

Microplastics in the Rhine River
From the Swiss catchment towards
the North Sea

Inauguraldissertation

zur

Erlangung der Würde eines Doktors der Philosophie
vorgelegt der
Philosophisch-Naturwissenschaftlichen Fakultät
der Universität Basel

von

Thomas Mani
aus Diemtigen, BE, Schweiz

2020

Genehmigt von der Philosophisch-Naturwissenschaftlichen Fakultät

auf Antrag von

Prof. Dr. Patricia Holm, MGU, Universität Basel

Prof. Dr. Helmut Segner, FIWI, Universität Bern

Basel, den 23. April 2019

Prof. Dr. Martin Spiess

Table of Contents

Summary	9
List of Papers	11
Introduction	13
Paper 1 Repeated detection of polystyrene microbeads in the Lower Rhine River	27
Abstract	29
1. Introduction.....	31
2. Materials and methods.....	32
2.1. Sampling sites	32
2.2. Sampling, processing and quantification.....	33
2.3. Raman microspectroscopy, FT-IR spectroscopy and SEM.....	34
2.4. Quality control and contamination protection	36
3. Results and discussion.....	37
3.1. Microbead concentrations and categories.....	37
3.2. Narrowing down the microbead influx area	38
3.3. Polymer composition.....	40
3.4. Fate of microbeads in the Rhine River	44
3.5. Current regulation on particulate matter emissions and future tasks	44
4. Conclusions.....	44
Acknowledgements	46

References	47
SI 1: Repeated detection of polystyrene microbeads in the Lower Rhine River.....	55
Paper 2 Using castor oil to separate microplastics from four different environmental matrices	75
Abstract	77
1. Introduction.....	79
2. Methods	80
2.1. Environmental sample collection	80
2.2. Microplastics for spiking	80
2.3. Castor oil microplastic and environmental matrix separation protocol.....	81
2.4. Quality control and protection against contamination.....	83
2.5. Statistical analysis	83
3. Results and discussion.....	84
3.1. Environmental matrix reduction and recovery of spiked microplastics	84
3.2. Properties and advantages of a castor oil-based separation approach.....	87
3.3. Chemical considerations and background to the lipophilic castor oil approach.....	88
4. Conclusions.....	89
Acknowledgements	90
References	91
SI 2: Using castor oil to separate microplastics from four different environmental matrices	97

Paper 3 Seasonal microplastics variation in nival and pluvial stretches of the Rhine River

– From the Swiss catchment towards the North Sea 111

Abstract	113
1. Introduction.....	115
2. Materials and methods.....	117
2.1. Sampling.....	117
2.2. Sample processing.....	118
2.3. Visual particle sorting for chemical analysis.....	118
2.4. FTIR analysis	119
2.5. Calculations, further data collection and statistics.....	120
2.6. Quality assurance and quality control	121
3. Results	122
3.1. Geographical and seasonal variations in MP concentrations.....	122
3.2. Geographical and seasonal occurrence of MP types	123
3.3. Types of MP and their polymers.....	125
4. Discussion.....	128
4.1. MP concentrations of the nival and pluvial locations	128
4.2. MP freight and fate downstream.....	130
4.3. Potential MP sources	131
4.4. Appraisal of methodology	133
5. Conclusion.....	134
Acknowledgements.....	135

References	136
SI 3: Seasonal microplastics variation in nival and pluvial stretches of the Rhine River – From the Swiss catchment towards the North Sea.....	145
Paper 4 Microplastic pollution in benthic midstream sediments of the Rhine River...	161
Abstract	163
1. Introduction.....	165
2. Materials and methods.....	166
2.1. Sampling.....	166
2.2. Drying, sieving, aliquoting and pooling	167
2.3. ZnCl ₂ density separation	167
2.4. Purification using Fenton’s Reagent	168
2.5. Focal plane array μFTIR analysis	169
2.6. Automated analysis of μFTIR data	169
2.7. Visual selection and ATR FTIR analysis of >500 μm fractions.....	169
2.8. Statistical analysis	170
2.9. Quality assessment and quality control	170
3. Results	170
3.1. Microplastic concentrations and sizes	170
3.2. Polymer composition.....	172
4. Discussion.....	173
4.1. MP sedimentation and retention in riverbed sediments.....	173
4.2. MP concentrations in riverbed sediments.....	174

4.3. Polymers in the Rhine riverbed sediments	176
4.4. Dominance of smallest-size MP in the Rhine riverbed	179
4.5. Sampling method and seasonal influences on sediment MP abundance.....	179
4.6. Appraisal of methodology	180
Acknowledgements.....	182
References	183
SI 4: Microplastic pollution in benthic midstream sediments of the Rhine River	193
Final Discussion Dissertation.....	207
Searching for MP sources on a way towards better accountability	207
Gearing up for the next challenges – method development for MP research	208
Taking into account seasonal changes in MP concentrations and fluxes.....	209
Getting to the bottom of things – investigating MP on the Rhine riverbed	210
Outlook and conclusion.....	211
References	214
Final Acknowledgements Dissertation	219
Final References Dissertation.....	221
Curriculum Vitae.....	248

Summary

The threat of plastic waste in the environment has evoked rising concern over the past decades. While these versatile and incredibly popular polymer materials undoubtedly fulfil unprecedented services, their extreme durability and alleged toxicity represent major downsides, once in the environment. As plastics break down into smaller microplastics (MP) they evidently pollute almost every thinkable habitat on the globe today. While an estimated 5–12 million tons of plastic end up in the oceans every year, rivers are important pathways, carrying an annual freight of 0.41–4 million tons downstream. The Rhine River, one of Europe's main streams and one of the World's busiest waterways, reportedly holds substantial amounts of MP in its near-surface waters and sediments. However, little is known about potential MP sources, seasonal dynamics and the MP pollution of benthic sediments of this major river. In my dissertation I address three pivotal knowledge gaps about MP in the Rhine River and investigate a new type of method to safely and efficiently separate MP from surrounding environmental sample matrices.

The surface water MP pollution of the Rhine River was earlier characterised by the distinct appearance of vast amounts (~60%) of rigid polystyrene microbeads of unknown origin and former purpose. In a sustained investigation of a defined river stretch in the Lower Rhine downstream Cologne, we managed to narrow down the entry region of these pollutants and close-to-certainly unveil the particle's former purpose as ion-exchange resin beads used in diverse fluid purification applications.

As more data on MP in rivers emerges, an interesting gap opens: empirical field studies tend to generate temporally restricted snapshot data while modellers, laudably seeking the bigger picture, are confronted with enormous uncertainties in their results. In a bid to reduce this void we embarked on a quadruplicate surface water MP observation in the Rhine catchment during 2016–2017. The investigation included three nival discharge regime tributaries and the Rhine in Switzerland as well as a pluvial Rhine River section towards the German-Dutch border. It became evident that despite a coherent increasing MP concentration gradient downstream, reflecting average discharge and catchment size, overall variability in environmental MP data was large. This hampers clear-cut estimations about concentration fluctuations but at the same time reinforces the theory of high MP seasonal pollution fluxes in the European winter months, when Rhine discharge is highest.

Seeking to contribute to the very scarce knowledge of MP and benthic sediment interaction in large dynamic rivers, we took a diving bell and a dredging vessel to the riverbed at two previously identified surface MP hotspots at the German Middle and Lower Rhine. Due to expected water turbulence and flow velocity, substantial settling of MP in such stretches is not necessarily anticipated. Interestingly, it showed that even the Rhine riverbed is not spared from vast MP pollution. The applied research technology allowed for reliable detection of MP down to particle sizes of 11 μm and yielded strongly varying concentrations of 260–11,000 MP kg^{-1} , with a strongly skewed size class distribution towards the smallest MP particles.

Experience showed us that environmental sample preparation for MP research can be a tedious and resource-intensive enterprise – including health and environmental hazards. Instead of attacking the unwanted portions in a sample (e.g. biogenic residue to isolate MP), a more efficient approach is to select the MP specifically. We refined a proposed lipophilicity-based separation technique and broadened its scope by successfully testing it to four different types of environmental matrices. This one-for-all approach may present a promising means for quicker, cheap, safe and efficient MP data compilation. The method was successfully applied for the seasonal surface MP investigation presented in this dissertation.

List of Papers

Paper 1

Mani, Thomas; Blarer, Pascal; Storck, Florian R.; Pittroff, Marco; Wernicke, Theo; Burkhardt-Holm, Patricia (2019): **Repeated detection of polystyrene microbeads in the Lower Rhine River.** In *Environmental Pollution* 245, pp. 634–641.
DOI: 10.1016/j.envpol.2018.11.036.

Paper 2

Mani, Thomas; Frehland, Stefan; Kalberer, Andreas; Burkhardt-Holm, Patricia (2019): **Using castor oil to separate microplastics from four different environmental matrices.** In *Analytical Methods* 11 (13), pp. 1788–1794. DOI: 10.1039/C8AY02559B.

Paper 3

Mani, Thomas; Burkhardt-Holm, Patricia (2020): **Seasonal microplastics variation in nival and pluvial stretches of the Rhine River – From the Swiss catchment towards the North Sea.** In *Science of the Total Environment* 707, 135579. DOI: 10.1016/j.scitotenv.2019.135579

Paper 4

Mani, Thomas; Primpke, Sebastian; Lorenz, Claudia; Gerdts, Gunnar; Burkhardt-Holm, Patricia (2019): **Microplastic pollution in benthic midstream sediments of the Rhine River.** In *Environmental Science & Technology* 53 (10), pp. 6053–6062.
DOI: 10.1021/acs.est.9b01363

All papers presented in this dissertation are accompanied by Supporting Information (SI).

For all papers the authors declare that no competing financial or other interests exist.

Introduction

Since the 19th century, breakthroughs in industrial chemistry spawned synthetic materials, which fundamentally revolutionised human life. The group of materials in question is – *plastics*. This general term refers to tens of thousands of synthetic, crude oil-based hydrocarbon polymer formulae in worldwide use today (Brydson, 1999). Plastics play a decisive role in almost every domain of life: automotive, aviation, medicine, agriculture, food packaging, clothing, electronics, building and construction, fishing, household, leisure and sports and many more (PlasticsEurope, 2017). But how is it possible that plastics can be key to such a myriad of modern life solutions? The answer lies in their miraculously versatile application due to unprecedented combinations of properties. Most synthetic polymers boast extreme mechanical, physical and chemical resilience as well as exceptional durability despite low specific density and enormous flexibility – even under smallest-quantity application. Furthermore, plastics are generally waterproof, electrically insulating, chemically inert, colourable and mouldable in to almost every thinkable colour and shape (Andrady, 2017). To only name a few applied benefits: cheap plastic food packaging can substantially prolong shelf life; energy demand to transport lightweight plastic water bottles is notably lower than for e.g. heavier glass bottles – a similar benefit results from lightweight plastic vehicle parts; also, plastic bottles yield improved survival upon collisions with hard surfaces; sterile, cheap, single use medical items, such as syringes, may help sustain affordable and efficient healthcare; the list almost indefinitely continues (Finkelstein, 2008). The minimal material requirement for many applications also explains the probably most pivotal factor for the material’s triumphal march through the economy: because little material is needed to produce useful items, using plastics is extremely cheap (Birley, 2012).

Today, over 320 million tonnes (mt) of plastics are produced in the world every year (PlasticsEurope, 2017). This is a >200-fold rise since the 1950s and 84 mt more than in 2004 (Andrady, 2017; PlasticsEurope, 2017; Thompson et al., 2004). By 2050, it is believed that this figure could rise to a staggering 33 billion annual tonnes (Ellen Mc Arthur Foundation, 2016; Rochman et al., 2013). Of the total 8.3 billion tonnes of plastics produced until today, 6.3 billion tonnes had turned to waste by 2015 already, of which 9% were recycled, 12% incinerated and 79% accumulated in landfills or the natural environment (Geyer et al., 2017). Once plastics end up in the environment, some of their formerly so distinguished properties become threats. Their high resilience and durability hinders natural forces to decompose and mineralise plastics at an ecologically beneficial rate, leading to the material’s survival in the environment for hundreds

to possibly thousands of years (O'Brine and Thompson, 2010; Ohtake et al., 1998). Considering the continually rising global output, their waste loss and persistence will invariably lead to an accumulation of plastics in the natural environment (Barnes et al., 2009). In 2010, 275 mt of plastic waste was generated in 192 coastal countries, of which 4.8–12.7 mt were calculated to enter the ocean (Jambeck et al., 2015), while also terrestrial habitats are far from spared from pollution (Dris et al., 2015; Dris et al., 2016; Rillig, 2012). In the ocean, large plastic items severely menace the wellbeing of wildlife through entanglement of animals e.g. in fishing lines and nets (Derraik, 2002; Gregory, 2009) or ingestion by marine mammals (Fossi et al., 2017; Secchi and Zarzur, 1999). As plastics break down in the environment into ever smaller fragments long before they decompose or mineralise, hardly visible *microplastics* (MP) result (Andrady, 2011; Barnes et al., 2009). The term generically refers to all synthetic polymer items of 0.001–5 mm in diameter (Hartmann et al., 2019). Their minute particle sizes collectively compile to a huge surface area potentially promoting toxic interaction, and the greater numerical probability for ingestion – even by smallest animals (Gallo et al., 2018; Holm et al., 2013). MP have increasingly been raising biological and ecological concerns for the past decades (Cole et al., 2011). Although hydrocarbon polymers are theoretically inert, plastics can contain low-molecular weight chemical species which may present a toxic hazard to ingesting organisms (Andrady, 2017): (i) additives enhancing stability, plasticity and flame retardation (Koelmans et al., 2014; Oehlmann et al., 2009); (ii) persistent organic pollutants (POP) present in the environment which are very efficiently sorbed by MP (Gallo et al., 2018; Lohmann, 2017; Mato et al., 2001) and (iii) residual monomers, e.g. styrene monomers in polystyrene (Andrady, 2017; Choi and Kim, 2012). It has been demonstrated, that toxic effects of MP upon ingestion in organisms can negatively alter behaviour (Ferreira et al., 2016) and lead to adverse health outcomes (Foley et al., 2018; Von Moos et al., 2012). However, it is of utmost importance to state that the scientific community does not yet conclusively agree on the extent of the potential ecological threats (Wagner et al., 2018). After years of potential confirmation bias in reporting negative effects of MP at unrealistic environmental concentrations more and more moderate, less alarmist and even non-effect papers on MP penetrate the peer-review process to balance the available body of publications (Backhaus and Wagner, 2018). Above aesthetic (recreation and tourism) and large item-related menaces, such as animal entanglement, the reported toxic threat of MP is regarded as the main global risk associated with plastic waste (Andrady, 2017) and this is also the driver for the vastly increasing environmental research output generated during the past decades (Eerkes-Medrano et al., 2015; Wright and Kelly, 2017). In 1972, for the first time in an academic context, small plastic particles were reported from the Sargasso

Sea (Carpenter et al., 1972; Carpenter and Smith, 1972). The authors already then speculated on ecological threats and environmental accumulation and at the same time unknowingly gave birth to a legacy of research on MP – which, however, would only pick up serious pace three decades later (Zeng, 2018). While environmental plastic pollution still is mainly a marine research topic (Klages et al., 2015), lakes and rivers are increasingly shifting into the spotlight of investigations (Wagner et al., 2014). More than 5 trillion floating plastic pieces weighing in total over 250,000 tons pollute the global oceans (Eriksen et al., 2014) and many more lie below the surface and on the seafloor (van Cauwenberghe et al., 2013). Rivers are major transport vectors for plastic waste (Faure et al., 2015; Schmidt et al., 2017) moving 0.41–4 million tons from land to sea every year (Lebreton et al., 2017; Schmidt et al., 2017). However, rivers are not simply conveyor belts for land-based plastic and MP pollution towards the seas – and therewith sources. River systems may function as plastic sinks retaining the pollutants in sediments of the shoreline (Klein et al., 2015) and the benthos (Castañeda et al., 2014; Hurley et al., 2018). Especially, when contaminated streams enter lentic waterbodies, residence time of the water masses and pollutants dramatically increase, keeping the pollution in the freshwater network (Boucher et al., 2019; Eriksen et al., 2013). Riverine fish (Sanchez et al., 2014; Silva-Cavalcanti et al., 2017) and crustaceans (Blarer and Burkhardt-Holm, 2016; Jemec et al., 2016) can ingest MP and are therefore potentially menaced by their adverse effects. In 2015, in a baseline study, we found out that the Rhine River is polluted with up to 21 MP particles m^{-3} in the water surface downstream highly urbanised areas (Mani et al., 2015). The work shed some light on some fundamental unknowns, such as MP distribution, particle types and polymers. One interesting finding, among others, was the vast numbers of specific microbeads. According to their chemistry (polystyrene, PS), physicality (rigid) and appearance these were not by then the widely reported care product additives. So, naturally, such insights lead to new questions, and so some pivotal areas for further research emerged. The presented dissertation is an in-depth follow-up of fundamental research to clarify the condition of the Rhine River and its catchment regarding MP pollution. Main research questions dealt with in this dissertation were:

- Where do the Rhine River PS microbeads come from, and what was their former purpose? In a geographically longitudinal and examination, these pearls were traced to find more answers (**Paper 1**).
- Is there a simple, effective, reliable, safe, environmentally friendly and cheap way to process environmental microplastic samples? After uncountable performances of tedious and tricky sample purification, we set out to seek a more straightforward solution (**Paper 2**).

- How valuable are one-off environmental studies? As most river MP assessments present temporal snapshot data, we raise the question: What are the seasonal dynamics of MP concentrations and fluxes downstream the Rhine River? Presented here is first insight on a one-year investigation of the Rhine River and three tributaries between Switzerland and the German-Dutch border (**Paper 3**).
- Finally, one question of paramount interest to me and my fellow researchers has always been: what goes on below the surface of the Rhine River? Much data is available on buoyant MP and sediment MP in slack waterbodies, but very little is known about MP interaction with dynamic river benthos. To find out if the pollution levels of the water surface are also reflected on the ground, we took a diving bell and a dredging vessel to the bottom of the Rhine in 2016 to investigate a potential pollution sink (**Paper 4**).

Paper 1: Repeated detection of polystyrene microbeads in the Lower Rhine River

One key finding published in 2015 was the severe proportion of almost 60% spherical, most probably primary, PS MP. By that time, plastic microbeads had been found e.g. in the Atlantic (Carpenter et al., 1972) and in the Great Lakes (Eriksen et al., 2013), but neither our team nor Carpenter et al., or Eriksen et al., had more to offer than mere speculation about potential source areas or former function of such spherules. On this ground, we embarked on a high-effort geographical and forensic investigation to unveil the possible entry area of these beads to the Rhine River as well as their former use in “Repeated detection of polystyrene microbeads in the Lower Rhine River” (**Paper 1**). As the remedial of MP pollution to date is technically and economically hardly viable, avoiding such pollution in the first place is absolutely key. For this, sources (geography as well as application) need to be known in order to lay promising cornerstones for effective pollution prevention measures. Apart from the focal investigation on source area and former use of the beads, the presented Paper is also a first technical proposal of how to answer such questions. Uncountable unregistered chemical plastic formulae and the lack of standard tracer technology, such as e.g. synthetic DNA implantation in the gem industry (Cartier et al., 2018), make it almost impossible to track down the sources of plastic waste after their superficial properties such as residual print or original object shape are lost. With the publication of **Paper 1** we hence aspire to additionally contribute to the body of knowledge on how to trace microscopic plastic waste and therewith foster producer/emitter accountability.

Paper 2: Using castor oil to separate microplastics from four different environmental matrices

One major flaw for the total field of environmental MP research is on the one hand the lack of standardisation in investigation methodology and the scarce availability of effective sample purification and separation methods (BASEMAN, 2017; Hidalgo-Ruz et al., 2012; Ivleva et al., 2017). In an aspirational bid to refine a suitable protocol, we set out to improve and expand an earlier proposed oil separation approach (Crichton et al., 2017). Our goal was to separate MP efficiently from four different surrounding environmental matrices. Many traditional sample preparation protocols involve (i) a purification step (e.g. using H₂O₂ and enzymes; Löder et al., 2017), where non-plastic content is targeted and (ii) a density separation step where MPs are floated above higher density particles such as silicate sediment e.g. using NaCl, (Hidalgo-Ruz et al., 2012; Thompson et al., 2004) or ZnCl₂, (Imhof et al., 2012). “Using castor oil to separate microplastics from four different types of environmental matrices” (**Paper 2**) demonstrates the combination of steps (i) and (ii) by attracting MP to the high molecular weight oil, taking advantage of their lipophilicity. This cheap, safe, simple and effective approach could promise harmonisation of MP research methodology as it proved to separate MP from soil, sediment and marine and freshwater surface samples. Instead of “removing the haystack and keeping the needle” (BASEMAN, 2017) we use a powerful magnet to find the needle and forget about the haystack. The refined protocol was applied to process 60 lotic water surface samples for the study presented in **Paper 3**.

Paper 3: Seasonal microplastics variation in nival and pluvial stretches of the Rhine River – From the Swiss catchment towards the North Sea

Despite the important baseline qualities of the earlier paper on the Rhine River (Mani et al., 2015), when sensibly evaluated, the results of 2015 are inevitably snapshot data. The lack of temporal replication, which would allow for more robust claims concerning total MP freight and potential seasonal changes as well as the omission of MP contributions upstream of Basel in Switzerland, constituted major remaining knowledge gaps. To satisfy these open points we elaborated a follow-up research design sending forth four further sampling campaigns covering four seasons and six focal locations between Switzerland and the German-Dutch border. The sites include nival and pluvial discharge regimes of the Rhine catchment, aiming to potentially identify regime driven dynamics of MP concentrations and fluxes. In the resulting **Paper 3**, we aim to validate the quantitative data brought forward by (Mani et al., 2015) and at the same time we expand the geographical scope to the Swiss Aare, Reuss and Limmat River tributaries.

Furthermore, **Paper 3** investigates potential seasonal and discharge alteration related effects on quantity and quality of present MP at the water surface (polymer and morphology).

Paper 4: Microplastic pollution in benthic midstream sediments of the Rhine River

MP are known to settle in slack water provided sufficient density, biofouling or heteroaggregation (Kooi et al., 2018). Little is known about their behaviour in dynamic, undammed stretches of major rivers (Wagner et al., 2014). Focusing on two locations with previously reported rising (Bad Honnef, Rh-km 640) and peak (Rees, Rh-km 837) surface water MP concentrations (Mani et al., 2015), our immense curiosity about potential MP in the mid-stream, benthic sediments of the Rhine River was met by diving to the floor at these locations. Are the characteristic MP pollution levels of the surface water reflected in the sediments? Considering the enormous inland waterway capacity of the Rhine (ICPR, 2018) – is there possibly shipping-related contamination? Exquisite riverbed access was provided by German Authorities and their diving bell as well as by a riverbed dredging vessel. With the support of Alfred-Wegener Institute Helgoland, highest standard, comprehensive sediment aliquot analysis was performed (Bergmann et al., 2017; Primpke et al., 2017).

With the four papers presented, this dissertation aims to significantly further the fundamental knowledge about occurrence and dynamics of MP in the Rhine River. It was a pleasure and a mighty experience to be part of this extraordinarily exciting research. I hope that the reader may share the enthusiasm on the presented work.

References

- Andrady, A.L., 2011. Microplastics in the marine environment. *Mar. Pollut. Bull.* 62 (8), 1596–1605. doi:10.1016/j.marpolbul.2011.05.030.
- Andrady, A.L., 2017. The plastic in microplastics: A review. *Mar. Pollut. Bull.* 119 (1), 12–22. doi:10.1016/j.marpolbul.2017.01.082.
- Backhaus, T., Wagner, M., 2018. Microplastics in the environment: Much ado about nothing? A debate. 26 pp. *Global Challenges*. doi:10.1002/gch2.201900022
- Barnes, D.K.A., Galgani, F., Thompson, R.C., Barlaz, M., 2009. Accumulation and fragmentation of plastic debris in global environments. *Philosophical transactions of the Royal Society of London. Series B, Biological sciences* 364 (1526), 1985–1998. doi:10.1098/rstb.2008.0205.
- BASEMAN, 2017. Interdisciplinary Research for Good Environmental Status. <http://www.jpi-oceans.eu/baseman>. Accessed 09 May 2018.
- Bergmann, M., Wirzberger, V., Krumpen, T., Lorenz, C., Primpke, S., Tekman, M.B., Gerdt, G., 2017. High quantities of microplastic in Arctic deep-sea sediments from the HAUSGARTEN observatory. *Environ. Sci. Technol.* 51 (19), 11000–11010. doi:10.1021/acs.est.7b03331.
- Birley, A.W., 2012 // 1991. *Plastic materials: Properties and applications*. Springer, 1205 pp.
- Blarer, P., Burkhardt-Holm, P., 2016. Microplastics affect assimilation efficiency in the freshwater amphipod *Gammarus fossarum*. *Environ. Sci. Pollut. R. Int.* 23 (23), 23522–23532. doi:10.1007/s11356-016-7584-2.
- Boucher, J., Faure, F., Pompini, O., Plummer, Z., Wieser, O., Felipe de Alencastro, L., 2019. (Micro) plastic fluxes and stocks in Lake Geneva basin. *TrAC Trend. Anal. Chem.* 112, 66–74. doi:10.1016/j.trac.2018.11.037.
- Brydson, J.A., 1999. *Plastics materials*. Elsevier Science, Oxford, United Kingdom.
- Carpenter, E.J., Anderson, S.J., Harvey, G.R., Miklas, H.P., Peck, B.B., 1972. Polystyrene spherules in coastal waters. *Science* 178 (4062), 749–750. doi:10.1126/science.178.4062.749.
- Carpenter, E.J., Smith, K.L., 1972. Plastics on the Sargasso sea surface. *Science* 175 (4027), 1240–1241.

- Cartier, L.E., Ali, S.H., Krzemnicki, M.S., 2018. Blockchain, chain of custody and trace elements: An overview of tracking and traceability opportunities in the gem industry. *Journ. of Gemm.* 36 (3), 212–227. doi:10.15506/JoG.2018.36.3.212.
- Castañeda, R.A., Avlijas, S., Simard, M.A., Ricciardi, A., Smith, R., 2014. Microplastic pollution in St. Lawrence River sediments. *Can. J. Fish. Aquat. Sci.* 71 (12), 1767–1771. doi:10.1139/cjfas-2014-0281.
- Choi, S.-S., Kim, Y.-K., 2012. Analysis of residual monomers in poly(acrylonitrile-co-butadiene-co-styrene). *Macromol. Res.* 20 (6), 585–589. doi:10.1007/s13233-012-0080-8.
- Cole, M., Lindeque, P., Halsband, C., Galloway, T.S., 2011. Microplastics as contaminants in the marine environment: A review. *Mar. Pollut. Bull.* 62 (12), 2588–2597. doi:10.1016/j.marpolbul.2011.09.025.
- Crichton, E.M., Noël, M., Gies, E.A., Ross, P.S., 2017. A novel, density-independent and FTIR-compatible approach for the rapid extraction of microplastics from aquatic sediments. *Anal. Methods* 9 (9), 1419–1428. doi:10.1039/C6AY02733D.
- Derraik, J.G.B., 2002. The pollution of the marine environment by plastic debris: A review. *Mar. Pollut. Bull.* 44 (9), 842–852. doi:10.1016/S0025-326X(02)00220-5.
- Dris, R., Gasperi, J., Rocher, V., Saad, M., Renault, N., Tassin, B., 2015. Microplastic contamination in an urban area: A case study in Greater Paris. *Environ. Chem.* 12 (5), 592. doi:10.1071/EN14167.
- Dris, R., Gasperi, J., Saad, M., Mirande, C., Tassin, B., 2016. Synthetic fibers in atmospheric fallout: A source of microplastics in the environment? *Mar. Pollut. Bull.* 104 (1-2), 290–293. doi:10.1016/j.marpolbul.2016.01.006.
- Eerkes-Medrano, D., Thompson, R.C., Aldridge, D.C., 2015. Microplastics in freshwater systems: A review of the emerging threats, identification of knowledge gaps and prioritisation of research needs. *Water Res.* 75, 63–82. doi:10.1016/j.watres.2015.02.012.
- Ellen Mc Arthur Foundation, 2016. The new plastics economy: Rethinking the future of plastics & catalysing action, 68 pp.
https://www.ellenmacarthurfoundation.org/assets/downloads/publications/NPEC-Hybrid_English_22-11-17_Digital.pdf. Accessed 01 April 2019.
- Eriksen, M., Lebreton, L.C.M., Carson, H.S., Thiel, M., Moore, C.J., Borerro, J.C., Galgani, F., Ryan, P.G., Reisser, J., 2014. Plastic pollution in the world's oceans: More than 5

- trillion plastic pieces weighing over 250,000 tons afloat at sea. *PloS one* 9 (12), e111913. doi:10.1371/journal.pone.0111913.
- Eriksen, M., Mason, S., Wilson, S., Box, C., Zellers, A., Edwards, W., Farley, H., Amato, S., 2013. Microplastic pollution in the surface waters of the Laurentian Great Lakes. *Mar. Pollut. Bull.* 77 (1-2), 177–182. doi:10.1016/j.marpolbul.2013.10.007.
- Faure, F., Demars, C., Wieser, O., Kunz, M., Alencastro, L.F. de, 2015. Plastic pollution in Swiss surface waters: Nature and concentrations, interaction with pollutants. *Environ. Chem.* 12 (5), 582. doi:10.1071/EN14218.
- Ferreira, P., Fonte, E., Soares, M.E., Carvalho, F., Guilhermino, L., 2016. Effects of multi-stressors on juveniles of the marine fish *Pomatoschistus microps*: Gold nanoparticles, microplastics and temperature. *Aquat. Toxicol.* 170, 89–103. doi:10.1016/j.aquatox.2015.11.011.
- Finkelstein, N.H., 2008. *Plastics*. New York, Marshall Cavendish Benchmark.
- Foley, C.J., Feiner, Z.S., Malinich, T.D., Höök, T.O., 2018. A meta-analysis of the effects of exposure to microplastics on fish and aquatic invertebrates. *Sci. Total Environ.* 631-632, 550–559. doi:10.1016/j.scitotenv.2018.03.046.
- Fossi, M.C., Baini, M., Panti, C., Galli, M., Jiménez, B., Muñoz-Arnanz, J., Marsili, L., Finoia, M.G., Ramírez-Macías, D., 2017. Are whale sharks exposed to persistent organic pollutants and plastic pollution in the Gulf of California (Mexico)? First ecotoxicological investigation using skin biopsies. *Comparative biochemistry and physiology. Toxicol. Pharm.: CBP* 199, 48–58. doi:10.1016/j.cbpc.2017.03.002.
- Gallo, F., Fossi, C., Weber, R., Santillo, D., Sousa, J., Ingram, I., Nadal, A., Romano, D., 2018. Marine litter plastics and microplastics and their toxic chemicals components: The need for urgent preventive measures. *Environ. Sci. Eur.* 30 (1), 13. doi:10.1186/s12302-018-0139-z.
- Geyer, R., Jambeck, J.R., Law, K.L., 2017. Production, use, and fate of all plastics ever made. *Sci. Adv.* 3 (7), e1700782. doi:10.1126/sciadv.1700782.
- Gregory, M.R., 2009. Environmental implications of plastic debris in marine settings—entanglement, ingestion, smothering, hangers-on, hitch-hiking and alien invasions. *Philosophical transactions of the Royal Society of London. Series B, Biological sciences* 364 (1526), 2013–2025. doi:10.1098/rstb.2008.0265.

- Hartmann, N.B., Hüffer, T., Thompson, R.C., Hassellöv, M., Verschoor, A., Daugaard, A.E., Rist, S., Karlsson, T., Brennholt, N., Cole, M., Herrling, M.P., Hess, M.C., Ivleva, N.P., Lusher, A.L., Wagner, M., 2019. Are we speaking the same language? Recommendations for a definition and categorization framework for plastic debris. *Environ. Sci. Technol.* 53 (3), 1039–1047. doi:10.1021/acs.est.8b05297.
- Hidalgo-Ruz, V., Gutow, L., Thompson, R.C., Thiel, M., 2012. Microplastics in the marine environment: A review of the methods used for identification and quantification. *Environ. Sci. Technol.* 46 (6), 3060–3075. doi:10.1021/es2031505.
- Holm, P., Schulz, G., Athanasopulu, K., 2013. Mikroplastik – ein unsichtbarer Störenfried. *Biologie in unserer Zeit* 43 (1), 27–33. doi:10.1002/biuz.201310497.
- Hurley, R., Woodward, J., Rothwell, J.J., 2018. Microplastic contamination of river beds significantly reduced by catchment-wide flooding. *Nat. Geosci.* 11 (4), 251–257. doi:10.1038/s41561-018-0080-1.
- ICPR, 2018. The Rhine. International Commission for the Protection of the Rhine. <https://www.iksr.org/en/rhine/>. Accessed 18 December 2018.
- Imhof, H.K., Schmid, J., Niessner, R., Ivleva, N.P., Laforsch, C., 2012. A novel, highly efficient method for the separation and quantification of plastic particles in sediments of aquatic environments. *Limnol. Oceanogr. Methods* 10 (7), 524–537. doi:10.4319/lom.2012.10.524.
- Ivleva, N.P., Wiesheu, A.C., Niessner, R., 2017. Microplastic in aquatic ecosystems. *Angew. Chem. Int. Edit.* 56 (7), 1720–1739. doi:10.1002/anie.201606957.
- Jambeck, J.R., Geyer, R., Wilcox, C., Siegler, T.R., Perryman, M., Andrady, A., Narayan, R., Law, K.L., 2015. Plastic waste inputs from land into the ocean. *Science* 347 (6223), 768–771. doi:10.1126/science.1260352.
- Jemec, A., Horvat, P., Kunej, U., Bele, M., Kržan, A., 2016. Uptake and effects of microplastic textile fibers on freshwater crustacean *Daphnia magna*. *Environ. Pollut.* 219, 201–209. doi:10.1016/j.envpol.2016.10.037.
- Klages, M., Gutow, L., Bergmann, M. (Eds.), 2015. *Marine anthropogenic litter*. Springer, 447 pp.

- Klein, S., Worch, E., Knepper, T.P., 2015. Occurrence and spatial distribution of microplastics in river shore sediments of the Rhine-Main area in Germany. *Environ. Sci. Technol.* 49 (10), 6070–6076. doi:10.1021/acs.est.5b00492.
- Koelmans, A.A., Besseling, E., Foekema, E.M., 2014. Leaching of plastic additives to marine organisms. *Environ. Pollut.* 187, 49–54. doi:10.1016/j.envpol.2013.12.013.
- Kooi, M., Besseling, E., Kroeze, C., van Wezel, A.P., Koelmans, A.A., 2018. Modeling the fate and transport of plastic debris in freshwaters: Review and guidance, in: Wagner, M., Lambert, S., Besseling, E., Biginagwa, F.J. (Eds.), *Freshwater microplastics. Emerging environmental contaminants? The handbook of environmental chemistry. Volume 58.* Springer, pp. 125–152. doi:10.1007/978-3-319-61615-5
- Lebreton, L.C.M., van der Zwet, J., Damsteeg, J.-W., Slat, B., Andrady, A., Reisser, J., 2017. River plastic emissions to the world's oceans. *Nat. Commun.* 8, 15611. doi:10.1038/ncomms15611.
- Löder, M.G.J., Imhof, H.K., Ladehoff, M., Löschel, L.A., Lorenz, C., Mintenig, S., Piehl, S., Primpke, S., Schrank, I., Laforsch, C., Gerdt, G., 2017. Enzymatic purification of microplastics in environmental samples. *Environ. Sci. Technol.* 51 (24), 14283–14292. doi:10.1021/acs.est.7b03055.
- Lohmann, R., 2017. Microplastics are not important for the cycling and bioaccumulation of organic pollutants in the oceans – But should microplastics be considered POPs themselves? *Integr. Environ. Assess.* 13 (3), 460–465. doi:10.1002/ieam.1914.
- Mani, T., Blarer, P., Storck, F.R., Pittroff, M., Wernicke, T., Burkhardt-Holm, P., 2019. Repeated detection of polystyrene microbeads in the Lower Rhine River. *Environ. Pollut.* 245, 634–641. doi:10.1016/j.envpol.2018.11.036.
- Mani, T., Frehland, S., Kalberer, A., Burkhardt-Holm, P., 2019b. Using castor oil to separate microplastics from four different environmental matrices. *Anal. Methods* 11 (13), 1788–1794. doi:10.1039/C8AY02559B.
- Mani, T., Hauk, A., Walter, U., Burkhardt-Holm, P., 2015. Microplastics profile along the Rhine River. *Sci. Rep.* 5, 17988. doi:10.1038/srep17988.
- Mato, Y., Isobe, T., Takada, H., Kanehiro, H., Ohtake, C., Kaminuma, T., 2001. Plastic resin pellets as a transport medium for toxic chemicals in the marine environment. *Environ. Sci. Technol.* 35 (2), 318–324. doi:10.1021/es0010498.

- O’Brine, T., Thompson, R.C., 2010. Degradation of plastic carrier bags in the marine environment. *Mar. Poll. Bull.* 60 (12), 2279–2283. doi:10.1016/j.marpolbul.2010.08.005.
- Oehlmann, J., Schulte-Oehlmann, U., Kloas, W., Jagnytsch, O., Lutz, I., Kusk, K.O., Wollenberger, L., Santos, E.M., Paull, G.C., van Look, K.J.W., Tyler, C.R., 2009. A critical analysis of the biological impacts of plasticizers on wildlife. *Philosophical transactions of the Royal Society of London. Series B, Biological sciences* 364 (1526), 2047–2062. doi:10.1098/rstb.2008.0242.
- Ohtake, Y., Kobayashi, T., Asabe, H., Murakami, N., 1998. Studies on biodegradation of LDPE – observation of LDPE films scattered in agricultural fields or in garden soil. *Polym. Degrad. Stabil.* 60 (1), 79–84. doi:10.1016/S0141-3910(97)00032-3.
- PlasticsEurope, 2017. Plastic – the Facts 2017, 44 pp.
https://www.plasticseurope.org/application/files/5715/1717/4180/Plastics_the_facts_2017_FINAL_for_website_one_page.pdf. Accessed 23 August 2018.
- Primpke, S., Lorenz, C., Rascher-Friesenhausen, R., Gerdt, G., 2017. An automated approach for microplastics analysis using focal plane array (FPA) FTIR microscopy and image analysis. *Anal. Methods* 9 (9), 1499–1511. doi:10.1039/C6AY02476A.
- Rillig, M.C., 2012. Microplastic in terrestrial ecosystems and the soil? *Environ. Sci. Technol.* 46 (12), 6453–6454. doi:10.1021/es302011r.
- Rochman, C.M., Browne, M.A., Halpern, B.S., Hentschel, B.T., Hoh, E., Karapanagioti, H.K., Rios-Mendoza, L.M., Takada, H., Teh, S., Thompson, R.C., 2013. Policy: Classify plastic waste as hazardous. *Nature* 494 (7436), 169–171. doi:10.1038/494169a.
- Sanchez, W., Bender, C., Porcher, J.-M., 2014. Wild gudgeons (*Gobio gobio*) from French rivers are contaminated by microplastics: Preliminary study and first evidence. *Environ. Res.* 128, 98–100. doi:10.1016/j.envres.2013.11.004.
- Schmidt, C., Krauth, T., Wagner, S., 2017. Export of plastic debris by rivers into the sea. *Environ. Sci. Technol.* 51 (21), 12246–12253. doi:10.1021/acs.est.7b02368.
- Secchi, E.R., Zarzur, S., 1999. Plastic debris ingested by a Blainville’s beaked whale, *Mesoplodon densirostris*, washed ashore in Brazil. *Aquat. Mamm.* 25 (1), 21–24.
- Silva-Cavalcanti, J.S., Silva, J.D.B., França, E.J.d., Araújo, M.C.B.d., Gusmão, F., 2017. Microplastics ingestion by a common tropical freshwater fishing resource. *Environ. Pollut.* 221, 218–226. doi:10.1016/j.envpol.2016.11.068.

- Thompson, R.C., Olsen, Y., Mitchell, R.P., Davis, A., Rowland, S.J., John, A.W.G., McGonigle, D., Russell, A.E., 2004. Lost at sea: Where is all the plastic? *Science*. 304 (5672), 838. doi:10.1126/science.1094559.
- Van Cauwenberghe, L., Vanreusel, A., Mees, J., Janssen, C.R., 2013. Microplastic pollution in deep-sea sediments. *Environ. Pollut.* 182, 495–499. doi:10.1016/j.envpol.2013.08.013.
- Von Moos, N., Burkhardt-Holm, P., Köhler, A., 2012. Uptake and effects of microplastics on cells and tissue of the blue mussel *Mytilus edulis* L. after an experimental exposure. *Environ. Sci. Technol.* 46 (20), 11327–11335. doi:10.1021/es302332w.
- Wagner, M., Lambert, S., Besseling, E., Biginagwa, F.J. (Eds.), 2018. Freshwater microplastics: Emerging environmental contaminants? The handbook of environmental chemistry. volume 58. Springer, 303 pp. doi:10.1007/978-3-319-61615-5
- Wagner, M., Scherer, C., Alvarez-Muñoz, D., Brennholt, N., Bourrain, X., Buchinger, S., Fries, E., Grosbois, C., Klasmeier, J., Marti, T., Rodriguez-Mozaz, S., Urbatzka, R., Vethaak, A.D., Winther-Nielsen, M., Reifferscheid, G., 2014. Microplastics in freshwater ecosystems: What we know and what we need to know. *Environ. Sci. Eur.* 26 (1), 12. doi:10.1186/s12302-014-0012-7.
- Wright, S.L., Kelly, F.J., 2017. Plastic and human health: A micro issue? *Environ. Sci. Technol.* 51 (12), 6634–6647. doi:10.1021/acs.est.7b00423.
- Zeng, E.Y., 2018. Microplastic contamination in aquatic environments: An emerging matter of environmental urgency. Elsevier Science. doi:10.1016/C2016-0-04784-8

Paper 1

Repeated detection of polystyrene microbeads in the Lower Rhine River

Thomas Mani ^a, Pascal Blarer ^b, Florian R. Storck ^c, Marco Pittroff ^c, Theo Wernicke ^c,
Patricia Burkhardt-Holm ^a

^a Department of Environmental Sciences, The Man-Society-Environment Program,
University of Basel, Vesalgasse 1, 4051 Basel, Switzerland

^b World Wide Fund for Nature (WWF) Switzerland, Department for Biodiversity,
Hohlstrasse 110, 8010 Zurich, Switzerland.

^c TZW: DVGW-Technologiezentrum Wasser, Karlsruher Strasse 84, 76139 Karlsruhe,
Germany.

Published 2019

in *Environmental Pollution* 245, pp. 634–641.

DOI: 10.1016/j.envpol.2018.11.036.

Abstract

Microplastics are emerging pollutants in water bodies worldwide. The environmental entry areas must be studied to localise their sources and develop preventative and remedial solutions. Rivers are major contributors to the marine microplastics load. Here, we focus on a specific type of plastic microbead (diameter 286–954 μm , predominantly opaque, white–beige) that was repeatedly identified in substantial numbers between kilometres 677 and 944 of the Rhine River, one of Europe’s main waterways. Specifically, we aimed (i) to confirm the reported abrupt increase in microbead concentrations between the cities of Leverkusen and Duisburg and (ii) to assess the concentration gradient of these particles along this stretch at higher resolution. Furthermore, we set out (iii) to narrow down the putative entry stretch from 81.3 km, as reported in an earlier study, to less than 20 km according to our research design, and (iv) to identify the chemical composition of the particles and possibly reveal their original purpose. Surface water filtration (mesh: 300 μm , $n = 9$) at regular intervals along the focal river stretch indicated the concentration of these spherules increased from 0.05 to 8.3 particles m^{-3} over 20 km. This spot sampling approach was supported by nine suspended solid samples taken between 2014 and 2017, encompassing the river stretch between Leverkusen and Duisburg. Ninety-five percent of microbeads analysed (202/212) were chemically identified as crosslinked polystyrene-divinylbenzene (PS-DVB, 146/212) or polystyrene (PS, 56/212) via Raman or Fourier-transform infrared spectroscopy. Based on interpretation of polymer composition, surface structure, shape, size and colour, the PS(-DVB) microbeads are likely to be used ion-exchange resins, which are commonly applied in water softening and various industrial purification processes. The reported beads contribute considerably to the surface microplastic load of the Rhine River and their potential riverine entry area was geographically narrowed down.

1. Introduction

Synthetic petrochemical polymer debris has been widely reported in the environment (Andrady, 2011; Eerkes-Medrano et al., 2015; Rillig, 2012). The demand for plastics is continuously rising worldwide – Europe consumed 49.9 million tons (mt) of new material and collected 27.1 mt of post-consumer plastics in 2016, of which 27.3%, 31.1%, and 41.6% was landfilled, recycled, or incinerated, respectively (PlasticsEurope, 2017). Microplastics (MP; <5 mm), which are either designed (primary MP) or fragmented to the relevant size range (secondary MP), have been in the spotlight of scientific research for over a decade (Cole et al., 2011; Thompson et al., 2004). The uptake of MP by aquatic and terrestrial organisms has been documented in species ranging from zooplankton (Steer et al., 2017) to worms (Huerta Lwanga et al., 2016), seabirds (Terepocki et al., 2017) and whales (Besseling et al., 2015). MP pollution is regarded as an emerging contaminant (Sedlak, 2017) and viewed as a possible planetary boundary threat (Jahnke et al., 2017).

Approximately 4.8–12.7 million tons of plastic waste reach the oceans from land-based sources every year (Jambeck et al., 2015). Rivers connect the terrestrial and marine biospheres, and thus represent important pathways for the passage of municipal, industrial and agricultural macro- and microplastic waste into the oceans (Faure et al., 2015; Mani et al., 2015; Schmidt et al., 2017). Every year the world's rivers carry between 0.47 and 2.75 million tons of plastic waste to the seas (Lebreton et al., 2017; Schmidt et al., 2017). The Rhine River transports approximately 10 tons of MP towards the North Sea in its surface waters annually (mean river discharge 2016 [MQ₂₀₁₆] at Rhine-km [Rh-km] 837.4: 2,367 m³ s⁻¹; BfG, 2017a; Mani et al., 2015).

Investigations of the origins of secondary MP varieties are usually ineffective due to the heterogeneity of polymers, shapes and colours. Furthermore, many characteristics that may enable identification of the origin or former purpose of MP are lost due to weathering and fragmentation (Ter Halle et al., 2016). Examination of a combination of primary microbead properties (i.e. size, shape, chemistry and surface structure) increases the chance of identifying their original purpose. Assessment of several characteristics, as well as the location of the occurrence of the MP, may facilitate identification of where the particles actually enter the environment. In our previous Rhine River study, opaque polystyrene (PS) microbeads ranging in size from 300 to 1000 µm accounted for over 60% of MP retrieved along an 835 km stretch of the Rhine ($n = 31$ samples at 11 sites; Mani et al., 2015). The concentration of these microbeads increased abruptly between the German cities of Leverkusen and Duisburg, located

at Rh-km 698 and 779.3, respectively. This finding obviously triggered a compelling follow-up mission to investigate this potential area of major microbead influx. Furthermore, this endeavour could offer a chance of identifying the original purpose and possibly hint towards the source of these spherules via a dedicated, spatially higher resolution sampling campaign in the relevant area. With reference to the morphology of the particles in question, we called this sampling campaign *pearl*.

The aims of this study were: (i) to confirm the abrupt increase in the concentration of spherical MP – predominantly polystyrene – observed at the surface of the Rhine River between the German cities of Leverkusen, Rh-km 698, and Duisburg, Rh-km 779.3 (Mani et al., 2015) through the longitudinal sampling campaign *pearl*; (ii) to assess the concentration gradient of these particles along this stretch of the Rhine; (iii) to narrow down the potential microbead entry area from 81.3 km (Mani et al., 2015) to less than 20 km; and (iv) to identify the chemical composition as well as further characteristics of these microbeads, such as surface structure, to possibly reveal their original purpose. By spatially confining the source area of a tangible type of primary MP, we sought to contribute to the so far limited knowledge of MP input pathways into aquatic environments. In this study, the findings from the *pearl* campaign (*p 1–9*) are consolidated with findings from sampling campaigns we conducted separately in the Rhine River between 2014 and 2017 (*s 1–9*).

2. Materials and methods

2.1. Sampling sites

Eighteen suspended solid samples were collected from the surface waters of the Rhine River: nine during the systematic longitudinal *pearl* campaign (*p 1–9*, Rh-km 691–780.3) on 29.11.2016 and another nine (*s 1–9* [*s 1–4* and *s 9* from Mani et al., 2015]) at five strategic locations geographically encompassing and overlapping the *pearl* sampling area during 2014–2017. Collectively, all samples cover the 267 km stretch of the Rhine River between Rh-km 677–944 (Table S1, Fig. S1).

For the *pearl* campaign, a longitudinal section from Cologne to Duisburg (both in Germany) was navigated by ship moving downstream. Sampling sites were selected based on previous data (Mani et al., 2015) and the following criteria: (i) most upstream sampling site: Cologne (*p 1*, Rh-km 691), centre of a 2 million-inhabitant metropolitan area, with only scarce previous evidence of opaque MP spherules (Mani et al., 2015); (ii) most downstream sampling site: Duisburg (*p 9*, Rh-km 780.3), a location previously reported to have high spherule concentrations (Mani et al., 2015); and (iii) strategic capture downstream of wastewater inlets,

resulting in a total of nine sampling sites at mean intervals \pm SD of 11.2 ± 5 km. A total of 76 direct wastewater dischargers (DID) and 14 communal wastewater treatment plants (WWTP) are directly connected to the main waterway along the 89.3 km investigated (Elwas, 2018; Table S2).

2.2. Sampling, processing and quantification

Samples were collected from the water surface to a depth of 18 cm using a Manta Trawl (5gyres Institute, Los Angeles, California, USA; 60×18 cm rectangular aperture, 300 μ m mesh; Faure et al., 2012). For each sample, the net was deployed for 10 min from a crane at the side of a steady-state, upstream facing ship. At every location, one sample was taken from the centre of the river cross section, always leaving a margin of 3 m between the Manta Trawl and the ship to dodge bow wave turbulence. After each sample, the ship moved downstream to the next location. Full and uniform inflow was achieved by maintaining a square net aperture angle facing the direction of river flow. The volume of sampled water was measured during all samplings using a mechanical flowmeter located at the centre of the Manta Trawl aperture (model 438 110; HYDRO-BIOS, Kiel, Germany). The Manta Trawl filtered a mean of 87 ± 17 m³ per sample during the *pearl* campaign. In deviations to the procedure described above, the *p 9* sample was collected on the right-hand side of the river cross section (Table S1), and 15 min sampling was used for *s 1–4* and *s 9*. For the *s 9* sample, the Manta Trawl was towed from the back of a vessel moving downstream in the Waal River (Mani et al., 2015), a lower branch of the Rhine (Table S1, Fig. S1). Turbulence caused by the flowmeter during Manta Trawl sampling is expected to be negligible because the net will capture all turbinated water. Furthermore, water volume loss due to mesh resistance is estimated to be below 2–3% (Currie and Foxton, 1957). The 10 min Manta Net trawls presented in this study usually resulted in a 2 cm thick filter cake in the cod end. The resulting clogged mesh area is roughly 0.4% of the total Manta Trawl mesh area and will therefore have a negligible effect regarding mass flow alterations (clogged mesh area: 0.02 m² of total 4.86 m²).

Samples were subsequently rinsed from the removable cod end into a 3 L glass beaker using 2 L of tap water from the ship. The cod end was thoroughly hand-rinsed between samples from the outside using ship tap water to avoid cross contamination from one sample to the next. Samples were subsequently reduced in volume (mesh 300 μ m) and transferred to sealable glass jars; 200 mL of ethanol (40%) was added to prevent fouling during transport and storage. In the lab, the samples were wet-sieved through a stainless-steel mesh (1000 and 300 μ m; Retsch, Haan, Germany) prior to density separation using saturated NaCl solution ($\rho \sim 1.2$ g cm⁻³) in a glass funnel equipped with a silicon tube and clamp as a separation device. The sedimented

fraction in the funnel was first drained into a separate glass container by easing the clamp on the silicon tube and the supernatant containing the microspheres was subsequently released through the tube into a glass Petri dish. From there, aliquots were transferred using a laboratory-grade stainless steel spoon to a Bogorov Chamber for visual inspection (10.5 × 7.3 cm, Hydro-Bios, Kiel, Germany). The abundance of putative MP spherules was quantified under a Leica Zoom 2000 stereomicroscope (10.5–45× with options for reflecting or transmitting light; Leica, Wetzlar, Germany) using a mechanical tally counter. Homogeneously spherical, opaque (including weakly translucent) particles smaller than 1000 µm in diameter of all colours that could be dented but not crushed using a pair of steel tweezers were considered.

On the basis of colour and translucency, 25 visual categories were generated among the 2,944 beads retrieved from the nine samples *p* 1–9 (Table S3). For each visual category, if the number of microbeads was sufficient, the first ten and every further fiftieth spherule were dried at room temperature, photographed and their diameter was measured ($n = 218$ [7.4%]; Olympus SZ61; Olympus SC50, Tokyo, Japan; CellSens Entry Version 1.17.16030.0). These 218 particles were subsequently stored in sealed polystyrene 96-well plates for backup and chemical analysis (Cellstar; ThermoFisher Scientific, Waltham, Massachusetts, USA).

2.3. Raman microspectroscopy, FT-IR spectroscopy and SEM

Chemical analysis was performed on a total of 212 environmental microbeads from *p* 3–9 and *s* 1–9. From the *pearl* campaign (*p* 3–9), 153 spherules (5.2% of the 2,944 retrieved beads) from the five most frequent categories A–E were analysed using either Raman microspectroscopy ($n = 98$) or attenuated total reflection Fourier-transform infrared (ATR FT-IR) spectroscopy ($n = 55$). A mean ± SD of 22 ± 5 beads were chemically analysed from each of the seven *pearl* samples *p* 3–9. Seventy-two category A beads and a mean ± SD of 20 ± 5 beads from the four categories B–E were analysed (Tables S1 and S3). From *s* 1–9, a total of 59 spherules were analysed using Raman spectroscopy ($n = 28$) or FT-IR ($n = 31$; Supporting Information, Table S1). As the project evolved, both Raman micro- and FT-IR spectroscopy – two complementary state-of-the-art techniques (Käppler et al., 2016) – were performed. For crosschecking, selected samples were analysed with both techniques. The techniques are complementary as they possess different strengths and weaknesses: Raman, for example, is known to have a higher sensitivity towards non-polar functional groups than FT-IR; however, Raman is prone to spectral interference due to fluorescence (Araujo et al., 2018). Further differences between Raman and FT-IR have been reported recently (Araujo et al., 2018; Barcelo et al., 2017; Ivleva et al., 2017; Silva et al., 2018).

Raman microspectroscopy was carried out using a Horiba XploRa Plus Raman-Microscope connected to a Sincerity EM-CCD detector (Horiba Jobin Yvon, Kyoto, Japan) and a confocal microscope (Olympus BX51, Olympus, Tokyo, Japan, consult Supporting Information for further details). Identification of chemical composition (polymers) was carried out using commercial reference databases (Bio-Rad, product code 470100, 1,600 entries, Hercules, CA, USA; All-Inclusive Bundle Raman Spectra Database [L60000], 16,898 entries, S.T. Japan Inc., Tokyo, Japan) as well as an internal reference database (180 entries, TZW, Karlsruhe, Germany). The hit quality index (HQI) and visual correlation, as assessed by the researchers, between the obtained and reference spectra were considered during identification of the assigned polymers. For example, when a shoulder in the 1620–1630 cm^{-1} Raman band region indicated the $\text{H}_2\text{C}=\text{CH}_2$ vibration of a vinyl group (Lin-Vien, 2006) and therefore the presence of DVB, this feature was registered (Fig. S2). Microbeads from *s 1*, *s 3*, *s 6* and *s 9* ($n = 28$, Table S1) were analysed by Raman microspectroscopy using the following parameters: 50 × objective (NA = 0.50, WD = 10.6 mm) and 10 accumulations. All other parameters were applied as described above.

Denoted spherules from *p 3–9*, *s 2*, *s 5*, *s 7* and *s 8* ($n = 71$, Table S1) were analysed using an ATR FT-IR spectrometer (Bruker ALPHA including a platinum Diamond-ATR QuickSnap Sampling Module, Bruker, Billerica, Massachusetts, USA). IR-Spectra were recorded over the wavenumber range of 400–4,000 cm^{-1} at a resolution of 4 cm^{-1} , applying 24 scans. Each spectrum was compared against a reference spectra library using Opus 7.5 software (B-KIMW ATR-IR Polymers, Plastics and Additives, 898 entries; Bruker, Billerica, Massachusetts, USA) and additionally against the BioRad KnowItAll library (KnowItAll IR Identification Pro, Spectral Library, 260,000 entries; BioRad, Hercules, CA, USA). Particles with a polymer hit above 75% were identified according to the reference polymer hit. Spherules from *s 4* and *s 9* (Mani et al., 2015; $n = 8$, Table S1) were analysed using a Varian ATR FT-IR with the BioRad KnowItAll reference database as described in a previous study (Mani et al., 2015; Supporting Information, ATR FT-IR spectroscopy).

Scanning electron micrographs of the surface structure of six environmental category A (3) and B (3) PS-DVB microbeads as well as two virgin ion-exchange resin types ($n = 2$ each) and non-expanded polystyrene (EPS) beads ($n = 2$) were taken using a Hitachi S-4800 high resolution cold emission SEM (Hitachi, Tokyo, Japan, Fig. S4). Microbeads were sputtered beforehand with 3 nm platinum in a Leica EM ACE600 Double Sputter Coater system (Leica, Wetzlar, Germany).

2.4. Quality control and contamination protection

A spike-recovery test was performed ($n = 3$) to assess the efficiency and contamination risk of NaCl density separation. Twenty blue polystyrene (PS) fragments ($\rho \sim 1.05 \text{ g cm}^{-3}$; diameter: 500–1000 μm) were added to $\sim 2 \text{ g}$ (w/w) of concentrated biogenic suspended solids (size fraction 300–1000 μm), mixed in 0.3 L of saturated NaCl solution ($\rho \sim 1.2 \text{ g cm}^{-3}$) and separated in a glass funnel. The mean recovery rate \pm SD was $90 \pm 5\%$. No microplastics other than the spikes were observed after the recovery experiment. The $<100\%$ recovery rate might possibly indicate a slight underestimation of environmental plastics; however, there are other factors, such as a minor leap of the Manta Trawl on the water or a few additional flowmeter-spins due to wind before water contact, which put this imperfection into perspective.

Procedural blanks were run in the laboratory ($n = 3$) for the duration of a sample density separation (90 min). Three glass Petri dishes (diameter 12 cm) were thoroughly rinsed with deionised water and placed without a cover on adjacent lab benches (Bergmann et al., 2017). There was no evidence of microbeads, however, some fibres were recorded in the procedural blanks. To assess the microbead contamination potential during field work, Rhine River samples from Basel (Switzerland, Rh-km 170.4) were inspected for comparison ($n = 3$). These three comparison samples were taken on 01.09.16 using the exact same sampling procedure and equipment (mean vol. 77 m^3). No microbeads were found in the visual investigation of these samples under a stereomicroscope (Olympus SZ61, Tokyo, Japan).

As an additional measure to the hand rinsing in between samples on board during *p 1–9*, the Manta Trawl cod end used for Rhine River surface sampling was hand rinsed in the same manner as between samples during field work and inspected in detail in the laboratory. The cod end was placed upside down inside a clean glass beaker and rinsed with 1 L of laboratory tap water. This procedure was repeated three times, using a fresh beaker each time ($n = 3$). The contents of the receiving glass beaker were filtered onto glass microfiber paper (Rotilabo Typ 112A, pore size 8–12 μm) and visually inspected for microbeads using a stereomicroscope. Had any microbeads from the field samples been retained in the mesh, they would have been expected to show in this examination. No evidence of remaining microbeads was recorded in any of the three inspections.

To prevent laboratory plastic contamination, glassware was used whenever possible. In cases where synthetic polymer items were necessary (e.g. silicone tubing for density separation), the items were rinsed thoroughly with deionised water and ethanol (70%) before first use. Sample containers were sealed with metal, colourless polyethylene (PE) or Parafilm covers at all times

when not in use. White lab coats (100% cotton) were worn at all times and blue nitrile rubber gloves were worn for sample sorting and counting.

3. Results and discussion

3.1. Microbead concentrations and categories

Microplastic spherule (MP-Sph) concentrations from the *pearl* campaign ranged between 0.03 and 9.2 particles m^{-3} . The lowest concentrations of MP-Sph were found in the three most upstream sampling sites, *p 1*, *p 2*, and *p 3* (Rh-km 691, 700, and 705; 0.03, 0.05, and 0.5 MP-Sph m^{-3} , respectively). The highest concentrations were 8.3 MP-Sph m^{-3} at *p 4* and 9.2 MP-Sph m^{-3} at *p 9* (Rh-km 720 and 780.3, respectively). Intermediate concentrations were measured at *p 5*, *p 6*, *p 7*, and *p 8* (Rh-km 737, 755, 766, and 772; 5.8, 4.2, 4.9, and 3.3 MP-Sph m^{-3} , respectively, Fig. 1). Samples *p 1* and *p 2* exclusively contained colourless, translucent microbeads; all other samples contained 85.4–99.9% opaque beads. During the *pearl* campaign, 2,944 MP-Sph were counted and assigned to 25 different categories based on their visual properties (Table S3). The five categories with the largest numbers of spherules accounted for 96% of all microbeads recovered during *pearl*. Category A accounted for 85% of MP-Sph (white/beige, opaque and smooth), followed by categories B (7%, white light-reflecting and reddish translucent light-transmitting), C (2%, colourless, translucent), D (1%, various shades of blue, opaque), and E (1%, orange/brown, opaque). The remaining 4% were assigned to categories F–Y (<1% each). Spherule sizes ranged between 286–954 μm (mean: 497 μm ; $n = 218$). The size range for category A was 338–931 μm (mean: 613 μm ; $n = 93$). Polystyrene microbeads of very similar colour, translucency and polymeric properties to the category A particles (spectral characteristics of Raman or FT-IR analysis) were also detected outside the *pearl* campaign between Rh-km 677 and 944 in *s 1–4* and *9* (Mani et al., 2015) and *s 5–8* (Table S1; Figs. S1 and S5). When comparing the samples from Leverkusen in 2014 (*s 2*, Rh-km 698) and 2016 (*p 2*, Rh-km 700) with the samples from Duisburg in 2014 and 2016 (*s 3*, Rh-km 779.3 and *p 9*, Rh-km 780.3, respectively), the microbead concentrations increased downstream by factors of 373 and 184, respectively (Table 1). Due to the most probably patchy (as opposed to homogeneous) distribution of microbeads across the river width and in the vertical water column as well as the relatively low sample numbers, we refrain from spatially or temporally extrapolating bead concentrations and total freights based on the current data.

Table 1

Comparison of microbead concentrations in surface water samples collected two years apart at Rhine kilometres 698/700 and 779.3/780.3 in 2014 and 2016 (MP m⁻³).

Rh-km	Microbeads m ⁻³ *	Sample
698.0	0.03	<i>s</i> 2; 14.07.2014 (Mani et al., 2015)
700.0	0.05	<i>p</i> 2; 29.11.2016
779.3	11.20	<i>s</i> 3; 15.07.2014 (Mani et al., 2015)
780.3	9.20	<i>p</i> 9; 29.11.2016

* Values represent single samples collected in the centre of the river cross section.

3.2. Narrowing down the microbead influx area

In the 89.3 km *pearl* campaign, we observed a 166-fold increase in microbead concentrations within a specific stretch of just 20 km (all microbead categories, Rh-km 700–720). This was the most striking concentration rise observed in this campaign, indicating a potential microbead influx. There are several possibilities of how and where these microbeads enter the Rhine River. Considering that the particles at hand are allegedly primary microplastics with a largely uniform appearance and possibly a specific origin, their environmental occurrence could be due to one or more point sources, such as waste water treatment plants (WWTP; Mintenig et al., 2017; Murphy et al., 2016) or direct industrial discharge (DID) outlets (Karlsson et al., 2018; Lechner and Ramler, 2015). Furthermore, locally restricted industrial run-off may be responsible for this phenomenon (Karlsson et al., 2018), or even more diffuse sources could be suspected such as loss during transport on water or land and subsequent road run-off (Duis and Coors, 2016). The river section investigated in the *pearl* campaign lies within one of Europe's most highly industrialised regions. The riparian German state of North Rhine-Westphalia (NRW) is home to around 1,000 companies in the plastic industry alone, employing circa 140,000 people (NRW Invest, 2016). Along the investigated river stretch of 20 km, three communal WWTP as well as eleven DID outlets from the chemical and food sector release effluent into the river between Rh-km 704.05–715.12 and 700.3–711.3, respectively (Elwas, 2018). Two of the WWTP directly discharging into the Rhine River (at Rh-km 704.05 and 711.86) also treat and release industrial wastewater, at rates of approximately 25% of their 6.2 and 4.7 million m³ a⁻¹, respectively, (Elwas, 2018), data from 2015). Presuming that the microbeads emerge from one or more of the fourteen potential WWTP or DID point sources, we could narrow down the major influx area to a 14.82 km river-stretch around the Dormagen area (DE).

The highest concentration of microbeads in the *pearl* campaign was detected at the most downstream site *p* 9 (9.2 MP-Sph m⁻³), which is located at the confluence of the Rhine and

Ruhr rivers at Duisburg (Rh-km 780.3). The relatively large amount of microbeads in this sample may be explained by (i) the substantial numbers of DID emitting into the Rhine upstream of *p 9* (32 DID between *p 7–9*, Table S2), or (ii) local hydrodynamic anomalies, potentially affected by the confluence and resulting lower water velocity compared to upstream sites ($v_{w p 9} = 0.7 \text{ m s}^{-1}$; $v_{w p 1-8} = 1.4 \text{ m s}^{-1}$). Hydrodynamic anomalies could result in patchily distributed suspended solid aggregation patterns on the water surface (Fujita et al., 1998; Park et al., 2017), and thus influence the amount of microbeads actually captured in the sampling net.

It is unlikely that the high surface water microbead concentrations at *p 9* can be explained by contributions from the Ruhr River (eight DID emitting within 23 km upstream of the confluence). Firstly, two spot samples collected from the Ruhr within 4 km upstream of the Rhine confluence (size range: $>5\text{--}0.02 \text{ mm}$) yielded only $0.7 \text{ microbeads m}^{-3}$ on average, with PS found in only one of the two samples at a concentration of $3.27 \text{ PS particles m}^{-3}$ (Hess et al., 2018). That report, however, did not specify if the PS particles occurred as microbeads. Secondly, during the *pearl* campaign (29.11.2016), the Ruhr was discharging 53% below its MQ_{2016} at $26.3 \text{ m}^3 \text{ s}^{-1}$ (measured 56 km upstream of the Rhine River confluence; BfG, 2017b), while $Q_{\text{km}780.8}$ of the Rhine River was $1590 \text{ m}^3 \text{ s}^{-1}$ (32% below its MQ_{2016} ; BfG, 2017c). Thus, the contribution of Ruhr water to the Rhine on the day of sampling was minimal. The water in the Ruhr is even likely to have backlogged before entering the Rhine. We therefore conclude that the Ruhr River could only have minorly contributed to the relatively high microbead abundance in sample *p 9*.

We acknowledge that the absence of sample replicates during the *pearl* campaign does not enable statistical confirmation of the potential microbead influx area. However, we were able to unambiguously and repeatedly detect this specific type of MP downstream of Rh-km 677, as well as the distinct increase in the microbead concentration within this geographically confined river stretch, in 18 samples taken on 10 different days between 2014 and 2017 (Fig. 1, Fig. S1, Table S1 and S2). Specific investigations of DID and WWTP effluents as well as high-risk runoff areas could help pinpoint the precise source(s) of these environmental microbeads.

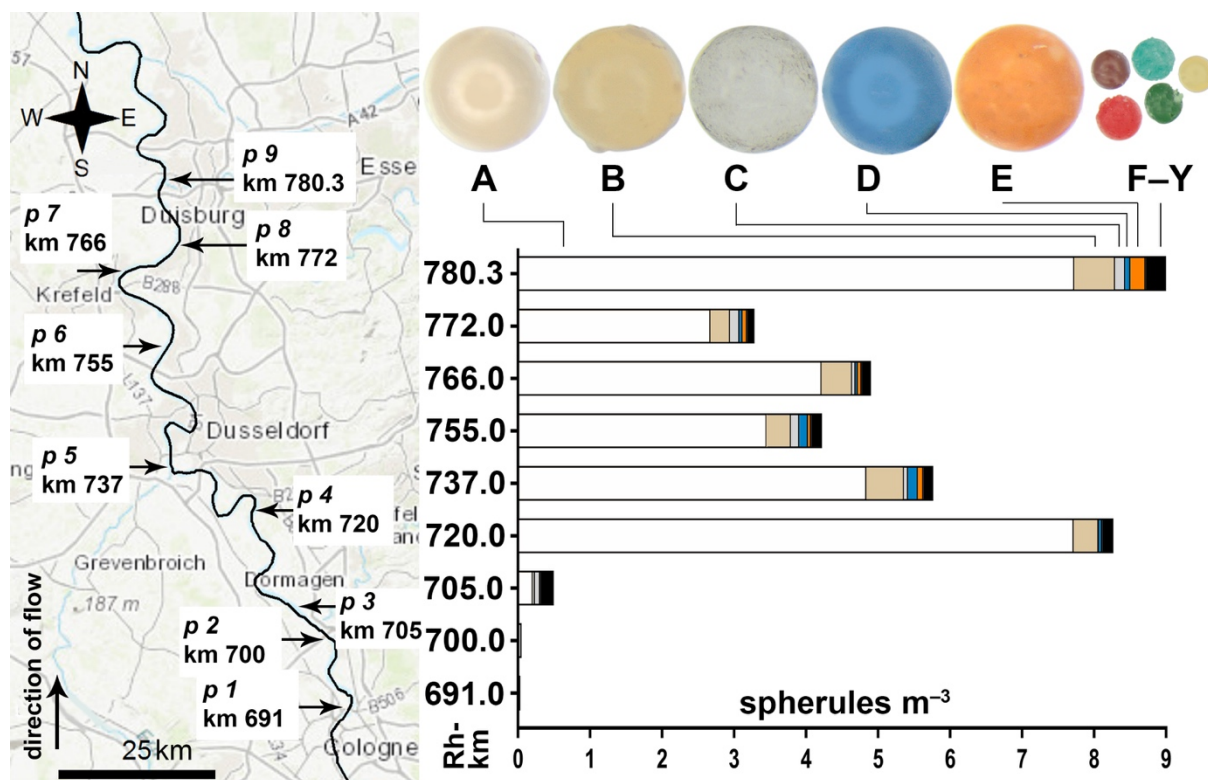


Fig. 1. Concentrations of plastic microbeads along the Cologne–Duisburg stretch of the Rhine River (Germany, Rh-km 691–780.3) in the *pearl* campaign. Sampling was carried out on 29.11.2016. Based on 218 microbeads (7.4% of the total 2,944) from all 25 categories (A–Y), average microbead diameter was 497 μm . Bead photos indicate colour and translucency, the bead sizes are not to scale. The map was obtained from Arc Map 10.3.

3.3. Polymer composition

Out of the 153 spherules analysed from the *pearl* campaign, 103 were identified as polystyrene-divinylbenzene (PS-DVB, Raman micro-spectroscopy, $n = 86$, hit quality index HQI: $97.8 \pm 1.2\%$; FT-IR spectroscopy, $n = 17$, HQI: $89.5 \pm 2.4\%$) and 42 as polystyrene (PS, Raman spectroscopy, $n = 9$, HQI: $88.6 \pm 8.4\%$; FT-IR, $n = 33$, HQI: $94.5 \pm 4.3\%$; Supporting Information Table S1). Three were polymethyl methacrylate (PMMA, Raman [$n = 2$], HQI: $98.2 \pm 1\%$; FT-IR [$n = 1$], HQI: 97.56%) and five were not identifiable, Raman ($n = 1$), FT-IR ($n = 4$). From *s 1–9*, out of the 59 beads analysed from these nine complementary campaigns during 2014 (Mani et al., 2015), 2016 and 2017, 43 beads were PS-DVB (Raman, $n = 28$, HQI: $96 \pm 1.7\%$; FT-IR, $n = 15$, HQI: $92.9 \pm 2.6\%$ [HQI only available for 2016 and 2017, $n = 10$]) and 14 were PS (FT-IR, HQI: $94.6 \pm 3.8\%$ [HQI only available for 2016 and 2017, $n = 11$]). Two further beads were polyethylene (PE, FT-IR, HQI: 97.1%) and polypropylene (PP, FT-IR, HQI: 96.9%), respectively (See Tables S1 and S3 for locations of PS-DVB and PS and respective bead categories).

Category conformity for the PS-DVB *pearl* beads was A ($n = 57$), B ($n = 19$), C ($n = 4$), D ($n = 15$), and E ($n = 8$); and A ($n = 15$), B ($n = 8$), C ($n = 10$), D ($n = 6$), and E ($n = 3$) for the PS-beads. All analysed *pearl* microbeads ($n = 153$ or 5.2% of all 2,944 retrieved beads) were taken from the five most abundant categories, to which ninety-six percent of all the beads found in the *pearl* campaign could visually be assigned: A ($n = 72$), B ($n = 27$), C ($n = 16$), D ($n = 22$), and E ($n = 16$; see Table S1 for the geographical occurrence of the analysed beads and Table S3 for detailed category descriptions and general geographical occurrences).

PS-DVB or PS was identified as the polymeric structure for 95.3% of the analysed beads from samples *p* 3–9 ($n = 153$) and *s* 1–9 ($n = 59$). As polymer spectra may alter due to weathering (Andrady et al., 1993; Feldman, 2002), it is possible that environmentally degraded PS-DVB beads could feature general PS characteristics but no longer exhibit a specific PS-DVB spectrum, due to degradation and a generally low degree of DVB cross-links (1–12%; Shim et al., 2004; Weaton & Lefevre, 2000). Also, differences may occur between the Raman and FT-IR results for a single particle (Käppler et al., 2016), potentially leading to PS as the top hit in one spectrum and PS-DVB in the other, and vice versa. The distinction between PS-DVB and pure PS is based on a small Raman peak at 1620–1630 cm^{-1} , indicating $\text{H}_2\text{C}=\text{CH}_2$ vibration of a vinyl group (Lin-Vien, 2006). Automatic correlation of spectra with database references is based on a pattern matching algorithm (width and position of broad peaks; Primpke et al., 2017; Primpke et al., 2018). Due to the marginal differences between PS-DVB and PS, it is therefore additionally necessary to rely on expert interpretation, which is only practicable if dealing with a reasonable number of spectra (Primpke et al., 2017).

3.3.1. Likely identification of microbeads as PS-DVB ion-exchange resins

Raman micro- and FT-IR spectroscopy, primarily yielding PS-DVB and PS (95.3%, $n = 212$), combined with the visual properties of the majority of beads (opaque, coloured, predominantly white–beige, 286–954 μm in diameter) and product data for comparison (Lenntech, 2018; Weaton & Lefevre, 2000) revealed that most of the retrieved spherical particles are possibly styrene-based macroporous ion-exchange resin (IER) beads (Tsyurupa and Davankov, 2006). For example, some Raman spectra of riverine category A microbeads exhibited very high correlations with virgin Purolite PS-DVB IER (HQI: >98%, Fig. S2). Furthermore, high-resolution Raman spectroscopy successfully performed on three environmental microbeads from category B ($n = 2$, *p* 3 and *p* 4, respectively) and category E ($n = 1$, *p* 3) revealed HQI >96% matching a PS-DVB and Dimethyl Sulfoxide IER product (AK-P-377, University of Marburg, Fig. S2). This finding could be an indication of an environmental PS-DVB IER with sulfonic functional groups. However, other beads from the same visual categories did not

reach equivalent HQIs, albeit yielding a styrenic polymer. Acknowledging that it is challenging to even distinguish virgin PS and PS-DVB materials, such high hits as described above may indicate an environmental IER finding but the result cannot be transferred to all other, not chemically successfully analysed, findings by default (Fig. S3). An examination of the product portfolios of three leading IER producers, Dow, Lanxess, and Purolite (Lenntech, 2018), 76–284 IER products each), revealed that 78–85% of their IER are crosslinked PS-DVB, of which 45% are macroporous and 55% are gel-type (Lenntech, 2018). Gel-type PS-DVB IER are translucent and microporous (pore diameters 10–20 Å), while macroporous PS-DVB IER are opaque (pore diameters 10–1000 Å; De Dardel, 2015; Lin et al., 2006).

To investigate the microbead surface pore structure of category A and B beads, scanning electron microscopy (SEM) was performed ($n = 3$ each) and the results were compared to two macroporous virgin Lewatit PS-DVB IER products ($n = 2$ each) as well as non-expanded polystyrene (EPS) beads used for producing materials like Styrofoam™ ($n = 2$, Fig. S4). SEM micrographs of category A and B microbeads from sample *p 5* ($n = 6$) revealed a distinct macroporous surface structure (pore diameters of 390–1430 Å) with high similarity to the reference virgin IERs (Fig. S4). The surface structure of the non-expanded, white, semi-transparent polystyrene beads (EPS, diameter 300–1000 µm) revealed a distinctly different, non-porous surface structure (Fig. S4). The EPS beads were included in the investigation due to their approximately similar size (300–1000 µm), shape and polystyrene backbone (matching spectra, Fig. S3). These features generally rendered them potential candidates for the repeatedly identified microbeads in the Rhine River. However, their lack of colouring, high translucency, distinct rigidity and smooth surface structure (SEM) clearly distinguished the EPS beads from the bead types abundantly found in the Rhine River. Also, after 72 h in water, the EPS beads did not gain additional visual, tactile or spectral similarity to the environmental beads investigated here.

In 1972, environmental polystyrene spherules with alleged possible “limited usage as absorbents for industrial water purification” were reported in the coastal waters of southern New England (average diameter: 0.5 mm; Carpenter et al., 1972). Recently, opaque plastic microbeads were found in the surface waters of the Lower Rhine River at average concentrations of 0.35 m^{-3} ($n = 5$, 20–5000 µm; Hess et al., 2018), 4.33 m^{-3} ; $n = 14$, 300–5000 µm, (Mani et al., 2015) and 9.72 m^{-3} ($n = 18$, 125–5000 µm; Urgert, 2015) as well as shoreline sediments of the Upper Rhine at 96.83 kg^{-1} ($n = 8$, only 200–5000 µm considered here; Klein et al., 2015). Microbeads in those studies were speculated to originate from care

products or cleaning products (Hess et al., 2018; Klein et al., 2015), air-blasting or industrial waste (Mani et al., 2015) or pre-expanded polystyrene beads (EPS; Urgert, 2015). The reported suspended Rhine microbead concentrations vary within a range of 0.35 and 9.72 particles m^{-3} likely due to their patchy distribution in the water and different times of sampling. Microbeads have also been found in other freshwater environments (Eriksen et al., 2013; Lechner et al., 2014; McCormick et al., 2014). This study is the first to attempt to geographically narrow down the environmental entry area of such beads, and to suspect that the vast majority of PS spherules found in an industrial, heavily used stretch of a large European river are likely polystyrene-divinylbenzene (PS-DVB) ion-exchange resin (IER) beads. This claim is based on (i) their chemical properties according to vibrational spectroscopy (Lenntech, 2018; Lin-Vien, 2006; Weaton & Lefevre, 2000); (ii) comparisons with manufacturers' descriptions (Lenntech, 2018); and (iii) the beads' near-to-perfect sphericity, (iv) colour, (v) size range (286–954 μm) and (vi) surface structure.

PS-DVB is produced by copolymerisation of styrene and divinylbenzene (DVB; Huck and Bonn, 2005; Miller et al., 2009). PS-DVB crosslinked IER beads typically contain 1–12% DVB (Weaton & Lefevre, 2000), are typically 0.1–1.2 mm in diameter and exhibit a specific gravity of 1.0–1.3 g cm^{-3} in their water-swollen state. PS-DVB IER may swell by between 4 and 30% upon contact with water (our unpublished experimental data; Lenntech, 2018). In this study, we measured the diameter of dry particles. Thus, these measurements could differ for particles in the water-swollen state (Miller et al., 2009); this discrepancy may have implications when comparing the findings of different studies and when consulting and comparing manufacturers' descriptions. Alterations in diameter and specific density could also influence recovery rates from surface samples, as the position and size of the particles in the water column could differ depending on a bead's swelling state.

Ion-exchangers are typically cross-linked synthetic resin spherules based on styrene or acryl, featuring evenly distributed special functional groups with mobile ions. These ions can be exchanged with other ions from a surrounding solution, e.g. for replacing calcium with sodium to soften water and prevent limescale accumulating in boiler tanks (Rohde and Wloka, 2011; Weaton & Lefevre, 2000). IER beads are widely applied in analytical laboratories, medicine, the food industry, horticulture and (waste-) water treatment (Inamuddin and Luqman, 2012). As IER beads are also employed to sequester heavy metals and other hazardous substances, they may potentially function as vectors for toxins, which could be released into organisms upon ingestion (Mato et al., 2001).

3.4. Fate of microbeads in the Rhine River

The microbeads described in this study may either be carried downstream to the North Sea (Besseling et al., 2017), ingested by organisms (Sanchez et al., 2014) or retained within shoreline (Klein et al., 2015), riverbed (Castañeda et al., 2014) or estuary (Nizzetto et al., 2016) sediments. The previously observed decrease in microbead concentrations in the surface waters of the Rhine River downstream of km 837 possibly indicates sedimentation of these particles as they reach the slower-flowing estuary water (Mani et al., 2015).

Conveniently, the round microbeads captured in the present study can be efficiently identified and quantified due to their distinct visual and chemical properties (according to vibrational spectroscopy). Thus, further studies on the distribution of these Rhine River microbeads could serve to validate riverine dispersion, sedimentation and retention models in rivers (Besseling et al., 2017; Nizzetto et al., 2016).

3.5. Current regulation on particulate matter emissions and future tasks

The emission of particulate matter into rivers and lakes is currently not sufficiently regulated by the law. For example, iron and steel manufacturing sites in Germany may legally emit 30 mg L^{-1} of filterable solids – including microplastics – without further qualitative specification (BMJV, 2016). Arguing in favour of an intact ecosphere, it is crucial to identify the actual point sources of these primary particles, so that their emission can be stopped as quickly as possible to prevent tons of avoidable MP contamination continuing to enter the Rhine and its connected ecosystems. The production, transport, application and disposal of manufactured primary microplastic products need to be performed within perfectly sealed-off systems. Once released, it is not realistic to retrieve innumerable small particles from the environment (1 kg of $497 \text{ }\mu\text{m}$ -diameter IER would contain ~ 15 million beads).

4. Conclusions

Identifying the sources and entry pathways of (primary) MP is an important step in the enforcement of pollution prevention, as opposed to more expensive (and not practicable) remedial end-of-pipe solutions. For this purpose, the sources of MP in the Rhine River and other waterbodies worldwide need to be identified.

This is the first report of microbeads, possibly polystyrene-divinylbenzene (PS-DVB) ion-exchange resins (IER), substantially contributing to the MP load of a major river. This specific type of primary MP has not previously been identified in the aquatic environment. IER may possibly contribute to the plastic load in other aquatic and also terrestrial compartments than the Rhine River catchment. As identification of the sources of MP in the environment remains

very difficult, we conducted a longitudinal spot sampling approach, which confirmed and spatially refined the entry area for a specific variety of MP to a maximum of 20 km. Further research is needed to examine the respective spillage risk for microbeads as a function of their specific application. Furthermore, toxicological assessments could shed light on the potential environmental risk of such applications upon leakage.

Acknowledgements

The authors gratefully acknowledge the officers and crew of the German Waterway and Shipping Administration (WSA) vessel *VSS Köln* as well as the head of the WSA Cologne branch office Mr. Rolf Nagelschmidt for their generous support in sampling. We would like to express great gratitude to WSA Duisburg-Rhein in Emmerich (Germany) for their valuable navigation for sampling at Rh-km 837. Furthermore, we would like to thank Sandrine Straub M.Sc. and lab technicians Nicole Seiler-Kurth and Heidi Schiffer from the Man-Society-Environment Programme, Department of Environmental Sciences, University of Basel for processing, quantifying and documenting the samples for this study and conducting the quality control proceedings. We would like to forward our special thanks to Evi Bieler from the Nano Imaging Lab at the University of Basel for her great work in SEM imaging. We would further like to give our thanks to the reviewers for critically evaluating our initial manuscript and providing input that substantially enhanced the quality of this work. Our gratitude also goes out to Sylvie Mittelheisser and Michael Pfeffer from the Department of Chemistry of the University of Basel for offering their valuable advice on various questions of analytics. Very special thanks go to Andrea Devlin, PhD, chief editor of Science Editing Experts, for her immaculate proof reading and language support. This study was partially funded by the World Wide Fund for Nature (WWF) Switzerland.

Author contributions

T.M., P.B. and P.B.-H. designed the research; T.M. and P.B. performed the field work. T.M. and P.B.-H. supervised the laboratory processing of samples and quality control, T.M. performed ATR FT-IR spectroscopy; F.R.S., M.P. and T.W. performed Raman microspectroscopy. T.M. and P.B.-H. wrote the manuscript.

References

- Andrady, A.L., 2011. Microplastics in the marine environment. *Mar. Pollut. Bull.* 62 (8), 1596–1605. doi:10.1016/j.marpolbul.2011.05.030.
- Andrady, A.L., Pegram, J.E., Tropsha, Y., 1993. Changes in carbonyl index and average molecular weight on embrittlement of enhanced-photodegradable polyethylenes. *J. Environ. Polym. Degr.* 1 (3), 171–179. doi:10.1007/BF01458025.
- Araujo, C.F., Nolasco, M.M., Ribeiro, A.M.P., Ribeiro-Claro, P.J.A., 2018. Identification of microplastics using Raman spectroscopy: Latest developments and future prospects. *Water Res.* 142, 426–440. doi:10.1016/j.watres.2018.05.060.
- Barcelo, D., Rocha-Santos, T.A.P., Duarte, A.C. (Eds.), 2017. Characterization of microplastics by Raman spectroscopy. *Comprehensive Analytical Chemistry* 75, 33 pp.
- Bergmann, M., Wirzberger, V., Krumpfen, T., Lorenz, C., Primpke, S., Tekman, M.B., Gerdt, G., 2017. High quantities of microplastic in Arctic deep-sea sediments from the HAUSGARTEN observatory. *Environ. Sci. Technol.* 51 (19), 11000–11010. doi:10.1021/acs.est.7b03331.
- Besseling, E., Foekema, E.M., van Franeker, J.A., Leopold, M.F., Kühn, S., Bravo Rebolledo, E.L., Heße, E., Mielke, L., IJzer, J., Kamminga, P., Koelmans, A.A., 2015. Microplastic in a macro filter feeder: Humpback whale *Megaptera novaeangliae*. *Mar. Pollut. Bull.* 95 (1), 248–252. doi:10.1016/j.marpolbul.2015.04.007.
- Besseling, E., Quik, J.T.K., Sun, M., Koelmans, A.A., 2017. Fate of nano- and microplastic in freshwater systems: A modelling study. *Environ. Pollut.* 220 (Pt A), 540–548. doi:10.1016/j.envpol.2016.10.001.
- BfG, 2017a. Pegel Rhein Rees. http://undine.bafg.de/rhein/pegel/rhein_pegel_rees.html. Accessed 10 January 2018.
- BfG, 2017b. Pegel Rhein Ruhr Hattingen. http://undine.bafg.de/rhein/pegel/rhein_pegel_hattingen.html. Accessed 5 January 2018.
- BfG, 2017c. Pegel Rhein Ruhrort Duisburg. http://undine.bafg.de/rhein/pegel/rhein_pegel_ruhrort.html. Accessed 5 January 2018.
- BMJV, 2016. Deutsches Bundesministerium für Justiz und Verbraucherschutz. Verordnung über die Anforderungen an das Einleiten von Abwasser in Gewässer, Annex 29: Eisen-

und Stahlerzeugung. BMJV. http://www.gesetze-im-internet.de/abwv/anhang_29.html. Accessed 15 January 2018.

- Carpenter, E.J., Anderson, S.J., Harvey, G.R., Miklas, H.P., Peck, B.B., 1972. Polystyrene spherules in coastal waters. *Science* 178 (4062), 749–750. doi:10.1126/science.178.4062.749.
- Castañeda, R.A., Avlijas, S., Simard, M.A., Ricciardi, A., Smith, R., 2014. Microplastic pollution in St. Lawrence River sediments. *Can. J. Fish. Aquat. Sci.* 71 (12), 1767–1771. doi:10.1139/cjfas-2014-0281.
- Cole, M., Lindeque, P., Halsband, C., Galloway, T.S., 2011. Microplastics as contaminants in the marine environment: A review. *Mar. Pollut. Bull.* 62 (12), 2588–2597. doi:10.1016/j.marpolbul.2011.09.025.
- Currie, R.I., Foxton, P., 1957. A new quantitative plankton net. *J. Mar. Biol. Ass.* 36 (01), 17. doi:10.1017/S0025315400017033.
- De Dardel, F., 2015. Ion exchange resin structure. http://dardel.info/IX/resin_structure.html#gel_macro. Accessed 3 October 2018.
- Duis, K., Coors, A., 2016. Microplastics in the aquatic and terrestrial environment: Sources (with a specific focus on personal care products), fate and effects. *Environ. Sci. Eur.* 28 (1), 2. doi:10.1186/s12302-015-0069-y.
- Eerkes-Medrano, D., Thompson, R.C., Aldridge, D.C., 2015. Microplastics in freshwater systems: A review of the emerging threats, identification of knowledge gaps and prioritisation of research needs. *Water Res.* 75, 63–82. doi:10.1016/j.watres.2015.02.012.
- Elwas, 2018. ELWAS KARTE NRW. <http://www.elwasweb.nrw.de/elwas-web/index.jsf#>. Accessed 10 January 2018.
- Eriksen, M., Mason, S., Wilson, S., Box, C., Zellers, A., Edwards, W., Farley, H., Amato, S., 2013. Microplastic pollution in the surface waters of the Laurentian Great Lakes. *Mar. Pollut. Bull.* 77 (1-2), 177–182. doi:10.1016/j.marpolbul.2013.10.007.
- Faure, F., Corbaz, M., Baecher, H., Alencastro, L.F. de, 2012. Pollution due to plastics and microplastics in Lake Geneva and in the Mediterranean Sea. *Arch. Sci.* 65 (157–164).
- Faure, F., Demars, C., Wieser, O., Kunz, M., Alencastro, L.F. de, 2015. Plastic pollution in Swiss surface waters: Nature and concentrations, interaction with pollutants. *Environ. Chem.* 12 (5), 582. doi:10.1071/EN14218.

- Feldman, D., 2002. Polymer weathering: Photo-oxidation. *J. Polym. Environ.* 10 (4), 163–173. doi:10.1023/A:1021148205366.
- Fujita, I., Muste, M., Kruger, A., 1998. Large-scale particle image velocimetry for flow analysis in hydraulic engineering applications. *J. Hydraul. Res.* 36 (3), 397–414. doi:10.1080/00221689809498626.
- Hess, M., Diel, P., Mayer, J., Rahm, H., Reifenhäuser, W., Stark, J., Schwaiger, J., 2018. Mikroplastik in Binnengewässern Süd- und Westdeutschlands: Bundesländerübergreifende Untersuchungen in Baden-Württemberg, Bayern, Hessen, Nordrhein-Westfalen und Rheinland-Pfalz, Karlsruhe, Augsburg, Wiesbaden, Recklinghausen, Mainz, 86 pp.
https://www.lanuv.nrw.de/fileadmin/lanuvpubl/6_sonderreihen/L%C3%A4nderbericht_Mikroplastik_in_Binnengew%C3%A4ssern.pdf. Accessed 25 May 2018.
- Huck, C.W., Bonn, G.K., 2005. Poly(styrene-divinylbenzene) based media for liquid chromatography. *Chem. Eng. Technol.* 28 (12), 1457–1472. doi:10.1002/ceat.200500265.
- Huerta Lwanga, E., Gertsen, H., Gooren, H., Peters, P., Salánki, T., van der Ploeg, M., Besseling, E., Koelmans, A.A., Geissen, V., 2016. Microplastics in the terrestrial ecosystem: Implications for *Lumbricus terrestris* (Oligochaeta, Lumbricidae). *Environ. Sci. Technol.* 50 (5), 2685–2691. doi:10.1021/acs.est.5b05478.
- Inamuddin, D., Luqman, M. (Eds.), 2012. *Ion Exchange Technology II: Applications*. Springer. 434 pp.
- Ivleva, N.P., Wiesheu, A.C., Niessner, R., 2017. Microplastic in aquatic ecosystems. *Angew. Chem. Int. Edit.* 56 (7), 1720–1739. doi:10.1002/anie.201606957.
- Jahnke, A., Arp, H.P.H., Escher, B.I., Gewert, B., Gorokhova, E., Kühnel, D., Ogonowski, M., Potthoff, A., Rummel, C., Schmitt-Jansen, M., Toorman, E., MacLeod, M., 2017. Reducing uncertainty and confronting ignorance about the possible impacts of weathering plastic in the marine environment. *Environ. Sci. Technol. Lett.* 4 (3), 85–90. doi:10.1021/acs.estlett.7b00008.
- Jambeck, J.R., Geyer, R., Wilcox, C., Siegler, T.R., Perryman, M., Andrady, A., Narayan, R., Law, K.L., 2015. Plastic waste inputs from land into the ocean. *Science* 347 (6223), 768–771. doi:10.1126/science.1260352.
- Käppler, A., Fischer, D., Oberbeckmann, S., Schernewski, G., Labrenz, M., Eichhorn, K.-J., Voit, B., 2016. Analysis of environmental microplastics by vibrational microspectroscopy:

- FTIR, Raman or both? *Anal. Bioanal. Chem.* 408 (29), 8377–8391. doi:10.1007/s00216-016-9956-3.
- Karlsson, T.M., Arneborg, L., Broström, G., Almroth, B.C., Gipperth, L., Hassellöv, M., 2018. The unaccountability case of plastic pellet pollution. *Mar. Pollut. Bull.* 129 (1), 52–60. doi:10.1016/j.marpolbul.2018.01.041.
- Klein, S., Worch, E., Knepper, T.P., 2015. Occurrence and spatial distribution of microplastics in river shore sediments of the Rhine-Main area in Germany. *Environ. Sci. Technol.* 49 (10), 6070–6076. doi:10.1021/acs.est.5b00492.
- Lebreton, L.C.M., van der Zwet, J., Damsteeg, J.-W., Slat, B., Andrady, A., Reisser, J., 2017. River plastic emissions to the world's oceans. *Nat. Commun.* 8, 15611. doi:10.1038/ncomms15611.
- Lechner, A., Keckeis, H., Lumesberger-Loisl, F., Zens, B., Krusch, R., Tritthart, M., Glas, M., Schludermann, E., 2014. The Danube so colourful: A potpourri of plastic litter outnumbers fish larvae in Europe's second largest river. *Environ. Pollut.* 188, 177–181. doi:10.1016/j.envpol.2014.02.006.
- Lechner, A., Ramler, D., 2015. The discharge of certain amounts of industrial microplastic from a production plant into the River Danube is permitted by the Austrian legislation. *Environ. Pollut.* 200, 159–160. doi:10.1016/j.envpol.2015.02.019.
- Lenntech, 2018. Ion exchange resins. <https://www.lenntech.com/products/resins/ixresins.htm>. Accessed 02 March 2020.
- Lin, Z.H., Guan, C.J., Feng, X.L., Zhao, C.X., 2006. Synthesis of macroreticular p-(ω -sulfonic-perfluoroalkylated) polystyrene ion-exchange resin and its application as solid acid catalyst. *J. Mol. Catal A-Chem.* 247 (1-2), 19–26. doi:10.1016/j.molcata.2005.11.008.
- Lin-Vien, D. (Ed.), 2006. *The Handbook of infrared and raman characteristic frequencies of organic molecules*, [Repr.] ed. Academic Press, San Diego, 503 pp.
- Mani, T., Hauk, A., Walter, U., Burkhardt-Holm, P., 2015. Microplastics profile along the Rhine River. *Sci. Rep.* 5, 17988. doi:10.1038/srep17988.
- Mato, Y., Isobe, T., Takada, H., Kanehiro, H., Ohtake, C., Kaminuma, T., 2001. Plastic resin pellets as a transport medium for toxic chemicals in the marine environment. *Environ. Sci. Technol.* 35 (2), 318–324. doi:10.1021/es0010498.

- McCormick, A., Hoellein, T.J., Mason, S.A., Schluep, J., Kelly, J.J., 2014. Microplastic is an abundant and distinct microbial habitat in an urban river. *Environ. Sci. Technol.* 48 (20), 11863–11871. doi:10.1021/es503610r.
- Miller, W.S., Castagna, C.J., Pieper, A.W., 2009. Understanding ion-exchange resins for water treatment systems. *Water Technologies & Solutions*, 13 pp.
<https://www.nguyenthanhmy.com/courses/Ion-Exchange-Polymers-01.pdf>. Accessed 02. March 2020.
- Mintenig, S.M., Int-Veen, I., Löder, M.G.J., Primpke, S., Gerdtts, G., 2017. Identification of microplastic in effluents of waste water treatment plants using focal plane array-based micro-Fourier-transform infrared imaging. *Water Res.* 108, 365–372.
doi:10.1016/j.watres.2016.11.015.
- Murphy, F., Ewins, C., Carbonnier, F., Quinn, B., 2016. Wastewater treatment works (wwtw) as a source of microplastics in the aquatic environment. *Environ. Sci. Technol.* 50 (11), 5800–5808. doi:10.1021/acs.est.5b05416.
- Nizzetto, L., Bussi, G., Futter, M.N., Butterfield, D., Whitehead, P.G., 2016. A theoretical assessment of microplastic transport in river catchments and their retention by soils and river sediments. *Environ. Sci. Proc. Imp.* 18 (8), 1050–1059. doi:10.1039/c6em00206d.
- NRW Invest, 2016. NI-Standortbroschuere, 28 pp.
<https://www.nrwinvest.com/fileadmin/Redaktion/branchen-in-nrw/NI-Standortbroschuere-DE-2016.pdf>. Accessed 13 September 2018.
- Park, I., Seo, I.W., Kim, Y.D., Han, E.J., 2017. Turbulent mixing of floating pollutants at the surface of the river. *J. Hydraul. Eng.* 143 (8), 4017019. doi:10.1061/(ASCE)HY.1943-7900.0001319.
- PlasticsEurope, 2017. Plastic – the Facts 2017, 44 pp.
https://www.plasticseurope.org/application/files/5715/1717/4180/Plastics_the_facts_2017_FINAL_for_website_one_page.pdf. Accessed 23 August 2018.
- Primpke, S., Lorenz, C., Rascher-Friesenhausen, R., Gerdtts, G., 2017. An automated approach for microplastics analysis using focal plane array (FPA) FTIR microscopy and image analysis. *Anal. Methods* 9 (9), 1499–1511. doi:10.1039/C6AY02476A.
- Primpke, S., Wirth, M., Lorenz, C., Gerdtts, G., 2018. Reference database design for the automated analysis of microplastic samples based on Fourier transform infrared (FTIR)

- spectroscopy. *Anal. Bioanal. Chem.* 410 (21), 5131–5141. doi:10.1007/s00216-018-1156-x.
- Rillig, M.C., 2012. Microplastic in terrestrial ecosystems and the soil? *Environ. Sci. Technol.* 46 (12), 6453–6454. doi:10.1021/es302011r.
- Rohde, W., Wloka, V., 2011. Ion exchanger moulded body and method for producing same PCT/EP09/64350. 2009. USA, 9 pp. <https://patents.google.com/patent/EP2352635A2/en>. Accessed 09 March 2020.
- Sanchez, W., Bender, C., Porcher, J.-M., 2014. Wild gudgeons (*Gobio gobio*) from French rivers are contaminated by microplastics: Preliminary study and first evidence. *Environ. Res.* 128, 98–100. doi:10.1016/j.envres.2013.11.004.
- Schmidt, C., Krauth, T., Wagner, S., 2017. Export of plastic debris by rivers into the sea. *Environ. Sci. Technol.* 51 (21), 12246–12253. doi:10.1021/acs.est.7b02368.
- Sedlak, D., 2017. Three lessons for the microplastics voyage. *Environ. Sci. Technol.* 51 (14), 7747–7748. doi:10.1021/acs.est.7b03340.
- Shim, S.E., Yang, S., Choi, H.H., Choe, S., 2004. Fully crosslinked poly(styrene-co-divinylbenzene) microspheres by precipitation polymerization and their superior thermal properties. *J. Polym. Sci. A Polym. Chem.* 42 (4), 835–845. doi:10.1002/pola.11028.
- Silva, A.B., Bastos, A.S., Justino, C.I.L., da Costa, J.P., Duarte, A.C., Rocha-Santos, T.A.P., 2018. Microplastics in the environment: Challenges in analytical chemistry – A review. *Anal. Chim. Acta.* 1017, 1–19. doi:10.1016/j.aca.2018.02.043.
- Steer, M., Cole, M., Thompson, R.C., Lindeque, P.K., 2017. Microplastic ingestion in fish larvae in the western English Channel. *Environ. Pollut.* 226, 250–259. doi:10.1016/j.envpol.2017.03.062.
- Ter Halle, A., Ladirat, L., Gendre, X., Goudouneche, D., Pusineri, C., Routaboul, C., Tenailleau, C., Duployer, B., Perez, E., 2016. Understanding the fragmentation pattern of marine plastic debris. *Environ. Sci. Technol.* 50 (11), 5668–5675. doi:10.1021/acs.est.6b00594.
- Terepocki, A.K., Brush, A.T., Kleine, L.U., Shugart, G.W., Hodum, P., 2017. Size and dynamics of microplastic in gastrointestinal tracts of Northern Fulmars (*Fulmarus glacialis*) and Sooty Shearwaters (*Ardenna grisea*). *Mar. Pollut. Bull.* 116 (1-2), 143–150. doi:10.1016/j.marpolbul.2016.12.064.

- Thompson, R.C., Olsen, Y., Mitchell, R.P., Davis, A., Rowland, S.J., John, A.W.G., McGonigle, D., Russell, A.E., 2004. Lost at sea: Where is all the plastic? *Science*. 304 (5672), 838. doi:10.1126/science.1094559.
- Tsyurupa, M.P., Davankov, V.A., 2006. Porous structure of hypercrosslinked polystyrene: State-of-the-art mini-review. *React. Funct. Polym.* 66 (7), 768–779. doi:10.1016/j.reactfunctpolym.2005.11.004.
- Urgert, W., 2015. Microplastics in the rivers Meuse and Rhine: Developing guidance for a possible future monitoring program. Masterthesis, Heerlen, The Netherlands, 106 pp. <https://www.riwa-rijn.org/wp-content/uploads/2015/11/master-thesis-NW-Wilco-Urgert-838144036-DEFINITIEF-16-10-2015.pdf> Accessed 09 March 2020.
- Weaton & Lefevre, 2000. Ion-Exchange resins. http://msdssearch.dow.com/PublishedLiteratureDOWCOM/dh_0032/0901b803800326ca.pdf. Accessed 15 January 2018.

SI 1: Repeated detection of polystyrene microbeads in the Lower Rhine River

Raman microspectroscopy

An air-cooled video camera (Infinity 3-1c; Lumenera Corporation, Ottawa, Canada) equipped with LEDs for illumination was used for visual inspection and photography. Daily spectral auto-calibration was performed using NIST polystyrene standard 1921b (band position 1001.4 cm^{-1}). A standardised set of parameters was used for all measurements to guarantee comparability between the acquired spectra: 100× objective (NA = 0.80, WD = 3.3 mm); 785 nm laser excitation (diode-laser, 90 mW, intensity: 100%); 600 gr mm^{-1} spectral grid-width (150–3,200 cm^{-1} wavelength range – Stokes shift); 300 μm aperture width; 100 μm gap width and 12 s integration time (30 accumulations). For one PS-spherule from *p* 5 (hit quality index [HQI] 87.1%, visual category B), the wavelength range was shortened to 150–1,800 cm^{-1} due to strong fluorescence. Exposure time was modified slightly if necessary to obtain clear spectra. Semi-automatic baseline correction was performed on all spectra.

ATR FT-IR spectroscopy

Spectroscopy on spherules from *s* 4 and *s* 9 (Mani et al., 2015; $n = 8$, Table S1) was performed using an ATR FT-IR spectrometer (Excalibur 3100; Varian, Palo Alto, California, USA) at Intertek AG, Basel, Switzerland. Spherules were photographed prior to analysis using a Zeiss Stereomicroscope SV8 with an Axio Cam MRC (Carl Zeiss Microscopy GmbH, Germany). Blow-dried samples were prepared on the crystal. IR-spectra were recorded at a resolution of 4 cm^{-1} , applying 32 scans, with a gain range radius of 40 and a sensitivity of 1 using a mercury cadmium telluride (MCT) detector. The spectrometer was equipped with a Golden Gate single reflection attenuated total reflection (ATR) unit with a diamond crystal. Spectra were compared to the KnowItAll Informatics Systems 7.5 library (Bio-Rad, Hercules, CA, USA; ~90,000 entries). All analyses were performed at room temperature. Images were processed using AxioVision software version 4.5 (Carl Zeiss Imaging Solutions GmbH, Oberkochen, Germany).

Table S1

Qualitative spectroscopic evidence of polystyrene (PS) and polystyrene-divinylbenzene (PS-DVB) microbeads in the surface waters of the Rhine River between kilometres 677–944 from 2014–2017 (including PMMA, PE and PP findings). Findings are sorted by Rhine River kilometre (Rh-km).

Rh-km	Code	Date	Opaque microbeads	Polymer ^a	Raman ^b	FT-IR ^c	Opaque microbead conc. (# m ⁻³)
677	<i>s 1</i> ^d	16.07.14	✓	PS-DVB ^e (<i>n</i> = 4) ^b	✓		0.07 (left-hand riverside) ^d
691	<i>p 1</i>	29.11.16	0 ^f	0 ^f	0 ^f	0 ^f	0.03 ^f
698	<i>s 2</i> ^d	14.07.14	✓	PS-DVB (<i>n</i> = 1) ^g ; PP (<i>n</i> = 1) ^g ; PE (<i>n</i> = 1) ^g		✓ ^g	0.2 (left-hand riverside) ^d
700	<i>p 2</i>	29.11.16	0 ^f	0 ^f	0 ^f	0 ^f	0.05 ^f
705	<i>p 3</i>	29.11.16	✓	PS-DVB (<i>n</i> = 4) ^b ; (<i>n</i> = 1) ^g ; PS ^h (<i>n</i> = 8) ^g	✓	✓ ^g	0.5
720	<i>p 4</i>	29.11.16	✓	PS-DVB (<i>n</i> = 11) ^b ; PS (<i>n</i> = 2) ^b ; (<i>n</i> = 6) ^g	✓	✓ ^g	8.3
737	<i>p 5</i>	29.11.16	✓	PS-DVB (<i>n</i> = 20) ^b ; (<i>n</i> = 4) ^g ; PS (<i>n</i> = 1) ^b , (<i>n</i> = 3) ^g	✓	✓ ^g	5.8
755	<i>p 6</i>	29.11.16	✓	PS-DVB (<i>n</i> = 15) ^b , (<i>n</i> = 3) ^g ; PS (<i>n</i> = 6) ^g ; Unknown (<i>n</i> = 1) ^b , (<i>n</i> = 1) ^g	✓	✓ ^g	4.2
766	<i>p 7</i>	29.11.16	✓	PS-DVB (<i>n</i> = 15) ^b , (<i>n</i> = 6) ^g ; PS (<i>n</i> = 2) ^g ; Unknown (<i>n</i> = 1) ^g	✓	✓ ^g	4.9
772	<i>p 8</i>	29.11.16	✓	PS-DVB (<i>n</i> = 10) ^b ; PS (<i>n</i> = 4) ^b , (<i>n</i> = 7) ^g ; PMMA (<i>n</i> = 1) ^b	✓	✓ ^g	3.3
779.3	<i>s 3</i> ^d	15.07.14 ^a	✓	PS-DVB (<i>n</i> = 3) ^b	✓		11.2
780.3	<i>p 9</i>	29.11.16	✓	PS-DVB (<i>n</i> = 12) ^b , (<i>n</i> = 3) ^g ; PS (<i>n</i> = 1) ^b , (<i>n</i> = 1) ^g ; PMMA (<i>n</i> = 1) ^b , (<i>n</i> = 1) ^g ; Unknown (<i>n</i> = 2) ^g	✓	✓ ^g	9.2
837	<i>s 4</i> ^d	17.07.14	✓	PS-DVB (<i>n</i> = 3) ⁱ ; PS (<i>n</i> = 1) ⁱ		✓ ⁱ	9.6
837	<i>s 5</i>	28.04.16	✓	PS-DVB (<i>n</i> = 1) ^g ; PS (<i>n</i> = 5) ^g		✓ ^g	n.a. ^j
837	<i>s 6</i>	08.09.16	✓	PS-DVB (<i>n</i> = 18) ^b	✓		n.a. ^j
837	<i>s 7</i>	01.12.16	✓	PS-DVB (<i>n</i> = 4) ^g ; PS (<i>n</i> = 3) ^g		✓ ^g	n.a. ^j
837	<i>s 8</i>	22.02.17	✓	PS-DVB (<i>n</i> = 4) ^g ; PS (<i>n</i> = 3) ^g		✓ ^g	n.a. ^j
944	<i>s 9</i> ^{d, k}	30.07.14	✓	PS-DVB (<i>n</i> = 3) ^b , (<i>n</i> = 2) ⁱ ; PS (<i>n</i> = 2) ⁱ	✓	✓ ⁱ	1.2 (right-hand riverside) ^d

^a (*n*) indicate positive polystyrene-divinylbenzene (PS-DVB) and polystyrene (PS) findings (PMMA, PE and PP findings included).

^b Raman microspectroscopy (Horiba XploRa Plus Raman-Microscope connected to a Syncrity EM-CCD detector; Horiba Jobin Yvon, Kyoto, Japan).

^c Fourier-transform infrared spectroscopy.

^d Published in (Mani et al., 2015).

^e Polystyrene–divinylbenzene.

^f These samples exclusively contained translucent microbeads.

^g FT-IR Bruker ALPHA; Bruker, Billerica, MA, USA.

^h Polystyrene.

ⁱ FT-IR Excalibur 3100, Varian, Palo Alto, CA, USA.

^j Microbead concentrations not assessed (n.a.).

^k This sample was taken downstream of the bifurcation of the Rhine River at Rh-km 866 in the Waal River channel.

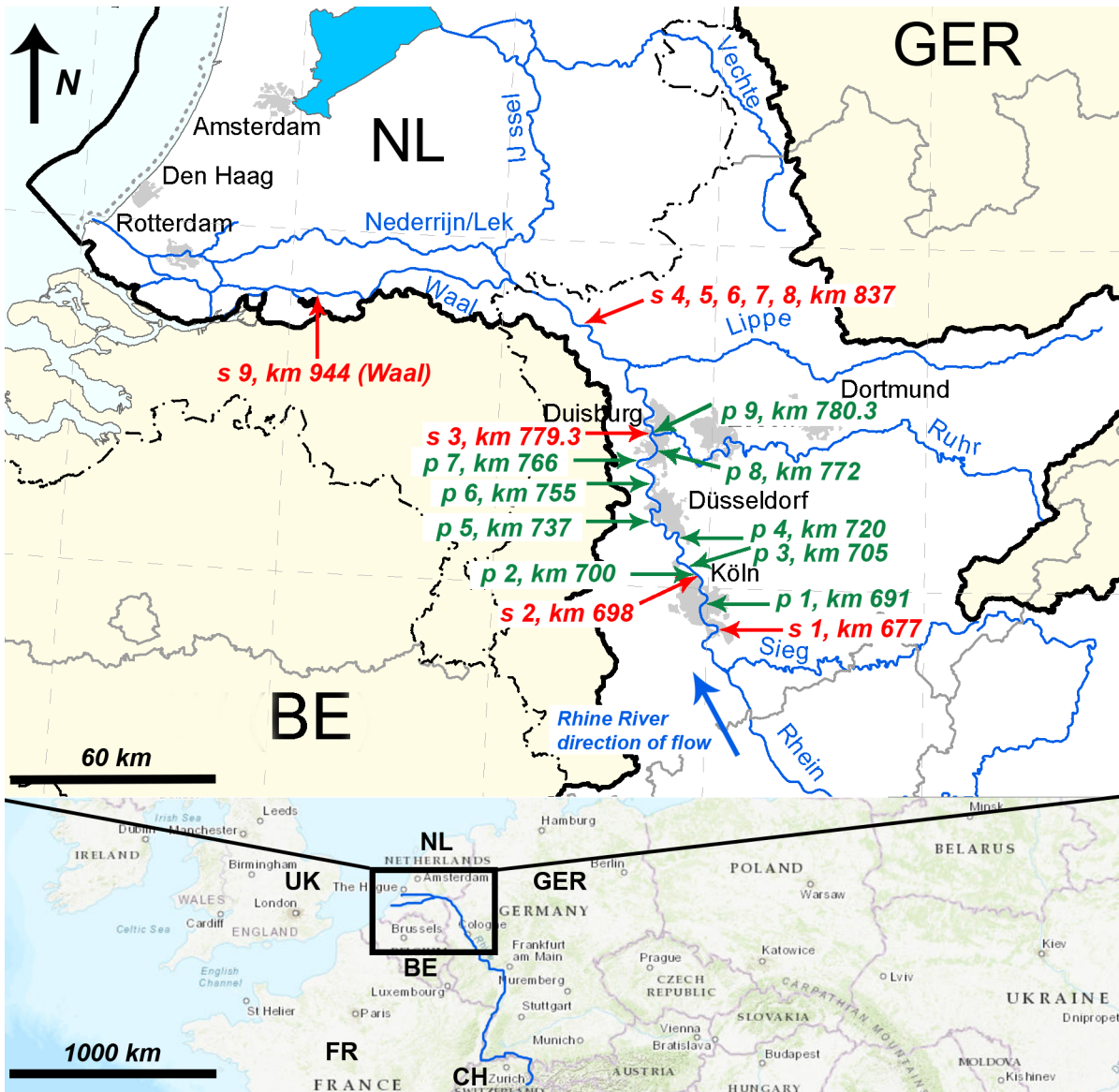


Fig. S1. Locations of the *s* 1–9 (red) and *p* 1–9 (green, 29.11.2016) sampling sites (*s* 1, 2, 3, 4 and 9 were first published in Mani et al. (2015)). Sampling dates: *s* 1: 16.07.2014; *s* 2: 14.07.2014; *s* 3: 15.07.2014; *s* 4: 17.07.2014; *s* 5: 28.04.2016; *s* 6: 08.09.2016; *s* 7: 01.12.2016; *s* 8: 22.02.2017 and *s* 9: 30.07.2014. The white area with a black margin indicates the Rhine watershed. Dashed lines indicate country borders. The upper depiction is a modified version of a map received from the ICPR Secretariat, 2011; the lower map is modified from ArcMap 10.3.

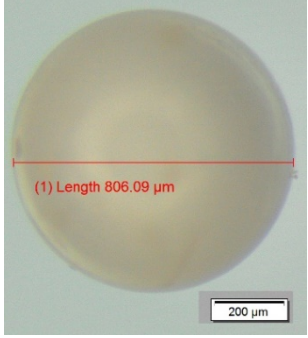
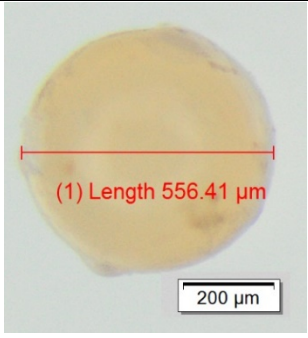
Table S2Metadata for the *pearl* sampling campaign (Cologne–Duisburg, GER; 29.11.2016)

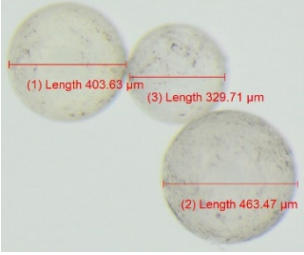
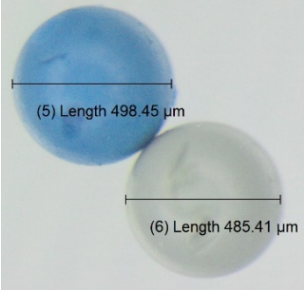
Site	Rhine-km	Coordinates	Microbead concentration (# m ⁻³)	Volume of water sampled (m ³)	DID ^a between <i>p_n</i> and <i>p_{n-1}</i>	WWTP ^b between <i>p_n</i> and <i>p_{n-1}</i>
<i>p</i> 1	691	50°57'27.80 N 6°59'8.37 E	0.03	90.5 ^c	-	-
<i>p</i> 2	700	51°1'24.41 N 6°58'25.16 E	0.05	80.7	12	1
<i>p</i> 3	705	51°3'14.32 N 6°55'10.07 E	0.5	96.7	3	1
<i>p</i> 4	720	51°8'44.30 N 6°51'2.28 E	8.3	96.0	8	3
<i>p</i> 5	737	51°11'51.88 N 6°43'51.40 E	5.8	88.6	4	1, 2 ^d
<i>p</i> 6	755	51°17'47.34 N 6°43'30.00 E	4.2	92.6	10	2
<i>p</i> 7	766	51°21'54.42 N 6°39'38.73 E	4.9	99.1	7 ^d	1
<i>p</i> 8	772	51°23'15.78 N 6°44'10.12 E	3.3	96.8	20	0
<i>p</i> 9	780.3 ^e	51°27'9.44 N 6°43'25.03 E	9.2	42.4	12	3
					Total DID, 76	Total WWTP, 14

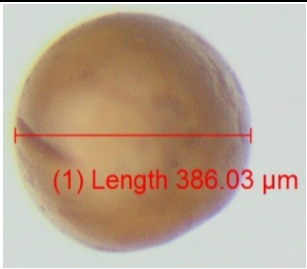
^a Direct industrial dischargers.^b Direct communal wastewater treatment plant dischargers.^c Flow velocity was calculated using the average of four subsequent samples.^d WWTP/DID connected to tributary within 5 km upstream of its Rhine confluence.^e Confluence of Ruhr and Rhine Rivers.

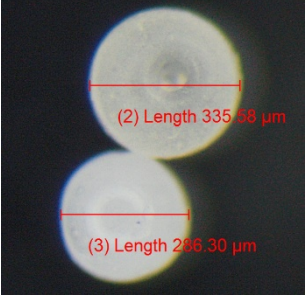
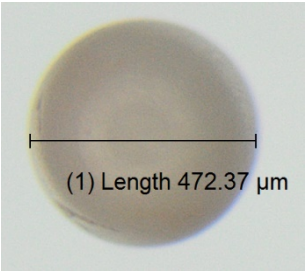
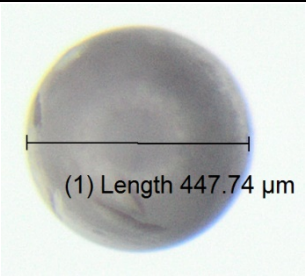
Table S3

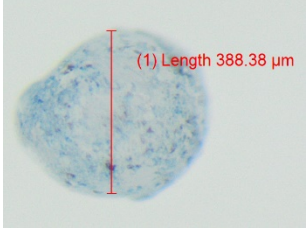
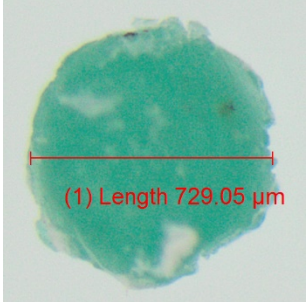
Overview of the 25 visual-based categories (A–Y) detected in the *pearl* campaign. Polymer composition and bead size range are given for the five most abundant categories A–E. Average sampling volume (\pm SD) at each site was $87 \pm 17 \text{ m}^3$.

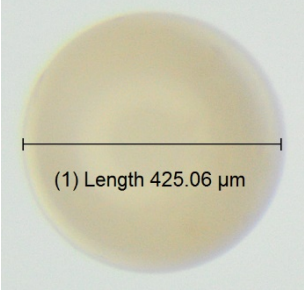
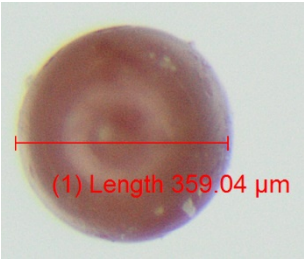
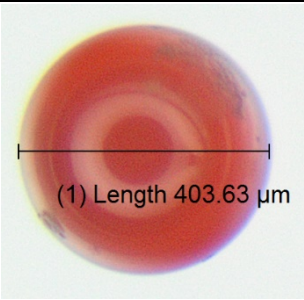
Visual Category	% of total bead count (<i>n</i> = 2,944)	Geographical occurrence (Rh-km bold); bead count (<i>n</i>) (Strike through = no occurrence)	Visual description and polymer (where available) of all beads from <i>p</i> 3–9 of the respective category	Photograph ^a
A Size range: 338–931 μm (mean = 613 μm <i>n</i> = 93)	85%	691 700 705 (20) 720 (741) 737 (429) 755 (320) 766 (418) 772 (259) 780.3 (328)	white/beige, opaque, glossy PS-DVB <i>n</i> = 57/72, PS <i>n</i> = 15/72	
B	7%	691 700 705 (3) 720 (33) 737 (46) 755 (31) 766 (42) 772 (26) 780.3 (24)	white (reflecting light), reddish translucent (transmitting light), glossy PS-DVB <i>n</i> = 19/27, PS <i>n</i> = 8/27	

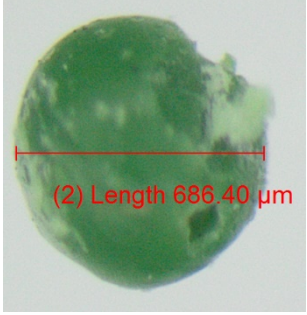
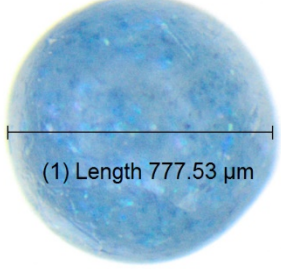
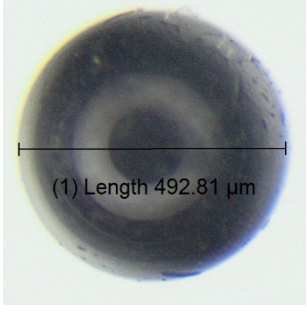
C	2%	691 (3) 700 (4) 705 (7) 720 (1) 737 (5) 755 (11) 766 (5) 772 (13) 780.3 (6)	colourless, translucent PS-DVB <i>n</i> = 4/16, PS <i>n</i> = 10/16, PMMA <i>n</i> = 2/16	
D	1%	691 700 705 720 (4) 737 (12) 755 (11) 766 (3) 772 (4) 780.3 (3)	shades of blue, glossy PS-DVB <i>n</i> = 15/22, PS <i>n</i> = 6/22, unknown <i>n</i> = 1/22	
E	1%	691 700 705 720 737 (7) 755 (4) 766 (5) 772 (6) 780.3 (9)	light brown, glossy PS-DVB <i>n</i> = 8/16, PS <i>n</i> = 3/16, PMMA <i>n</i> = 1/16, unknown <i>n</i> = 4/16	

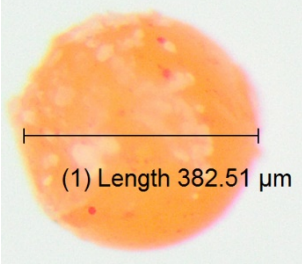
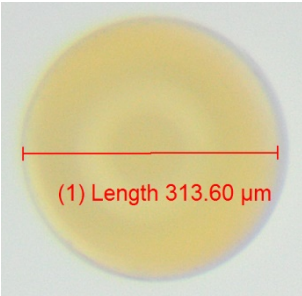
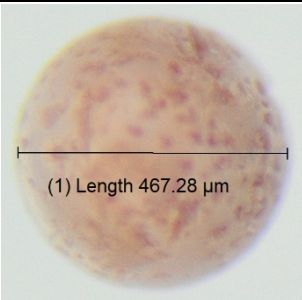
F	<1%	691 700 705 720 737 (3) 755 (10) 766 (3) 772 (2) 780.3 (6)	light grey, sometimes glossy	
G	<1%	691 700 705 (4) 720 (4) 737 (1) 755 (1) 766 (1) 772 780.3 (5)	white, inhomogeneous surface, weathered	
H	<0.5%	691 700 705 (3) 720 (6) 737 755 (2) 766 (1) 772 780.3 (1)	dark brown, inhomogeneous surface	

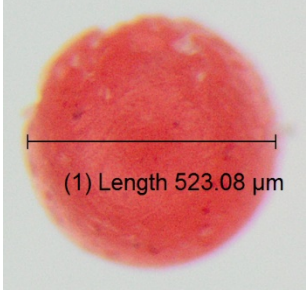
I	<0.5%	691 700 705 720 737 755 766 (5) 772 (4) 780.3 (1)	colourless, translucent, milky, dented	
J	<0.5%	691 700 705 (2) 720 (1) 737 755 766 (1) 772 780.3 (3)	grey, fragile, glossy	
K	<0.5%	691 700 705 (1) 720 737 (2) 755 766 772 (2) 780.3	grey, dented, porous	

L	<0.5	691 700 705 (5) 720 737 755 766 772 780.3	light brown, dented	
M	<0.5%	691 700 705 (2) 720 (1) 737 755 766 772 780.3	colourless, translucent, inhomogeneous shape	
N	<0.5%	691 700 705 720 (1) 737 755 766 772 (1) 780.3 (1)	mint green, brittle, weathered	

O	<0.5%	694 700 705 720 737 (2) 755 766 772 780.3 (1)	grey (reflecting light), golden-red (transmitting light), glossy	 <p>(1) Length 425.06 μm</p>
P	<0.1%	694 700 705 (1) 720 (1) 737 755 766 772 780.3	bordeaux red, glossy	 <p>(1) Length 359.04 μm</p>
Q	<0.1%	694 700 705 720 (1) 737 (1) 755 766 772 780.3	bright red, translucent, glossy	 <p>(1) Length 403.63 μm</p>

R	<0.1%	691 700 705 720 (1) 737 755 766 772 780.3	grass green, brittle, weathered	 <p>(2) Length 686.40 μm</p>
S	<0.1%	691 700 705 720 737 (1) 755 766 772 780.3	blue, glitter, glossy	 <p>(1) Length 777.53 μm</p>
T	<0.1%	691 700 705 720 737 (1) 755 766 772 780.3	black, glitter, glossy	 <p>(1) Length 492.81 μm</p>

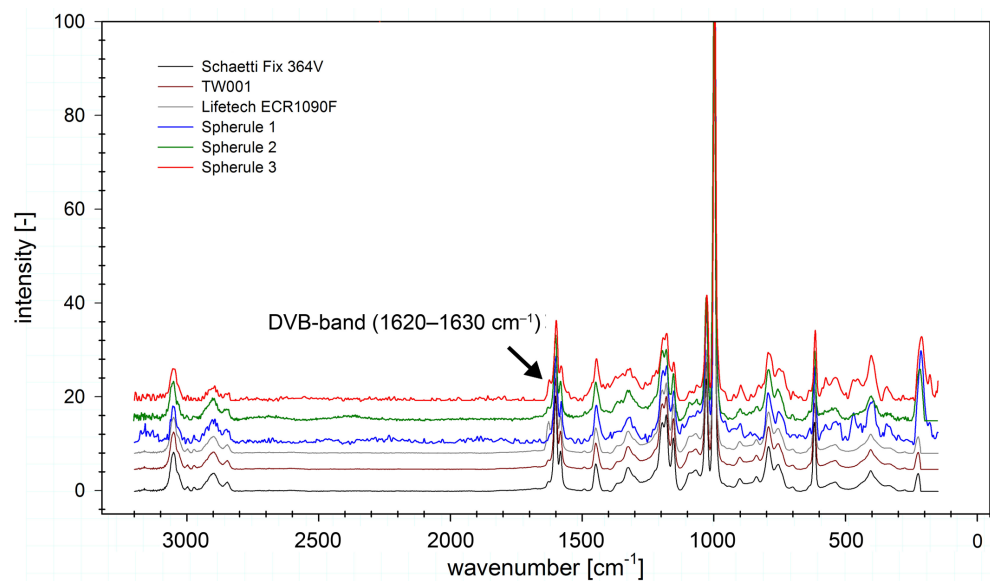
U	<0.1%	694 700 705 720 737 (1) 755 766 772 780.3	orange, red dots	
V	<0.1%	694 700 705 720 737 755 766 (1) 772 780.3	golden-green, translucent, glossy	
W	<0.1%	694 700 705 720 737 755 766 (1) 772 780.3	pink, red dots, indented surface	

X	<0.1%	691 700 705 720 737 755 766 772 (1) 780.3	red, red dots	
Y	<0.1%	691 700 705 720 737 755 766 772 780.3 (1)	grey, granite pattern	

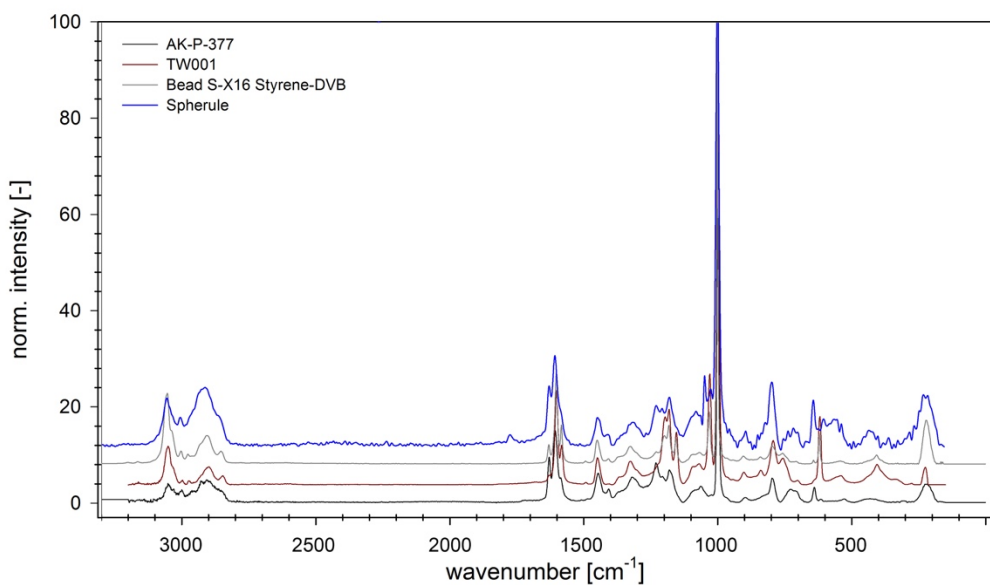
Samples were collected on 29.11.2016.

Size range for all categories was 286–954 μm (mean = 497 μm, $n = 218$).

^a Olympus SZ61; Olympus SC50; CellSens Entry Version 1.17.16030.0.



HQI	DB	specification	material	manufacturer
99.04	EDB	TW001 (DVB based ion exchanger)	8%-cross-linked PS/DVB	Uni Marburg
99.02	EDB	Schaetti Fix 364V	polystyrene	Schaetti
98.58	EDB	Lifetech ECR1090F (DVB based ion exchanger)	macroporous DVB	Purolite



HQI	DB	specification	material	manufacturer
96.47	EDB	AK-P-377 (DVB based ion exchanger)	PS/DVB with DMSO	Uni Marburg
96.21	EDB	TW001 (DVB based ion exchanger)	8%-cross-linked PS/DVB	Uni Marburg
95.80	QRX	Bio Beads S-X16	PS-DVB	Bio-Rad Inc.

Fig. S2. Top: Raman spectra for three category A microbeads as well as three reference spectra. Below: Category E microbead from sample *p* 3 matching the sulfonated PS-DVB IER AK-P-377 at a HQI of 96.47%.

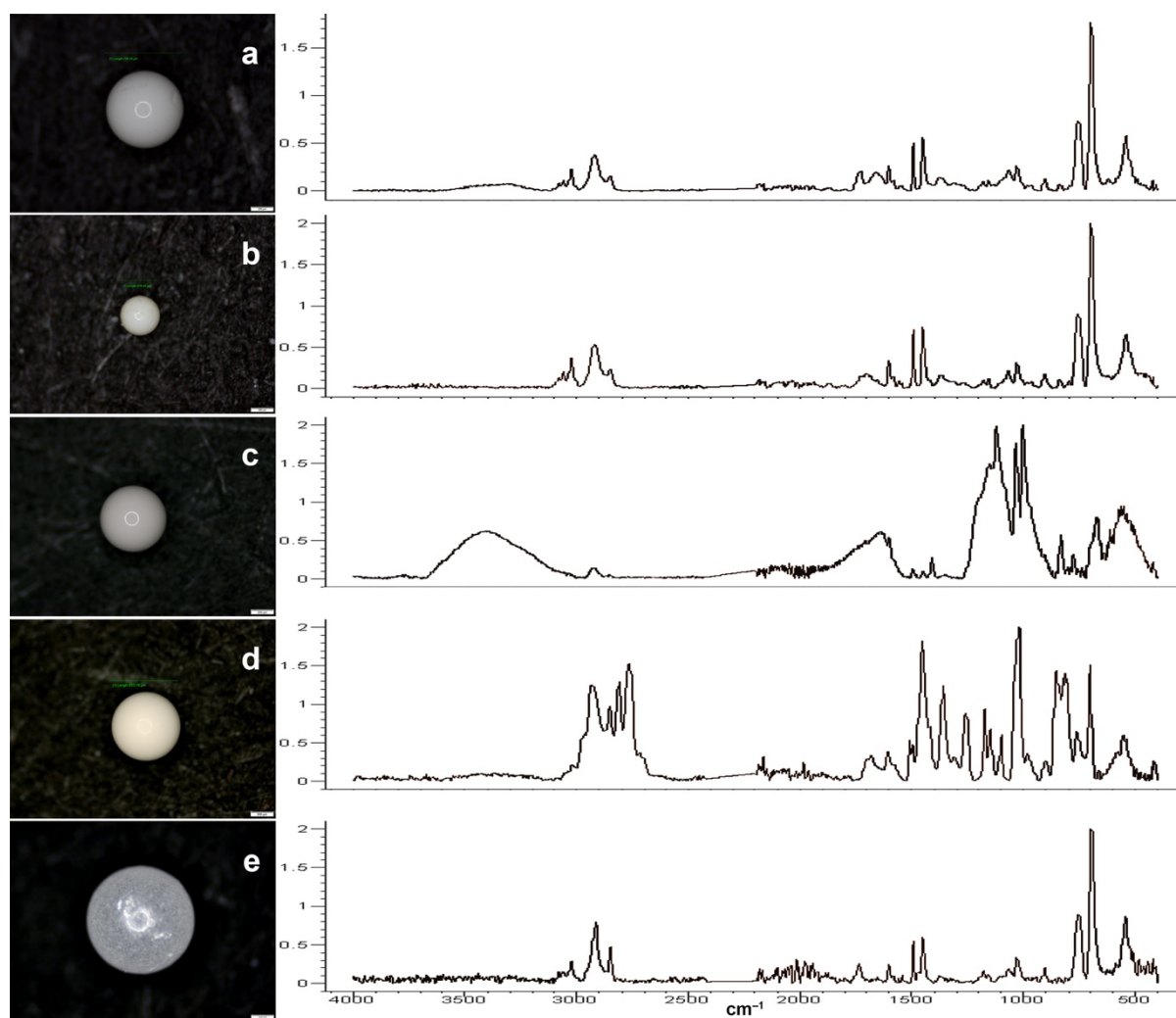


Fig. S3. Microbead stereomicrographs with respective FT-IR spectra. Environmental polystyrene(-divinylbenzene), PS-DVB category A and B microbeads (a, b, respectively). Lewatit Monoplus SP 112 H and MP 62 PS-DVB ion-exchange resins (IER; c and d, respectively) and non-expanded polystyrene (EPS) bead (e) for reference. Scale bars are 200 μm . Spectra were baseline-corrected and normalised. To exclude the CO₂ band, a straight line was created in the wavenumber range of 2420–2200 cm^{-1} (Primpke et al., 2018).

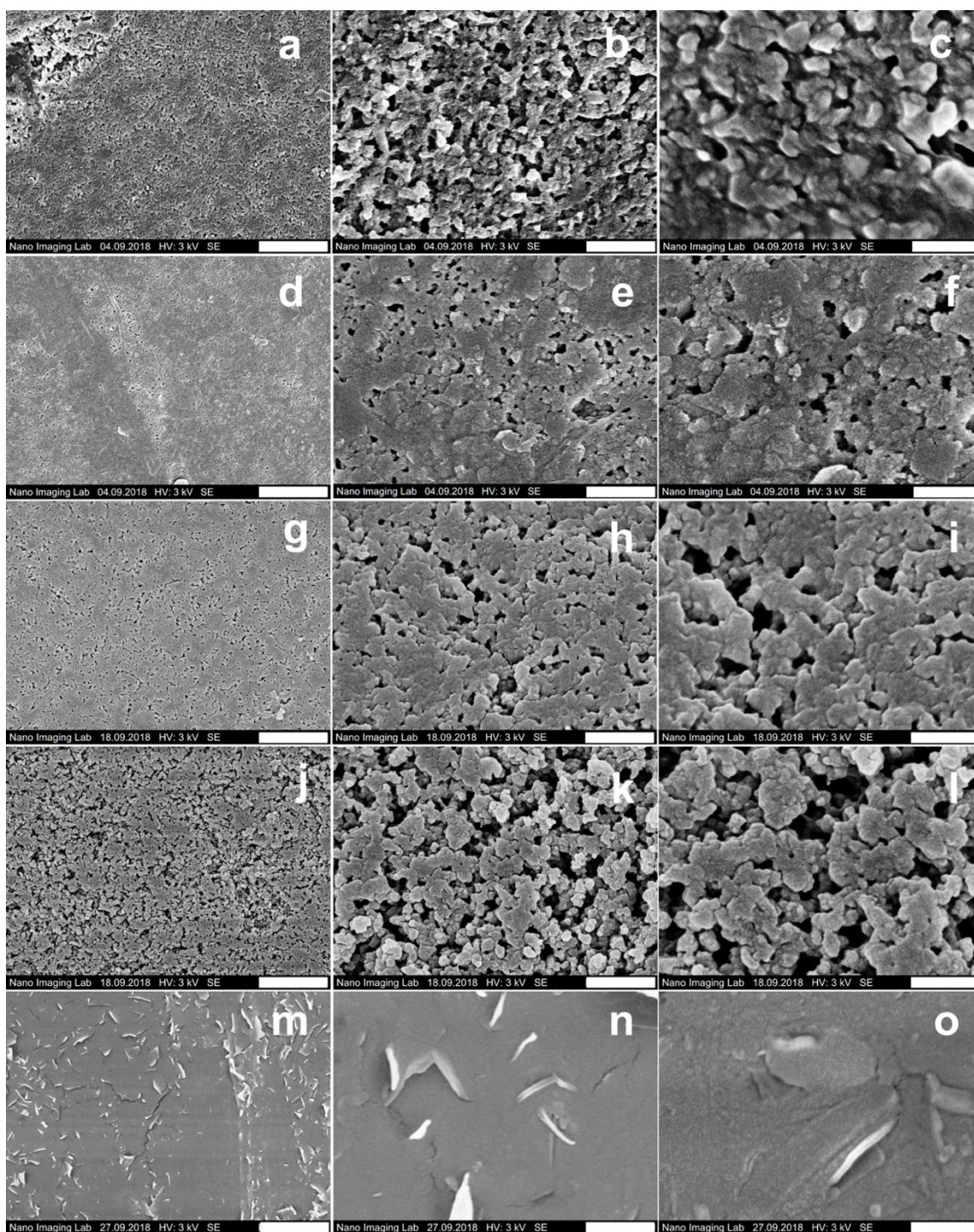


Fig. S4. Scanning electron micrographs (SEM) of environmental (a–f) and reference (g–o) polystyrene microbeads taken of the surface of the particles after 3 nm platinum layer sputtering. Category A (a–c) and B (d–f) polystyrene(-divinylbenzene), PS-DVB microbeads from the Rhine River sampled at p 5 (Rh-km 737, pore diameters: 390–1430 Å). Reference materials: PS-DVB ion-exchange resin (IER) bead types Lewatit SP 112 H and Lewatit MP 62 (g–i and j–l, respectively) and non-expanded polystyrene beads (EPS; m–o). Visible (macro-)porous surface structure in (a–l), smooth surface with spikes and fine cracks (m–o). Scale bars, left column: 2 μm; middle column: 400 nm and right column: 200 nm. Image (c) exhibits some distortion due to the electric charge of the material surface and hence challenging imaging.



Fig. S5. Examples of category A microbeads (opaque, white–beige) collected at sampling site *s 6* (Rh-km 837, 08.09.16). The translucent spherules containing gas bubbles were not specifically considered in this study; their source area and distribution are yet to be investigated. Former research has indicated polymethyl methacrylate (PMMA) for the beads containing bubbles and PMMA or polystyrene (PS) for the translucent, colourless beads without large internal bubbles.

References

- Mani, T., Hauk, A., Walter, U., Burkhardt-Holm, P., 2015. Microplastics profile along the Rhine River. *Sci. Rep.* 5, 17988. doi:10.1038/srep17988.
- Primpke, S., Wirth, M., Lorenz, C., Gerdt, G., 2018. Reference database design for the automated analysis of microplastic samples based on Fourier transform infrared (FTIR) spectroscopy. *Anal. Bioanal. Chem.* 410 (21), 5131–5141. doi:10.1007/s00216-018-1156-x.

Paper 2

Using castor oil to separate microplastics from four different environmental matrices

Thomas Mani ^a, Stefan Frehland ^a, Andreas Kalberer ^a, and Patricia Burkhardt-Holm ^a

^a Department of Environmental Sciences, The Man-Society-Environment Program,
University of Basel, Vesalgasse 1, 4051 Basel, Switzerland

Published 2019

in *Analytical Methods* 11 (13), pp. 1788–1794.

DOI: 10.1039/C8AY02559B.

Abstract

The detection of environmental microplastics (MP) is limited by the need to rigorously separate polymers from the surrounding sample matrix. Searching for an affordable, low-risk and quick separation method, we developed a protocol to separate microplastics (size range: 0.3–1 mm; virgin polymers: PP, PS, PMMA and PET-G) from suspended surface solids (marine and fluvial) as well as soil and sediment using castor oil. We demonstrate effective separation of the four polymers in a spike-recovery experiment. The mean \pm SD MP spike-recovery rate was $99 \pm 4\%$ with an average matrix reduction of $95 \pm 4\%$ (dry weight, $n = 16$). The protocol was validated by separating non-spiked environmental Rhine River suspended solids samples recovering $74 \pm 13\%$ of MP. There PS comprised 76% of the non-retrieved MP and additional H₂O₂ digestion was needed to sufficiently reduce the highly abundant natural matrix. This castor oil lipophilicity-based protocol (i) achieves high MP recovery rates as a function of its environmental matrix reduction ability and (ii) provides environmentally friendly, non-hazardous and resource-efficient separation of MP from four different, typically investigated environmental compartments using one and the same method. Based on the Rhine River sample validation, the protocol is a potent replacement for traditional density separation techniques. Samples with high biogenic concentrations may require additional digestion.

1. Introduction

Microplastics (MP; <5 mm) are an emerging contaminant with planetary boundary implications (Jahnke et al., 2017; Sedlak, 2017). MP have been widely reported in marine (Cole et al., 2011), freshwater (Eerkes-Medrano et al., 2015; Rodrigues et al., 2018) and terrestrial (Rillig, 2012; Zhang and Liu, 2018) environments, and their rising environmental concentrations, high bioavailability and ecotoxicological potential have led to escalating global concern regarding the effects of MP (GESAMP, 2016). Surveys on environmental MP are published nearly every week; however, vast inconsistencies prevail in the methodologies used for sampling, purification, quantification and chemical analysis (BASEMAN, 2017). To minimise the interference of natural residues during chemical analysis (for instance Fourier Transform Infrared [FTIR] or Raman spectroscopy; K  ppler et al., 2016), it is vital to rigorously separate synthetic polymers from the environmental matrix. A number of separation and purification processes are known in preparatory protocols for MP analysis, including electro- (Felsing et al., 2018) and density separation based on NaCl, ZnCl₂ or NaI, and purification protocols using NaClO, HNO₃, H₂O₂ or KOH (Ivleva et al., 2017; Silva et al., 2018). However, many of these techniques are complex, time consuming and require extensive sample manipulation, and are thus prone to contamination and loss (Silva et al., 2018).

Moreover, some reagents used for density separation or chemical purification of MP samples e.g., ZnCl₂ (Imhof et al., 2012), NaI (Nuelle et al., 2014), HCl (Cole et al., 2014), or H₂O₂ (L  der et al., 2017) pose a threat to health and/or the environment if mismanaged. These risks may be of particular concern when laypersons employ such techniques, for example in nowadays emerging microplastics citizen science surveys (Bergmann et al., 2017a; Bosker et al., 2017; Gewert et al., 2017; Lots et al., 2017). Apart from their ecological hazards, many of these reagents are costly, may consume precious resources that could be better used elsewhere, or – depending on the economic resources or geographical location of the investigating unit – may not be easily available (Crichton et al., 2017). Due to the increasing, widespread demand for monitoring and risk assessment of environmental MP, simplification and democratisation of standardized methods for MP sampling, purification and quantification are urgently required (BASEMAN, 2017; European Union, 2018). A generally applicable, efficient, accurate, rapid, cheap purification method could aid the compilation of valuable extensive datasets on the distribution of MP in different environments.

In this study, we aimed to develop a method that enables the separation of some of the most common types of MP particles found in the environment from a diverse set of typically

investigated matrices. We based our approach on an oil extraction protocol for separating MP from sediments that employs canola oil (Crichton et al., 2017). Here, we report a simple, rapid, cheap extraction protocol based on castor oil – which has a higher molecular weight than canola oil (933.45 vs. 876.6 g mol⁻¹) – for efficient and accurate recovery of various MP particles (PP, PS, PMMA and PET-G) from four typical environmental sample matrices: fluvial suspended surface solids (FSS), marine suspended surface solids (MSS), marine beach sediments (MBS) and agricultural soil (AS). In order to validate the microplastic recovery as well as the matrix reduction potential on non-spiked environmental samples the castor oil separation protocol was executed on five Rhine River FSS samples. These were collected at different locations between Switzerland and the German-Dutch border in order to capture a variety of microplastics and biogenic residue abundance as well as diversity in polymers and state of polymer degradation (Mani et al., 2015; Mani et al., 2019).

2. Methods

2.1. Environmental sample collection

Fluvial suspended surface solids (FSS) and marine suspended surface solids (MSS) were collected using a 0.3 mm-neuston net mesh (see Table S1 for the details of all hereinafter mentioned materials and instruments) and marine beach sediments (MBS) and agricultural soil (AS) were collected using a stainless-steel spoon (Table S2, Fig. S1). The samples were fractionated (0.3–1.0 mm for FSS and MSS and 0.063–1 mm for MBS and AS) using geological sieves and stored at 7 °C. Prior to analysis, all samples were dried at 40 °C for 24 h. Each environmental matrix was divided into four replicates with specific target dry weights to the nearest mg: 1.0 g for FSS and MSS and 10.0 g for MBS and AS. Due to formation of aggregates in the MSS and FSS after drying, these samples were disaggregated by adding 100 mL distilled water (aq. dest.) and stirring at 400 rpm and 60 °C for 15 min prior to the separation protocol. Five additional Rhine River FSS samples were collected to examine whether non-spiked field samples potentially containing MP could be efficiently separated using the oil separation protocol. The Rhine River samples were collected at different locations (Table S2). Each sample was collected over 10 min from the centre of the river cross section using a Manta Trawl (mesh: 300 µm), resulting in a mean (± SD) filtered volume of 84.2 ± 8.7 m³ (Supporting Information, Table S2).

2.2. Microplastics for spiking

The environmental samples were spiked with synthetic polymer particles to assess the MP recovery rate of the protocol. Selection of the polymers was based on (i) global production

volumes (Geyer et al., 2017b) and the frequency of reported identification in the environment (Hong et al., 2017) and (ii) the inclusion of a range of polymer densities from below to above the specific density values of fresh water and saltwater.

We used fragments of four common polymer types: polypropylene (PP; specific density, $\rho = 0.84 \text{ g cm}^{-3}$, Table S4, Fig. S5), polystyrene (PS; 1.05 g cm^{-3} , Table S5, Fig. S7), polymethyl methacrylate (PMMA; 1.19 g cm^{-3} , Table S6, Fig. S9) and glycol modified polyethylene terephthalate (PET-G; 1.27 g cm^{-3} , Table S7, Fig. S11). PP, PS and PET are among the six most commonly produced plastics (including PE, PVC and PUR; Geyer et al., 2017a). PP and PS are typically two of the three most commonly identified polymers in environmental plastic studies (the other is PE; Hong et al., 2017). PMMA was additionally selected as it had been previously identified as a major MP representative in the Rhine River (Mani et al., 2015). Particle sizes ranged from 0.3–1 mm.

As the oil separation protocol involves an aqueous phase with a specific density (ρ) of $\sim 1 \text{ g cm}^{-3}$, polymers that covered the specific density range of $0.84\text{--}1.27 \text{ g cm}^{-3}$ were deliberately selected. This density-range coverage is also important for separation of MP from heavier matrices, such as MBS ($\rho \sim 2.6 \text{ g cm}^{-3}$), as the aqueous phase of the water-matrix mixture in every separation process will have a specific density $\rho \sim 1 \text{ g cm}^{-3}$ after the heavier solid fraction has settled.

Particles were mechanically fragmented and sieved into small (0.3–0.5 mm) and large (0.5–1.0 mm) fractions (see Table S1 for material and instrument details). Each fraction was numerically quantified using a stereomicroscope and chemically analysed by attenuated total reflection (ATR)-FTIR. Spectra were compared against a reference spectra library using Opus 7.5 software.

2.3. Castor oil microplastic and environmental matrix separation protocol

For the four environmental matrices, the four replicates of each pre-weighed residue were transferred into a separation funnel ($n = 16$, see Table S1 for all material and instrument details), suspended in 100 mL aq. dest. water and spiked with 100 MP particles (15 small and 10 large fragments of each polymer type, resulting in $n = 1,600$ MP particles for the entire experiment).

The sealed funnels were shaken for 30 s by hand to ensure thorough mixing of the spiked samples. Ten mL of castor oil (Table S1) was added to each replicate. To guarantee that the entire sample made contact with the castor oil, the separation funnel was inverted and shaken for 1 min by hand. For this the separation funnel was firmly held using two hands at the top and

the bottom, respectively, and vigorously shaken and rotated at shoulder level. Subsequently, the separation funnels were rotated back to their upright position and the walls and lid of the funnel were rinsed with 400 mL aq. dest. water to ensure any remaining residue and oil droplets were returned to the mixture. Thereafter, the MBS and AS samples were left to settle for 15 min and the MSS and FSS samples for 45 min, according to previous experience (please refer to Fig. S2 for a schematic diagram of the entire procedure).

The lower aqueous and solid phase was then drained from the separation funnel into a clean glass jar, sealed and stored at 7 °C. The remaining oil phase was drained, vacuum filtered onto ash-less hardened cotton/cellulose filter paper (pore size: 25 µm), and the filter was washed with 100 mL ethanol (EtOH, 96%). Before and during draining, the lid and walls of the funnel were thoroughly rinsed using an additional 100 mL EtOH to transfer all residue onto the filter. The filter paper was transferred to a glass Petri dish, sealed with Parafilm and stored at 7 °C for visual polymer spike-recovery and further FTIR analysis.

For visual spike-recovery, the filters containing the separated oil fraction filtrates were dried at 40 °C for 24 h and weighed to define dw-reduction (in %, Table S3). Finally, the extracted spiked polymer particles on the filter (Fig. S3) were picked by hand, quantified using a stereomicroscope and then chemically analysed by FTIR (as described in the section “microplastics for spiking”).

The five Rhine River FSS samples collected to examine non-spiked environmental microplastic recovery rates and matrix reduction efficiency (Table S2) were subjected to the same castor oil separation protocol. Subsequently the separated sample fractions were rinsed with aq. dest. and dried. All resulting fractions (oil as well as the water and solid phase) were visually assessed for MP within the size range of 0.3–1 mm. Totally 978 putative environmental microplastic particles were detected in both the oil and water and solid phase of all five Rhine River samples combined, of which 40% were chemically investigated using FTIR. After the oil separation, further dw matrix reduction potential of these five FSS-samples was investigated by subjecting the oil-extracted, rinsed and dried fractions to H₂O₂. For this, the pre-weighed dry sample residues from the upper oil-phase were placed in separate glass Petri dishes (diameter 6 cm), covered with 10 mL of H₂O₂ (30%) and incubated at 50 °C for 18 hours (adapted from Löder et al., 2017). Subsequently, the sample residues were rinsed on a 300 µm mesh using aq. dest., re-transferred back to the Petri dishes, dried for 6.5 h at 60 °C and weighed (dw).

2.4. Quality control and protection against contamination

The effect of EtOH rinsing on preventing castor oil-FTIR interference (Crichton et al., 2017) was quantified. For this, spectral hit quality indices (HQI) of PS and PP MP (size range longest axis: 0.5–1.2 mm) were compared after four different treatments in triplicate: (i) untreated, pure MP, (ii) MP submerged in EtOH (96%) for 30 min, (iii) MP submerged in castor oil for 30 min and (iv) MP submerged in castor oil for 30 min and subsequently submerged in EtOH (96%) for 5 min. MP from treatment (iv) reached significantly higher HQIs compared to treatment (iii) (Fig. S13). Interestingly, MP submerged in EtOH reached higher HQIs than untreated pure MP (Fig. S13), indicating a general benefit of EtOH treatment for MP spectroscopy, also outside the application of the presented protocol. To prevent samples from contamination, glassware was used whenever possible. Containers, such as Petri dishes, were always covered with a lid or aluminium foil when not in use. Where the use of plastic materials for processing was unavoidable (e.g. the PTFE stopcock in the separation funnel), the item was thoroughly rinsed before use with deionised water and EtOH (70%). White lab coats (100% cotton) were worn in the laboratory at all times. Nitrile gloves were worn whenever the operator's hands came into close contact with samples and glassware. To prevent cross-contamination between instruments or receptacles, all used items were thoroughly washed with warm water and labware detergent. Procedural blanks were run during the visual sample examination phase (~4 h) to assess the laboratory atmosphere contamination potential (adapted from Bergmann et al., 2017b). For this, three thoroughly rinsed glass Petri dishes (diameter: 13 cm) were placed uncovered on the laboratory bench during the entire visual sample examination phase. Subsequently they were rinsed and drained onto cotton/cellulose filter paper and the filter paper was visually examined under a super-lighted stereomicroscope. No MP fragments were recorded in any of the blanks.

2.5. Statistical analysis

Statistical analyses were performed using GraphPad Prism 7.03 for Windows (GraphPad Software, La Jolla, CA, USA). A Kruskal-Wallis test was performed to evaluate differences between the four dw matrix reduction rates in the spike-recovery experiment. A Friedman test was run to assess differences of total microplastic recovery rates between the different matrices in the spike-recovery experiment. Both tests were followed by a Dunn's multiple comparison test to evaluate where differences lie. To compare matrix dw reduction of the five non-spiked Rhine River samples (i) after oil separation and (ii) after additional H₂O₂ treatment, a Kolmogorov–Smirnov test was applied. To compare HQIs of PS and PP particles after four different treatments as described in “2.4. Quality control and protection against contamination” unpaired *t* tests were carried out after a Shapiro–Wilk normality test.

3. Results and discussion

3.1. Environmental matrix reduction and recovery of spiked microplastics

The oil separation protocol reduced the irrelevant part of the environmental matrices by a mean of $95 \pm 4\%$ (\pm SD, dw, $n = 16$). The highest matrix reduction was achieved for AS ($98 \pm 1\%$), followed by MBS ($97 \pm 1\%$), MSS ($94 \pm 1\%$) and FSS ($91 \pm 4\%$, $n = 4$ each). AS dw reduction was significantly higher than FSS ($p < 0.01$). The mean recovery rate for all four synthetic polymers (PP, PS, PMMA and PET-G) over all sample replicates was $99 \pm 4\%$. Spiked MP with a large diameter (0.5–1 mm) were recovered at a rate of $100 \pm 2\%$, and those with a small diameter (0.3–0.5 mm) were recorded at a rate of $98 \pm 4\%$. The highest spike recovery rate was observed for the MSS samples, from which $100 \pm 2\%$ of spiked MP (of all polymer types and sizes) were recovered, followed by $99 \pm 3\%$ for the AS replicates, $99 \pm 3\%$ for the FSS replicates and $97 \pm 5\%$ for the MBS replicates. PP (both size fractions) had the highest recovery rate from all four environmental matrices ($99 \pm 3\%$), followed by PS ($99 \pm 3\%$), PMMA ($99 \pm 4\%$), and PET-G ($98 \pm 5\%$; Fig. 1, Table S3).

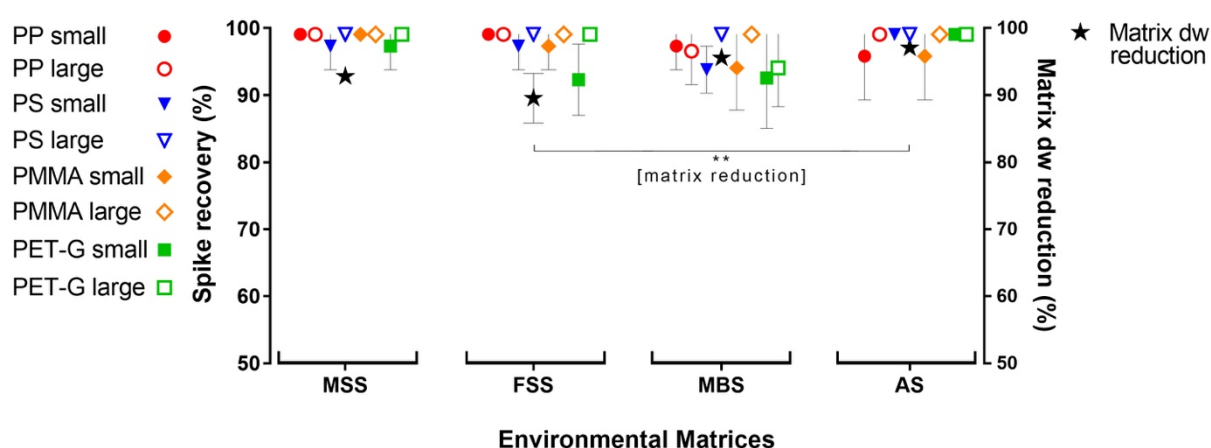


Fig. 1 Mean matrix dry weight (dw) reduction and spike recovery rates (both in %) for the four polymer fragment types (PP, PS, PMMA and PET-G) from four environmental matrices: marine suspended surface solids (MSS), fluvial suspended surface solids (FSS), marine beach sediments (MBS), and agricultural soil (AS). Error bars indicate the standard deviation ($n = 4$ for every data point plotted). The small spiked polymer particles had a diameter of 0.3–0.5 mm ($n = 15$ per polymer and replicate), the large spiked particles were 0.5–1 mm in diameter ($n = 10$ per polymer and replicate; resulting in a total of 4×25 MP particles = 100 spikes for each of the 16 experimental replicates). There was no significant difference in total microplastics recovery rates between tested environmental matrices ($p > 0.05$). The dw matrix reduction rates of FSS and AS samples differed significantly (** = $p < 0.01$).

A before-and-after comparison using ATR-FTIR spectroscopy confirmed that the spiked polymers were not chemically altered during treatment (Fig. S6, S8, S10 and S12). The non-destructive nature of the protocol is an important factor for bias-reduced environmental analysis; some published protocols involve potentially plastic-modifying steps such as acidic or alkaline purification (Claessens et al., 2013; Liebezeit and Dubaish, 2012) or ultrasonication (Löder and Gerdts, 2015).

Fluvial suspended solids samples (FSS) turned out to be the hardest to separate (Fig. 1), due to their high proportions of low-density biogenic particulate matter. Therefore, five non-spiked Rhine River FSS samples were subjected to the oil separation protocol for validation. Through the castor oil separation the environmental matrix could initially be reduced by $51 \pm 11\%$ dw. A subsequent H_2O_2 treatment of these remaining residues resulted in a significantly higher final dw matrix reduction of $82 \pm 6\%$ (Fig. 2). Clearing up the environmental matrix generally will also have a positive effect on the visual microplastic recovery rates, as sample insight improves on removal of non-plastic particles (Ivleva et al., 2017). We identified a total of 978 synthetic particles, distributed very heterogeneously between the five samples. This large range of MP concentrations represents the highly variable pollution levels of the different Rhine River stretches (Mani et al., 2015; Mani et al., 2019). Using the castor oil separation protocol, a mean $74 \pm 13\%$ of environmental MP could be retrieved in the upper oil phase (totally 773 MP particles retrieved from the upper oil phase, Fig. 2). Of the totally 205 MP particles retrieved from the lower aqueous and solid phase upon oil separation, the non-spiked Rhine River samples exhibited a large proportion of PS (76%, Fig. S4). This was unexpected, as the overall recovery rate for PS particles in the spike-recovery experiment was 99%. PS opaque microbeads (33%) and PS foam (29%) were the largest contributors to the aqueous and solid PS abundance (Fig. S4). The microbeads in the aqueous and solid phase ($n = 67$) stemmed from only one of the five environmental Rhine River samples. In an earlier study of the Rhine River such microbeads were identified to most likely be ion exchange resin (IER) beads (Mani et al., 2019). Possibly, the ion-active surface of IER beads weakens their lipophilicity, thus resulting in their relatively low recovery rate upon oil separation (67%). The other dominant shape-category found in the lower aqueous and solid phase was foams (68 of 205 MP, of which 60 were PS). Remarkably, despite their very low density ($0.01\text{--}0.45 \text{ g cm}^{-3}$; Winterling and Sonntag, 2011) only 70% of foamed PS retained in the oil phase after separation. Possibly, their rough, scraggly surface promotes heteroaggregation with ambient, denser solid environmental particles and thus causes their settling below the oil phase (Kooi et al., 2018). Nevertheless, the Rhine River sample findings demonstrates the applicability of the method to genuine field samples, albeit

not quite yielding the same high level of recovery as in the spiking experiment. Among both the oil as well as the aqueous and solid phase of the Rhine River samples after separation, there was a high congruence of MP category abundance (solid fragments, foams, spherules, etc., Fig. S4). However, the variety and abundance of different polymer types was distinctively poorer in the aqueous and solid phase (Fig. S4). Fibres were present in both fractions but not accounted for in this investigation as their sound environmental and polymer identification is reportedly highly bias-afflicted (Löder and Gerdts, 2015; Hidalgo-Ruz et al., 2012). Due to the vast heterogeneity of MP abundance among the five Rhine River samples (11–692 MP) a statistical investigation of shape-related separation efficiency was not possible. Two samples with the highest MP abundances (692 and 235 MP) majorly influence the shape-related MP separation patterns depicted in Fig. S4. This test reveals that weathered environmental MP, potentially clustered in compact heteroaggregates with non-plastic suspended solids, are not as well separable from the surrounding matrix as the spiked MP.

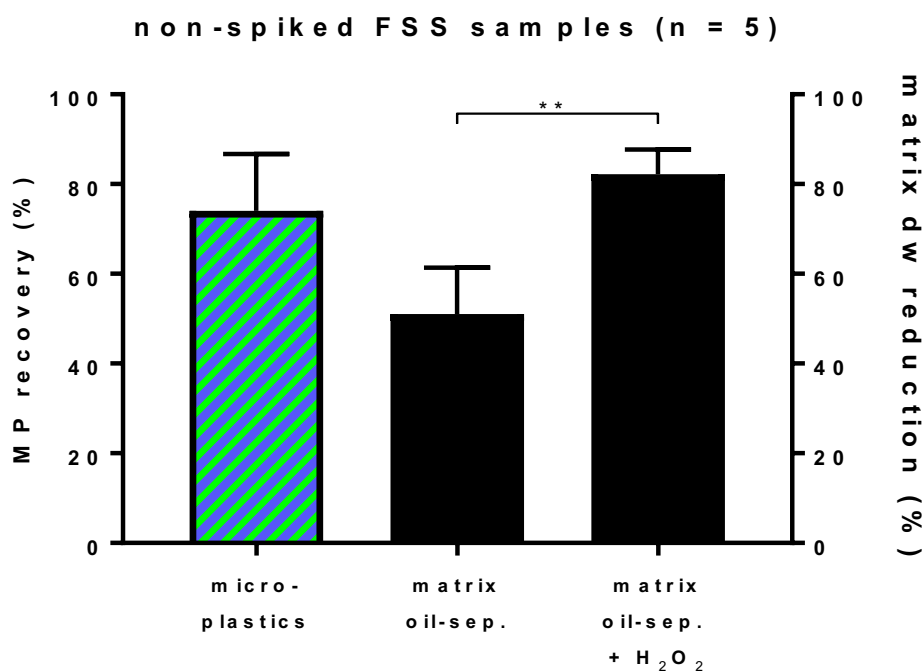


Fig. 2 Mean percentage (+ SD) of recovered microplastics (MP) from the five non-spiked Rhine River fluvial surface suspended solids samples (FSS, green and blue hatched column, left). The centre and right-hand columns show the mean percentage (+ SD) of dw matrix reduction after the oil separation and after subsequent H₂O₂ treatment, respectively ($n = 5$). The dw matrix reduction was significantly higher after H₂O₂ treatment (** = $p < 0.01$).

Characteristics and composition of the environmental matrices, such as FSS, may strongly vary depending on the season of collection, yielding varying abundance of e.g. lipophilic chitin crustacean exoskeletons (Löder et al., 2017). Furthermore, weathered, environmental MP are prone to alterations in their visual and chemical characteristics (Ter Halle et al., 2016). Such potential modifications were apparent in the retrieved environmental microplastics in the form of e.g. fading colours and surface cracks. This finding alludes to the potential need for better disaggregation of environmental FSS samples prior to, and additional purification after oil separation.

3.2. Properties and advantages of a castor oil-based separation approach

In this study, we present a rapid, reliable method to extract commonly found MP with various polymeric characteristics from four typical environmental matrices, FSS, MSS, MBS and AS, that yields high polymer recovery and matrix reduction rates. In contrast to separation and purification protocols involving numerous treatment and sample transfer steps (e.g. Löder et al., 2017), the presented oil separation is non-toxic and performed practically entirely within a closed system, which is a great advantage in terms of reducing the risk of sample contamination. Furthermore, there is minimal necessity for sample transfer between containers during the protocol, and hence the risks of sample losses or contamination during transfer exposure are minimised. We show, however, that depending on the quality of the environmental matrix, additional purification after oil separation can be highly beneficial (e.g. using H₂O₂). Therefore, this oil separation protocol may, depending on the matrix at hand, serve as a valuable alternative to density separation, but not always as a replacement for further purification measures. Application of this single protocol to an array of distinct matrices fosters the potential for comparative research on MP pollution across different environmental compartments (BASEMAN, 2017), while avoiding the need to use expensive and potentially hazardous reagents such as ZnCl₂ (Imhof et al., 2012) and NaI (Nuelle et al., 2014) in density-based separation protocols or H₂O₂ (Löder and Gerdts, 2015) in enzymatic/oxidative purification protocols. The efficient isolation of any sample residue offered by the oil separation protocol represents an immensely important factor required for the success of both automatic and manual spectroscopic MP assessment techniques (Löder et al., 2017).

Previously reported separation techniques resulted in matrix reduction rates of up to 80% for MBS using fluidisation and flotation (Nuelle et al., 2014) and 98% for MSS using enzymatic digestion (Löder et al., 2017). In comparison, the matrix reduction rate of this oil separation protocol (95 ± 4%) lies in the upper ranges of these other techniques. The presented castor oil separation protocol achieved very high MP spike-recoveries from four different matrices which

are almost identical to an earlier published oil extraction protocol (Crichton et al., 2017) which was only tested on sediments (99 ± 4 vs. $99 \pm 1.4\%$). Previous work on MBS using fluidisation and flotation reported spike recovery rates of between 18 and 100% (Stolte et al., 2015) and 91–99% (Nuelle et al., 2014). Spiked MP were recovered from MSS at a rate of $84 \pm 3\%$ using an enzymatic digestion protocol (Löder et al., 2017) and 96–100% using the Munich Plastic Sediment Separator (MPSS; Imhof et al., 2012). In comparison, the here presented protocol resulted in spike recovery rates of $99 \pm 4\%$ over all tested matrices.

3.3. Chemical considerations and background to the lipophilic castor oil approach

The natural castor oil employed in this protocol consists of approximately 99% long-chain C_{18} fatty acids (~90% ricinoleic acid, $C_{18}H_{34}O_3$; Salimon et al., 2010). The high molecular weight of these long-chain aliphatic hydrocarbon-dominated fatty acids enables stable attraction between the non-polar lipophilic component of the fatty acid molecules and the non-polar lipophilic carbohydrate surface of synthetic polymer fragments (e.g. PP $[C_3H_6]_n$) in a quasi-micellar manner. Furthermore, castor oil features one of the highest viscosities of the natural plant oils (>300 cP vs. <200 cP for canola oil), allowing the formation of a thick oil layer around the polymer fragments. The oil-polymer clusters have a lower overall density than water – even for high-density plastics such as PET-G (1.27 g cm^{-3}). Therefore, these clusters move to the top of the separation funnel, where they merge with the castor oil and become separated from the lower aqueous environmental matrix phase. Due to the presence of a hydroxyl group on its twelfth C atom, ricinoleic acid is sufficiently polar to easily dissolve in EtOH following the oil separation procedure.

In contrast to density-based separation approaches the here presented castor oil based microplastic separation protocol relies on the lipophilic and at the same time hydrophobic properties of synthetic hydrocarbon polymers (Rice and Gold, 1984; Mato et al., 2001). Within the separation funnel, separation and stratification of the liquid water/matrix and oil phases are driven by both chemical and gravitational forces. Hence, suspended solids with a specific density lower than water ($\sim 1 \text{ g cm}^{-3}$) but higher than castor oil ($\sim 0.96 \text{ g cm}^{-3}$) settle in the top layer of the water and solid phase, just below the oil phase. This phenomenon presents a challenge to precise manual separation of the water and oil phases while handling the polytetrafluorethylene (PTFE) stopcock during sample release for filtration. Especially during the separation of FSS, large residues settled at the oil-water interface, which ultimately increased the total mass of solids oil-extracted from the matrix, thus limiting the matrix reduction rate for this matrix. In a previously published canola oil separation method, an additional enzymatic digestion step was applied when excess biomass was encountered during

separation (Crichton et al., 2017). Indicated by the strong reduction rates of non-oleophilic matrix, as presented in our manuscript, it is most probable that highly biofouled MP, where contact between the castor oil and the polymer is inhibited, would not be separated as efficiently as unfouled MP. For samples where MP are strongly biofouled (Zettler et al., 2013; Kirstein et al., 2016) we would recommend applying sample digestion (Löder et al., 2017) prior to oil separation to remove excess biogenic material from polymers. Further research is needed concerning the castor oil recovery potential specifically of biofouled, weathered, smaller (<0.3 mm) and denser MP (e.g. polytetrafluorethylene [PTFE] $\sim 2.2 \text{ g cm}^{-3}$; AFT Fluorotec, 2016). We suggest repeating the separation process for the lower lying water-matrix phase in a series of further separation run-throughs. In our hands, a series of further separation run-throughs led to further separation and enhanced the rates of recovery, but residue reduction and MP recovery clearly depended on the environmental matrix and the characteristics of the MP particles (such as size, tendency to form aggregates etc.).

4. Conclusions

Still today, after more than a decade of intensive research on microplastics worldwide, at least two major handicaps prevail: (i) there is a downright lack of uniformity in sampling, processing and analysis within the scientific community, and (ii) the inevitable separation and purification of environmental samples prior to the identification and analysis of potential plastics is more often than not enormously time and material consuming as well as prone to sample manipulation. Every methodology (e.g. oil-, density-, electro- or visual separation) ultimately quantifies a spectrum of the possible variables. Besides developing uniform protocols to guarantee comparability of environmental data, knowing the limits of each method is crucial, as it will facilitate to identify the most appropriate approach for every given case. Here, we were able to present a separation protocol for microplastics from environmental matrices which is highly simple and extremely efficient regarding the investments of time, material resources and health/environmental risk. The very same procedure was successfully demonstrated on four different types of environmental samples from the hydro- and lithosphere where the anthroposphere overlaps or affects them. This advance could possibly lead to a break-through in improving methodical homogeneity across the field and accelerate the accumulation of ever so important data for moving to the next crucial steps in microplastics sciences – namely, evaluating their ecological impact and finding mitigation and solution measures.

Acknowledgements

The authors gratefully acknowledge the officers and crew of the Swiss police vessels in Brugg and Basel, the Spanish vessel FIRMM Vision in Tarifa, as well as the German Waterway and Shipping Administration (WSA) vessels VSS Köln in Bad Honnef and VSS Grieth in Rees for their generous support in collecting the environmental samples. We would also like to extend our appreciation to Prof. Dr. Luiz Felipe De Alencastro and his team from the Swiss Federal Institute of Technology Lausanne, for the loan of a Manta Trawl and valuable counselling. Warm gratitude for impeccable laboratory guidance is expressed towards the technical assistants Nicole Seiler-Kurth and Heidi Schiffer at the Man-Society-Environment Program, Department of Environmental Sciences, University of Basel. We would also like to forward our gratitude to the reviewers for critically evaluating our initial manuscript and providing input that substantially enhanced the quality of this work. And finally, very special thanks go to Andrea Devlin, PhD, chief editor of Science Editing Experts, for her immaculate and fast proof reading and language support. This study was partially funded by the World Wide Fund for Nature (WWF) Switzerland.

References

- AFT Fluorotec, 2016. The properties and advantages of PTFE.
<https://www.fluorotec.com/news/blog/the-properties-and-advantages-of-polytetrafluoroethylene-ptfe/>. Accessed 21 February 2019.
- BASEMAN, 2017. Interdisciplinary Research for Good Environmental Status.
<http://www.jpi-oceans.eu/baseman>. Accessed 9 May 2018.
- Bergmann, M., Lutz, B., Tekman, M.B., Gutow, L., 2017a. Citizen scientists reveal: Marine litter pollutes Arctic beaches and affects wild life. *Mar. Pollut. Bull.* 125 (1-2), 535–540. doi:10.1016/j.marpolbul.2017.09.055.
- Bergmann, M., Wirzberger, V., Krumpfen, T., Lorenz, C., Primpke, S., Tekman, M.B., Gerdt, G., 2017. High quantities of microplastic in Arctic deep-sea sediments from the HAUSGARTEN observatory. *Environ. Sci. Technol.* 51 (19), 11000–11010. doi:10.1021/acs.est.7b03331.
- Bosker, T., Behrens, P., Vijver, M.G., 2017. Determining global distribution of microplastics by combining citizen science and in-depth case studies. *Integr. Environ. Assess. Manag.* 13 (3), 536–541. doi:10.1002/ieam.1908.
- Claessens, M., van Cauwenberghe, L., Vandegehuchte, M.B., Janssen, C.R., 2013. New techniques for the detection of microplastics in sediments and field collected organisms. *Mar. Pollut. Bull.* 70 (1-2), 227–233. doi:10.1016/j.marpolbul.2013.03.009.
- Cole, M., Lindeque, P., Halsband, C., Galloway, T.S., 2011. Microplastics as contaminants in the marine environment: A review. *Mar. Pollut. Bull.* 62 (12), 2588–2597. doi:10.1016/j.marpolbul.2011.09.025.
- Cole, M., Webb, H., Lindeque, P.K., Fileman, E.S., Halsband, C., Galloway, T.S., 2014. Isolation of microplastics in biota-rich seawater samples and marine organisms. *Sci. Rep.* 4, 4528. doi:10.1038/srep04528.
- Crichton, E.M., Noël, M., Gies, E.A., Ross, P.S., 2017. A novel, density-independent and FTIR-compatible approach for the rapid extraction of microplastics from aquatic sediments. *Anal. Methods* 9 (9), 1419–1428. doi:10.1039/C6AY02733D.
- Eerkes-Medrano, D., Thompson, R.C., Aldridge, D.C., 2015. Microplastics in freshwater systems: A review of the emerging threats, identification of knowledge gaps and prioritisation of research needs. *Water Res.* 75, 63–82. doi:10.1016/j.watres.2015.02.012.

- European Union, 2018. Strategy for plastics in a circular economy. https://ec.europa.eu/commission/publications/documents-strategy-plastics-circular-economy_en. Accessed 10 October 2018.
- Felsing, S., Kochleus, C., Buchinger, S., Brennholt, N., Stock, F., Reifferscheid, G., 2018. A new approach in separating microplastics from environmental samples based on their electrostatic behavior. *Environ. Pollut.* 234, 20–28. doi:10.1016/j.envpol.2017.11.013.
- GESAMP, 2016. Sources, fate and effects of microplastics in the marine environment: Part two of a global assessment 93. GESAMP, 221 pp. <http://www.gesamp.org/site/assets/files/1275/sources-fate-and-effects-of-microplastics-in-the-marine-environment-part-2-of-a-global-assessment-en.pdf>. Accessed 14 December 2018.
- Gewert, B., Ogonowski, M., Barth, A., MacLeod, M., 2017. Abundance and composition of near surface microplastics and plastic debris in the Stockholm Archipelago, Baltic Sea. *Mar. Pollut. Bull.* 120 (1-2), 292–302. doi:10.1016/j.marpolbul.2017.04.062.
- Geyer, R., Jambeck, J.R., Law, K.L., 2017a. Production, use, and fate of all plastics ever made. *Sci. Adv.* 3 (7), e1700782. doi:10.1126/sciadv.1700782.
- Geyer, R., Jambeck, J.R., Law, K.L., 2017b. Supplementary Material, Production, use, and fate of all plastics ever made. *Sci. Adv.* 3 (7), e1700782. doi:10.1126/sciadv.1700782.
- Hidalgo-Ruz, V., Gutow, L., Thompson, R.C., Thiel, M., 2012. Microplastics in the marine environment: A review of the methods used for identification and quantification. *Environ. Sci. Technol.* 46 (6), 3060–3075. doi:10.1021/es2031505.
- Hong, S.H., Shim, W.J., Hong, L., 2017. Methods of analysing chemicals associated with microplastics: A review. *Anal. Methods* 9 (9), 1361–1368. doi:10.1039/C6AY02971J.
- Imhof, H.K., Schmid, J., Niessner, R., Ivleva, N.P., Laforsch, C., 2012. A novel, highly efficient method for the separation and quantification of plastic particles in sediments of aquatic environments. *Limnol. Oceanogr. Methods* 10 (7), 524–537. doi:10.4319/lom.2012.10.524.
- Ivleva, N.P., Wiesheu, A.C., Niessner, R., 2017. Microplastic in aquatic ecosystems. *Angew. Chem. Int. Edit.* 56 (7), 1720–1739. doi:10.1002/anie.201606957.
- Jahnke, A., Arp, H.P.H., Escher, B.I., Gewert, B., Gorokhova, E., Kühnel, D., Ogonowski, M., Potthoff, A., Rummel, C., Schmitt-Jansen, M., Toorman, E., MacLeod, M., 2017.

- Reducing uncertainty and confronting ignorance about the possible impacts of weathering plastic in the marine environment. *Environ. Sci. Technol. Lett.* 4 (3), 85–90.
doi:10.1021/acs.estlett.7b00008.
- Käppler, A., Fischer, D., Oberbeckmann, S., Schernewski, G., Labrenz, M., Eichhorn, K.-J., Voit, B., 2016. Analysis of environmental microplastics by vibrational microspectroscopy: FTIR, Raman or both? *Anal. Bioanal. Chem.* 408 (29), 8377–8391. doi:10.1007/s00216-016-9956-3.
- Kirstein, I.V., Kirmizi, S., Wichels, A., Garin-Fernandez, A., Erler, R., Löder, M., Gerdt, G., 2016. Dangerous hitchhikers? Evidence for potentially pathogenic *Vibrio* spp. on microplastic particles. *Mar. Environ. Res.* 120, 1–8. doi:10.1016/j.marenvres.2016.07.004.
- Kooi, M., Besseling, E., Kroeze, C., van Wezel, A.P., Koelmans, A.A., 2018. Modeling the fate and transport of plastic debris in freshwaters: Review and guidance, in: Wagner, M., Lambert, S., Besseling, E., Biginagwa, F.J. (Eds.), *Freshwater microplastics. Emerging environmental contaminants? The handbook of environmental chemistry. Volume 58.* Springer, pp. 125–152. doi:10.1007/978-3-319-61615-5
- Liebezeit, G., Dubaish, F., 2012. Microplastics in beaches of the East Frisian islands Spiekeroog and Kachelotplate. *Bull. Environ. Contam. Toxicol.* 89 (1), 213–217.
doi:10.1007/s00128-012-0642-7.
- Löder, M.G.J., Gerdt, G., 2015. Methodology used for the detection and identification of microplastics – A critical appraisal, in: Klages, M., Gutow, L., Bergmann, M. (Eds.), *Marine Anthropogenic Litter.* Springer, pp. 201–227.
- Löder, M.G.J., Imhof, H.K., Ladehoff, M., Löschel, L.A., Lorenz, C., Mintenig, S., Piehl, S., Primpke, S., Schrank, I., Laforsch, C., Gerdt, G., 2017. Enzymatic purification of microplastics in environmental samples. *Environ. Sci. Technol.* 51 (24), 14283–14292.
doi:10.1021/acs.est.7b03055.
- Lots, F.A.E., Behrens, P., Vijver, M.G., Horton, A.A., Bosker, T., 2017. A large-scale investigation of microplastic contamination: Abundance and characteristics of microplastics in European beach sediment. *Mar. Pollut. Bull.* 123 (1-2), 219–226.
doi:10.1016/j.marpolbul.2017.08.057.
- Mani, T., Blarer, P., Storck, F.R., Pittroff, M., Wernicke, T., Burkhardt-Holm, P., 2019. Repeated detection of polystyrene microbeads in the Lower Rhine River. *Environ. Pollut.* 245, 634–641. doi:10.1016/j.envpol.2018.11.036.

- Mani, T., Hauk, A., Walter, U., Burkhardt-Holm, P., 2015. Microplastics profile along the Rhine River. *Sci. Rep.* 5, 17988. doi:10.1038/srep17988.
- Mato, Y., Isobe, T., Takada, H., Kanehiro, H., Ohtake, C., Kaminuma, T., 2001. Plastic resin pellets as a transport medium for toxic chemicals in the marine environment. *Environ. Sci. Technol.* 35 (2), 318–324. doi:10.1021/es0010498.
- Nuelle, M.-T., Dekiff, J.H., Remy, D., Fries, E., 2014. A new analytical approach for monitoring microplastics in marine sediments. *Environ. Pollut.* 184, 161–169. doi:10.1016/j.envpol.2013.07.027.
- Rice, M.R., Gold, H.S., 1984. Polypropylene as an adsorbent for trace organics in water. *Anal. Chem.* 56 (8), 1436–1440. doi:10.1021/ac00272a052.
- Rillig, M.C., 2012. Microplastic in terrestrial ecosystems and the soil? *Environ. Sci. Technol.* 46 (12), 6453–6454. doi:10.1021/es302011r.
- Rodrigues, M.O., Abrantes, N., Gonçalves, F.J.M., Nogueira, H., Marques, J.C., Gonçalves, A.M.M., 2018. Spatial and temporal distribution of microplastics in water and sediments of a freshwater system (Antuã River, Portugal). *Sci. Total Environ.* 633, 1549–1559. doi:10.1016/j.scitotenv.2018.03.233.
- Salimon, J., Noor, D.A.M., Nazrizawati, A.T., Firdaus, M.Y.M., Noraishah, A., 2010. Fatty acid composition and physicochemical properties of Malaysian castor bean *Ricinus communis* L. seed oil. *Sains Malays.* 39 (5), 761–764.
- Sedlak, D., 2017. Three lessons for the microplastics voyage. *Environ. Sci. Technol.* 51 (14), 7747–7748. doi:10.1021/acs.est.7b03340.
- Silva, A.B., Bastos, A.S., Justino, C.I.L., da Costa, J.P., Duarte, A.C., Rocha-Santos, T.A.P., 2018. Microplastics in the environment: Challenges in analytical chemistry – A review. *Anal. Chim. Acta* 1017, 1–19. doi:10.1016/j.aca.2018.02.043.
- Stolte, A., Forster, S., Gerdt, G., Schubert, H., 2015. Microplastic concentrations in beach sediments along the German Baltic coast. *Mar. Pollut. Bull.* 99 (1-2), 216–229. doi:10.1016/j.marpolbul.2015.07.022.
- Ter Halle, A., Ladirat, L., Gendre, X., Goudouneche, D., Pusineri, C., Routaboul, C., Tenailleau, C., Duployer, B., Perez, E., 2016. Understanding the fragmentation pattern of marine plastic debris. *Environ. Sci. Technol.* 50 (11), 5668–5675. doi:10.1021/acs.est.6b00594.

- Winterling, H., Sonntag, N., 2011. Rigid Polystyrene Foam (EPS, XPS). *Kunststoffe international* 10, 18–22.
- Zettler, E.R., Mincer, T.J., Amaral-Zettler, L.A., 2013. Life in the “plastisphere”: Microbial communities on plastic marine debris. *Environ. Sci. Technol.* 47 (13), 7137–7146. doi:10.1021/es401288x.
- Zhang, G.S., Liu, Y.F., 2018. The distribution of microplastics in soil aggregate fractions in southwestern China. *Sci. Total Environ.* 642, 12–20. doi:10.1016/j.scitotenv.2018.06.004.

Supporting Information

SI 2: Using castor oil to separate microplastics from four different environmental matrices

Table S1 Details of materials and instruments used in the protocol, as mentioned in section 2. *Materials and Methods* in their respective order of occurrence.

Material / Instrument	Details
Neuston net mesh	0.3 mm mesh cods, attached to a metal and bamboo construction.
Geological sieves	1.0, 0.5, 0.3 mm; Retsch, Haan, Germany
Incubator for drying samples at 40 °C	BINDER BD 115, Tuttlingen, Germany
Scales for weighing samples to nearest mg	Mettler Toledo XS 105 DualRange, Columbo OH, USA
Heated laboratory stirrer	Schott laboratory stirrer SLR, Mainz, Germany
Grinder for polymer fragmentation	Merlin 123 household grinder, WS-Teleshop, Neudorf, Austria
Stereomicroscope	Olympus SZ61, Tokyo, Japan
Fourier-Transform Infrared Spectrometer (FT-IR)	Bruker ALPHA, platinum Diamond-ATR QuickSnap Sampling Module, Bruker, Billerica, MA, USA
Software Opus 7.5	Bruker, Billerica, Massachusetts, USA; B-KIMW ATR-IR Polymers, Plastics and Additives, 898 entries, library is available upon request
Castor oil	Cold pressed, organic, lot-no.: 1703A0138, Armonia GmbH, Azmoos, Switzerland https://www.armonia-shop.ch/online-shop/basis%C3%B6le-1/
Separation funnel	Lenz, Sqibb-F., grad., 2000 mL, PTFE-cock NS 18,8; ground joint NS 29/32
Filter paper	Hahnemühle DP 1505 110, pore size: 25 µm, diameter: 11 cm, Dassel, Germany
Labware detergent	Mucasol universal detergent, Schülke, Norderstedt, Germany
Hydrogen peroxide, H ₂ O ₂ (30%)	Sigma-Aldrich, St. Louis, MO, USA

Table S2 Basic characteristics of the four environmental matrices separated with the oil separation protocol.

Name	Sample description	sampling location	date	Figs.
MBS Marine Beach Sediment	Clastic sediment, consisting mainly of quartz; low organic content (< 1%)	36°00'42.8"N, 5°36'31.3"W, Atlantic, Tarifa, Andalusia, Spain	09/2017	S1 (A)
AS Agricultural Soil	Agricultural soil	47°31'57.6"N, 7°36'53.5"E, Münchenstein, canton of Basel Country, Switzerland	10/2017	S1 (B)
MSS Marine Suspended Surface Solids	Suspended surface solids; mainly algae and fine sand	36°00'40.9"N, 5°35'41.7"W, Mediterranean, Tarifa, Andalusia, Spain	09/2017	S1 (C)
FSS Fluvial Suspended Surface Solids	Suspended surface solids; 90% organic biogenic content	47°32'26.3"N, 7°36'59.3"E, Saint-Albanteich, Basel, canton of Basel-City, Switzerland	01/2018	S1 (D)
<i>FSS (n = 5)</i> environmental samples for the calibration of the oil separation protocol	Suspended surface solids; 90% organic biogenic content	<ol style="list-style-type: none"> 1. 47°30'16.8"N 8°14'14.0"E, 86.3 m³, Limmat River, Untersiggenthal, canton of Aargau, Switzerland 2. 47°33'19.6"N, 7°35'54.8"E, 94.4 m³, Rhine River, Basel, canton of Basel-City, Switzerland 3. 47°33'25.9"N, 7°36'27.8"E, 85.6 m³, Rhine River, Basel, canton of Basel-City, Switzerland 4. 50°37'47.0"N, 7°12'47.1"E, 70.3 m³, Rhine River, Bad Honnef, North Rhine-Westphalia, Germany 5. 51°45'22.6"N, 6°24'06.7"E, 84.7 m³, Rhine River, Rees, North Rhine-Westphalia, Germany 	<p>08/2016</p> <p>09/2016</p> <p>09/2016</p> <p>09/2016</p> <p>09/2016</p>	No fotos

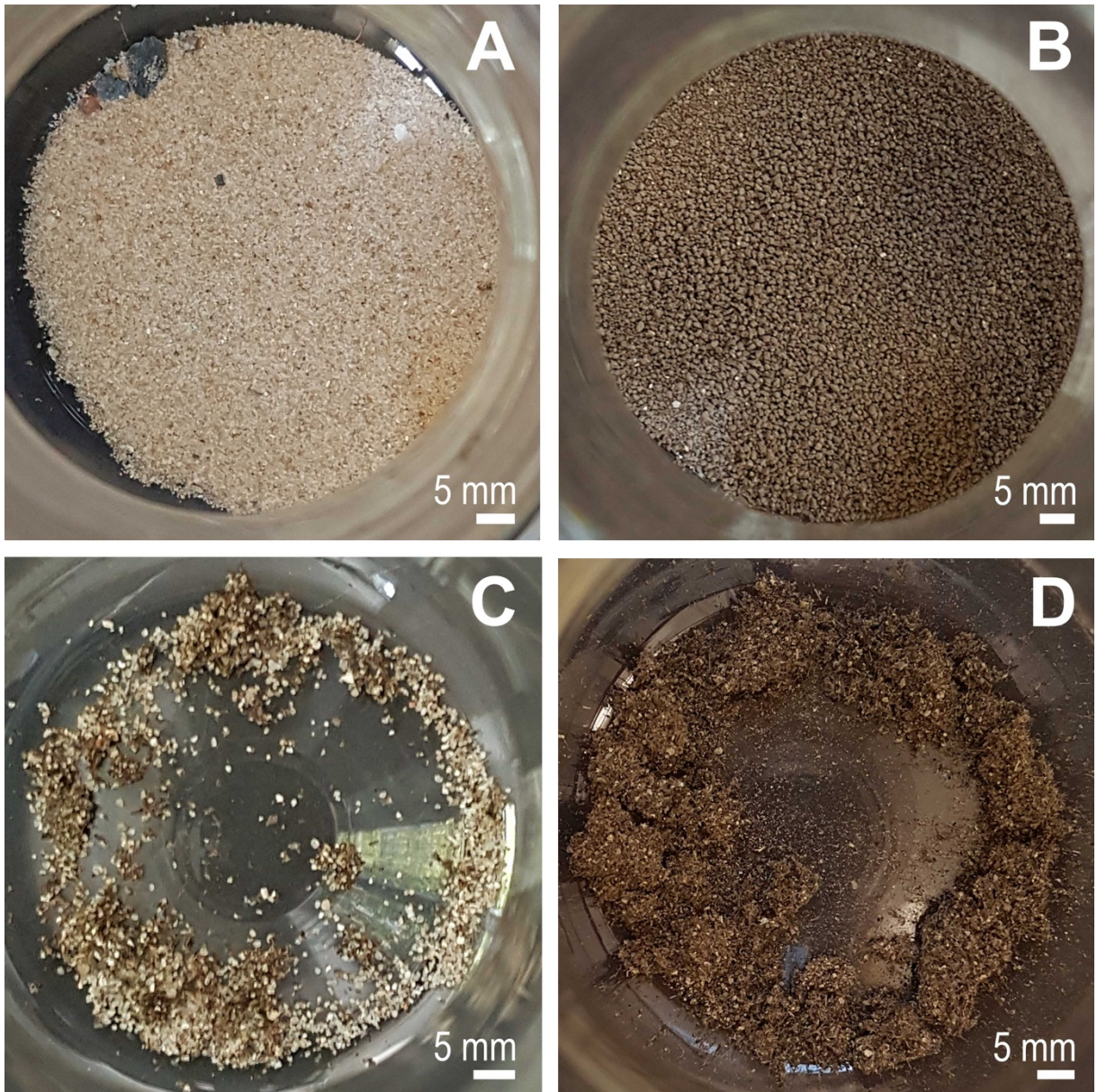


Fig. S1 Environmental matrix samples before performing the oil separation protocol. (A) Marine beach sediment (MBS), (B) agricultural soil (AS, 10 g each) and (C) marine suspended surface solids (MSS), (D) fluvial suspended surface solids (FSS, 1 g each).

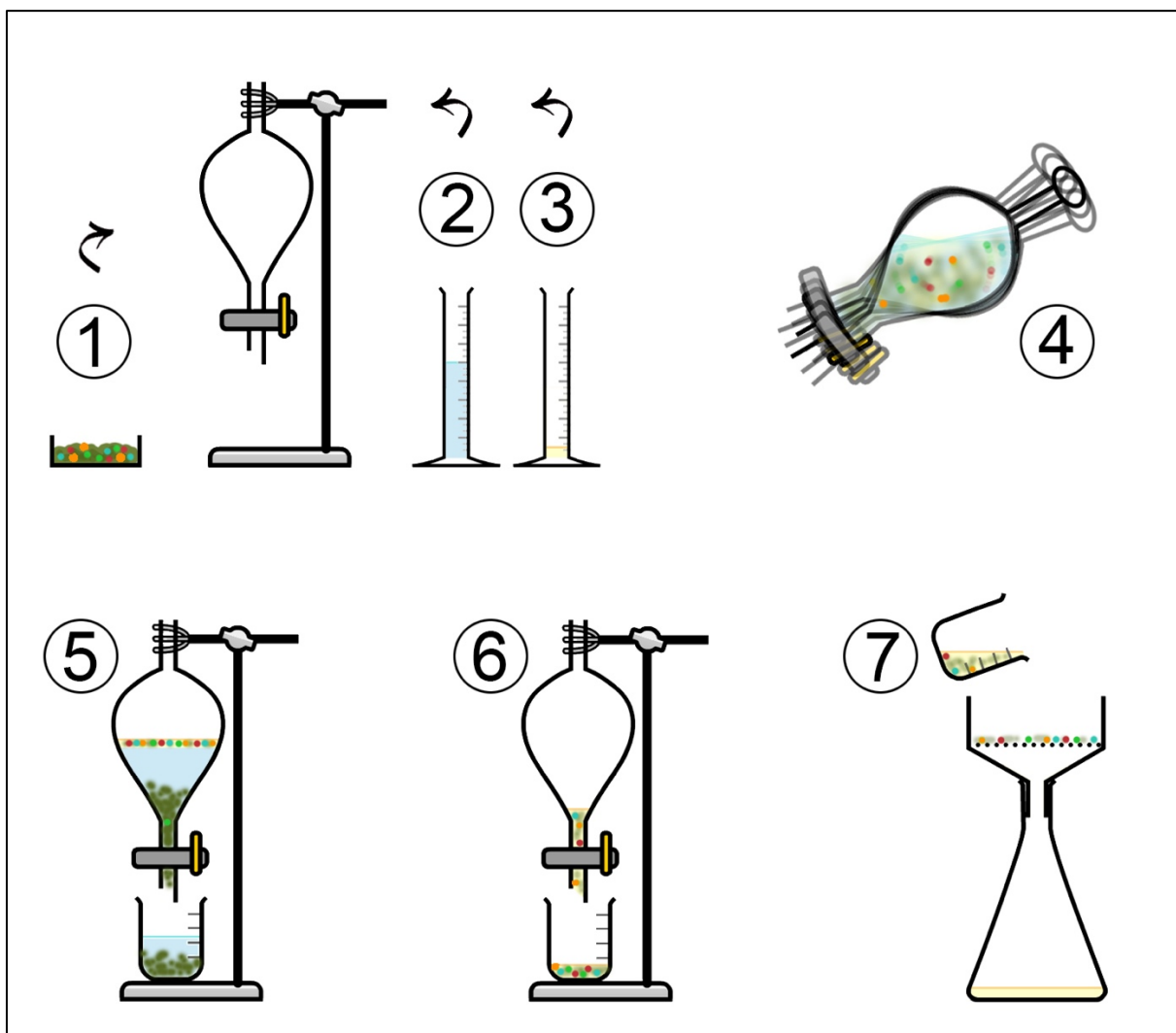


Fig. S2 Castor oil separation protocol depicted in seven steps: add environmental sample (1) and 100 mL of aq. dest. water (2) to the separation funnel and make sure to wet the entire sample. Next, add 10 mL of Castor oil (3) to the separation funnel. Seal and shake the separation funnel for 1 min (4). Let the mixture separate and release lower, aqueous and solid phase (5). Release oil phase to different container (6) and filter oil phase for the recovery of microplastics (7). Diagram was constructed using the CHEMIX School software v2.8.1 (Arne Standnes, Bergen, Norway).

Table S3 Petrochemical polymer spike recovery rates and environmental matrix reduction rates for all experiment replicates ($n = 4$ for each matrix).

Environmental matrix	replicate	Recovery rate for reference polymer particles								Environmental matrix dw reduction
		Small particles (0.3–0.5 mm)				Large particles (0.5–1 mm)				
		PP ($n = 15$)	PS ($n = 15$)	PMMA ($n = 15$)	PET-G ($n = 15$)	PP ($n = 10$)	PS ($n = 10$)	PMMA ($n = 10$)	PET-G ($n = 10$)	
MSS	1	100%	100%	100%	100%	100%	100%	100%	100%	94%
	2	100%	100%	100%	100%	100%	100%	100%	100%	95%
	3	100%	93%	100%	100%	100%	100%	100%	100%	93%
	4	100%	100%	100%	93%	100%	100%	100%	100%	93%
FSS	1	100%	100%	100%	100%	100%	100%	100%	100%	92%
	2	100%	100%	100%	93%	100%	100%	100%	100%	93%
	3	100%	93%	93%	87%	100%	100%	100%	100%	92%
	4	100%	100%	100%	93%	100%	100%	100%	100%	85%
MBS	1	100%	93%	87%	87%	100%	100%	100%	100%	96%
	2	100%	100%	100%	100%	100%	100%	100%	100%	98%
	3	100%	93%	100%	100%	90%	100%	100%	90%	96%
	4	93%	93%	93%	87%	100%	100%	100%	90%	96%
AS	1	100%	100%	100%	100%	100%	100%	100%	100%	97%
	2	100%	100%	100%	100%	100%	100%	100%	100%	99%
	3	100%	100%	100%	100%	100%	100%	100%	100%	98%
	4	87%	100%	87%	100%	100%	100%	100%	100%	98%

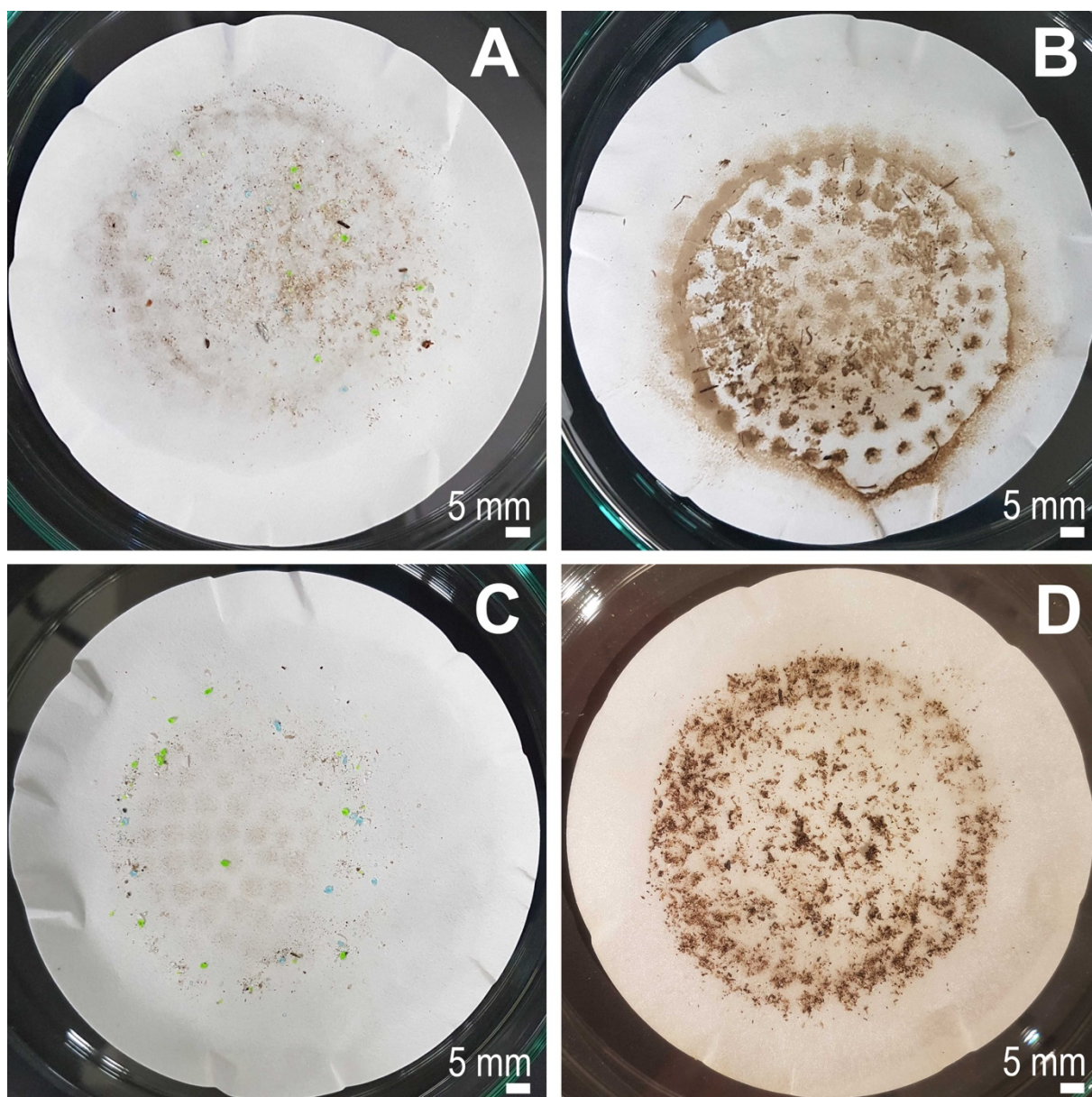


Fig. S3 Environmental matrix residues and recovered spiked microplastic particles (blue: PS, green: PET-G; size range: 0.3–1 mm, visible in panels A and C) on cotton/cellulose filter paper (Hahnemuehle DP 1505 110, pore size: 25 μm , diameter: 11 cm, Dassel, Germany) after performing the MOSeS protocol. (A) Marine beach sediment (MBS), (B) agricultural soil (AS), (C) marine suspended surface solids (MSS) and (D) fluvial suspended surface solids (FSS).

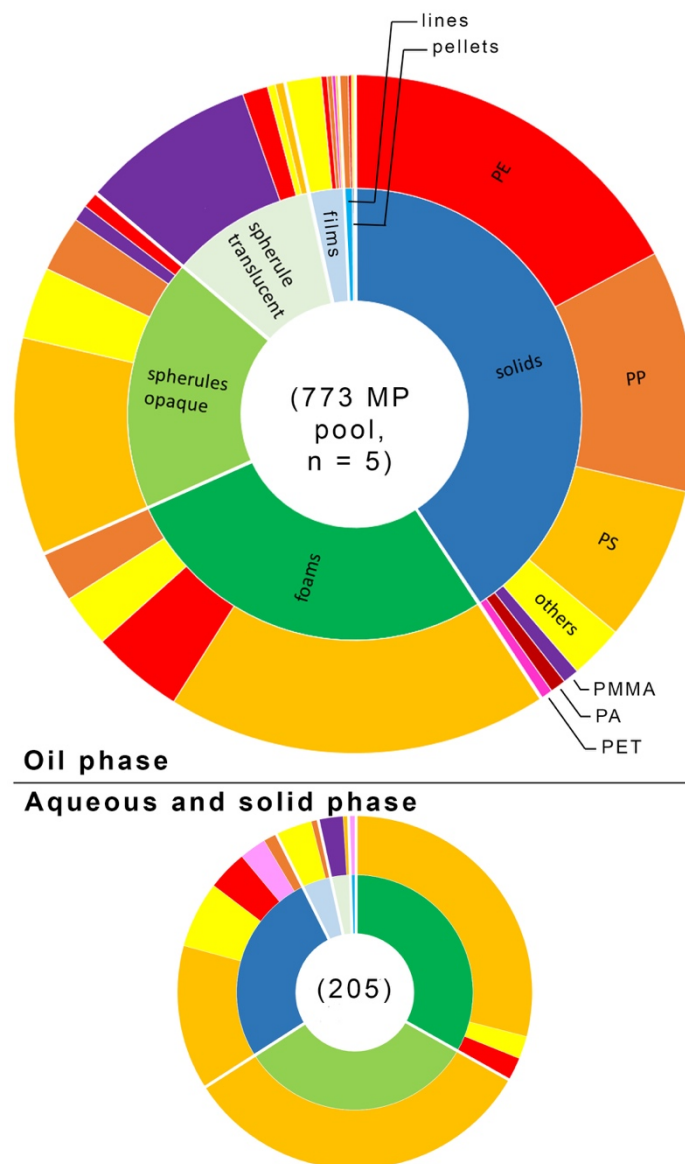


Fig. S4 Relative proportions of microplastic (MP) categories (inner ring) and polymer types (outer ring) retrieved from the oil (above) and the aqueous and solid phases (below), respectively. The two diagrams together represent the pooled amount of MP from five Rhine River surface samples. After oil separation the five upper oil phases combined contained 773 (79.1%) and the lower aqueous and solid phases contained 205 (20.9%) of the total 978 (100%) MP particles from all five samples. The two inner rings, representing the relative shares of MP categories, are scaled in percental proportion to each other by surface area according to number of particles.

Table S4 Characteristics of the polypropylene (PP) used for spiking.

Polymer/Density	Product	Retailer	Fragmentation method (0.3–0.5; 0.5–1.0 mm)
Polypropylene (PP), 0.84 g cm ⁻³	Kitchen strainer RONDO 32.5 cm red https://www.rothoshop.de/Kueche/Sieb-RONDO-32-5-cm.html , accessed on 05.06.18	Rotho Kunststoff AG, Würenlingen, Switzerland	Coffee grinder (Merlin 123 household grinder, WS-Teleshop, Neudorf, Austria), geological sieves (1 mm, 0.5 mm and 0.3 mm, Retsch, Haan, Germany)



Fig. S5 Large (left) and small (right) PP particles after recovery

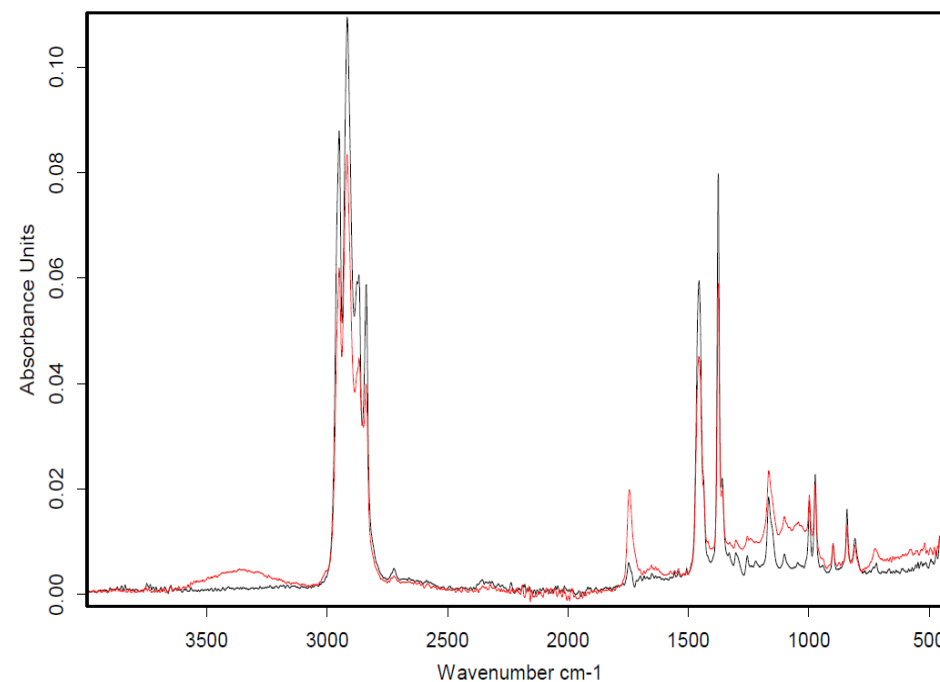


Fig. S6 FT-IR Spectrum of PP before (black) and after (red) separation using the MoSeS protocol (Bruker ALPHA, Billerica, MA, USA)

Table S5 Characteristics of the polystyrene (PS) used for spiking.

Polymer/Density	Product	Retailer	Fragmentation method (0.3–0.5; 0.5–1.0 mm)
Polystyrene (PS), 1.05 g cm ⁻³	Colourplast melting pellets medium-blue, article-ID: 607199 https://www.aduis.ch/colourplast-200-g.-mittelblau-art607199.aspx , accessed on 05.06.18	Creartec trend-design, Lindenberg, Germany	Coffee grinder (Merlin 123 household grinder, WS-Teleshop, Neudorf, Austria), geological sieves (1 mm, 0.5 mm and 0.3 mm, Retsch, Haan, Germany)



Fig. S7 Large (left) and small (right) PS particles after recovery

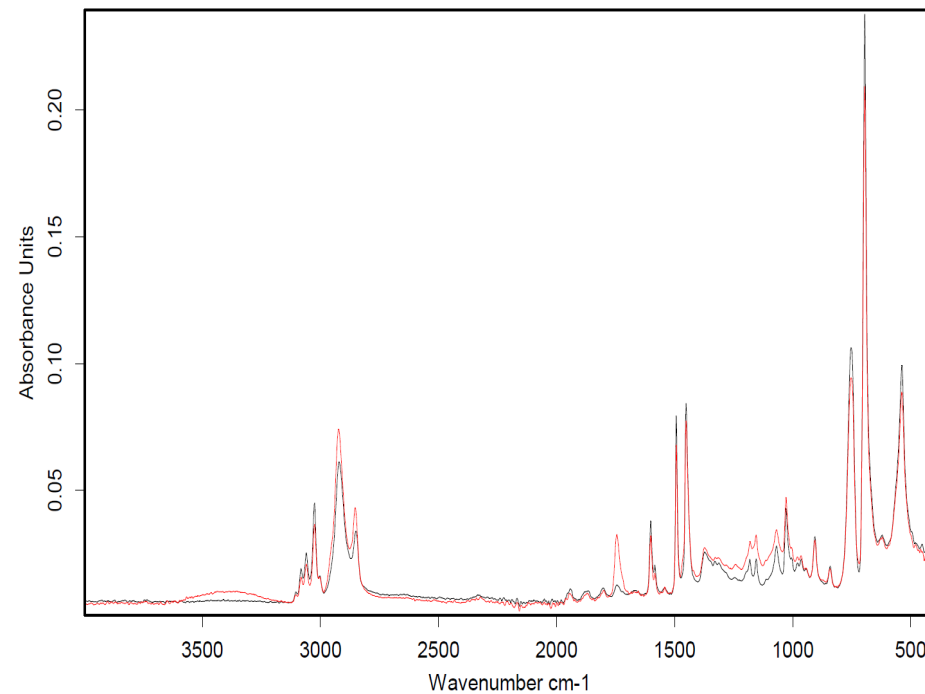


Fig. S8 FT-IR Spectrum of PS before (black) and after (red) separation using the MoSeS protocol (Bruker ALPHA, Billerica, MA, USA)

Table S6 Characteristics of the polymethyl methacrylate (PMMA) used for spiking.

Polymer/Density	Product	Retailer	Fragmentation method (0.3–0.5; 0.5–1.0 mm)
Polymethyl methacrylate (PMMA), 1.19 g cm ⁻³	Acrylic glass sheet (3 mm) Evonik, article-ID: 3000813 https://www.modulor.de/plexiglas-gs-farbig-3-mm-3-0-x-120-x-250-mm-orange-transparent-2c04.html , accessed on 05.06.18	Modulor Material Total, Berlin, Germany	coffee grinder (Merlin 123 household grinder, WS-Teleshop, Neudorf, Austria), geological sieves (1 mm, 0.5 mm and 0.3 mm, Retsch, Haan, Germany)



Fig. S9 Large (right) and small (left) PMMA particles after recovery

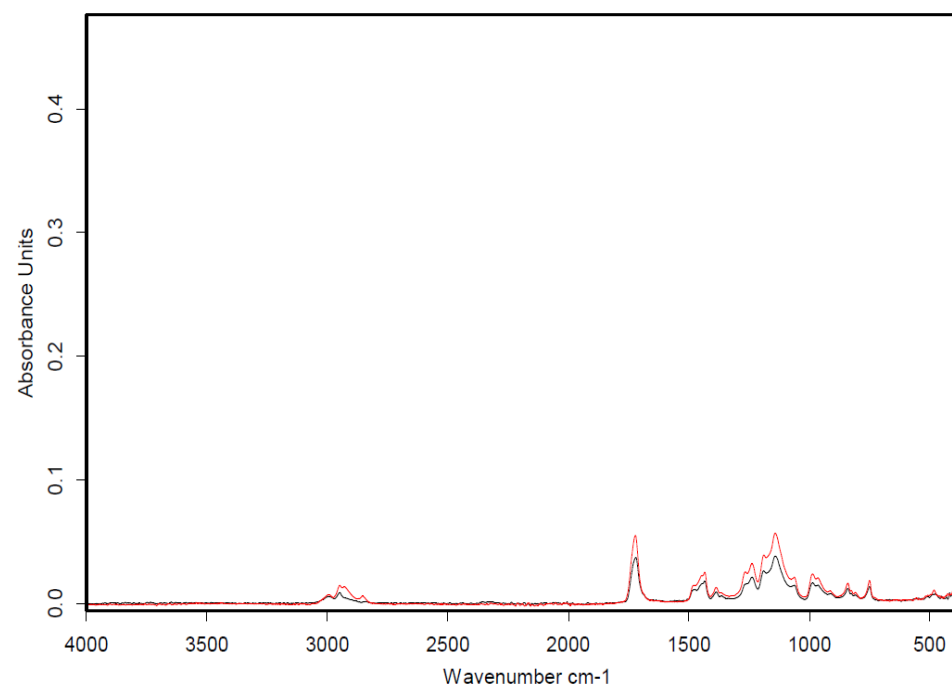


Fig. S10 FT-IR Spectrum of PMMA before (black) and after (red) separation using the MoSeS protocol (Bruker ALPHA, Billerica, MA, USA)

Table S7 Characteristics of the polyethylene glycol-modified (PET-G) used for spiking.

Polymer/Density	Product	Retailer	Fragmentation method (0.3–0.5; 0.5–1.0 mm)
Polyethylene terephthalate glycol-modified (PET-G), 1.27 g cm ⁻³	3D printer filament Minadax, article-ID: 16863 https://www.amazon.de/Qualitaet-PET-Filament-transparent-3D-Drucker-hergestellt-gr%C3%bcn/dp/B01781ERXE , Accessed on 05.06.18	Minadax online retail services, Dortmund, Germany	Coffee grinder (Merlin 123 household grinder, WS-Teleshop, Neudorf, Austria), geological sieves (1 mm, 0.5 mm and 0.3 mm, Retsch, Haan, Germany)

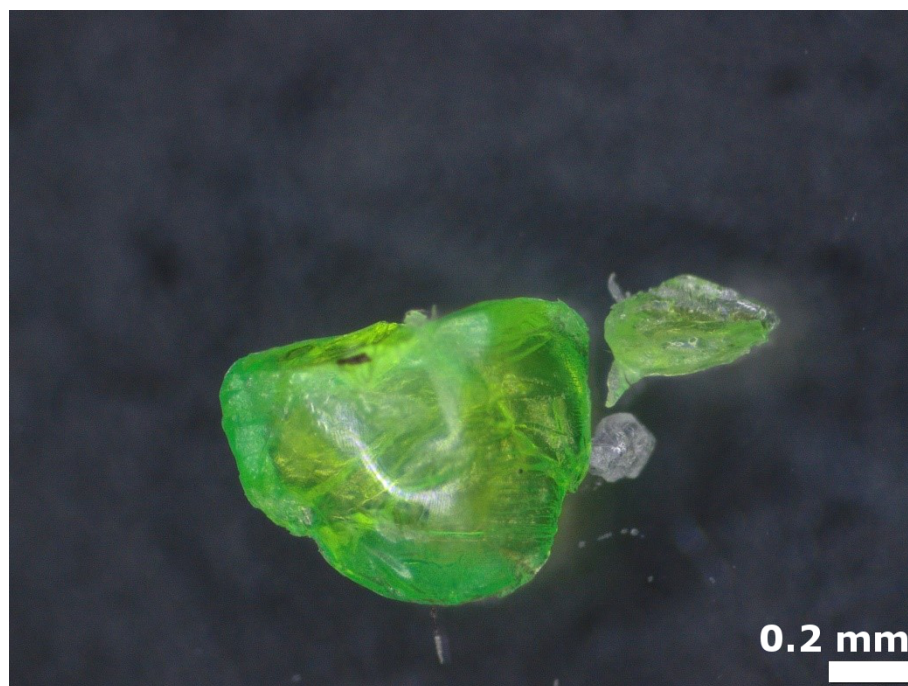


Fig. S11 Large (left) and small (right) PET-G particles after recovery

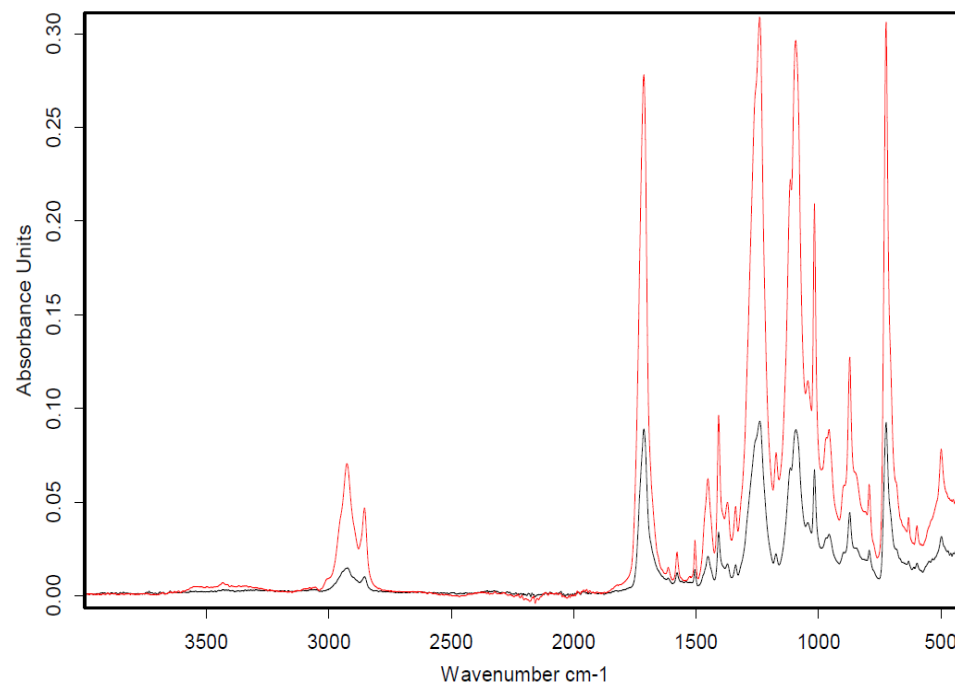


Fig. S12 FT-IR Spectrum of PET-G before (black) and after (red) separation using the MoSeS protocol

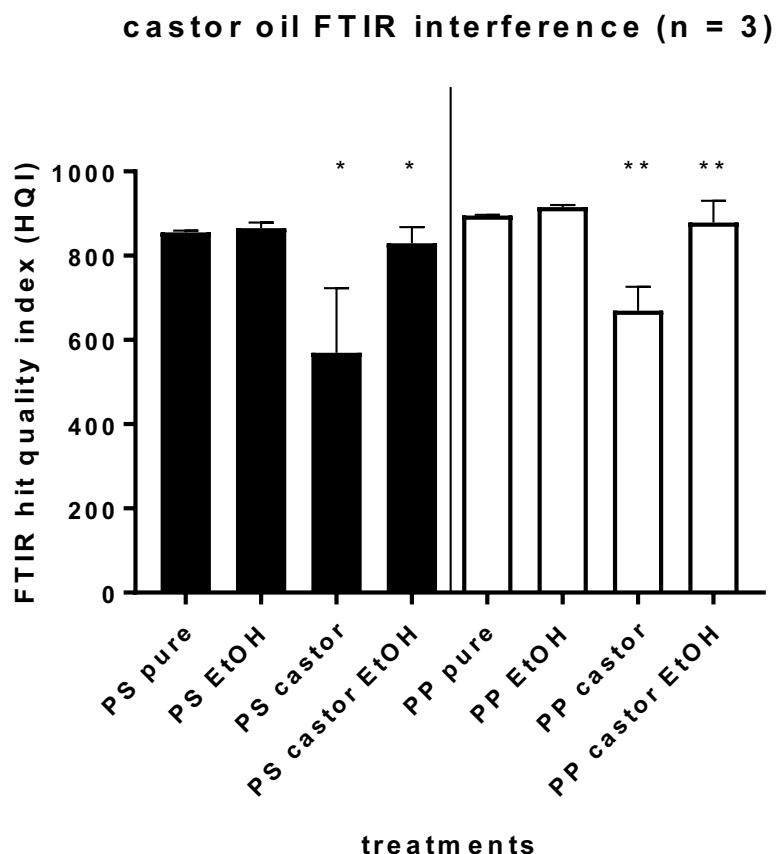


Fig. S13 Comparison of ATR-FTIR hit quality indices for four treatments of PS and PP virgin microplastics (0.5–1.2 mm, longest axis) using unpaired t tests. Columns marked with asterisks indicate significant differences between the treatments of interest (castor oil removal using EtOH; * = $p < 0.05$, ** = $p < 0.01$). $HQI > 700$ is regarded as a reliable level for confirming synthetic polymers (Obbard et al., 2014; Thompson et al., 2004).

References

- Obbard, R.W., Sadri, S., Wong, Y.Q., Khitun, A.A., Baker, I., Thompson, R.C., 2014. Global warming releases microplastic legacy frozen in Arctic Sea ice. *Earth's Future* 2 (6), 315–320. doi:10.1002/2014EF000240.
- Thompson, R.C., Olsen, Y., Mitchell, R.P., Davis, A., Rowland, S.J., John, A.W.G., McGonigle, D., Russell, A.E., 2004. Lost at sea: Where is all the plastic? *Science*. 304 (5672), 838. doi:10.1126/science.1094559.

Paper 3

Seasonal microplastics variation in nival and pluvial stretches of the Rhine River – From the Swiss catchment towards the North Sea

Thomas Mani ^a and Patricia Burkhardt-Holm ^a

^a Department of Environmental Sciences, The Man-Society-Environment Program,
University of Basel, Vesalgasse 1, 4051 Basel, Switzerland

Published 2020

in *Science of the Total Environment* 707, 135579.

DOI: 10.1016/j.scitotenv.2019.135579

Abstract

Rivers are pivotal carriers of microplastic (MP) towards the oceans. Investigative data on MP pollution in rivers at specific timepoints is continuously compiling. However, such snapshot data can only roughly indicate the long-term extent of contamination and particle fluxes; modelling studies informed by this limited data are prone to large uncertainties. The present study sought to narrow this knowledge gap by examining the differences in MP concentrations, loads and compositions at three nival tributaries and the Rhine River in Basel, Switzerland, as well as two downstream pluvial Lower Rhine River locations in Germany over four seasons throughout 2016–2017. MP concentrations (>0.3 mm) correlated positively with average water discharge and catchment size of the evaluated stream locations and MP concentrations were significantly higher at the downstream pluvial than upstream nival sites. There was no coherent pattern in MP concentration fluctuations between seasons across the six sites investigated, and no correlation with recent precipitation. These findings suggest that temporal variations in MP fluxes towards the North Sea through the year are dominated by the different discharge regimes along the river. This study also corroborates theoretical models that predict the highest MP loads move downstream the Rhine River during the European winter months.

1. Introduction

Plastic waste is an emerging contaminant on the global scale (Jahnke et al., 2017; Sedlak, 2017). Every year, an estimated 4.8–12.7 million tons of plastic enter the oceans (Cózar et al., 2014; Jambeck et al., 2015). Mechanical, physical and chemical stresses eventually fragment larger plastic items into secondary microplastic (MP, <5 mm; Andrady, 2017; Barnes et al., 2009). Together with emitted primary particles (e.g. exfoliating agents in care products; Fendall and Sewell, 2009) and ion-exchange resin beads (Mani et al., 2019a), secondary MP account for an estimated over 5 trillion MP particles afloat at sea (Eriksen et al., 2014), with many more below the surface and on the sea floor (van Cauwenberghe et al., 2013). It takes decades to centuries for MP to mineralise into their molecular and atomic constituents (O'Brine and Thompson, 2010; Ohtake et al., 1998), which contributes to severe environmental accumulation potential as global plastic demand and waste continue to dramatically increase (Andrady, 2017; Ellen Mc Arthur Foundation, 2016). Furthermore, MP are highly bioavailable and facilitate the transfer of inherent as well as adherent toxic compounds into organisms (Cole et al., 2011; Triebkorn et al., 2019).

Approximately 80% of marine polymer debris is widely believed to originate from land-based sources (Andrady, 2011; Jambeck et al., 2015; Wagner et al., 2014). Rivers, pivotal pathways for anthropogenic waste, transport 0.41–4 million tons of plastic to the oceans annually (Lebreton et al., 2017; Lechner et al., 2014; Schmidt et al., 2017). Consequentially, attention has turned to freshwater MP, with increasing numbers of rivers and lakes investigated (Eerkes-Medrano et al., 2015). The top 20 polluting rivers are responsible for 67% of the global riverine ocean plastic input, and 15 of these rivers are located in Asia. The peak is between May–October when, according to a worldwide model, over 74% of the annual riverine plastic transport towards the oceans occurs (Jambeck et al., 2015; Lebreton et al., 2017). In Europe, the Danube and the Rhine Rivers are two major ocean contributors moving reported annual plastic freights of 530–1,500 tons and 20–105 tons towards the Black and North Sea, respectively, in suspected seasonal patterns characterised by high winter loads (Lebreton et al., 2017; Lechner et al., 2014; Mani et al., 2015; Van der Wal et al., 2015).

MP have been studied in snapshot water surface data along the length of the Rhine River (Hess et al., 2018; Mani et al., 2015), at single strategic locations (Leslie et al., 2017; Van der Wal et al., 2015), in a one-off study of the shoreline surface sediments at the Rhine-Main confluence (Klein et al., 2015) and in the riverbed sediments at each one mid-stream location of the Middle and Lower Rhine (Mani et al., 2019c). Reported MP concentrations at the water surface range

from 1 to 17 particles m⁻³ (0.3–5 mm; Hess et al., 2018; Mani et al., 2015). The high variability in concentrations between samples and studies is generally attributed to different sampling seasons, environmental and anthropogenic factors, as well as laboratory processing and analysis methods (Hidalgo-Ruz et al., 2012). Above all, most MP investigations rely on single sampling campaigns that are temporally restricted to a few days (Blettler et al., 2018). In contrast, assessments of annual and multi-annual emission dynamics are often based on theoretical modelling approaches, which are prone to high uncertainty (Lebreton et al., 2017; Schmidt et al., 2017). Empirical, long-term investigations on the temporal and spatial dynamics of MP distribution in rivers worldwide are scarce (Blettler et al., 2018).

There is a knowledge gap regarding the seasonal differences in MP concentrations and fluxes, especially considering the characteristics of different river discharge regimes (e.g. nival or pluvial). In order to validate existing models and inform new simulations, extended insight into the interplay between regimes along a river catchment are vital. While anthropogenic activity will determine MP pollution levels at a given river section, the discharge regime will govern its fluxes downstream. Therefore, empirical investigations that include both varied anthropogenic activities and environmental factors, such as discharge dynamics, are essential. This study documents MP abundance, types and polymers in three Swiss tributaries and the Rhine River across an entire year, over four seasons (2016–2017). The geographical scope encompasses three previously identified Rhine River locations with characteristic MP findings, Basel (km 168), Bad Honnef (640) and Rees (837; Mani et al., 2015), as well as – for the first time – three major tributaries of its Swiss catchment, the Aare, Reuss and Limmat Rivers. The four rivers investigated in the present study cover nival (the Limmat, Reuss, Aare and the Rhine at Basel) as well as pluvial (the Rhine at Bad Honnef and Rees) discharge regimes. The nival regime displays low discharge in the winter months due to retention of liquid water in ice and snow and peaks around June due to the release of meltwater. The pluvial sections, in contrast, are characterised by the interplay of rain and evaporation and thus carry the most water in the winter months around January (Kleinn et al., 2005; Verbunt et al., 2006). The research design applied in this study sought to capture these discharge mannerisms over four samplings of the selected geographical locations throughout one year. We assessed the seasonal variation in MP concentrations, type (e.g. hard, foam, spherule; primary, secondary) and polymer compositions. We expect to observe upstream to downstream gradients in MP abundance, types and polymers, as well as an impact of seasonal discharge on particle concentrations and total particle fluxes.

2. Materials and methods

2.1. Sampling

Between April 2016 and February 2017, four sampling campaigns (SC1–SC4) were conducted at six locations between the Swiss Rhine River catchment at Brugg and the downstream German-Dutch border at Rees ($n = 15$ samples in total per sampling campaign, total of $n = 60$ for the entire study; see Fig. 1 as well as Supporting Information, Table S1). In Switzerland (CH), the Rhine tributaries Limmat and Reuss Rivers ($n = 2$ and $n = 1$ samples per campaign) were sampled immediately upstream of their Aare River confluences. The larger Aare itself was sampled both upstream ($n = 2$) and downstream ($n = 1$) of its Limmat and Reuss confluences for comparison. This whole region of river confluences (Aare, Reuss and Limmat) is called the *Swiss Wasserschluss*; their waters finally enter the Rhine River at Koblenz (CH) approximately 95 km downstream. Together with the Rhine, these three rivers are responsible for draining 68% of the Swiss geographical surface area towards the North Sea (Spreatico et al., 1992). In the Rhine River, samples were taken at Basel (CH, Rhine-kilometre [Rh-km] ~ 165 , $n = 3$), Bad Honnef (DE, Rh-km 640, $n = 3$) and Rees (Rh-km 837, $n = 3$) during each of the four campaigns. The sampling campaigns were conducted within one year at ~ 3 -month intervals in April (SC1), August/September (SC2), November/December (SC3) of 2016 and February 2017 (SC4). The temporal intervals were defined to capture the distinctive discharge patterns of the four nival discharge regime locations in Switzerland and the two pluvial discharge regime locations in Germany. MP were previously studied in the Swiss lakes relevant to the here investigated rivers: Lake Constance (Rhine), Lake Zurich (Limmat) and Lake Brienz (Aare; all Faure et al., 2015). However, this study is the first assessment of MP in the outflowing rivers of these lakes. The Rhine locations of Basel, Bad Honnef and Rees were selected to represent major points of interest identified in the first comprehensive investigation of surface MP in the Rhine River: Basel is the most upstream location of notable industry and commercial shipping and Bad Honnef and Rees yielded dramatically rising and peaking MP concentrations, respectively (Mani et al., 2015). The water surface was sampled using a Manta Trawl (aperture: 60×18 cm; Faure et al., 2012) equipped with a 0.3 mm mesh, a removable cod end (5Gyres, Los Angeles, CA, USA) and a mechanical flowmeter at the aperture centre (model 438 110; HYDRO-BIOS, Kiel, Germany). The Manta Trawl was deployed at the side of one vessel on the Limmat, Reuss and Aare Rivers and each a different vessel on the Rhine River at Basel, Bad Honnef and Rees, leaving a margin between the hull and the net to avoid bow-induced turbulence (Faure et al., 2012; Mani et al., 2015; Silva et al., 2018). Ten-minute samples were collected with the vessel facing upstream at a steady state relative to the shore, resulting in a

range of 25.2–200.9 m³ filtered water per trawl, amounting to a total of 5613.2 m³ for the entire study. For the Aare, Limmat, Reuss and Rhine at Basel, samples were taken from the centre of the river cross-section, at Bad Honnef and Rees, one sample was taken from the left-hand side, the centre and the right-hand side of the river cross-section per campaign. Intercepted suspended solids were transferred from the cod end of the Manta Trawl to clean glass jars (0.5 L) using adjacent river water in a glass Schott bottle as a rinsing agent. Each sample was mixed in ~40% ethanol (EtOH) in the glass jar before sealing the receptacle with a metal lid for transport to the lab. Samples were stored at room temperature (RT, ~21 °C) prior to further processing.

2.2. Sample processing

Samples were wet sieved using 0.3 mm, 1 mm and 5 mm mesh geological sieves (Retsch, Haan, Germany) and running distilled water (aq. dest.), creating three particle diameter fractions (0.3–1 mm, 1–5 mm and >5 mm; Mani et al., 2015). The 1–5 mm and >5 mm fractions were suspended in ~40% EtOH and stored in sealed glass jars at RT for subsequent visual and chemical analysis, while the 0.3–1 mm fractions underwent castor oil separation (Mani et al., 2019b) prior to visual and chemical analysis. In brief, the castor oil separation protocol is a refined approach based on the initial oil-based microplastic separation technique proposed by (Crichton et al., 2017), in which MP (lipophilic) are extracted from their surrounding environmental matrix by attracting the MP to an oil layer and segregating the non-MP suspended solids in a separation funnel. The protocol is capable of efficiently recovering different polymer types from various environmental matrices, including fluvial suspended solids, within a sealed off processing system, as well as omitting sample transfer, thus preventing sample contamination and loss (Mani et al., 2019b).

2.3. Visual particle sorting for chemical analysis

In the first step, the larger 1–5 mm and >5 mm fractions were rinsed and drained from the EtOH solution by filtration with running aq. dest. onto 0.3 mm mesh and subsequently transferred to glass Petri dishes. The smaller oil-separated 0.3–1 mm fractions were left on their filter paper from the oil separation (Hahnemühle DP 1505 110, pore size: 25 µm, diameter: 11 cm, Dassel, Germany), sealed in glass Petri dishes and remained untouched until the subsequent step.

Visual sorting of all three fractions on the residue filters was performed using delicate stainless-steel forceps and a stereomicroscope with LED super-lighting (Olympus SZ61, Tokyo, Japan). Due to an excess abundance of biogenic and plastic particles in 10 of the 36 smaller oil-separated 0.3–1 mm fractions from Basel (2 samples), Bad Honnef (4) and Rees (4), one geometrical quarter of each of these 10 round sample filters (resembling a pie slice of $\frac{1}{4}$ of the

filter area) were randomly selected and visually investigated. All four sampling seasons (SC1–4) are represented in this selection. The findings on these filters were subsequently multiplied by four to enable quantitative assessment of MP. Particles were identified as putative MP if they fulfilled two main characteristics on a 13-criterion decision chart that includes the tactile (e.g. denting capacity) and visual (e.g. shape and/or colour) properties of the particles (Fig. S1); the chart was assembled and extended based on (Masura et al., 2015; Norén, 2007). Positively selected particles were classified into one of eight possible shape categories (e.g. “fragment hard”, “fragment foam” or “spherule opaque”; Fig. S2). Fibres were not accounted for (i) because their polymer composition cannot be reliably analysed using applied attenuated total reflection Fourier transform infrared spectroscopy (ATR-FTIR) due to insufficient particle diameter and (ii) their high rate of false-positive identification as MP in visual investigation (Hidalgo-Ruz et al., 2012; Ivleva et al., 2017; Löder and Gerdt, 2015). Each particle was classified into one of seven predefined colour groups (Fig. S4). Particles were stored in sealed polystyrene 96-well plates for chemical analysis and backup (Cellstar; ThermoFisher Scientific, Waltham, MA, USA). All suspected particles for the 1–5 mm and >5 mm fractions, and using a high-spot sample approach, the first ten and every further tenth putative MP particle for every shape + colour category for the 0.3–1 mm fractions (i.e. “fragment hard_blue” Nos 1–10, 20, 30, ..., 100, 110, etc.) were photographed and their diameters were measured at the longest axis using a stereomicroscope equipped with a camera and imaging software (Olympus SZ61; Olympus SC50; Olympus CellSens Entry Version 1.17.16030.0). For 27 of the sixty 0.3–1 mm sample fractions, colour was not considered for the morphological category “fragment hard” in the FTIR analysis, due to the lack of substantial differences in polymer/colour combinations (Wang et al., 2017). Recently, a comprehensive guideline on monitoring and assessment of (micro)plastic litter was published, elaborating on the decisive methodological aspects of environmental investigations (GESAMP, 2019).

2.4. FTIR analysis

All photographed particles were chemically analysed using an ATR-FTIR spectrometer (Bruker ALPHA including a platinum Diamond-ATR QuickSnap Sampling Module; Bruker, Billerica, MA, USA or Excalibur 3100; Varian, Palo Alto, CA, USA). IR-Spectra were recorded over the wavenumber range of 4000–400 cm^{-1} at a resolution of 4 cm^{-1} , applying 24 scans (Fig. S3). Each spectrum was compared using Opus 7.5 software (Bruker) and the spectral correlation option with vector normalisation against two combined reference spectra libraries (BASEMAN, 2017; Bergmann et al., 2017; Primpke et al., 2018); Bruker B-KIMW ATR-IR Polymers, Plastics and Additives, 898 entries, Bruker or Bio-Rad, Hercules, CA, USA; ~90,000 entries).

The Bruker and Varian ATR-FTIR devices were used in succession as the research project evolved. The comparability of the spectral results was confirmed in collaboration with polymer analysis experts from Intertek, Switzerland. Particles achieving a synthetic polymer hit quality index (HQI) of >60% were considered confirmed MP. Of the total of 15,783 visually and tactually identified putative MP particles, 6522 were analysed by ATR-FTIR (~41%). Polymer types were grouped according to (Primpke et al., 2018).

2.5. Calculations, further data collection and statistics

Not all visually suspected MP particles were confirmed as synthetic polymers. To avoid overestimation of environmental concentrations, the confirmed MP concentrations $MP_{conc.}$ per sample were calculated using the following formula:

$$MP_{conc.} = \left(\frac{MP_{n\ vis}}{Spl.Vol.} \right) \times HQI_{600\ hit-rate} \times OilSep_{comp.} \quad (1)$$

where $MP_{conc.}$ is the confirmed MP concentration, $MP_{n\ vis}$ is the number of visually identified MP, $Spl.Vol.$ is the volume of filtered surface water in m³ of the respective sample, $HQI_{600\ hit-rate}$ is the ratio of HQI >60% hits to the total number of FTIR-analysed particles from the respective size range (0.3–1 mm, 1–5 mm or >5 mm) and $OilSep_{comp.}$ is the coefficient ((1/74)*100) to compensate for MP potentially lost during oil separation (74 ± 13% MP recovery rate according to Mani et al., 2019). The $HQI_{600\ hit-rate}$ for the 0.3–1 mm fraction was 0.609, 0.515 for the 1–5 mm fraction, and 0.246 for the >5 mm fraction; these were the ratios of positive HQI >60% hits in the respective size classes.

The relationship between MP concentrations, MP loads and precipitation (polluted runoff and flush events) was investigated. For this, the mean of the daily rainfall sums (mm day⁻¹) on the day of sampling and the two previous days were compared to MP concentrations and loads. For the nival locations, rainfall data was collected from the respective river watershed between the sampling location and the next upstream lake from IDAWEB (Swiss Confederation, meteorology and climatology department). For the pluvial sites, rainfall data was consulted from the Rhine River watershed within a 50 km radius upstream of the respective sampling sites from the Environmental Department Rhineland-Palatinate and North Rhine-Westphalia, respectively.

In an exploratory survey to observe putative MP foam-type origin (packaging and insulation material), riparian construction activity data within 10 km upstream of the sampling sites was collected from canton and commune agencies. Construction activity from the communes of

Brugg and Windisch (both canton of Aargau, Switzerland) was considered within a perimeter of 500 m to the respective riverbanks.

Statistical tests were performed using Graphpad Prism 8.1.2 (227) for macOS.

2.6. Quality assurance and quality control

To avoid plastic contamination, glassware and metalware were used whenever possible for processing samples. PTFE squirt bottles were used for aq. dest. and EtOH (70% and 96%). Samples were covered with glass (Petri dish) or metal (sealable jars) lids at all times when not under treatment or investigation. The lab was equipped with a sticky entrance doormat to prevent contamination of external particulate matter from the soles of the investigator's shoes. White lab coats (100% cotton) were worn at all times. Wet or residual castor oil-coated putative MP particles (0.3–1 mm fraction) were left to dry for 1 minute on the warm steel sample table of the Bruker device before FTIR analysis or rinsed with a drop of EtOH (96%; Mani et al., 2019b), respectively. Between FTIR analysis of different particles, the FTIR crystal was cleaned with a drop of EtOH (96%) and a Kimwipe (Kimberly-Clark, Irving, TX, USA). Approximately every 30 min, a blank background FTIR spectrum was recorded on the free, freshly cleaned sample crystal. To assess the contamination potential of samples exposed to the laboratory environment by airborne MP, the lab was periodically evaluated for airborne particles. Thoroughly rinsed glass Petri dishes exposed for 1.5–24 h (Bergmann et al., 2017) yielded potential MP fibres, but no evidence of other conspicuous particulate matter.

While the 1–5 mm and >5 mm fractions of the 60 samples were visually examined for MP by a single investigator, the samples from the 0.3–1 mm fraction were randomly distributed and sorted by five different investigators (pers. A, $n = 9$ samples; B, $n = 16$; C, $n = 17$; D, $n = 12$; E, $n = 6$). Despite rigorous guidelines for identification and categorisation of putative MP (Figs. S1–S4), differences between the detection rates of each investigator are inevitable (Hidalgo-Ruz et al., 2012; Ivleva et al., 2017; Löder and Gerdts, 2015). To assess these interindividual differences for the 0.3–1 mm fraction, three samples were selected for blind cross-checking by four of the five investigators. At random, the same quarters of the three selected filters were independently visually inspected and MP were quantified by all four investigators. The mean numbers (\pm SD) of identified putative MP varied from 101 ± 65 (Sample 1), 290 ± 147 (Sample 2) and 151 ± 104 (Sample 3) among the four investigators, demonstrating the great challenge of consistent visual identification (Dekiff et al., 2014). However, we found that the investigators who included larger numbers of visually putative MP generally achieved lower polymer hit ratios after FTIR, as a larger proportion of visually selected potential MP were not

confirmed to be plastic. Therefore, we can rely on the buffering effect of the hit ratio after FTIR to compensate for visual overestimation.

3. Results

3.1. Geographical and seasonal variations in MP concentrations

A total of 15,783 putative MP particles (0.3–5 mm) were visually selected from all samples, of which 6522 were analysed with FTIR (41%) and 3799 were finally verified as synthetic polymers (resulting in an overall 59% positive plastic hit ratio for analysed particles). Of the suspected 69 mesoplastics particles (>5 mm; Hartmann et al., 2019), 24% of the analysed particles were verified as polymers by FTIR (Table S2).

Verified mean MP (0.3–5 mm) concentrations ranged from 0.04–9.97 MP m⁻³ per sample ($n = 60$). Mesoplastics (>5 mm) were detected in 27 of the 60 samples, but at much lower concentrations of 5×10^{-4} –0.013 MP m⁻³. Mean MP concentrations per sampling campaign significantly increased from the Swiss Rhine catchment (0.04 ± 0.04 – 3.3 ± 2.1 MP m⁻³) downstream towards the German locations on the Rhine (2.7 ± 0.4 – 6.3 ± 2.6 MP m⁻³; Fig. 1). In Switzerland, over all four campaigns SC1–SC4, the Reuss River yielded the lowest average MP concentrations of 0.04–0.18 MP m⁻³ ($n = 1$ per campaign), followed by the Limmat River (0.09 ± 0.07 – 0.52 ± 0.03 MP m⁻³, $n = 2$), the Aare River (0.36 ± 0.38 – 0.67 ± 0.09 MP m⁻³, $n = 3$) and the Rhine River at Basel, just upstream of the Swiss-German Border (1.1 ± 1.5 – 3.3 ± 2.1 MP m⁻³, $n = 3$). We observed positive correlations between MP concentrations, average yearly discharge and catchment size (Fig. S5); but no persistent relation between MP concentrations and relative discharge levels in the 72 h leading up to the sampling event (Fig. S6).

For the German pluvial regime sample locations at Bad Honnef and Rees (each $n = 3$ per campaign), MP concentrations were highly variable and there was no visible trend in MP concentrations at specific times of year (Fig. 1). While the highest mean MP concentration at Bad Honnef (Rh-km 640) occurred in February 2017 (in SC4), the same campaign yielded the lowest mean concentrations at Rees (Rh-km 837), 197 km downstream of Bad Honnef (Fig. 1). Moreover, while the two lowest mean concentrations at Bad Honnef were recorded in April and September 2016 (2.7 ± 0.4 MP m⁻³, SC1; 4 ± 1.4 MP m⁻³, SC2), Rees yielded its highest concentrations in the same two campaigns (5.5 ± 3 MP m⁻³, SC1; 6.32 ± 2.6 MP m⁻³ SC2, Fig. 1). There was no correlation between rainfall amounts in the three days leading up to the sampling events and MP concentrations or MP loads, neither in the nival nor the pluvial sections.

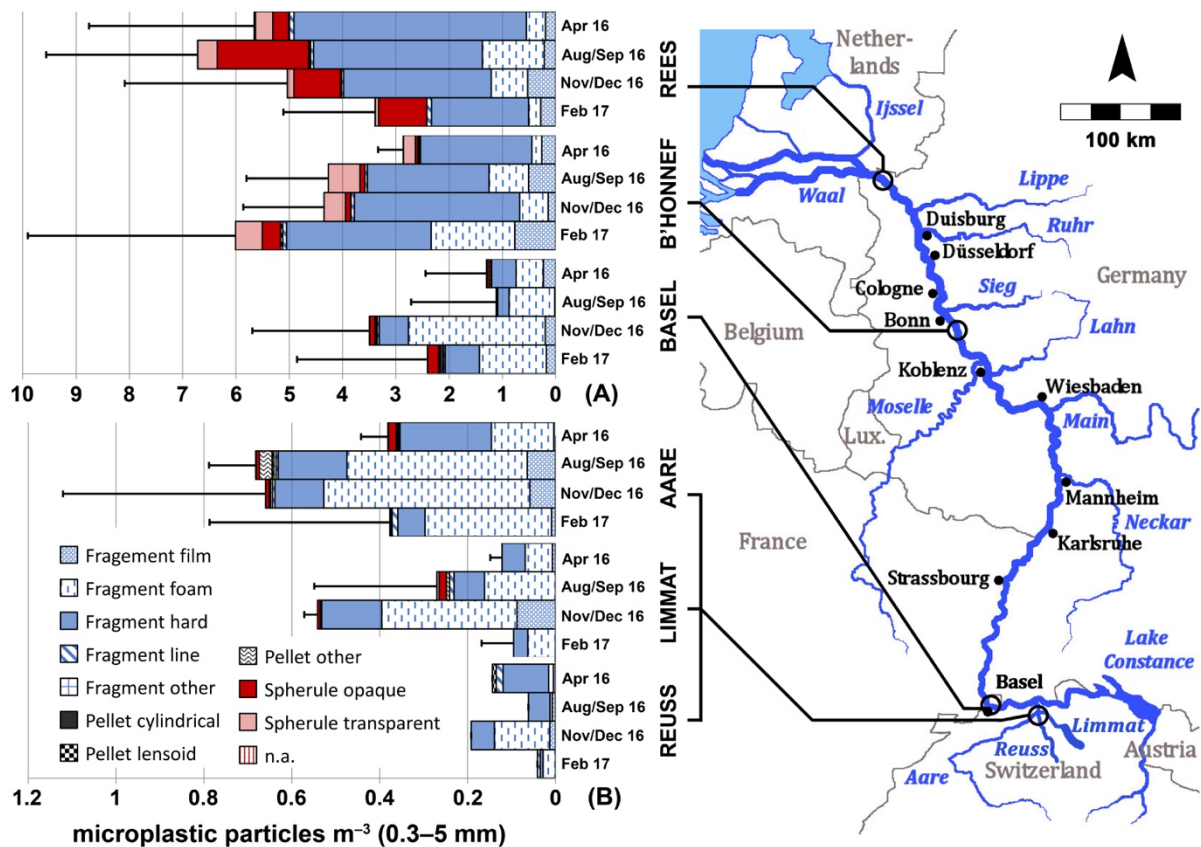


Fig. 1: Mean microplastic surface water concentrations (MP m^{-3}) in the Rhine River catchment recorded at four discrete times of year during 2016–2017. Error bars indicate standard deviation. Axes (A) and (B) feature different scales to improve visual access of lower MP concentration samples (B). Sampling locations comprise the three major Swiss tributaries Reuss ($n = 1$ per campaign), Limmat ($n = 2$) and Aare ($n = 3$) at Brugg, and the Rhine River at Basel, Switzerland as well as Bad Honnef ($n = 3$) and Rees ($n = 3$) on the Lower Rhine in Germany. Samples were collected in April (SC1), August/September (SC2) and November/December (SC3) of 2016 and February 2017 (SC4).

3.2. Geographical and seasonal occurrence of MP types

MP category diversity increased downstream from the Swiss nival tributaries towards the pluvial German sites (Figs. 1, S7). While the Reuss, Limmat, and Aare Rivers exhibited 3–5, 2–6, and 6–7 different MP categories per campaign, respectively, 6–8 MP categories were identified at every location from Basel downstream to Bad Honnef and Rees in all four sampling campaigns. Foam and hard-type fragment secondary MPs were the only types of MP found at all locations during every sampling campaign.

Specific geographical patterns in the relative abundance of MP types were observed. The four Swiss upstream locations yielded distinctly higher mean proportions of foam MP per sampling campaign ($53.8 \pm 20\%$) compared to the two downstream German locations ($13.2 \pm 6.8\%$). In contrast, the German locations yielded clearly higher proportions of hard fragments

($59.5 \pm 12.3\%$) than the Swiss sites ($33.1 \pm 18.1\%$; Fig. S7). Considering the increase in overall MP concentrations downstream from the nival to the pluvial section, the increase in the proportion of hard fragments is an indication of accumulating hard fragment input over the course of the river, rather than a decrease in the numbers of foam-type fragments, the concentrations of which remained comparable in Germany and Basel. In the Reuss and Limmat Rivers, film-type fragments occurred in all but three sampling events at proportions of 1.8–16.8% (the exceptions being SC4 Reuss, SC2 and SC4 Limmat). Suspected pre-production pellets occurred in very low proportions in 16 of the 24 sampling events (samples combined per location and SC, Fig. 1). The highest share of preproduction pellets was recorded in the Swiss Aare River (6.7%) where the verified mean MP concentration was at a mere $0.7 \pm 0.09 \text{ MP m}^{-3}$. Such primary MP occurrence phenomena may generally indicate discrete spillage events; however, the relatively small sample size and lack of comprehensive upstream spillage surveillance data hamper a conclusive assessment of this claim. There was a positive relationship between the occurrence of smaller (0.3–1 mm) and larger (1–5 mm) MP particles at all sites investigated (Fig. S8).

Primary MP occurred at distinctly higher concentrations at the downstream study sites Bad Honnef and Rees compared to the upstream Swiss investigation sites. Opaque and colourless transparent spherules occurred in Bad Honnef and Rees in 18 and 11 of the 24 sampling events, respectively.

Compared to the upstream Swiss locations, the concentrations and mean proportions of total MP per campaign were significantly higher in the downstream locations of Bad Honnef and Rees. While opaque MP spherules occurred in only a few samples at relatively low concentrations of 2×10^{-3} – 0.2 MP m^{-3} at the Swiss sites, similar beads were found in all Bad Honnef and Rees sample events. The concentration of opaque MP spherules ranged from 0.04– 0.34 MP m^{-3} in Bad Honnef, and was notably higher (0.3 – 1.7 MP m^{-3}) at Rees. Hence, the highest concentration of opaque spherules in a single sample was recorded at Rees in the September 2016 campaign at 2.9 MP m^{-3} , representing 29% of all MP in that single sample. Colourless, transparent spherules only occurred at three Swiss sampling events at mean concentrations of 2 – $8 \times 10^{-3} \text{ MP m}^{-3}$ (SC2 and SC4 in Basel and SC2 in the Aare), and peaked at Bad Honnef, where the mean proportion of colourless, transparent spherules over all four sampling campaigns was $9.7 \pm 2.9\%$ (up to 0.5 MP m^{-3}). Interestingly, 197 km downstream at Rees, the proportion of colourless, transparent spherules decreased to only $3.8 \pm 1.7\%$ over all

four campaigns (max. 0.37 MP m^{-3}). The seasonal variations in MP types followed no recognisable pattern.

3.3. Types of MP and their polymers

Fourteen main polymer types were identified among the 3799 confirmed microplastic particles by FTIR in the entire study (plus the category “others” denoting additive hits and non-polymer substances). Polyethylene (PE) was by far the most frequently found plastic. At the four Swiss sites, the analysed particles were represented by foam (50.3%), hard (36.9%) and film-type fragments (6.7%), followed by opaque spherules (4.4%) and a combined remainder (1.7%) of line fragments, lensoid pellets and transparent spherules (Fig. 2). The four most common MP type categories were dominated by PE, at proportions of 82.9% (foam), 60.8% (hard), 66.7% (film), and 51.4% (opaque spherules). Polystyrene (PS) was the second most common polymer for foam (12.1%), film (9.3%) and opaque spherules (17.1%), while, in contrast, polypropylene (PP) was the second most common hard fragment (25%, Fig. 2).

Compared with the nival Swiss region described above, the two German pluvial sample locations yielded clearly different MP category proportions and corresponding polymers: hard (46.5%), followed by foam fragments (16.8%), opaque (14.3%) and transparent (10.3%) spherules. Fragmented films represented 8.4% of MPs and line fragments and supposed pre-production nurdles accounted for the remaining 3.7%. Similar as in the upstream nival section, PE was the major polymer for foam (58.8%), hard (58.3%) and film-type fragments (55%) in the pluvial section. However, 73.3% of the opaque spherules in the pluvial section were PS (in contrast to 51.4% PE at the nival sites). Only 14.6% of the opaque spherules in the nival section were PE. Transparent spherules only occurred in substantial numbers in the pluvial section, and 76.8% were polymethyl methacrylate (PMMA, Fig. 2; see Fig. 3 for image examples of retrieved MP in the eight type categories).

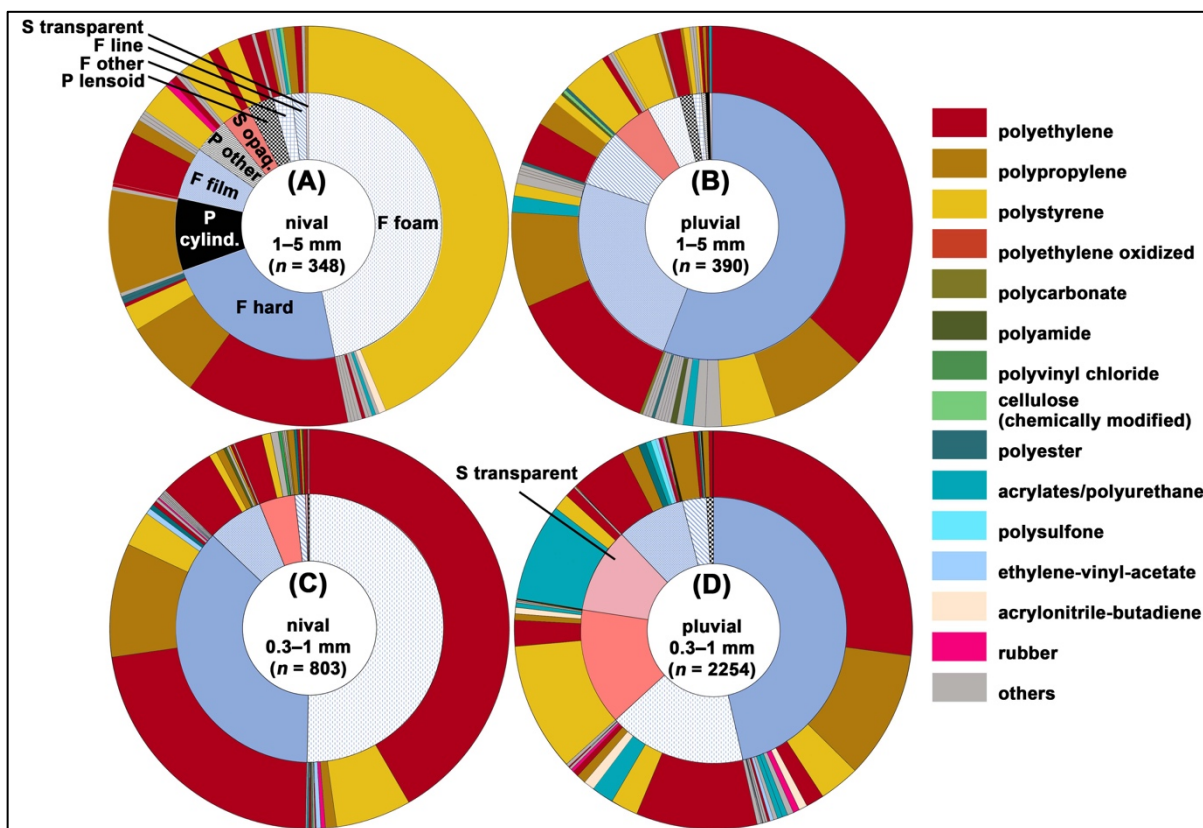


Fig. 2: Microplastic (MP) type categories and the respective polymers encountered in the 1–5 mm fractions (A, nival locations: Reuss, Limmat, Aare and Rhine at Basel; B, pluvial locations: Bad Honnef and Rees) and 0.3–1 mm fractions (C, nival; D, pluvial). “Others” denotes plastics additive and plastic related non-polymer findings. Data represents combined total FTIR-confirmed MP particles for the four sampling campaigns during April 2016 to February 2017. S = spherule; P = pellet; F = fragment.

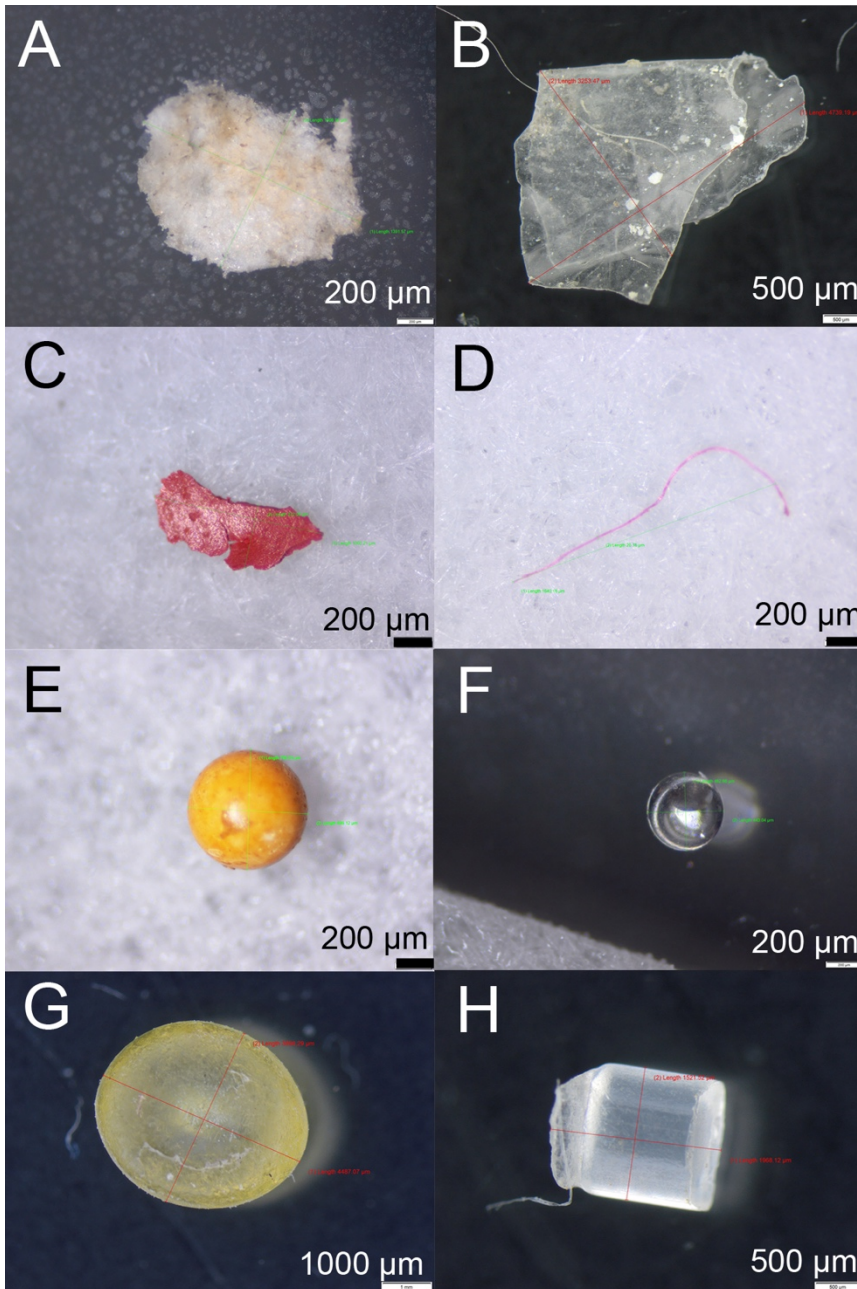


Fig. 3: Retrieved riverine microplastic particles according to the eight type categories applied. Secondary fragments: foam (A), film (B), hard (C), line (D); primary particles: spherule opaque (E), spherule transparent (F), pellet lensoid (G) and pellet cylindrical (H). Scale bars vary in length and are given at the bottom right of each image including length description (μm).

4. Discussion

4.1. MP concentrations of the nival and pluvial locations

The increase in mean MP concentrations from the Swiss tributaries downstream to the German Rhine locations in this study corroborates previously reported trends (Mani et al., 2015; Urgert, 2015). The higher MP concentrations at the downstream German Rhine River locations compared to the Rhine in Basel and upstream Swiss tributaries are associated with greater anthropogenic pressure and mismanaged waste (Lebreton et al., 2017; McCormick et al., 2014; Yonkos et al., 2014). However, another investigation by (Hess et al., 2018) did not observe a MP concentration gradient along the downstream direction of the Rhine, indicating generally high variability in MP concentrations and also the potential of effects related to the season and methodology. That said, the present study was based on a temporal four-fold visitation of the same sites, and therefore holds multiple explanatory power compared to one-off assessments. The differences in the mean MP concentrations within the Swiss rivers potentially reflect varying plastic immission along the river courses and catchments (Dris et al., 2018; Scheurer and Bigalke, 2018). This assumption is supported by the positive correlations between catchment area (km^2), average discharge ($\text{m}^3 \text{s}^{-1}$) and mean MP concentrations (MP m^{-3} ; Fig. S5). Gauges close to the sampling locations in this study reveal the Limmat (catchment area: 2416 km^2) and Reuss (3425 km^2) rivers yield similar ten-year average discharges of $99 \text{ m}^3 \text{ s}^{-1}$ and $139 \text{ m}^3 \text{ s}^{-1}$, respectively, while the Aare ($17,755 \text{ km}^2$) discharges $309 \text{ m}^3 \text{ s}^{-1}$ and the Rhine at Basel ($36,472 \text{ km}^2$) discharges $1037 \text{ m}^3 \text{ s}^{-1}$ (2006–2017; Bundesamt für Umwelt BAFU, 2019; Fig. S9). These findings appear to corroborate the work of Scheurer and Bigalke (2018), who observed higher MP concentrations in the floodplain soils of the rivers examined in this study with larger catchments compared to those with smaller catchments. Various diffuse river sources, as well as aeolian transport, are plausible factors that may explain the higher probability of MP input into rivers with larger catchments, resulting in higher MP concentrations (Dris et al., 2016; Scheurer and Bigalke, 2018). Additionally, considering the diluting effect of high-discharge rivers, their higher MP concentrations may in fact reflect a dramatically higher MP input (Xiong et al., 2019). Interestingly, a comparison of Aare River MP concentrations recorded up- and downstream the Reuss and Limmat confluences, did not reflect this tendency. Samples taken downstream of these confluences in the Aare River yielded lower MP concentrations than the samples taken upstream of the confluences in three out of four sampling campaigns. Turbulence, induced by a rapid flow zone where the water rushed over shallow lying rocks could have compromised a steady water intake of the Manta Trawl there due to increased vertical oscillation of the device on the water surface, thus “missing”

some of the pollution. Generally, it is plausible that the MP input of the Reuss and the Limmat Rivers is overcompensated by the additionally inflowing diluting water masses, resulting in lower MP concentrations downstream.

High discharge periods may wash shoreline plastic waste into the stream of a river (Eerkes-Medrano et al., 2015); furthermore, high discharge is often the result of rainfall events that promote additional urban and agricultural run-off, which potentially increases MP input (Karlsson et al., 2018; Lechner et al., 2014; Lechner and Ramler, 2015; Yonkos et al., 2014). However, this tendency is not supported by our data, as there was no correlation between river discharge levels on the days of sampling and MP concentrations (Table S1). Also, there was no correlation of rainfall amounts leading up to the date of sampling and MP concentrations. This suggests that the generally higher mean MP concentrations for SC2 and SC3 are potentially the result of sporadic upstream MP immissions prior to sampling. The low Swiss MP concentrations at SC4 may be the result of limited terrestrial polluted runoff, as these samples temporally coincided with the extremely dry 2017 Swiss winter period, with precipitation rates at only half the 1981–2010 average for the same season (Bundesamt für Umwelt BAFU, 2018).

The absence of distinct patterns in the variations of MP concentrations between the four sampling campaigns potentially indicates anthropogenic effects have a stronger influence on MP concentrations than environmental factors. With a time lag of approximately one day, Rees encounters almost parallel changes in discharge levels to Bad Honnef located 197 km upstream (BfG, 2017a, 2017b). However, these two sites encompass the vastly industrialised and populated areas of Cologne, Leverkusen and the Rhine-Ruhr region around Duisburg. Therefore Rees, in contrast to Bad Honnef, receives Rhine water that has flown through some of Europe's most highly anthropogenically pressured regions (ICPR, 2018; IT NRW, 2018). Indeed, the average MP concentration was higher at Rees than Bad Honnef over all four sampling campaigns (4.9 ± 1.3 vs. 4.1 ± 1.2 MP m⁻³). However, there was no coherent pattern in the variation in MP concentrations between these locations in any sampling campaign. Additionally, there is no evidence to support a river discharge-based argument to explain MP concentrations in the German pluvial section of this study (Fig. 1).

As obviously high discharge cannot be clearly linked to higher MP concentrations, as in this study, an important discussion arises about the causality of MP concentrations and freight in a moving water body. Xiong et al. (2019) found for the Yangtze River that elevated flow velocity correlated negatively with MP concentrations on the water surface. They argued this is possibly the result of favoured accumulation of MP in slack water as opposed to dynamic water. An

alternative argument could be the diluting effect of greater and faster water masses on the abundance of MP in a moving waterbody. Thinking of the moving fluid as a conveyor belt, a higher MP input is required to maintain a certain concentration when the belt is moving faster. The general, weak negative correlation between MP concentrations and flow velocity in the present study could support this claim. However, this phenomenon can only be substantiated by clear-cut correlations at the Reuss River ($R^2 = 0.8$) and Rhine at Basel ($R^2 = 0.4$; Fig. S10, Fig. S11).

MP-concentrations were in the range between 10^{-1} – 10^1 MP m^{-3} . This is below the predicted no effect concentrations, which reportedly lie between 10^5 – 10^7 MP m^{-3} for numerous freshwater organisms (Adam et al., 2019). However, identified >0.3 mm MP are highly likely indicators for higher concentrations of <0.3 mm MP and potentially nanoplastics, of which the hazardous potential is still largely unknown (Adam et al., 2019; Triebkorn et al., 2019). Furthermore, MP of proven, as well as suspected smaller size ranges, accumulate in locally restricted high-abundance hotspots in natural or artificial traps (e.g. harbour areas or groyne fields), culminating into potentially effect-relevant concentrations (Lebreton et al., 2017). Predicted rising plastic production and waste rates (Koelmans et al., 2017) indicate increasing environmental MP concentrations for the future, emphasising the relevance of current observations as well as raising concern for potential ecological impacts (SAPEA, 2019).

4.2. MP freight and fate downstream

Global models of riverine plastic input to the oceans have produced highly variable estimates of between 0.47 and 2.75 million tons annually (Lebreton et al., 2017; Schmidt et al., 2017). Yearly microplastic transport from the Rhine River to the North Sea has been estimated at 20–105 tons (Siegfried et al., 2017; Van der Wal et al., 2015). Globally, May–October is the highest-input period, during which $>74\%$ of the annual MP load is discharged into the oceans; in contrast, the peak interval for riverine plastic input in Europe is estimated to occur between November–May (Lebreton et al., 2017). The Swiss nival locations investigated in this study discharge the highest amounts of water in June (Bundesamt für Umwelt BAFU, 2019 and Fig. S12), while the pluvial section has the highest average discharge in the winter months around January (BfG, 2017b and Fig. S13).

It seems highly plausible that the periods of highest MP contribution from the Rhine River towards the North Sea is mainly driven by the discharge regime, rather than seasonal differences in MP concentrations in the waterbody. Thus, the peak freight would occur between November and May, as modelled by (Lebreton et al., 2017). This suggestion is supported by (i) the

critically higher MP concentrations in the pluvial (highest discharge in winter) as opposed to nival (highest discharge in summer) sections of the Rhine, as identified in the present and earlier studies (Leslie et al., 2017; Mani et al., 2015; Urgert, 2015) and (ii) the absence of any distinct patterns in MP concentrations between the four sampling dates throughout 2016–2017. According to points (i) and (ii), the differences in the MP concentrations between sampling campaigns would be starkly overcompensated for by the varied water masses running off towards the North Sea during different seasons. Multiplying the combined mean MP concentrations observed at Bad Honnef and Rees in this study by the corresponding ten-year discharge averages of Bad Honnef/Rees for the respective months (assuming homogenous distribution of MP in the entire water column; Liedermann et al., 2018) indicates the total number of MP discharged downstream is approximately $1.35 \times$ higher in February than e.g. in September.

4.3. Potential MP sources

Almost half of the smaller (0.3–1 mm) as well as larger (1–5 mm) MP retrieved from the nival section were foams. While the smaller foam particles were mainly PE, the larger particles were nearly all PS. A very similar foam-polymer-size distribution was also observed at the pluvial sample sites. The striking difference in the polymer composition of the two foam size classes suggests different sources and fragmentation behaviours for these polymer materials. PE foam is widely used for vibration dampening and insulation (Biron, 2004) and appears to enter the waterbody in smaller pieces, or possibly fragments faster in the environment than larger PS foams that potentially originate from the crumbled Styrofoam cells of insulation or packaging products (Andrady, 2011; PlasticsEurope, 2017). PS foam particles with larger diameters (>1 mm) may be an indication of very recent immission, as this material is expected to easily fragment under e.g. mechanical stress (Song et al., 2017). PS, including expanded polystyrene (EPS), constitutes ~7% of European plastics converter demand (PlasticsEurope, 2017). While up to half of EPS waste in Europe is landfilled, the vast majority of EPS in Switzerland is incinerated, as landfilling has been banned since the early 2000s (Kawecki et al., 2018; Kettler, 2001). Despite this Swiss waste management practice, Styrofoam objects were among the top eight waste types identified in a citizen science shoreline investigation at 112 locations along numerous Swiss freshwater waterbodies (Blarer and Kull, 2018). Such plastic debris is likely to enter rivers and lakes through runoff or wind action (Dris et al., 2018), and will fall apart into its constituent foam cells (Zhang et al., 2015) and eventually fragment to even smaller particles (Barnes et al., 2009; Song et al., 2017). Riparian construction activity surveyed from roadworks and two Aargau communes was constant (26–29 active projects during all sampling campaigns,

personal communications G. Sabato, L. Angelini and E. Hofmänner, 2019), thus failing to explain variation in typical construction foam-type MP occurrence.

The large combined proportion of hard, film and line-type secondary MP particles in both the nival and the pluvial sections of this study is representative of a myriad of fragmented consumer products, construction and industrial abrasives (Barnes et al., 2009). PE, PP and PS were by far the major polymers allocated to these highly abundant MP types (Fig. 2). These three polymers represent ~60% of European plastics demand and are mainly used to produce food packaging, pipes, automotive parts, toys, care product containers and insulation (PlasticsEurope, 2017); they are also the most commonly identified MP polymers in the environment (Andrady, 2011; Fahrenfeld et al., 2019; Wagner et al., 2018). Preproduction pellets were rarely found in this study. The highest mean pellet concentrations were all detected in Basel – during the February 2017 (SC4), April (SC1) and November 2016 (SC3) sampling campaigns – at 0.08 (SC4) and 0.05 MP m⁻³ (SC1/SC3), respectively. During SC4, Bad Honnef yielded the next highest pellet concentration of 0.04 MP m⁻³, a possible indication of widely reported erratic pellet loss events from industrial spillage, or loss during transport or transshipment (Cole and Sherrington, 2016; Karlsson et al., 2018). Opaque PS MP spherules, which yielded the highest concentrations in Rees, have repeatedly been detected in the Lower Rhine and are most likely polystyrene-divinylbenzene (PS-DVB) ion exchange resin beads (Mani et al., 2015; Mani et al., 2019a). Opaque spherules were also found at the Swiss locations in this study; however, these MP either had generally larger diameters (>1 mm) or were mainly PE – a potential indicator of personal care product microbeads (Eriksen et al., 2013; Fendall and Sewell, 2009). The high proportions of transparent, colourless spherules at Bad Honnef and Rees are a known component of the Rhine River MP load (Mani et al., 2015; Urgert, 2015; Van der Wal et al., 2015). These MP likely stem from spilled suspension polymerisation polymethyl methacrylate (PMMA) products (Arshady, 1992). In order to avoid further MP contamination as well as to enable remediation of affected habitats, (i) emissions of primary MP (e.g. pre-production pellets or ion-exchange resin beads) need to be eliminated through rigorously sealed and controlled production, transport, application and waste management processes; while (ii) production and demand of excess plastic (e.g. single-use items or unreasonable packaging), potentially releasing secondary MP after end of life or upon littering, need to be dramatically reduced; and (iii) on a higher level, it is believed that a circular economy approach will highly benefit resolving the obvious plastic waste crisis (SAPEA, 2019).

The positive relationship between 0.3–1 mm and 1–5 mm MP in this study (Fig. S8) generally suggests either similar environmental regions of entry for the different size classes or rapid

fragmentation once in the river (Scheurer and Bigalke, 2018; Xiong et al., 2019). Fibres were present in all samples, but were not quantified due to technical limitations (*cf.* section 2.3.). Fibre-type MP commonly originate from synthetic textiles and are frequently emitted into the aquatic environment via wastewater discharge and aeolian transport (Hernandez et al., 2017; Mintenig et al., 2017; Napper and Thompson, 2016). Interestingly, while approaches for modelling MP in the environment often predict substantial proportions (>50%) of tyre and road wear particles (TRWP) and care product abrasives (Siegfried et al., 2017), these particles are hardly ever detected at high concentrations in environmental investigations, including the present sampling campaigns. Technical limitations of most field surveys (Hidalgo-Ruz et al., 2012; Silva et al., 2018), non-realistic modelling scenarios, or both, may account for this discrepancy.

4.4. Appraisal of methodology

As visual identification of MP is highly bias-afflicted (Ivleva et al., 2017; Löder and Gerdts, 2015), we selected a high spot sample proportion of 6522 of the 15,783 total conspicuous particles in all size classes for FTIR chemical assessment (~41%). The threshold for positive plastic identification was set at 60% HQI and mean MP concentrations were multiplied by the positive hit factor ($HQI \geq 60\%$, *cf.* section 2.5.), which may lead to an underrepresentation of MP concentrations compared to earlier Rhine investigations where this calculation and strict HQI threshold were not applied (Mani et al., 2015). All putative mesoplastics were investigated by a single investigator. The relatively low hit ratio is the result of a highly cautious visual selection approach, which included a wide interpretation of the plastic properties listed in the guidance protocols. Furthermore, the buffering effect of the chemical analysis (FTIR) counteracts the pitfall of overestimating plastic particles (*cf.* section 2.6.). Despite its many advantages compared to traditional approaches, the novel oil separation protocol performed in this study yields slightly below-state-of-the-art riverine environmental MP recovery rates, especially for PS (Crichton et al., 2017; Mani et al., 2019b). Therefore, the verified MP concentrations were multiplied with the reported MP loss factor of ~26% to compensate for this underestimation. The 0.3 mm sampling mesh, as used in the present as well as in the majority of freshwater MP investigations (Adam et al., 2019), allows for the assessment of >0.3 mm MP. Size-frequency distributions of environmental MP are usually skewed towards the smallest (single digit micron) size ranges (Adam et al., 2019; Burns and Boxall, 2018). The choice of a 0.3 mm mesh is the consequence of a trade-off in favour of greater sample analysis throughput and therewith broader numerical, geographical and temporal explanatory power. Based on the knowledge that secondary MP result from the fragmentation of larger plastic particles (Barnes

et al., 2009) and of size-frequency distribution of MP particles, >0.3 mm MP investigations, such as the present one, serve as pivotal indicators for the presence of smaller size MP and potentially nanoplastics (Triebkorn et al., 2019) which need to be considered in environmental policy and determined through further research. Moreover, as the Manta Trawl sampling technique only accesses the top 18 cm of the water column, MP concentrations and freight in the lower water column remain unknown. The vast proportion of low density MP are believed to float or be slightly submerged in the top layers of rivers; however, there is growing evidence of deeper submerged MP, which are best captured by multipoint sampling techniques where operating includes various depths of below-surface water column compartments (Liedermann et al., 2018).

5. Conclusion

The MP concentrations and freight in the Rhine River and its Swiss tributaries reflect the size of the river catchments and mean discharge levels. The MP concentrations of the Swiss nival Rhine River tributaries were significantly lower than the pluvial German Rhine River sites of Bad Honnef and Rees approximately 400 and 600 km further downstream, respectively. While secondary particles dominate the MP pollution load upstream, the proportions of primary MP increase at the downstream locations. As the occurrence of MP at a given location is expected to be affected by anthropogenic as well as environmental factors, the difficulty of dissecting these multiple factors complicates final conclusions about causality. No consistent seasonal patterns in the fluctuations in MP concentrations were observed among the six sampling sites. Based on the observed MP concentrations and discharge regimes of the investigated river locations, it seems highly plausible that the largest flux of MP from the Rhine River towards the North Sea occurs between November and May, as predicted by transport and fate models. As the bigger picture for Rhine River MP gradually crystallises in seasonal and geographical terms, below-surface, mid-water-column investigations are still required to inform reliable and comprehensive flux predictions.

Acknowledgements

The authors would like to thank the Police authorities in Brugg and Basel, Switzerland, as well as the Waterway and Shipping Administration of Niederkassel and Rees, Germany for their generous use of their professional vessel services for field sampling. We also thank Pascal Blarer, Christian Hossli (both World Wide Fund for Nature WWF, Switzerland) and Sandrine Straub (MGU, University of Basel, Switzerland) for invaluable support during field work. Heidi Schiffer, Nicole Seiler-Kurth, Hedwig Scharlipp and Sophie Bosshart, (all MGU) are greatly acknowledged for their enduring and precise work in sample analysis. We thank Ulrich Walter, Peter Mühlischlegel and Marco Solari, Intertek, Switzerland, for assistance with FTIR analysis and spectral interpretation. Many thanks for impeccable data analysis support go to M.Sc. Denise M. Staubli, consultant to the Mekong River Commission (MRC). Andrea Devlin, PhD, chief editor of Science Editing Experts, is owed great gratitude for her immaculate proof reading and language support. This study was partially funded by the World Wide Fund for Nature (WWF), Switzerland.

References

- Andrady, A.L., 2011. Microplastics in the marine environment. *Mar. Pollut. Bull.* 62 (8), 1596–1605. doi:10.1016/j.marpolbul.2011.05.030.
- Andrady, A.L., 2017. The plastic in microplastics: A review. *Mar. Pollut. Bull.* 119 (1), 12–22. doi:10.1016/j.marpolbul.2017.01.082.
- Arshady, R., 1992. Suspension, emulsion, and dispersion polymerization: A methodological survey. *Colloid Polym. Sci.* 270 (8), 717–732. doi:10.1007/BF00776142.
- Barnes, D.K.A., Galgani, F., Thompson, R.C., Barlaz, M., 2009. Accumulation and fragmentation of plastic debris in global environments. *Philosophical transactions of the Royal Society of London. Series B, Biological sciences* 364 (1526), 1985–1998. doi:10.1098/rstb.2008.0205.
- BASEMAN, 2017. Interdisciplinary Research for Good Environmental Status. <http://www.jpi-oceans.eu/baseman>. Accessed 9 May 2018.
- Bergmann, M., Wirzberger, V., Krumpen, T., Lorenz, C., Primpke, S., Tekman, M.B., Gerdt, G., 2017. High quantities of microplastic in Arctic deep-sea sediments from the HAUSGARTEN observatory. *Environ. Sci. Technol.* 51 (19), 11000–11010. doi:10.1021/acs.est.7b03331.
- BfG, 2017a. Pegel Rhein Bonn. http://undine.bafg.de/rhein/pegel/rhein_pegel_bonn.html. Accessed 10 January 2018.
- BfG, 2017b. Pegel Rhein Rees. http://undine.bafg.de/rhein/pegel/rhein_pegel_rees.html. Accessed 10 January 2018.
- Biron, M. (Ed.), 2004. *Thermosets and Composites*. Elsevier Science, Oxford.
- Blarer, P., Kull, G., 2018. *Swiss Litter Report*, Zurich, 65 pp. https://storage.googleapis.com/wzukusers/user-15533811/documents/5b867b8f51528JrYbIoW/Swiss%20Litter%20Report_final_180710.pdf. Accessed 30 March 2019.
- Blettler, M.C.M., Abrial, E., Khan, F.R., Sivri, N., Espinola, L.A., 2018. Freshwater plastic pollution: Recognizing research biases and identifying knowledge gaps. *Water Res.* 143, 416–424. doi:10.1016/j.watres.2018.06.015.
- Bundesamt für Umwelt BAFU, 2018. *Hydrologisches Jahrbuch der Schweiz 2017*. 44 pp. <https://naturwissenschaften.ch/uuid/61b20431-cbe0-5f94-8511->

[c50e3c95b90b?r=20190807115818_1565140005_88713df7-d203-5932-ae9a-0b9e3ecb3adf](https://www.hydrodaten.admin.ch/de/messstationen_zustand.html). Accessed 31 March 2020.

Bundesamt für Umwelt BAFU, 2019. Hydrologische Daten und Vorhersagen.

https://www.hydrodaten.admin.ch/de/messstationen_zustand.html. Accessed 14 April 2019.

Cole, G., Sherrington, C., 2016. Study to quantify pellet emission in the UK – Report to Fidra. Eunomia. <https://www.eunomia.co.uk/reports-tools/study-to-quantify-pellet-emissions-in-the-uk/>. Accessed 09 June 2018.

Cole, M., Lindeque, P., Halsband, C., Galloway, T.S., 2011. Microplastics as contaminants in the marine environment: A review. *Mar. Pollut. Bull.* 62 (12), 2588–2597. doi:10.1016/j.marpolbul.2011.09.025.

Cózar, A., Echevarría, F., González-Gordillo, J.I., Irigoien, X., Ubeda, B., Hernández-León, S., Palma, A.T., Navarro, S., García-de-Lomas, J., Ruiz, A., Fernández-de-Puelles, M.L., Duarte, C.M., 2014. Plastic debris in the open ocean. *P. Natl. Acad. Sci. USA* 111 (28), 10239–10244. doi:10.1073/pnas.1314705111.

Crichton, E.M., Noël, M., Gies, E.A., Ross, P.S., 2017. A novel, density-independent and FTIR-compatible approach for the rapid extraction of microplastics from aquatic sediments. *Anal. Methods* 9 (9), 1419–1428. doi:10.1039/C6AY02733D.

Dekiff, J.H., Remy, D., Klasmeier, J., Fries, E., 2014. Occurrence and spatial distribution of microplastics in sediments from Norderney. *Environ. Pollut.* 186, 248–256. doi:10.1016/j.envpol.2013.11.019.

Dris, R., Gasperi, J., Saad, M., Mirande, C., Tassin, B., 2016. Synthetic fibers in atmospheric fallout: A source of microplastics in the environment? *Mar. Pollut. Bull.* 104 (1-2), 290–293. doi:10.1016/j.marpolbul.2016.01.006.

Dris, R., Gasperi, J., Tassin, B., 2018. Sources and fate of microplastics in urban areas: A focus on Paris Megacity, in: Wagner, M., Lambert, S., Besseling, E., Biginagwa, F.J. (Eds.), *Freshwater microplastics. Emerging environmental contaminants? The handbook of environmental chemistry. Volume 58*. Springer, pp. 69–83. doi:10.1007/978-3-319-61615-5

Eerkes-Medrano, D., Thompson, R.C., Aldridge, D.C., 2015. Microplastics in freshwater systems: A review of the emerging threats, identification of knowledge gaps and prioritisation of research needs. *Water Res.* 75, 63–82. doi:10.1016/j.watres.2015.02.012.

- Ellen Mc Arthur Foundation, 2016. The new plastics economy: Rethinking the future of plastics & catalysing action, 68 pp.
https://www.ellenmacarthurfoundation.org/assets/downloads/publications/NPEC-Hybrid_English_22-11-17_Digital.pdf. Accessed 01 April 2019.
- Eriksen, M., Lebreton, L.C.M., Carson, H.S., Thiel, M., Moore, C.J., Borerro, J.C., Galgani, F., Ryan, P.G., Reisser, J., 2014. Plastic pollution in the world's oceans: More than 5 trillion plastic pieces weighing over 250,000 tons afloat at sea. *PloS one* 9 (12), e111913. doi:10.1371/journal.pone.0111913.
- Eriksen, M., Mason, S., Wilson, S., Box, C., Zellers, A., Edwards, W., Farley, H., Amato, S., 2013. Microplastic pollution in the surface waters of the Laurentian Great Lakes. *Mar. Pollut. Bull.* 77 (1-2), 177–182. doi:10.1016/j.marpolbul.2013.10.007.
- Fahrenfeld, N.L., Arbuckle-Keil, G., Naderi Beni, N., Bartelt-Hunt, S.L., 2019. Source tracking microplastics in the freshwater environment. *TrAC Trend. Anal. Chem.* 112, 248–254. doi:10.1016/j.trac.2018.11.030.
- Faure, F., Corbaz, M., Baecher, H., Alencastro, L.F. de, 2012. Pollution due to plastics and microplastics in Lake Geneva and in the Mediterranean Sea. *Arch. Sci.* 65 (157–164).
- Faure, F., Demars, C., Wieser, O., Kunz, M., Alencastro, L.F. de, 2015. Plastic pollution in Swiss surface waters: Nature and concentrations, interaction with pollutants. *Environ. Chem.* 12 (5), 582. doi:10.1071/EN14218.
- Fendall, L.S., Sewell, M.A., 2009. Contributing to marine pollution by washing your face: Microplastics in facial cleansers. *Mar. Pollut. Bull.* 58 (8), 1225–1228. doi:10.1016/j.marpolbul.2009.04.025.
- Hartmann, N.B., Hüffer, T., Thompson, R.C., Hassellöv, M., Verschoor, A., Daugaard, A.E., Rist, S., Karlsson, T., Brennholt, N., Cole, M., Herrling, M.P., Hess, M.C., Ivleva, N.P., Lusher, A.L., Wagner, M., 2019. Are we speaking the same language? Recommendations for a definition and categorization framework for plastic debris. *Environ. Sci. Technol.* 53 (3), 1039–1047. doi:10.1021/acs.est.8b05297.
- Hernandez, E., Nowack, B., Mitrano, D.M., 2017. Polyester textiles as a source of microplastics from households: A mechanistic study to understand microfiber release during washing. *Environ. Sci. Technol.* 51 (12), 7036–7046. doi:10.1021/acs.est.7b01750.
- Hess, M., Diel, P., Mayer, J., Rahm, H., Reifenhäuser, W., Stark, J., Schwaiger, J., 2018. Mikroplastik in Binnengewässern Süd- und Westdeutschlands:

- Bundesländerübergreifende Untersuchungen in Baden-Württemberg, Bayern, Hessen, Nordrhein-Westfalen und Rheinland-Pfalz, Karlsruhe, Augsburg, Wiesbaden, Recklinghausen, Mainz, 86 pp.
https://www.lanuv.nrw.de/fileadmin/lanuvpubl/6_sonderreihen/L%C3%A4nderbericht_Mikroplastik_in_Binnengew%C3%A4ssern.pdf. Accessed 25 May 2018.
- Hidalgo-Ruz, V., Gutow, L., Thompson, R.C., Thiel, M., 2012. Microplastics in the marine environment: A review of the methods used for identification and quantification. *Environ. Sci. Technol.* 46 (6), 3060–3075. doi:10.1021/es2031505.
- ICPR, 2018. The Rhine. International Commission for the Protection of the Rhine.
<https://www.iksr.org/en/rhine/>. Accessed 18 December 2018.
- IT NRW, 2018. Bevölkerung in Nordrhein-Westfalen. Information und Technik Nordrhein-Westfalen. <https://www.it.nrw/bevoelkerung-am-31122017-und-30062018-nach-gemeinden-93051>. Accessed 15 January 2019.
- Ivleva, N.P., Wiesheu, A.C., Niessner, R., 2017. Microplastic in aquatic ecosystems. *Angew. Chem. Int. Edit.* 56 (7), 1720–1739. doi:10.1002/anie.201606957.
- Jahnke, A., Arp, H.P.H., Escher, B.I., Gewert, B., Gorokhova, E., Kühnel, D., Ogonowski, M., Potthoff, A., Rummel, C., Schmitt-Jansen, M., Toorman, E., MacLeod, M., 2017. Reducing uncertainty and confronting ignorance about the possible impacts of weathering plastic in the marine environment. *Environ. Sci. Technol. Lett.* 4 (3), 85–90. doi:10.1021/acs.estlett.7b00008.
- Jambeck, J.R., Geyer, R., Wilcox, C., Siegler, T.R., Perryman, M., Andrady, A., Narayan, R., Law, K.L., 2015. Plastic waste inputs from land into the ocean. *Science* 347 (6223), 768–771. doi:10.1126/science.1260352.
- Karlsson, T.M., Arneborg, L., Broström, G., Almroth, B.C., Gipperth, L., Hassellöv, M., 2018. The unaccountability case of plastic pellet pollution. *Mar. Pollut. Bull.* 129 (1), 52–60. doi:10.1016/j.marpolbul.2018.01.041.
- Kawecki, D., Scheeder, P.R.W., Nowack, B., 2018. Probabilistic material flow analysis of seven commodity plastics in Europe. *Environ. Sci. Technol.* 52 (17), 9874–9888. doi:10.1021/acs.est.8b01513.
- Kettler, R., 2001. Statistique des déchets 2000, Avec données 2001 sur la planification des UIOM.: Doc. Environ. 95. Off. fédéral l'environnement.

<https://www.admin.ch/gov/fr/accueil/documentation/communiqués.msg-id-8421.html>.

Accessed 02 March 2020.

- Klein, S., Worch, E., Knepper, T.P., 2015. Occurrence and spatial distribution of microplastics in river shore sediments of the Rhine-Main area in Germany. *Environ. Sci. Technol.* 49 (10), 6070–6076. doi:10.1021/acs.est.5b00492.
- Kleinn, J., Frei, C., Gurtz, J., Lüthi, D., Vidale, P.L., Schär, C., 2005. Hydrologic simulations in the Rhine basin driven by a regional climate model. *J. Geophys. Res.* 110 (D4), 224. doi:10.1029/2004JD005143.
- Lebreton, L.C.M., van der Zwet, J., Damsteeg, J.-W., Slat, B., Andrady, A., Reisser, J., 2017. River plastic emissions to the world's oceans. *Nat. Commun.* 8, 15611. doi:10.1038/ncomms15611.
- Lechner, A., Keckeis, H., Lumesberger-Loisl, F., Zens, B., Krusch, R., Tritthart, M., Glas, M., Schludermann, E., 2014. The Danube so colourful: A potpourri of plastic litter outnumbered fish larvae in Europe's second largest river. *Environ. Pollut.* 188, 177–181. doi:10.1016/j.envpol.2014.02.006.
- Lechner, A., Ramler, D., 2015. The discharge of certain amounts of industrial microplastic from a production plant into the River Danube is permitted by the Austrian legislation. *Environ. Pollut.* 200, 159–160. doi:10.1016/j.envpol.2015.02.019.
- Leslie, H.A., Brandsma, S.H., van Velzen, M.J.M., Vethaak, A.D., 2017. Microplastics en route: Field measurements in the Dutch river delta and Amsterdam canals, wastewater treatment plants, North Sea sediments and biota. *Environ. Int.* 101, 133–142. doi:10.1016/j.envint.2017.01.018.
- Liedermann, M., Gmeiner, P., Pessenlehner, S., Haimann, M., Hohenblum, P., Habersack, H., 2018. A methodology for measuring microplastic transport in large or medium rivers. *Water* 10 (4), 414. doi:10.3390/w10040414.
- Löder, M.G.J., Gerds, G., 2015. Methodology used for the detection and identification of microplastics – A critical appraisal, in: Klages, M., Gutow, L., Bergmann, M. (Eds.), *Marine Anthropogenic Litter*. Springer, pp. 201–227.
- Mani, T., Blarer, P., Storck, F.R., Pittroff, M., Wernicke, T., Burkhardt-Holm, P., 2019. Repeated detection of polystyrene microbeads in the Lower Rhine River. *Environ. Pollut.* 245, 634–641. doi:10.1016/j.envpol.2018.11.036.

- Mani, T., Frehland, S., Kalberer, A., Burkhardt-Holm, P., 2019b. Using castor oil to separate microplastics from four different environmental matrices. *Anal. Methods* 11 (13), 1788–1794. doi:10.1039/C8AY02559B.
- Mani, T., Hauk, A., Walter, U., Burkhardt-Holm, P., 2015. Microplastics profile along the Rhine River. *Sci. Rep.* 5, 17988. doi:10.1038/srep17988.
- Mani, T., Primpke, S., Lorenz, C., Gerdt, G., Burkhardt-Holm, P., 2019c. Microplastic pollution in benthic midstream sediments of the Rhine River. *Environ. Sci. Technol.* 53 (10), 6053–6062. doi:10.1021/acs.est.9b01363.
- Masura, J., Baker, J.E., Foster, G.D., Arthur, C., Herring, C., 2015. Laboratory methods for the analysis of microplastics in the marine environment: recommendations for quantifying synthetic particles in waters and sediments. NOAA technical memorandum NOS-OR&R 48. NOAA, Silver Spring, Maryland, USA.
<https://repository.library.noaa.gov/view/noaa/10296#tabs-2>. Accessed 16 August 2018.
- McCormick, A., Hoellein, T.J., Mason, S.A., Schlupe, J., Kelly, J.J., 2014. Microplastic is an abundant and distinct microbial habitat in an urban river. *Environ. Sci. Technol.* 48 (20), 11863–11871. doi:10.1021/es503610r.
- Mintenig, S.M., Int-Veen, I., Löder, M.G.J., Primpke, S., Gerdt, G., 2017. Identification of microplastic in effluents of waste water treatment plants using focal plane array-based micro-Fourier-transform infrared imaging. *Water Res.* 108, 365–372. doi:10.1016/j.watres.2016.11.015.
- Napper, I.E., Thompson, R.C., 2016. Release of synthetic microplastic plastic fibres from domestic washing machines: Effects of fabric type and washing conditions. *Mar. Pollut. Bull.* 112 (1-2), 39–45. doi:10.1016/j.marpolbul.2016.09.025.
- Norén, F., 2007. Small plastic particles in coastal Swedish waters. n-research, Lysekil, Sweden.
https://www.researchgate.net/profile/Fredrik_Noren/publication/284312290_Small_plastic_particles_in_Coastal_Swedish_waters/links/571203c608ae4ef74525ec38/Small-plastic-particles-in-Coastal-Swedish-waters.pdf?origin=publication_detail. Accessed 23 May 2018.
- O’Brine, T., Thompson, R.C., 2010. Degradation of plastic carrier bags in the marine environment. *Mar. Poll. Bull.* 60 (12), 2279–2283. doi:10.1016/j.marpolbul.2010.08.005.

- Ohtake, Y., Kobayashi, T., Asabe, H., Murakami, N., 1998. Studies on biodegradation of LDPE – observation of LDPE films scattered in agricultural fields or in garden soil. *Polym. Degrad. Stabil.* 60 (1), 79–84. doi:10.1016/S0141-3910(97)00032-3.
- PlasticsEurope, 2017. Plastic – the Facts 2017, 44 pp.
https://www.plasticseurope.org/application/files/5715/1717/4180/Plastics_the_facts_2017_FINAL_for_website_one_page.pdf. Accessed 23 August 2018.
- Primpke, S., Wirth, M., Lorenz, C., Gerdt, G., 2018. Reference database design for the automated analysis of microplastic samples based on Fourier transform infrared (FTIR) spectroscopy. *Anal. Bioanal. Chem.* 410 (21), 5131–5141. doi:10.1007/s00216-018-1156-x.
- Scheurer, M., Bigalke, M., 2018. Microplastics in Swiss floodplain soils. *Environ. Sci. Technol.* 52 (6), 3591–3598. doi:10.1021/acs.est.7b06003.
- Schmidt, C., Krauth, T., Wagner, S., 2017. Export of plastic debris by rivers into the sea. *Environ. Sci. Technol.* 51 (21), 12246–12253. doi:10.1021/acs.est.7b02368.
- Sedlak, D., 2017. Three lessons for the microplastics voyage. *Environ. Sci. Technol.* 51 (14), 7747–7748. doi:10.1021/acs.est.7b03340.
- Siegfried, M., Koelmans, A.A., Besseling, E., Kroeze, C., 2017. Export of microplastics from land to sea. A modelling approach. *Water Res.* 127, 249–257. doi:10.1016/j.watres.2017.10.011.
- Silva, A.B., Bastos, A.S., Justino, C.I.L., da Costa, J.P., Duarte, A.C., Rocha-Santos, T.A.P., 2018. Microplastics in the environment: Challenges in analytical chemistry – A review. *Anal. Chim. Acta.* 1017, 1–19. doi:10.1016/j.aca.2018.02.043.
- Song, Y.K., Hong, S.H., Jang, M., Han, G.M., Jung, S.W., Shim, W.J., 2017. Combined effects of uv exposure duration and mechanical abrasion on microplastic fragmentation by polymer type. *Environ. Sci. Technol.* 51 (8), 4368–4376. doi:10.1021/acs.est.6b06155.
- Spreafico, M., Weingartner, R., Leibundgut, C. (Eds.), 1992. Hydrological atlas of Switzerland. EDMZ, Bern, 11 pp.
- Triebkorn, R., Braunbeck, T., Grummt, T., Hanslik, L., Huppertsberg, S., Jekel, M., Knepper, T.P., Kraus, S., Müller, Y.K., Pittroff, M., Ruhl, A.S., Schmieg, H., Schür, C., Strobel, C., Wagner, M., Zumbülte, N., Köhler, H.-R., 2019. Relevance of nano- and

- microplastics for freshwater ecosystems: A critical review. *TrAC Trend. Anal. Chem.* 110, 375–392. doi:10.1016/j.trac.2018.11.023.
- Urgert, W., 2015. Microplastics in the rivers Meuse and Rhine: Developing guidance for a possible future monitoring program. Masterthesis, Heerlen, The Netherlands, 106 pp. <https://www.riwa-rijn.org/wp-content/uploads/2015/11/master-thesis-NW-Wilco-Urgert-838144036-DEFINITIEF-16-10-2015.pdf>. Accessed 09 March 2020.
- Van Cauwenberghe, L., Vanreusel, A., Mees, J., Janssen, C.R., 2013. Microplastic pollution in deep-sea sediments. *Environ. Pollut.* 182, 495–499. doi:10.1016/j.envpol.2013.08.013.
- Van der Wal, M., Van der Meulen, M., Tweehuijsen, G., Peterlin, M., Palatinus, A., Virsek, M.K., Coscia, L., Krsan, A., 2015. SFRA0025: Identification and assessment of riverine input of (marine) litter.: Final report for the European Commission DG Environment under framework contract No ENV. D, Bristol (Vol. 25). 2/FRA/2012., 208 pp. <http://ec.europa.eu/environment/marine/good-environmental-status/descriptor-10/pdf/iasFinal%20Report.pdf>. Accessed 29 March 2019.
- Verbunt, M., Zappa, M., Gurtz, J., Kaufmann, P., 2006. Verification of a coupled hydrometeorological modelling approach for alpine tributaries in the Rhine basin. *Journal of Hydrology* 324 (1-4), 224–238. doi:10.1016/j.jhydrol.2005.09.036.
- Wagner, M., Lambert, S., Besseling, E., Biginagwa, F.J. (Eds.), 2018. Freshwater microplastics: Emerging environmental contaminants? The handbook of environmental chemistry. Volume 58. Springer, 303 pp. doi:10.1007/978-3-319-61615-5
- Wagner, M., Scherer, C., Alvarez-Muñoz, D., Brennholt, N., Bourrain, X., Buchinger, S., Fries, E., Grosbois, C., Klasmeier, J., Marti, T., Rodriguez-Mozaz, S., Urbatzka, R., Vethaak, A.D., Winther-Nielsen, M., Reifferscheid, G., 2014. Microplastics in freshwater ecosystems: What we know and what we need to know. *Environ. Sci. Eur.* 26 (1), 12. doi:10.1186/s12302-014-0012-7.
- Wang, W., Ndungu, A.W., Li, Z., Wang, J., 2017. Microplastics pollution in inland freshwaters of China: A case study in urban surface waters of Wuhan, China. *Sci.Total Environ.* 575, 1369–1374. doi:10.1016/j.scitotenv.2016.09.213.
- Xiong, X., Wu, C., Elser, J.J., Mei, Z., Hao, Y., 2019. Occurrence and fate of microplastic debris in middle and lower reaches of the Yangtze River – From inland to the sea. *Sci. Total Environ.* 659, 66–73. doi:10.1016/j.scitotenv.2018.12.313.

Yonkos, L.T., Friedel, E.A., Perez-Reyes, A.C., Ghosal, S., Arthur, C.D., 2014. Microplastics in four estuarine rivers in the Chesapeake Bay, U.S.A. *Environ. Sci. Technol.* 48 (24), 14195–14202. doi:10.1021/es5036317.

Zhang, K., Gong, W., Lv, J., Xiong, X., Wu, C., 2015. Accumulation of floating microplastics behind the Three Gorges Dam. *Environ. Pollut.* 204, 117–123. doi:10.1016/j.envpol.2015.04.023.

Supporting Information

SI 3: Seasonal microplastics variation in nival and pluvial stretches of the Rhine River – From the Swiss catchment towards the North Sea

Table S1: Metadata for field samples (table distributed over two pages).

Sampling Campaign	Regime	Location	Sample	Coordinates N	Coordinates E	River width (m)	Date	Sample volume	Verified MP m ⁻³ (0.3-5)	72 hour average discharge (sample)*	10 year average monthly discharge*
SC1	Nival	Reuss	1	47°29.448333'	8°14.268833'	87	06.04.2016	99.8244	0.14339	124.75	129.77
		Limmat	1	47°30.109920'	8°14.373240'	49	07.04.2016	58.5144	0.14075	78.11	90.99
			2	47°30.259620'	8°14.262360'	26	07.04.2016	80.19	0.10270	78.11	90.99
		Aare	1	47°29.375700'	8°13.945740'	71	06.04.2016	168.1884	0.40525	306.16	327.44
			2	47°29.412420'	8°14.022720'	64	06.04.2016	109.2204	0.42703	306.16	327.44
			3	47°30.519840'	8°14.093460'	123	07.04.2016	188.9892	0.31220	330.65	327.44
		Basel	1	47°33.322140'	7°35.910060'	197	20.04.2016	90.882	0.72516	1619.07	1000.10
			2	47°36.878333'	7°35.152167'	191	20.04.2016	122.2128	0.56121	1619.07	1000.10
			3	47°33.072000'	7°36.077167'	213	20.04.2016	90.1044	2.61442	1619.07	1000.10
	Pluvial	Bad Honnef	1	50°37.803833'	7°12.771000'	296	26.04.2016	96.39	3.31631	2513.33	1984.97
			2	50°37.809667'	7°12.725000'	296	26.04.2016	112.0392	2.36524	2513.33	1984.97
			3	50°37.805000'	7°12.648833'	296	26.04.2016	104.7816	2.89159	2513.33	1984.97
		Rees	1	51°45.357167'	6°23.344833'	442	28.04.2016	107.6004	3.56615	2733.33	2205.73
			2	51°45.304500'	6°23.323333'	442	28.04.2016	111.3912	4.18550	2733.33	2205.73
			3	51°45.281167'	6°23.351167'	442	28.04.2016	90.558	9.21612	2733.33	2205.73
SC2	Nival	Reuss	1	47°29.448333'	8°14.268833'	87	31.08.2016	105.1056	0.06172	127.56	189.95
		Limmat	2	47°30.046667'	8°14.038833'	30	31.08.2016	86.2812	0.07279	66.23	117.47
			3	17°30.020833'	8°14.042000'	93	31.08.2016	75.3624	0.46723	66.23	117.47
			Aare	1	47°29.059333'	8°13.165500'	79	31.08.2016	135.594	0.80260	262.73
		2		47°29.070500'	8°14.010000'	73	31.08.2016	100.926	0.60194	262.73	351.39
		3		47°30.103667'	8°14.005500'	100	31.08.2016	121.014	0.64327	262.73	351.39
		Basel	1	47°35.490000'	7°35.708000'	190	01.09.2016	52.2612	2.95889	910.97	972.22
			2	47°36.878333'	7°35.152167'	191	01.09.2016	94.4136	0.26725	910.97	972.22
			3	47°33.072000'	7°36.077167'	213	01.09.2016	85.5684	0.11673	910.97	972.22
	Pluvial	Bad Honnef	1	50°37.130333'	7°12.111333'	295	06.09.2016	84.6288	5.70766	1233.33	1478.73
			2	50°37.794667'	7°12.751000'	297	06.09.2016	84.1752	4.44451	1233.33	1478.73
			3	50°37.783167'	7°12.785500'	302	06.09.2016	70.2756	2.64712	1233.33	1478.73
		Rees	1	51°45.062833'	6°24.018500'	404	08.09.2016	84.6936	5.43367	1343.33	1653.64
			2	51°45.054167'	6°24.016167'	404	08.09.2016	84.6936	9.97478	1343.33	1653.64
			3	51°45.050667'	6°24.007167'	384	08.09.2016	91.2384	4.74148	1343.33	1653.64

Sampling Campaign	Regime	Location	Sample	Coordinates N	Coordinates E	River width (m)	Date	Sample volume	Verified MP m ⁻³ (0.3-5)	72 hour average discharge (sample)*	10 year average monthly discharge*
SC3	Nival	Reuss	1	47°29.448333'	8°14.268833'	87	22.11.2016	78.3108	0.19195	101.44	96.55
		Limmat	1	47°30'7.4	8°14'17.3	75	22.11.2016	25.2396	0.56292	70.40	75.70
			2	47°30'15.99	8°14'15.15	28	22.11.2016	70.4376	0.52034	70.40	75.70
			3	47°29'22.426	8°13'56.980	70	22.11.2016	200.88	0.19015	430.39	263.03
		Aare	1	47°29'25.5	8°14'3.03	64	22.11.2016	166.3416	1.11157	430.39	263.03
			2	47°30'32.506	8°14'4.989	112	22.11.2016	173.4372	0.67798	430.39	263.03
			3	47°33'27.078"	7°36'30.409"	210	23.11.2016	100.5696	1.11688	965.90	846.71
		Basel	1	47°33'20.6"	7°35'49.082"	178	23.11.2016	79.8012	3.91552	965.90	846.71
			2	47°35'17.12"	7°35'15.056"	193	23.11.2016	62.9856	5.45285	965.90	846.71
	3		50°37'47"	7°12'38"	299	28.11.2016	77.2092	5.25763	1533.33	1699.29	
	Pluvial	Bad Honnef	1	50°37'48"	7°12'43"	300	28.11.2016	83.0088	5.18412	1533.33	1699.29
			2	50°37'48"	7°12'46"	300	28.11.2016	71.0208	2.59628	1533.33	1699.29
			3	51°45.276	6°23.767	328	01.12.2016	71.2476	4.03863	1506.67	2555.75
		Rees	1	51°45.328	6°23.770	328	01.12.2016	71.2476	8.46014	1506.67	2555.75
			2	51°45.365	6°23.763	328	01.12.2016	71.2476	2.60965	1506.67	2555.75
3			47°29'27.2	8°14'17.6	78	16.02.2017	132.3864	0.04122	69.96	74.32	
SC4	Nival	Reuss	1	47°30'7.5	8°14'21.7	48	16.02.2017	31.5252	0.14697	57.88	77.44
		Limmat	2	47°30'18.2	8°14'11.9	35	16.02.2017	112.3308	0.04399	57.88	77.44
			1	47°29'22.1	8°13'56.4	70	16.02.2017	99.2088	0.17122	138.05	240.14
			2	47°29'24.0	8°14'1.1	66	16.02.2017	62.6616	0.84940	138.05	240.14
		3	47°30'35.4	8°14'3.0	96	16.02.2017	78.1812	0.11070	138.05	240.14	
		Basel	1	47°33'27.6	7°36'30.5	209	17.02.2017	73.9368	0.54462	547.62	794.18
			2	47°33'20.1	7°35'49.5	188	17.02.2017	68.364	1.49860	547.62	794.18
			3	47°35'17.4	7°35'14.2	190	17.02.2017	42.0552	5.17850	547.62	794.18
		Pluvial	Bad Honnef	1	50°37.8020	7°12.6590	302	20.02.2017	85.536	1.52140	1283.33
	2			50°37.8034	7°12.7139	305	20.02.2017	84.4668	7.88569	1283.33	2291.27
	3			50°37.8054	7°12.7868	306	20.02.2017	75.8484	8.60931	1283.33	2291.27
	Rees		1	51°45'22.7"	6°24'2.8"	402	22.02.2017	82.9764	2.92484	1443.33	2602.08
			2	51°45'19.85"	6°24'2.98"	402	22.02.2017	86.832	5.29281	1443.33	2602.08
			3	51°45'7.9"	6°24'3.94"	402	22.02.2017	106.8228	1.94786	1443.33	2602.08

*Stations: Reuss (Mellingen, CH), Limmat (Baden, CH), Aare (Brugg, CH), Basel (Rhein/Rheinhalle, CH), Bonn, DE (14.8 km downstream of Bad Honnef), Rees, DE; data from (BfG, 2017a, 2017b; Bundesamt für Umwelt BAFU, 2019)

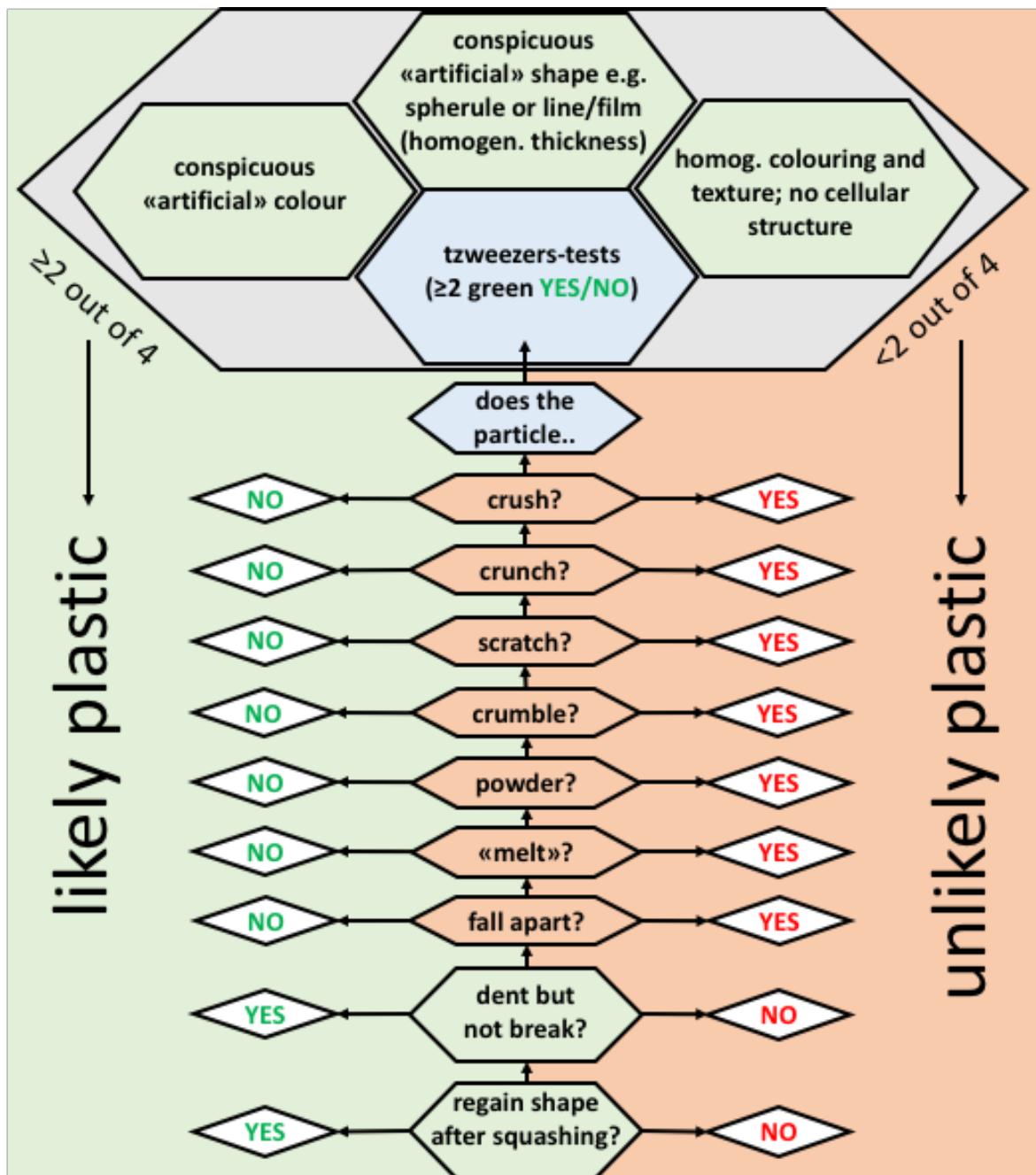


Fig. S1: Decision chart for visual identification of putative microplastics used in the lab; based on (Masura et al., 2015; Norén, 2007). An investigated particle qualified as likely plastic if it fulfils two of the main criteria (large grey hexagon). Particles reaching two green YES/NO-assessments succeed the tweezer-test.

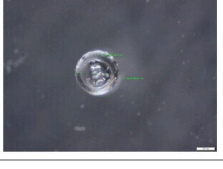
FRAGMENT			SPHERULE		
Foam		Spongy texture, no biogenic appearance (cellular structure, etc.)	Opaque		Homogenous, spherical shape, opaque
Film		Flat fragment with even thickness	Transparent		Homogenous, spherical shape, transparent
Hard		Random fragment shape with a solid, rogorous texture	PELLET		
Line		Longish fragment with homogenous thickness (analogy: part of a fishing line)	Lensoid		Pre-production plastic pellet, lensoid shape
			Cylindrical		Pre-production plastic pellet, cylindrical shape

Fig. S2: Visual shape prototypes for categorisation based on (Masura et al., 2015; Norén, 2007).

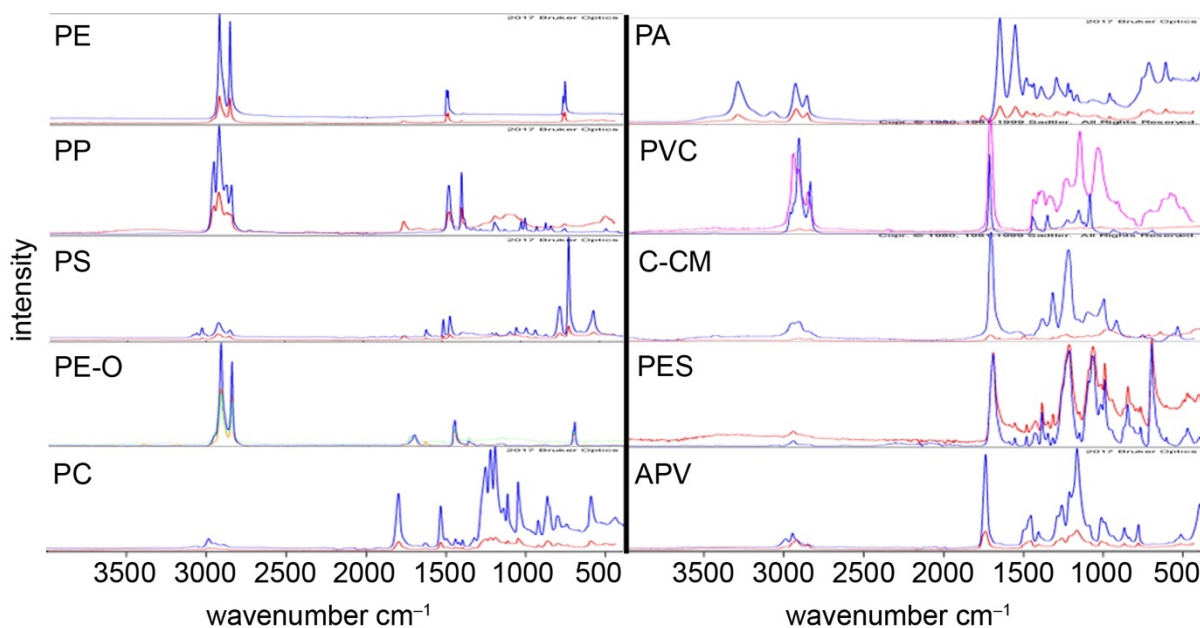


Fig. S3: FTIR spectra of the ten most commonly identified main polymer types: PE = polyethylene; PP = polypropylene; PS = polystyrene; PE-O = polyethylene oxidized; PC = polycarbonate; PA = polyamide; PVC = polyvinyl chloride; C-CM = cellulose (chemically modified); PES = polyester; APV = acrylates/polyurethane. Blue lines represent the reference spectra from the database. All shown spectra achieved a hit quality index (HQI) of >60%, except for C-CM.

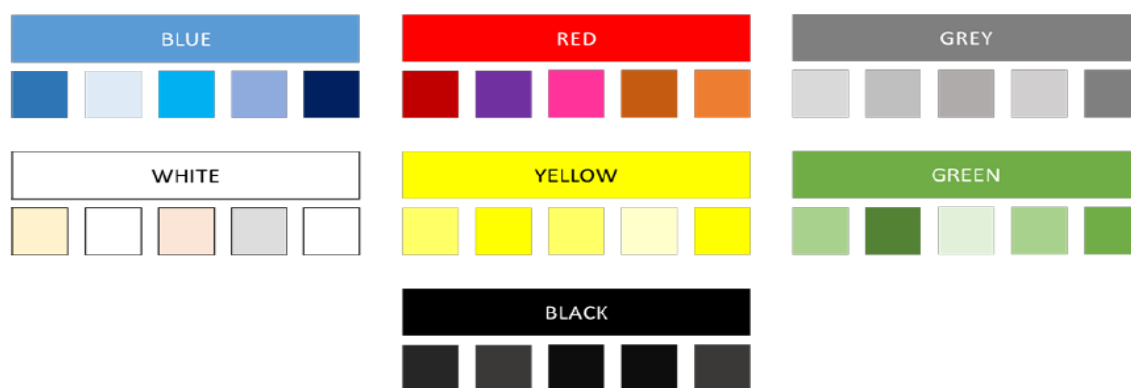


Fig. S4: Example chart for colour merging.

Table S2: Visually identified (A) and chemically verified (B) micro- (0.3–1 mm; 1–5 mm) and mesoplastics from 60 samples taken in the surface waters of the Rhine River and Swiss tributaries.

Plastics particles	Total	0.3–1 mm	1–5 mm	>5 mm
(A) Vis. ident.	15,783	14,277	1,437	69
(B) FTIR analysis	6,522 (41.3% of A)	5,016 (35.1% of A)	1,437 (100.0% of A)	69 (100.0% of A)
(C) HQI retrieved	5,946 (91.2% of B)	4,965 (99.0% of B)	919 (63.9% of B)	62 (89.9% of B)
(D) HQI >600	3,815 (58.5% of B)	3,057 (60.9% of B)	741 (51.6% of B)	17 (24.6% of B)

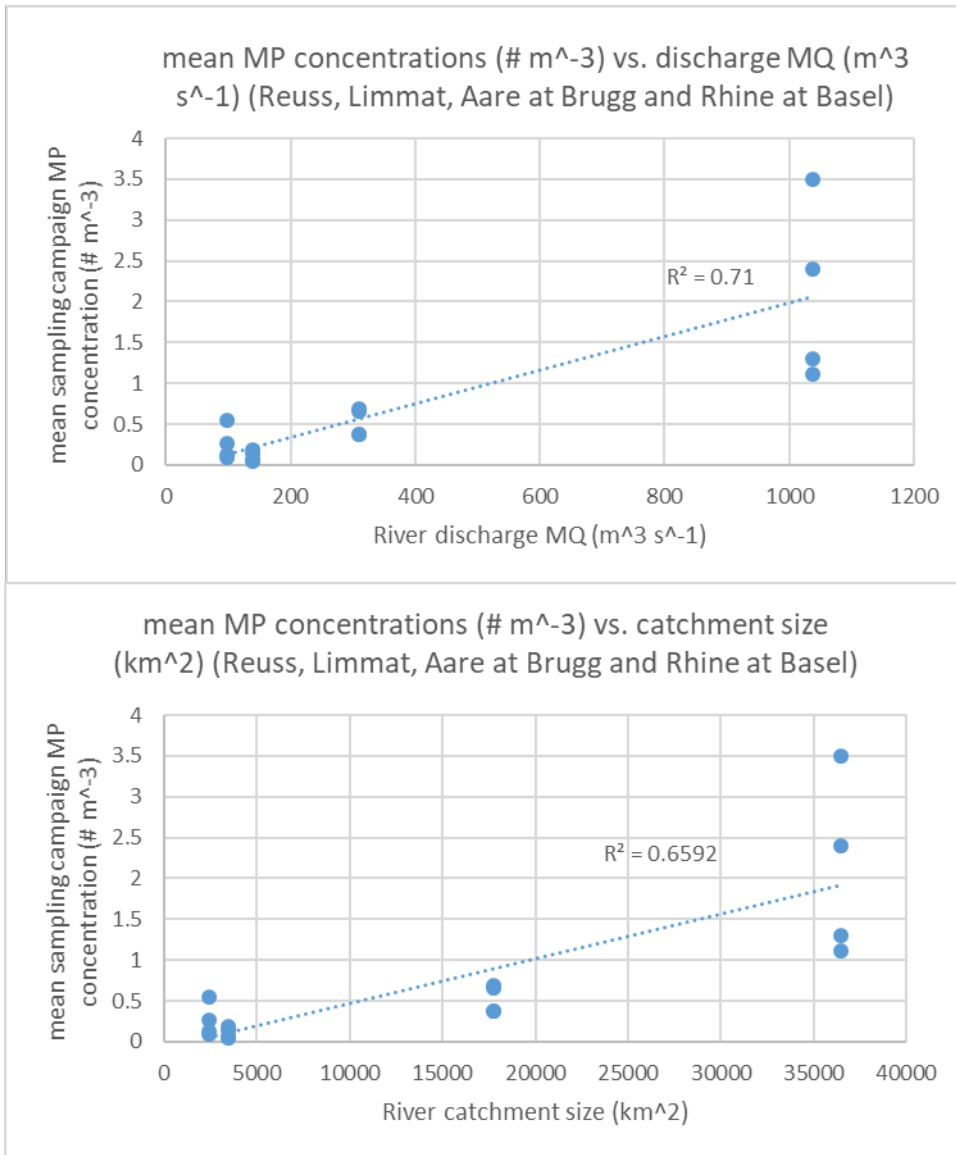


Fig. S5: Relationship for mean MP concentrations ($\# \text{ m}^{-3}$) vs. mean river discharge (MQ, $\text{m}^3 \text{ s}^{-1}$, top graph) and vs. river catchment size (km^2 , bottom graph). Locations Reuss, Limmat, Aare and Rhine at Basel are plotted from left to right on the x-axis (data: Bundesamt für Umwelt BAFU, 2019).

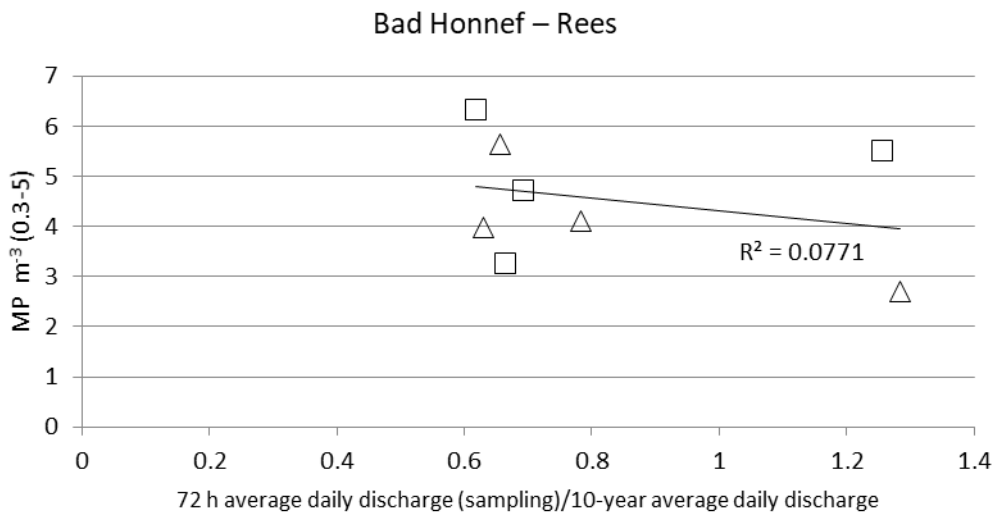
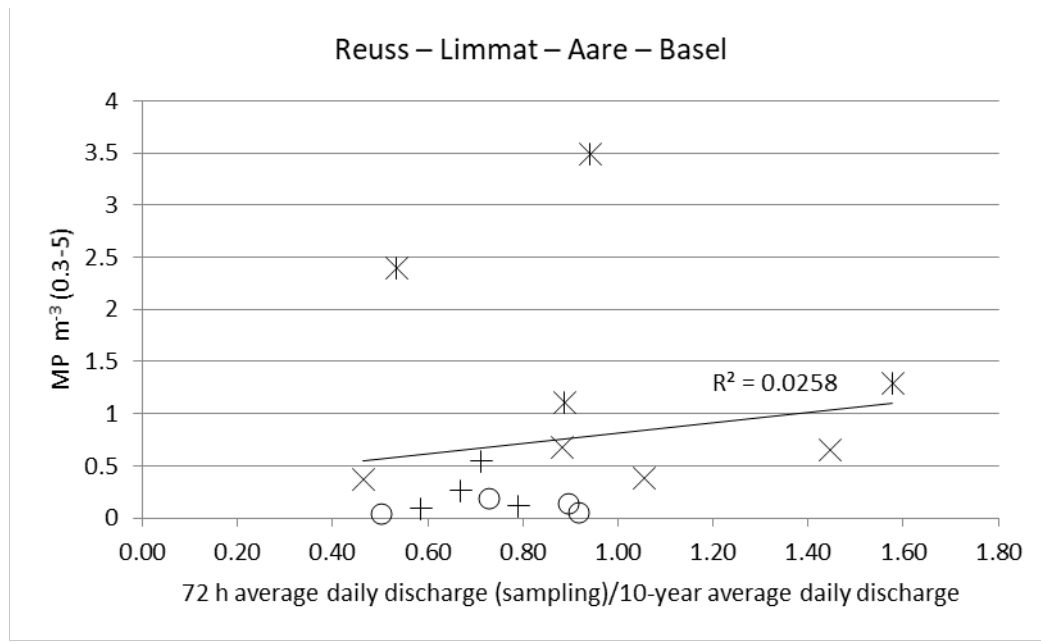


Fig. S6: Relationship between 72 h average discharge up to the day of sampling at the respective location divided by 10-year average discharge and mean MP concentrations (MP m³) per sampling campaign and location. Upper graph: * = Basel, x = Aare, + = Limmat and circle = Reuss. Lower graph: squares = Rees and triangles = Bad Honnef (hydrological data: (Bundesamt für Umwelt BAFU, 2019)).

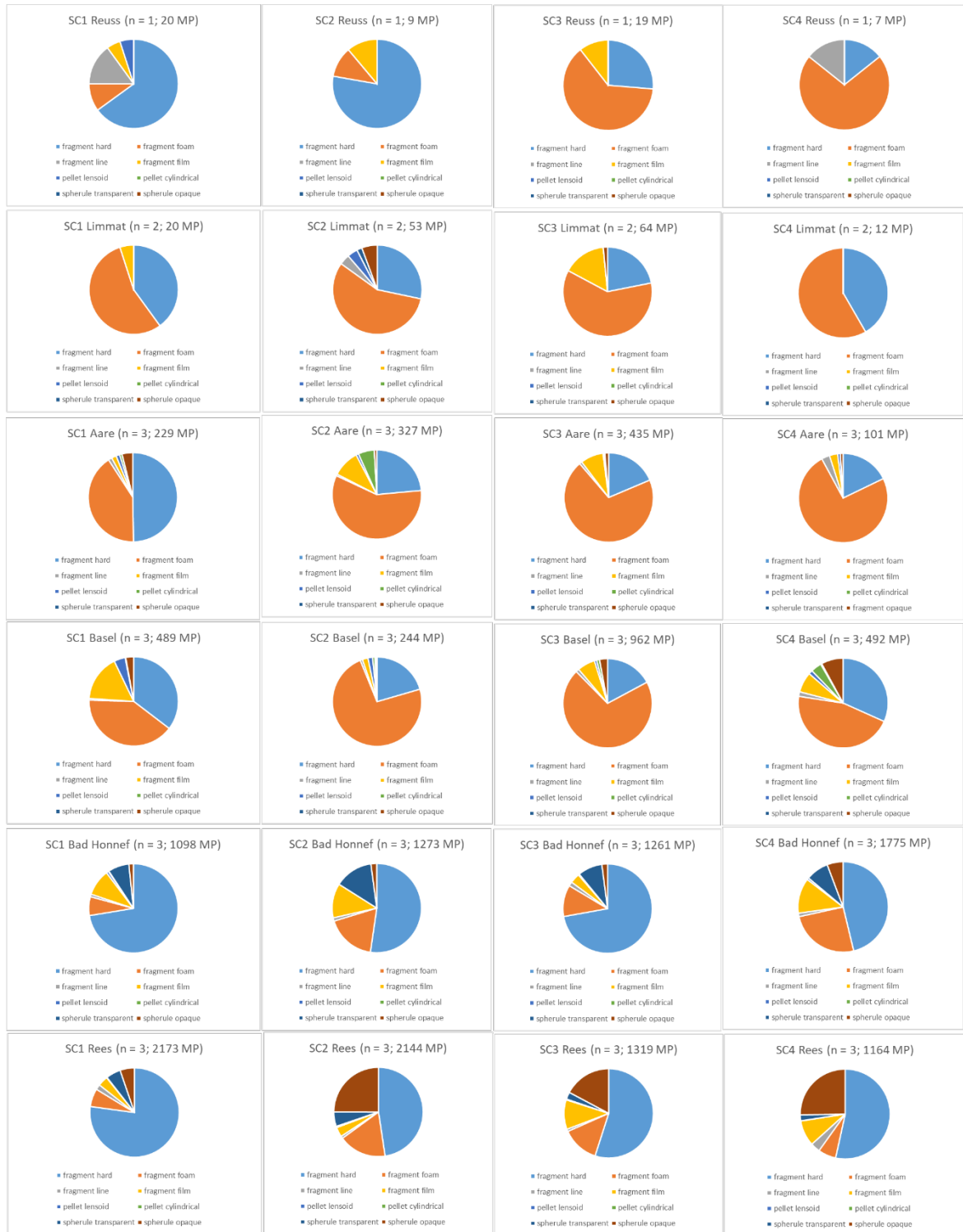


Fig. S7: Microplastic types for particles with a diameter of 0.3–5 mm at six locations at four distinct time-points during one year (April 2016 to February 2017).

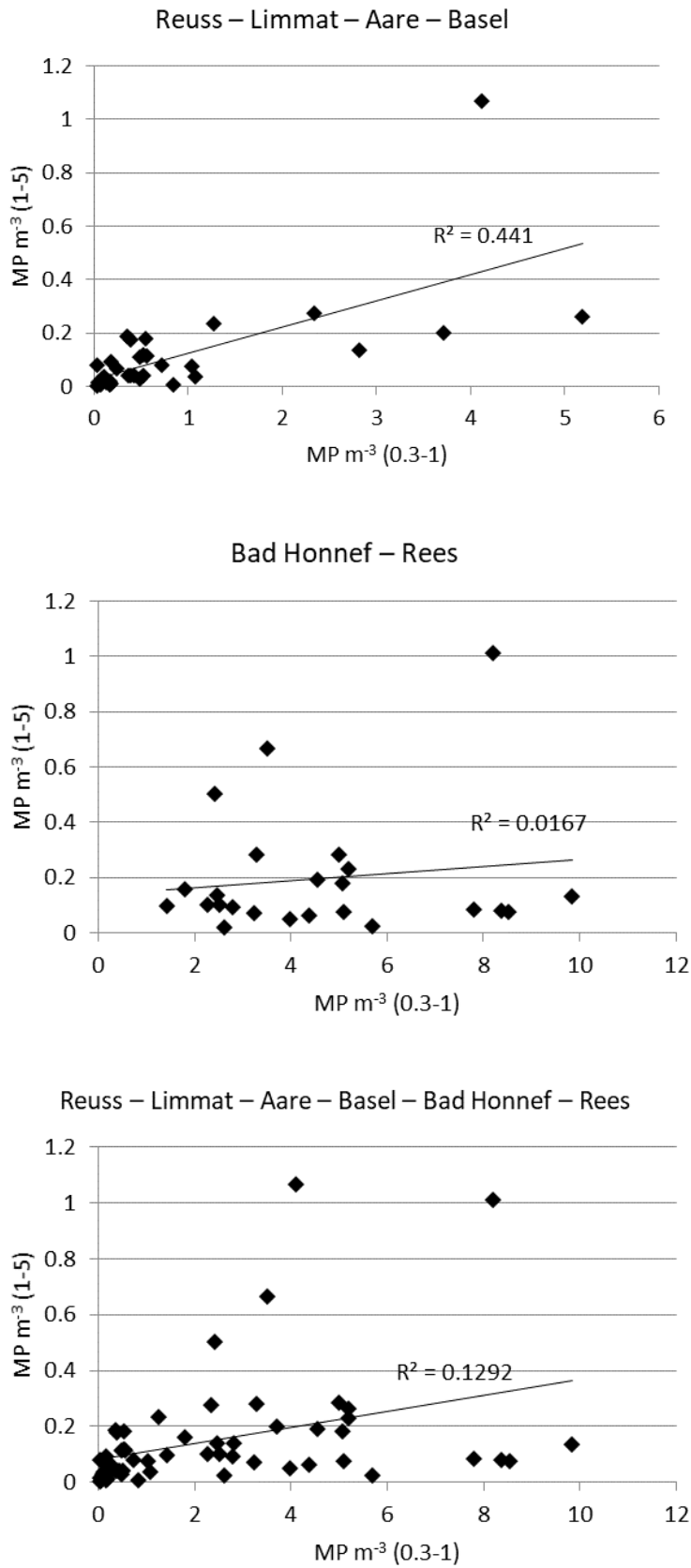


Fig. S8: Relationship between the concentrations of larger (1–5 mm) and smaller (0.3–1 mm) MP per sample (data: BfG, 2017a, 2017b; Bundesamt für Umwelt BAFU, 2019).

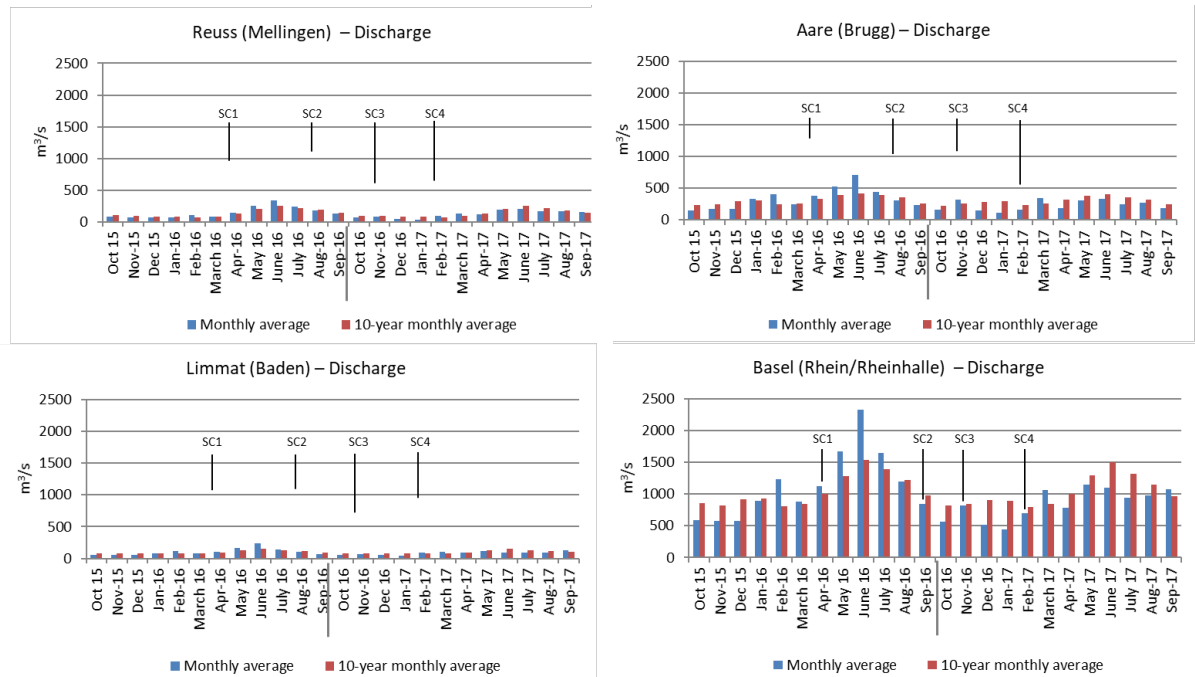


Fig. S9: Monthly average and ten-year average discharges of the four Swiss rivers investigated for the two hydrological years Oct 2016–Sep 2017. The four sampling campaigns are indicated (data: Bundesamt für Umwelt BAFU, 2019).

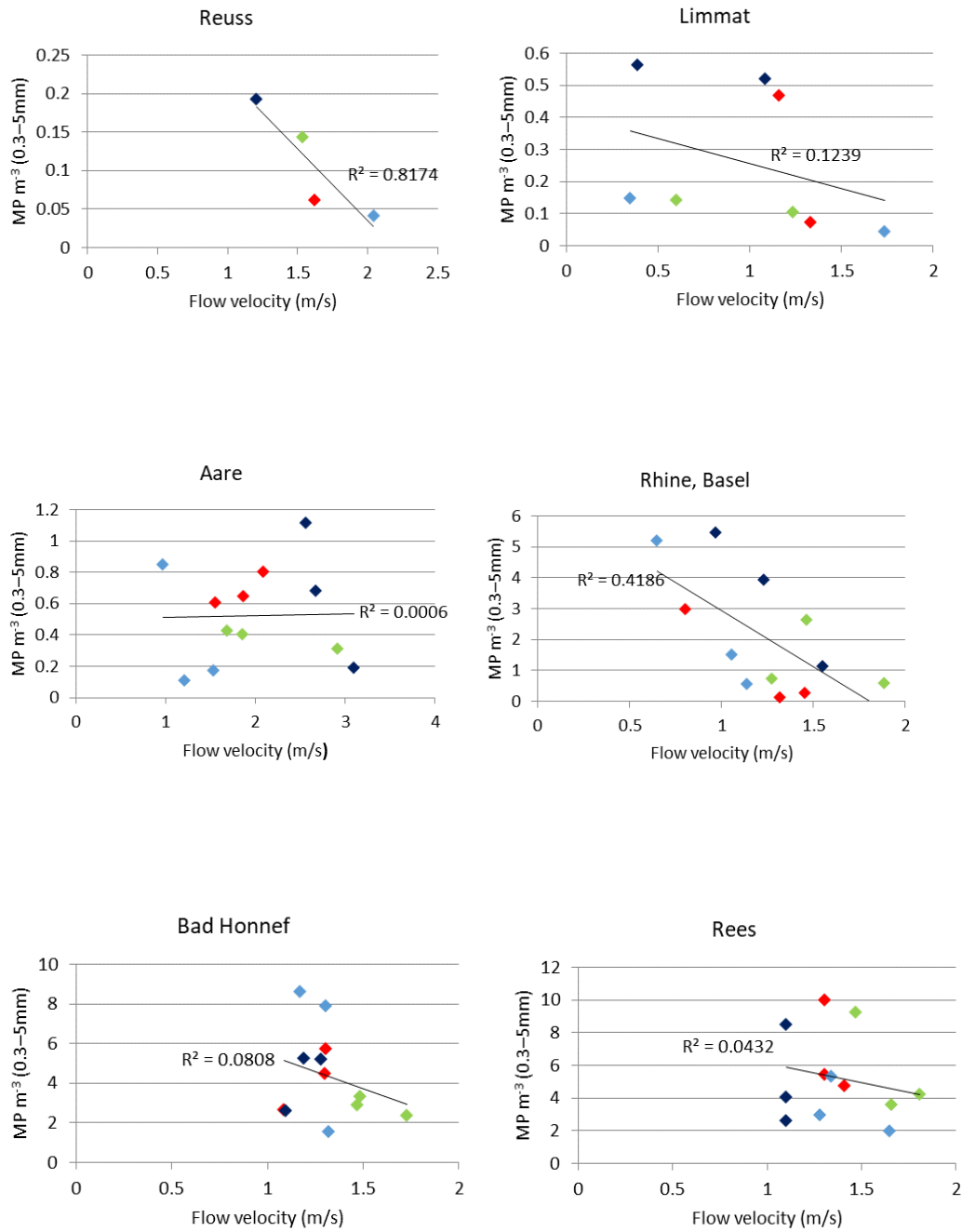


Fig. S10: Regression analysis of mean MP concentrations ($\# \text{ m}^{-3}$; 0.3–1 mm) and surface water flow velocity for the single samples from each sampling campaign. Green: SC1, April 2016; red: SC2, August/September 2016; dark blue: SC3, November 2016 and light blue: February 2017 (data: BfG, 2017a, 2017b; Bundesamt für Umwelt BAFU, 2019).

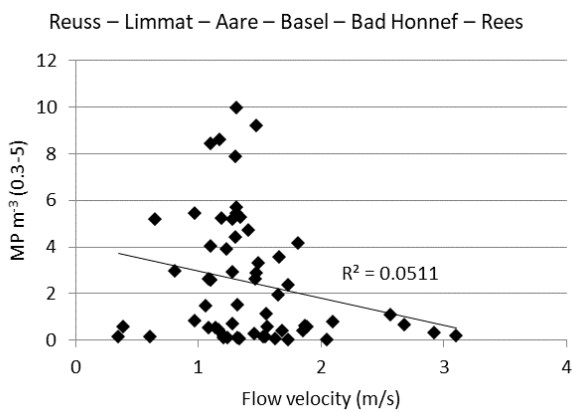
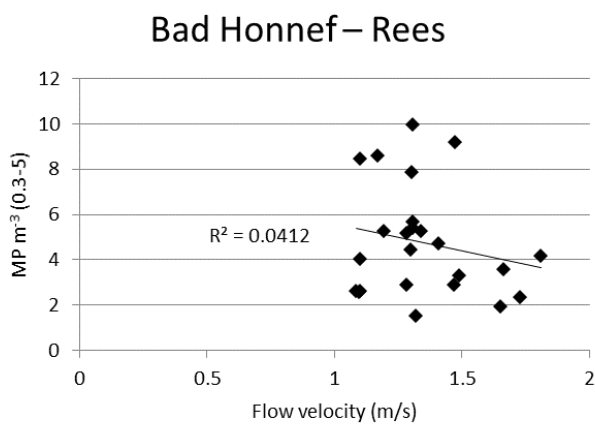
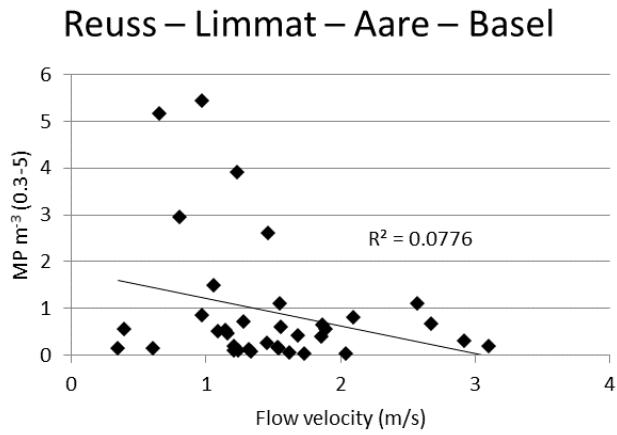


Fig. S11: Relationship between MP concentrations ($\# \text{ MP m}^{-3}$) and surface water flow velocity measured during sampling. Data for all samples is presented in the three charts above (data: BfG, 2017a, 2017b; Bundesamt für Umwelt BAFU, 2019).

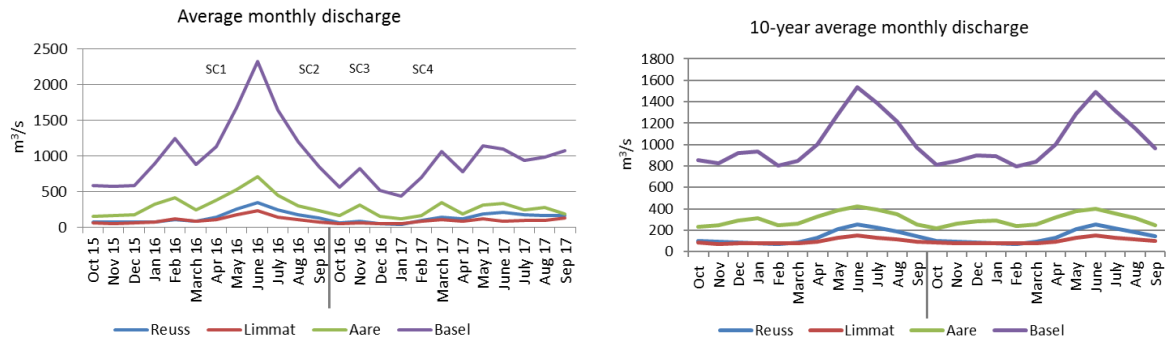


Fig. S12: Average monthly discharge (left) and ten-year average monthly discharge (right) calculated for the hydrological years Oct 2015–Sep 2017 for the four Swiss rivers investigated (data: Bundesamt für Umwelt BAFU, 2019).

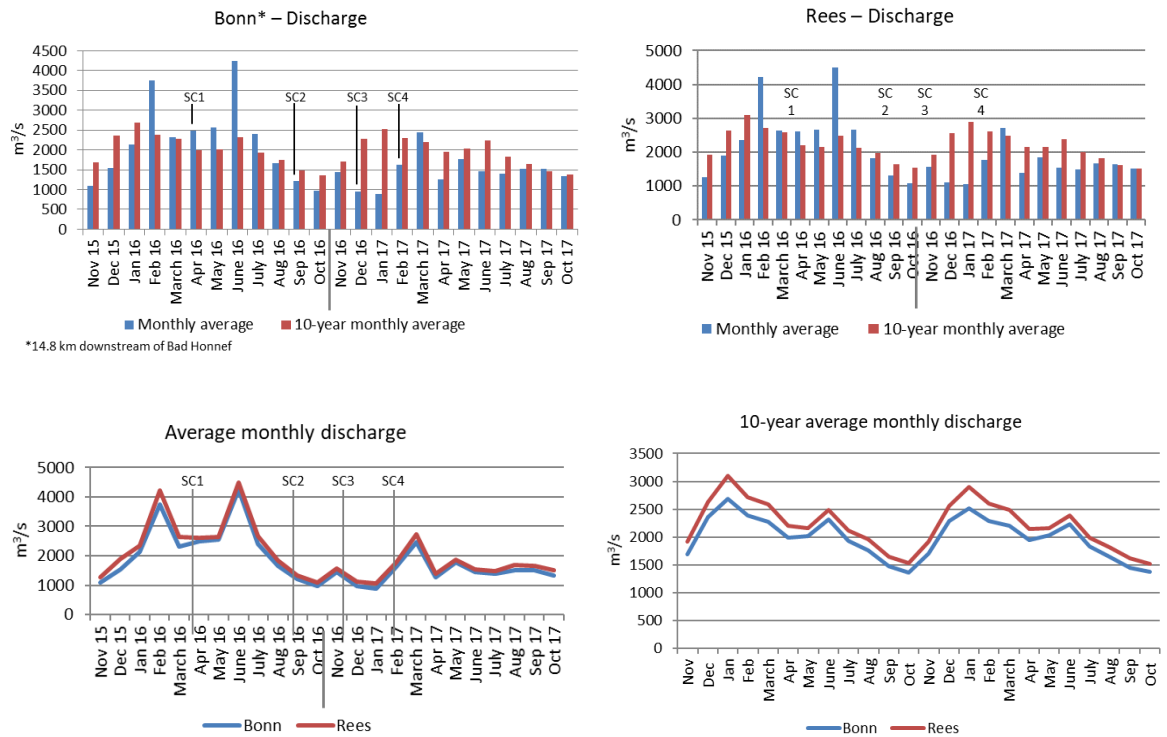


Fig. S13: Top row: Monthly average discharge and ten-year monthly average discharge for the Rhine at Bonn (left) and Rees (right) for the two hydrological years Nov 2015–Oct 2017. Bottom row: Monthly average discharge for the Rhine at Bonn and Rees Nov 2015–Oct 2017 (left) and ten-year monthly average for the two hydrological years Nov 2015–Oct 2017 (right, data: BfG, 2017a, 2017b; Bundesamt für Umwelt BAFU, 2019).

References

- BfG, 2017a. Pegel Rhein Bonn. http://undine.bafg.de/rhein/pegel/rhein_pegel_bonn.html. Accessed 10 January 2018.
- BfG, 2017b. Pegel Rhein Rees. http://undine.bafg.de/rhein/pegel/rhein_pegel_rees.html. Accessed 10 January 2018.
- Bundesamt für Umwelt BAFU, 2019. Hydrologische Daten und Vorhersagen. https://www.hydrodaten.admin.ch/de/messstationen_zustand.html. Accessed 14 April 2019.
- Masura, J., Baker, J.E., Foster, G.D., Arthur, C., Herring, C., 2015. Laboratory methods for the analysis of microplastics in the marine environment: recommendations for quantifying synthetic particles in waters and sediments. NOAA technical memorandum NOS-OR&R 48. NOAA, Silver Spring, Maryland, USA. <https://repository.library.noaa.gov/view/noaa/10296#tabs-2>. Accessed 16 August 2018.
- Norén, F., 2007. Small plastic particles in coastal Swedish waters. n-research, Lysekil, Sweden. https://www.researchgate.net/profile/Fredrik_Noren/publication/284312290_Small_plastic_particles_in_Coastal_Swedish_waters/links/571203c608ae4ef74525ec38/Small-plastic-particles-in-Coastal-Swedish-waters.pdf?origin=publication_detail. Accessed 23 May 2018.

Paper 4

Microplastic pollution in benthic midstream sediments of the Rhine River

Thomas Mani ^a, Sebastian Primpke ^b, Claudia Lorenz ^b, Gunnar Gerdts ^b, and Patricia Burkhardt-Holm ^a

^a Department of Environmental Sciences, The Man-Society-Environment Program,
University of Basel, Vesalgasse 1, 4051 Basel, Switzerland

^b Department of Microbial Ecology, Biologische Anstalt Helgoland, Alfred-Wegener-Institut
Helmholtz-Zentrum für Polar- und Meeresforschung, Kurpromenade, 27498 Helgoland,
Germany

Published 2019

in *Environmental Science & Technology* 53 (10), pp. 6053–6062.

DOI: 10.1021/acs.est.9b01363

Abstract

Rivers are major transport vectors for microplastics (MP) toward the sea. However, there is evidence that MP can temporarily or permanently be inhibited from migrating downstream by retention in sediments or ingestion by organisms. MP concentrations, compositions and fate within the different compartments of the fluvial environment are poorly understood. Here, benthic, midstream sediments of two undammed, open-flowing stretches were investigated in the Rhine River, one of the world's busiest inland waterways. Twenty-five samples were collected at ten sites via riverbed access through a diving bell or dredging. We performed the first comprehensive analysis of riverbed sediment aliquots that avoids visual selection bias using state-of-the-art automated micro-Fourier-transform infrared spectroscopy (μ FTIR) imaging. MP numbers ranged between 0.26 ± 0.01 – $11.07 \pm 0.6 \times 10^3$ MP kg⁻¹ while MP particles <75 μ m accounted for a mean numerical proportion \pm SD of $96 \pm 6\%$. MP concentrations decreased with sediment depth. Eighteen polymers were identified in the size range of 11–500 μ m; the acrylates/polyurethane/varnish (APV) cluster was found at all sites (mean numerical proportion, $70 \pm 19\%$), possibly indicating particulate pollution from ship antifouling paint. Overall, polymers denser than freshwater (>1 g cm⁻³) dominated ($85 \pm 18\%$), which contrasts the large proportions of low-density polymers previously reported in near-surface compartments of the Rhine.

1. Introduction

An estimated 4.8–12.7 million tonnes of plastic waste entered the oceans from land in 2010 (Jambeck et al., 2015). Rivers alone reportedly carry 0.47–2.75 million tonnes of plastic waste toward the seas every year (Lebreton et al., 2017; Schmidt et al., 2017) and it is suggested there are 4.85 trillion microplastic (MP, <5 mm) particles in the world's oceans today (Eriksen et al., 2014). MP emerge from varnish, paint, tire wear, textiles, agriculture, industry, uncountable consumer products and packaging (Dris et al., 2015; Dris et al., 2018; Kooi et al., 2018). Diffuse sources include municipal, agricultural, industrial and road runoff (Duis and Coors, 2016; Karlsson et al., 2018; Mani et al., 2019), while wastewater treatment plants (WWTP; Mintenig et al., 2017; Murphy et al., 2016) and (direct) industrial dischargers (Karlsson et al., 2018; Lechner and Ramler, 2015) represent potential point sources. Although land-based sources are widely regarded as the main contributors to the marine plastic load (~80%; GESAMP, 2016), rivers cannot be simply regarded as linear vectors that transport all of the MP they are polluted with (Eerkes-Medrano et al., 2015; Lechner et al., 2014; Wagner et al., 2014) to downstream seas and oceans (Kooi et al., 2018; Lebreton et al., 2017). Indeed, there is evidence that MP in lotic waters may be prevented from directly reaching downstream lentic waterbodies due to ingestion by organisms (Peters and Bratton, 2016; Sanchez et al., 2014) or retention in sediments (Castañeda et al., 2014; Klein et al., 2015; Leslie et al., 2017).

The Rhine River catchment is home to ~60 million people (ICPR, 2018), with over 10 million inhabitants in the Rhine-Ruhr metropolitan area alone (IT NRW, 2018). The Middle and Lower Rhine stretches host approximately 10% of the world's chemical industry (NRW Invest, 2016) and every year over 110,000 vessel sailings carry ~150 million tonnes of goods through the Lower Rhine alone, (WSV DE, 2017) qualifying the Rhine as one of the world's most frequented inland waterways (CCNR, 2018). The surface waters of the Rhine (Hess et al., 2018; Leslie et al., 2017; Mani et al., 2015) as well as shoreline sediments (Klein et al., 2015) and estuary benthos (Leslie et al., 2017) have been investigated for MP. The Rhine transports 10–30 tons of plastic litter toward the North Sea every year (Mani et al., 2015; van der Wal et al., 2015). However, there is a knowledge gap regarding the role of benthic, midstream sediments as potential temporary or permanent MP sinks in the Middle and Lower Rhine stretches. Until now, it was unclear (i) which types and sizes of polymers may be retained in the riverbed; (ii) if the retained polymers are complementary to those found in near-surface compartments; and (iii) if the “polymer footprint” could possibly indicate specific dominant emission sources (e.g., shipping). Two sites where MP concentrations at the water surface notably increased and peaked, respectively, were previously identified at Rhine kilometres (Rh–km) 640 and 837

(Mani et al., 2015). For the present study, two geographically proximal stretches (at Koblenz, Rh-km 593.95–598.77 and Rees, 837.41–837.52) were chosen to investigate if these high surface water MP concentrations are reflected in the midstream bed sediments (Di and Wang, 2018). Until now, the interaction of MP with benthic riverbed sediments in stretches of dynamic flow represented a highly unknown factor in the mass balancing of MP downstream transportation (Lebreton et al., 2017). We hypothesised that (hA) the sediments mainly contain MP polymers that are denser than freshwater ($>1 \text{ g cm}^{-3}$) with small diameters ($<100 \mu\text{m}$), based on the preferential heteroaggregation of small MP with ambient suspended solids, which increases MP settling capability (Besseling et al., 2017), and second, as a result of the continuous attrition of polymers into ever smaller particles in the bedload (Frings, 2008). Furthermore, we hypothesized (hB) that the polymer composition in the sediments would complement the dominance of low-density polymers in the near-surface compartments of the Rhine (Hess et al., 2018; Klein et al., 2015) and that (hC) the exceptionally high shipping frequency leaves a characteristic polymer footprint due to the loss of antifouling paint particles from vessels (Frings, 2008; Mani et al., 2018).

Acknowledging that the size-frequency distribution of MP in sediments is reportedly strongly skewed toward the smallest particle sizes (Bergmann et al., 2017) and that visual selection of small MP is highly bias-afflicted (Hidalgo-Ruz et al., 2012), riverbed MP were quantified down to $11 \mu\text{m}$ by MP analysis using automatic focal plane array (FPA) micro-Fourier-transform infrared spectroscopy (μFTIR) microscopy and image analysis (Primpke et al., 2017b). Riverine water-sediment interfaces are highly important biological zones that provide significant food sources for benthic organisms (Shumchenia et al., 2016), thus, MP-contaminated riverbed sediments increase the probability of plastic ingestion (Eerkes-Medrano et al., 2015) and ultimately threaten the health of the riverine ecosystem (Hurley et al., 2017). Therefore, detailed knowledge on the amount, sizes, and polymer compositions of the MP in benthic riverbed sediments is necessary to devise mitigation and remedial measures.

2. Materials and methods

2.1. Sampling

Twenty-five samples (n) were collected at ten sites (N) from the Rhine riverbed close to the German settlements of Koblenz ([K], $n = 10$, $N = 5$; Rhine kilometres [Rh-km] 593.95–598.77) and Rees ([R], $n = 15$, $N = 5$; Rh-km 837.41–837.52) at water depths of 5–7.5 m during February–June 2016 (Fig. 1, Table S1). Nineteen samples were taken by accessing the riverbed through the German diving bell [B] vessel *Carl Straat* ($n = 10$, $N = 5$ at Koblenz

[KB1-1–KB5-2] and $n = 9$, $N = 3$ at Rees [RB1-1–RB3-3], Supporting Information [SI Fig. S1). The sediment was sampled down to ~ 7 cm using a 10×10 cm wooden frame and wooden ruler to monitor the approximate sample volume. A diving bell vessel was selected for sampling to access the riverbed manually to minimise sediment disturbance and sample loss (Tittizer et al., 1988) as opposed to, e.g., using a grab approach (Blomqvist, 1991). For a method and depth comparison, six further opportunistic samples were collected at two sites at Rees using the buckets of a chain dredging [D] vessel to sediment depths of 42 cm (RD1) and 111 cm (RD2, Fig. S2, Table S1). All samples ($n = 25$) were collected using a steel spade with a wooden handle, aiming for approximately 700 cm^3 of wet sediment per sample. Samples were subsequently transferred to distilled water (aq. dest.)-rinsed 1 L glass jars, conserved with 200 mL of ethanol (96%) and sealed with metal lids. Mean (\pm SD) sample wet weight (ww) was 1.3 ± 0.3 kg (Table S1).

2.2. Drying, sieving, aliquoting and pooling

Samples were dried at $60 \text{ }^\circ\text{C}$ for 4 days; mean sample dry weight was 1.2 ± 0.2 kg (dw \pm SD; Table S1). Effective sediment volumes (sediment bulk volume minus the voids in-between pebbles and grains) were determined by separately and thoroughly mixing each dry sample with 300 mL of aq. dest. in a 1,000 mL glass cylinder and subtracting the 300 mL from the resulting total volume after the aq. dest. had intruded the sediment voids. Mean effective sample volume (\pm SD) was $459.3 \pm 77.6 \text{ cm}^3$ (Table S1). The sample grains were highly heterogeneous in size and ranged from clay to coarse pebbles; therefore, the grains were fractionated ($n = 25$) into three grain-size categories: <2 mm (clay–silt–sand); 2–5 mm (gravel–fine pebbles) and >5 mm (fine–coarse pebbles) using stainless steel geological sieves (see Table S1 and Fig. S3 for the grain size ratios of each sample). Subsequently, the replicate aliquots of the clay–silt–sand fraction ($n = 25$) from each of the ten sampling sites were pooled, resulting in ten 60 g dw pools (five each for Koblenz and Rees). Aliquots of 30 g were pooled in pairs for the five Koblenz sites (KB1–5) and aliquots of 20 g were pooled in triplets for the five Rees sites (RB1–3 and RD1–2).

2.3. ZnCl_2 density separation

Samples were density separated using a protocol inspired by the Munich Plastic Sediment Separator (Imhof et al., 2012). The ten 60 g pools of clay–silt–sand sediment (<2 mm) were separately transferred into 100 mL Erlenmeyer flasks under a fume hood. The flasks were filled with a ZnCl_2 solution ($\rho \sim 1.7 \text{ g cm}^{-3}$), leaving a 1.5 cm margin below the brim, and covered with aluminium foil to prevent entry of airborne particles. To disaggregate clusters of sediment

and potential MP particles, the glass receptacles were submerged in an ultrasonic bath, until the mouth of the flask was 3 cm above the brim, and sonicated for 15 min at 160 W/35 kHz (Sonorex RK255 H; Bandelin Electronic GmbH & Co., Berlin, Germany). Subsequently, the samples were stirred for 1 h at 250 rpm using PTFE-coated magnetic stirrer bars to suspend particles with $\rho < 1.7 \text{ g cm}^{-3}$. Subsequently, the exteriors of the flasks were cleaned with aq. dest. and the flasks were placed onto 14 cm-diameter glass Petri dishes. The flasks were fully topped up with ZnCl_2 and left to settle for 30 min, before adding another 20 mL of ZnCl_2 and allowing the excess fluid, as well as the suspended solids therein, to run down into the underlying Petri dishes (Figs. S4 and S5). Using aq. dest. the exteriors of the flasks were rinsed down into the Petri dishes, and the collected supernatants were funnelled into 250 mL glass volumetric flasks and sealed with glass stoppers and Parafilm and stored at 4 °C.

2.4. Purification using Fenton's Reagent

To reduce the interference of organic material in the μFTIR analysis, samples were purified using Fenton's reagent (Tagg et al., 2017). As μFTIR analysis in transmission mode only reliably identifies MP $< 500 \text{ }\mu\text{m}$, suspended samples were sieved through stainless steel $500 \text{ }\mu\text{m}$ mesh and the filtrates were subsequently vacuum filtered onto stainless steel $10 \text{ }\mu\text{m}$ mesh disks. The $> 500 \text{ }\mu\text{m}$ fraction was retained for subsequent manual MP analysis (*cf.* section 2.7). Each disk was placed into a dry 200 mL glass beaker in a 20 °C water bath; 10 mL of FeSO_4 solution (7.2 mM, pH 5) was added, and then 20 mL of H_2O_2 (30%) was added dropwise over 15 min to induce the exothermic Fenton's reaction while the temperature of the water bath was monitored (step A). To remove residual particles from the steel meshes, the filters and beakers were placed into an ultrasonic bath and sonicated at 215 W/35 kHz for 5 min (step B; Sonorex RK514). Steps A and B were both repeated in the same succession. Next, three 1 mL subsamples from every sample were analysed using a FlowCam (Fluid Imaging Technologies, Inc., Scarborough, ME, U.S.A.) to calculate a feasible suspension volume for filtration onto the Anodisc for μFTIR imaging (Bergmann et al., 2017; Lorenz et al., 2017). Accordingly, the calculated volumes of suspension for each sample (between 7.5–100%; Table S1) were filtered onto aluminium oxide filters (pore size: $0.2 \text{ }\mu\text{m}$, diameter: 25 mm, Anodisc; Whatman, Merck, Darmstadt, Germany). Sample pools KB3, KB5, and RB2 underwent additional density separation using ZnCl_2 and were passed through a separation funnel to remove excess hydrated iron oxide particles that formed during the Fenton reaction.

2.5. Focal plane array μ FTIR analysis

The sample fractions (<500 μm) on Anodisc filters were analysed using a Hyperion 3000 μ FTIR microscope equipped with a Focal Plane Array (FPA) detector (64×64 detector elements) and TENSOR 27 spectrometer (Bruker Optics GmbH., Billerica, MA, U.S.A.). Measurements were performed at wavenumbers from 3600–1250 cm^{-1} at a resolution of 8 cm^{-1} and binning factor of 4 with six scans per field (see Löder et al., 2015 for details). Filters were dried for at least 2 days at 30 °C and placed onto a calcium fluoride window under the μ FTIR microscope, a visual overview image was recorded (Fig. S6) and then the concentrates on the filter (166 mm^2 , 73×73 FPA fields, 1.36 million spectra) were assessed (ca. 13 h per filter).

2.6. Automated analysis of μ FTIR data

Each FTIR spectrum was automatically analysed using two library search methods to confirm the identities of the polymers via automated analysis (Primpke et al., 2017b) combined with a database with an adaptable design (Primpke et al., 2018). Each identified pixel was recorded, together with its position, analysis quality, and polymer type, and further investigated via image analysis based on Python 3.4 scripts and Simple ITK functions (Primpke et al., 2017b). This method excludes human selection bias and enables identification, quantification and size determination for all polymer particles (Primpke et al., 2017b). MP particle numbers were assessed on the aliquot filters with an accuracy of 5%; size classes were introduced to reduce the complexity of the size distribution (e.g. 11 μm , 11–25 μm , etc., see Primpke et al., 2017b) for details). Error calculation and error values are provided in the SI.

2.7. Visual selection and ATR FTIR analysis of >500 μm fractions

Putative MP >500 μm in the <2 mm aliquots were visually and tactually investigated on cellulose filter paper (pore size: 0.45 μm , diameter: 47 mm; Whatmann ME25, mixed cellulose ester, Merck) using ultra-fine forceps and a stereomicroscope equipped with a camera and imaging software (Olympus SZ61, Olympus SC50, Tokyo, Japan; CellSens Entry Version 1.17.16030.0). Selection criteria (though not exclusive) were (i) homogeneous texture with an absence of cellular structure and absence of (ii) crushing or powdering upon applying force with forceps, and (iii) conspicuous artificial colouring and (iv) shape (e.g., spherule or filament; Masura et al., 2015; Norén, 2007). Particles meeting at least one of these four criteria ($n = 126$) were analysed using an attenuated total reflection (ATR) FTIR spectrometer (Bruker ALPHA with a Platinum Diamond-ATR QuickSnap Sampling Module, Bruker). IR-Spectra were recorded over the wavenumber range of 4,000–400 cm^{-1} at a resolution of 4 cm^{-1} , applying 24 scans. Each spectrum was compared against a reference spectra library using Opus 7.5 software

(Bruker; B-KIMW ATR-IR Polymers, Plastics and Additives, 898 entries, principle component analysis). Particles with a synthetic polymer hit quality index (HQI) above 70% were considered MP. The entire 2–5 mm and >5 mm fractions were visually investigated on a stainless steel tray and a stereomicroscope in the case of conspicuous particles.

2.8. Statistical analysis

MP concentrations were compared using unpaired *t*-tests with Welch's correction. Data normality was assessed using the Shapiro-Wilk test ($p > 0.05$). Linear regression analysis of MP concentrations and sample sand proportions was performed using Spearman's rank correlation. All statistical analyses were carried out using GraphPad Prism version 7.03 for Windows (GraphPad Software, La Jolla, CA, U.S.A.).

2.9. Quality assessment and quality control

Sampling, processing, and analysis steps were performed using glass, stainless steel, wood, or PTFE materials instead of other plastics whenever possible; PTFE cannot be identified in the spectral IR range between 3600–1250 cm^{-1} applied for automatic μFTIR imaging (Primpke et al., 2017b). All items were rinsed with aq. dest. before use. The one exception was a PE squirt bottle used for aq. dest. rinsing; otherwise a PTFE squirt bottle was used. Samples were processed under a fume hood whenever possible and white 100% cotton lab coats were worn at all times. Dustboxes (DB1000, G4 prefiltration, HEPA-H14 final filtration, $Q = 950 \text{ m}^3 \text{ h}^{-1}$; Möcklinghoff Lufttechnik, Gelsenkirchen, Germany) that filter airborne particles were installed in the laboratories for Fenton's reagent purification, additional density separation (ZnCl_2) after Fenton's and μFTIR imaging. Fenton's reagent purification, additional density separation and Anodisc filtration were performed in a laminar flow cabinet (Scanlaf Fortuna, Labogene, Allerød, Denmark). The H_2O_2 and FeSO_4 solutions were filtered through polycarbonate filters (0.2 μm , GTTP; Merck Millipore, Darmstadt, Germany) to remove particulate contaminants before use. Sample receptacles were always covered or sealed as soon as possible after each treatment step using glass lids, Parafilm or aluminium foil. Three procedural blanks were run and analysed with automated μFTIR imaging to detect potential sample processing-introduced MP in the samples (Fig. S7); accordingly, all reported MP concentrations were blank corrected with consideration to polymer types and size classes (SI).

3. Results

3.1. Microplastic concentrations and sizes

MP were identified at all sites from Koblenz and Rees at sizes ranging between 11–5033 μm (orthogonal longest axis). Concentrations were in the range 0.26 ± 0.01 – $11.07 \times 10^3 \text{ MP}$

particles kg^{-1} in the 11–500 μm size range, Fig. 1). The MP concentrations for the five diving bell sites at Koblenz were: $0.26 \pm 0.01 \times 10^3 \text{ kg}^{-1}$ (KB1), $2.05 \pm 0.13 \times 10^3 \text{ kg}^{-1}$ (KB3), $2.54 \pm 0.14 \times 10^3 \text{ kg}^{-1}$ (KB4), $2.74 \pm 0.15 \times 10^3 \text{ kg}^{-1}$ (KB2), and $5.22 \pm 0.75 \times 10^3 \text{ kg}^{-1}$ (KB5, Fig. 1). At Rees, the three diving bell sites yielded $3.13 \pm 0.44 \times 10^3 \text{ kg}^{-1}$ (RB1), $3.43 \pm 0.19 \times 10^3 \text{ kg}^{-1}$ (RB3), and $11.07 \pm 0.6 \times 10^3 \text{ kg}^{-1}$ (RB2). The two Rees bucket chain dredge sites contained $1.79 \pm 0.1 \times 10^3 \text{ kg}^{-1}$ (RD1) and $0.89 \pm 0.05 \times 10^3 \text{ kg}^{-1}$ (RD2). Mean MP concentrations were higher at Rees than Koblenz (only diving bell considered) and higher for the diving bell sites than the bucket chain dredge sites (only Rees considered); however, statistical comparisons yielded no significant differences, possibly due to the relatively low sample pool numbers ($N = 10$, $p > 0.05$; Fig. S8). The lowest MP concentrations at Rees were recorded in the bucket chain sites RD1 and RD2. The deeper dredge sediment sampling depths (compared to the diving bell) may be responsible for “dilution” of MP concentrations with clean, deeper lying sand, and the open dredging bucket possibly allowed for loss of smaller MP during sample hauling. The highest MP pollution level in the central Rees site RB2 may possibly be explained by its position within the highly frequented navigation channel, where high shipping-related MP emissions may occur. Strikingly, MP concentrations at the five Koblenz sites along the 4.82 km stretch between Rh-km 593.95–598.77 increased from $0.26 \pm 0.01 \times 10^3 \text{ kg}^{-1}$ at the most upstream, central site (KB1) to $5.22 \pm 0.75 \times 10^3 \text{ kg}^{-1}$ at the most downstream site (KB5), located immediately downstream of the Rhine island Graswerth; the three sites in-between KB2–4 yielded a mean MP concentration of $2.45 \pm 0.26 \times 10^3 \text{ kg}^{-1}$. The increase in MP concentrations along this stretch may possibly be explained by changes in the riverbed’s flow velocity exposition moving downstream. Site KB1 contained a low MP concentration, most probably due to its central location in the river cross-section upstream of Niederwerth island, resulting in unsheltered exposure to higher flow velocity. In contrast, site KB5 had the highest concentration of all Koblenz sites, presumably due to its location downstream of Graswerth island that is sheltered from stronger flow dynamics. The sites in between (KB2 to KB4) yielded a narrower range of MP concentrations, possibly as they are exposed to similar water dynamics. However, linear regression analysis of MP concentrations and fine-grain sediment proportions ($< 2 \text{ mm}$) as a proxy for near-bed flow velocity at all ten sites yielded no significant relationship (Fig. S9). MP $< 75 \mu\text{m}$ accounted for $96.3 \pm 5.7\%$ of all MP in the sample fractions analysed by μFTIR imaging from all ten sites; $68.2 \pm 15.9\%$ of all MP were $< 25 \mu\text{m}$ (Fig. S10).

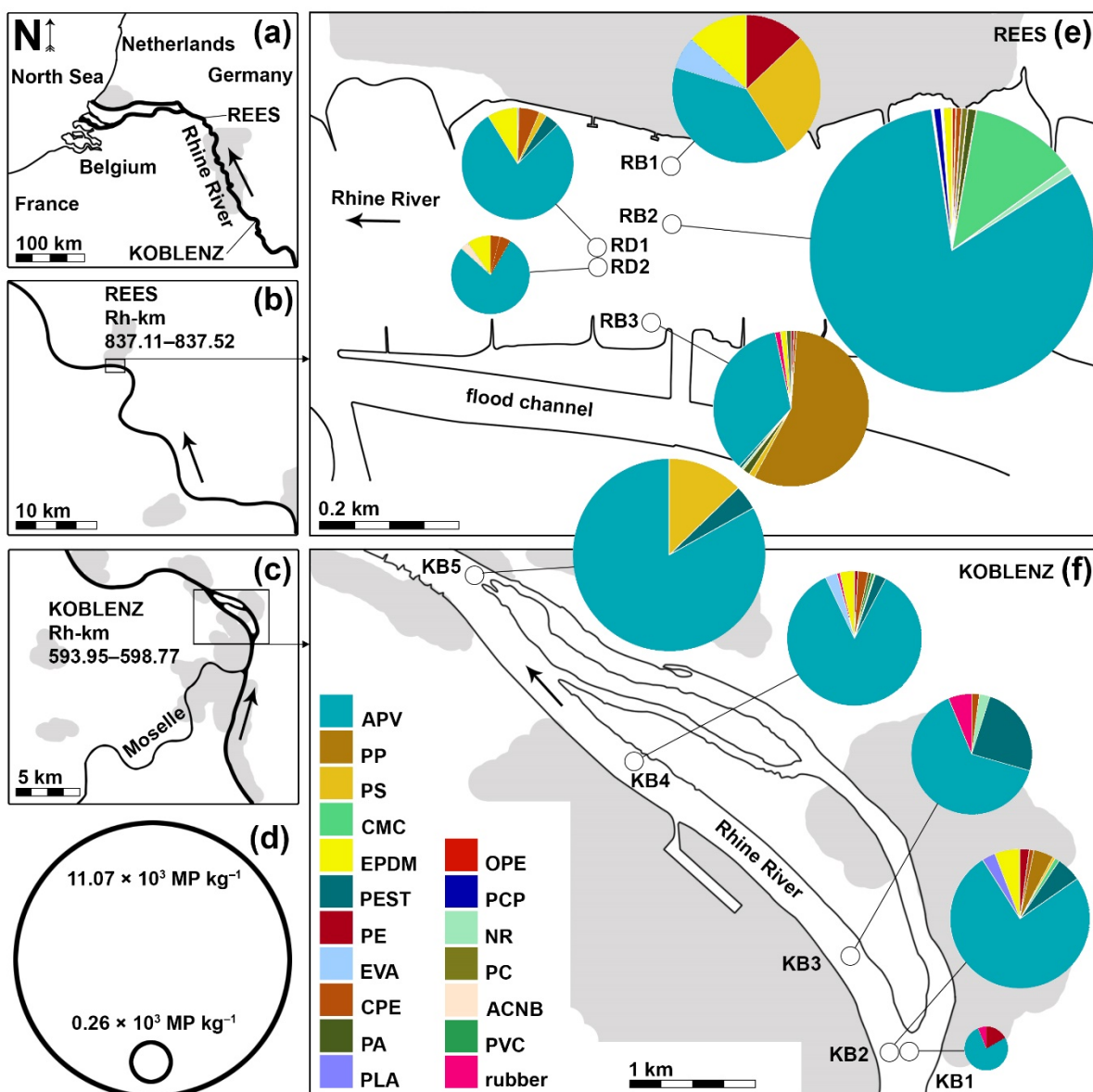


Fig. 1: Microplastics concentrations at Rees and Koblenz in the size range 11–500 μm . Location of the sampling sites at Rees and Koblenz (a–c); MP concentrations correspond to the area of the circles (d); microplastics particle concentrations in MP kg^{-1} and polymer numerical proportions at Rees (e) and Koblenz (f). APV: acrylates/polyurethanes/varnish cluster; PP: polypropylene; PS: polystyrene; CMC: chemically modified cellulose; EPDM: ethylene-propylene-diene rubber; PEST: polyester; PE: polyethylene; EVA: ethylene-vinyl-acetate; CPE: chlorinated polyethylene; PA: polyamide; PLA: polylactide acid; OPE: oxidised polyethylene; PCP: polychloroprene; NR: nitrile rubber; PC: polycarbonate; ACNB: acrylonitrile-butadiene; PVC: polyvinyl chloride.

3.2. Polymer composition

Eighteen polymer types were identified through μFTIR imaging in the 11–500 μm size fraction (18 types in Rees and 14 in Koblenz, Fig. 1). The acrylates/polyurethane/varnish cluster (representing 27 different spectra; Primpke et al., 2018), henceforth termed APV, was found at

all ten sites. The sites lying within the shipping channel (all except RB1 and RB3) yielded a mean numerical proportion of $78 \pm 6.4\%$ APV MP compared to 39% and 33% at the two peripheral diving bell sites at Rees. The next most widely distributed polymers were chlorinated polyethylene (CPE, 7 sites), ethylene-propylene-diene rubber (EPDM, 7), polyester (PEST, 6), and polyethylene (PE, 6, Table S3). The most polymer-diverse sites were RB3 (11 polymers), RB2 (10), KB4 (10), and KB2 (9). RB3 lies at the slip-off slope of a sharp, left turning riverbend at Rees, where the lowest flow velocity of all investigated sites was reflected by the highest fine-grain sediment proportion (Fig. S3). The low exposure to currents at RB3, resulting in sediment accumulation, is a possible explanation for the settling of a wider density range of polymers, manifested in the by far highest share of the low density PP for any site (57.2%). At RB2, with the exception of APV (81.8%) and chemically modified cellulose (CMC, 12.2%), all other polymer types accounted for less than 1.1% of particles. Hence, the high diversity there is due to the presence of a wide variety of scarcely represented polymers. Riverbed dredging does not take place at RB2, potentially enabling this modest retention of a wide array of polymers. KB4 and KB2 are similarly positioned on the left-hand border of the shipping channel downstream of Koblenz. Their relatively high diversity is the result of the presence of several types of polymer at proportions of 0.3–5.9% (apart from APV, $80.4 \pm 6.7\%$). The lowest polymer diversities were found at the Koblenz sites KB1 and KB5, which featured only three types each (Fig. 1). At Rees, the diving bell sampling sites yielded higher mean polymer diversities than the dredged sites (9 ± 3.6 vs. 5.5 ± 0.7).

From the manually sorted $>500 \mu\text{m}$ sediment fractions, eight of the total 126 putative microplastic particles analysed by ATR-FTIR (6.3%) were confirmed as synthetic polymers (HQI $>70\%$; *cf.* section 2.7): PTFE in KB1 (1), RB2 (2) and RB3 (2); urea formaldehyde (UF) resin in KB5 (1) and RD1 (1); and PE in RB3 (1). PTFE was not considered further in this study, as it could not be detected by μFTIR imaging (Primpke et al., 2017b; *cf.* section 2.9). No putative MP were detected in the 2–5 mm and >5 mm fractions.

4. Discussion

4.1. MP sedimentation and retention in riverbed sediments

Aquatic suspended particulate matter, including MP, is expected to preferentially settle in low-dynamic environments (Mahmood, 1987). Rivers are characterised by an elevation gradient resulting in time-averaged motion of water in the longitudinal direction (Ji, 2017). As dynamics increase, the probability of MP sedimentation, retention and burial decrease (Besseling et al., 2017; Kooi et al., 2018; Nizzetto et al., 2016). Density and shear forces within a moving

waterbody counter the settling of MP (Kooi et al., 2018); thus, among others, the factors relevant to midstream riverbed MP sedimentation include (i) specific polymer density (Corcoran, 2015; Kowalski et al., 2016), (ii) local hydrodynamics (Hurley et al., 2018; Nizzetto et al., 2016), and (iii) formation of biofilms on MP (Fazey and Ryan, 2016; Lobelle and Cunliffe, 2011; Rummel et al., 2017) that alter (iv) the attachment efficiency of MP to ambient non-MP suspended solids (Farley and Morel, 1986; Quik et al., 2014) and hence influence (v) heteroaggregation with ambient particulate matter (Besseling et al., 2017), potentially allowing MP settling and riverbed retention, even in coarse substrates (Pye, 1994). In this evaluation of the Rhine riverbed sediments, we focused on specific polymer density, local hydrodynamics, and potential heteroaggregation.

4.2. MP concentrations in riverbed sediments

Considering the preferable MP settling conditions of low water dynamics (Kooi et al., 2018), the presence of high MP concentrations in the midstream Rhine riverbed sediments from open-flowing, dynamic stretches with mean flow velocities of 1.2–1.4 m s⁻¹ (WSV DE, 2016a) is unexpected. The higher mean MP concentrations at Rees compared to Koblenz may be due to general differences in natural and artificial sedimentation and erosion regimes, as well as almost impossible to predict local hydrodynamics. Downstream of Koblenz, the Rhine riverbed is subject to high erosion due to sporadic discharge increases of the inflowing Moselle river, which carries suspended solids but no bedload (Ries, 2019). Therefore, on average, every 18 months, 35,000 m³ of terrestrially quarried basalt rubble (grain size: <100 mm) is artificially introduced into the Rhine immediately downstream of the Moselle inflow (Ries, 2019) – just at the stretch where the Koblenz samples were taken for this study. In contrast, at Rees, the slip-off slope on the inside of the sharp river bend (samples RD1, RD2, and RB3) is a net sedimentation zone, where periodic dredging is required to maintain the depth of the shipping channel (Wolters, 2019). According to the responsible authorities, the artificially introduced basalt rubble downstream the Moselle-Rhine confluence at Koblenz is unlikely to be MP-contaminated (Ries, 2019). This possibly explains the generally lower MP concentrations at Koblenz, compared to Rees where sediment and MP may accumulate on the riverbed over time.

The Rhine sediments at RB1–3 and KB5, sampled 163 and 402 km upstream of the estuary, yielded MP concentrations of a comparable magnitude as findings in the downstream, tidal harbour benthic sediments of Rotterdam (3.01–3.6 × 10³ kg⁻¹, >10 μm; Leslie et al., 2017). Although the MP concentrations at six sites (KB1–4 and RD1 and RD2) in the present study are lower than the Rotterdam figures, the MP concentrations at KB5 and RB2 remarkably exceeded the concentrations in the Rotterdam harbour (while RB1 and RB3 are within the

Rotterdam range). This finding is remarkable as Rotterdam lies (a) at the mouth of the Rhine and is (b) home to Europe's busiest and the World's twelfth busiest port (Eurostat, 2018; World Shipping Council, 2016). Hence, (a') in the absence of stronger flow dynamics, water dynamics are largely reduced to tidal, seiche and shipping influences (Jong and Battjes, 2004) which facilitates MP settling (Kooi et al., 2018) and (b') the estuary is under enormous anthropogenic pressure, receiving high pollution immissions (Ng and Song, 2010), and is thus expected to retain high amounts of MP in its sediments. Due to massive sedimentation at the mouth of the Rhine, regular dredging is necessary at Rotterdam to maintain smooth shipping operations (Verlaan and Spanhoff, 2000). Thereby, anthropogenic pollutants, including MP, may be removed from the estuary (van den Hurk et al., 1997). A previous longitudinal study of the Rhine indicated decreasing water surface MP concentrations between Rees and downstream Rotterdam which led to speculation that the "lost" MP could all be retained in the estuarine sediments (Mani et al., 2015). If this were true, we would expect to observe lower riverbed concentrations at upstream sites (this study) than in the estuary (Leslie et al., 2017). However, this assumption is not supported by our nor by other studies (Di and Wang, 2018; Hurley et al., 2018; Nel et al., 2018). On a technical note, it is important to state that existing comparisons of upstream (present study) and estuary (Leslie et al., 2017) Rhine riverbed MP concentrations are based on two individual studies, each with limited sample numbers, highly variable concentrations (in this study), and different sampling, purification and polymer analysis approaches and techniques. Furthermore, the depth, timing and season of sampling, as well as previous dredging or artificial sediment supply events and the position of the sites relative to the shipping channel may affect the resulting MP concentrations and polymer compositions. Looking to other European waters, the MP concentrations of the present study are comparable with those of canals in Amsterdam (Leslie et al., 2017) and England (Hurley et al., 2018), which yielded $0.07\text{--}10.5 \times 10^3 \text{ kg}^{-1}$ ($>10 \mu\text{m}$) and $0.3\text{--}4.8 \times 10^3 \text{ kg}^{-1}$ ($>63 \mu\text{m}$), respectively. While (Hurley et al., 2018) may have reported higher concentrations if smaller particles had been included (due to the likely dominance of small MP; Bergmann et al., 2017), it is completely unforeseen that Rhine midstream sediments contain similar concentrations of MP as the almost static downtown canals (Leslie et al., 2017) of the 850,000-inhabitant Dutch capital (Statista, 2018). Generally, it seems that the local, small-scale variability in MP pollution and retention is highly diverse (Wagner et al., 2014) and that these effects may superimpose on other, larger scale factors such as general suspended solid transport and sedimentation regimes. The coexistence of hydrological, physical, hydraulic engineering, and pollution influences plays a crucial role in the outcome of MP investigations and will always lay the curse of high

uncertainty on the interpretation of the data. However, putting the European figures into perspective, the highest riverbed sediment MP concentrations reported to date were found in the Wen-Rui Tang River at $18.69\text{--}74.8 \times 10^3 \text{ kg}^{-1}$, albeit very small MP particles $>0.4 \mu\text{m}$ were included (Wang et al., 2018). In that study, the low-elevation gradient dictated flow velocities below 0.05 m s^{-1} during the sampling process close to the >3 million-citizen Wenzhou metropolis (Wenzhou Municipal Statistic Bureau, 2011) where the Wen-Rui Tang canal system enters the Oujiang river slightly upstream of the East China Sea (Wang et al., 2018), providing two highly favourable preconditions for MP in sediments: calm water (Kooi et al., 2018) and a high population (Dris et al., 2015).

4.3. Polymers in the Rhine riverbed sediments

The high proportions of APV in the riverbed sediments are a novel finding for the entire Rhine ecosystem. Two main members of the APV cluster, acrylates (ACR) and polyurethanes (PU, both $\sim 1.2 \text{ g cm}^{-3}$; Primpke et al., 2017a), are common components of antifouling paint used to protect and reduce friction on ship hulls (Mellor and Khanna, 2006). Antifouling paint formulas can reach specific densities of up to 2 g cm^{-3} (Jones, 2007; Turner, 2010) and substantial loads of antifouling paint particles reportedly erode into the environment from vessel hulls as a result of chemical, physical or mechanical stress impact (Turner, 2010). Given the high traffic density on the Rhine River, it is likely that considerable proportions of the reported benthic APV particles stem from antifouling paint. The highest APV concentration was detected at the centre-riverbed at RB2 (Table S3), which spatially coincides with the navigation channel (WSV DE, 2016b). However, ACR and PU polymers are also used in other applications, including construction, automobiles, glass substitutes, textiles, biomedicine and optics (ACR; Ali et al., 2015; Penzel et al., 2000) as well as construction, automobiles, refrigerator insulation and furniture (PU; Covestro, 2017). The areas upstream of all sampling sites feature dense human populations as well as intense construction and industrial activities (ICPR, 2018; NRW Invest, 2016), which may also contribute to the frequent occurrence of APV in the sediments, as widely used APV materials are potentially emitted to the environment due to riparian mismanagement (Dris et al., 2015; Eerkes-Medrano et al., 2015). It is remarkable that the highest APV concentration was identified at RB2 in the centre of the riverbed, which is exposed to stronger water currents, than in the peripheral sites closer to the riverbank. The stronger central water currents are corroborated by the comparatively low clay–silt–sand proportion of only $8.4 \pm 3.8\%$ in these samples (Fig. S3 and Table S1). This finding possibly indicates that the concentrations of APV MP in the central benthic Rhine sediment may at times be much higher or lower than those reported here, but that these particles are continuously resuspended and

washed downstream due to riverbed erosion (Hurley et al., 2018; van Rijn, 1984). The limited data on polymer types in benthic river sediments around the world indicates low proportions of APV polymers. PU accounted for 6.5% of identified MP particles ($n = 293$) in the Chinese Wen-Rui Tang watershed in Wenzhou (Wang et al., 2018); where the narrow canal system does not facilitate high shipping activity and the high levels of heavy metal pollution in sediments are attributed to industrial activities (Xia et al., 2018). No APV-relevant MP were found in the Yangtze River upstream of the Three Gorges Dam ($n = 174$, $>48 \mu\text{m}$; Di and Wang, 2018) despite this area seeing an increase in shipping in the past few years (Zheng and Yang, 2016). Similarly, benthic sediments from the Canadian St. Lawrence River did not yield APV polymers; however, it should be noted that the study only included MP $>500 \mu\text{m}$ and focused on PE microbeads (Castañeda et al., 2014). It is important to state that the Chinese and Canadian studies (Castañeda et al., 2014; Di and Wang, 2018) both relied on visual preselection of potential MP particles, and employed different polymer identification algorithms to the present study. Therefore, it remains unclear what the investigations at those sites would yield if they were conducted with the same methodology as employed in this investigation. Turning to other studies of the Rhine River near-surface compartments, the proportion of APV-type polymers ranged from 1.5% (Klein et al., 2015) and 2.5% (Hess et al., 2018) to 18.6% (Mani et al., 2015). However, the latter study (Mani et al., 2015) relied on a visual pre-selection of only 118 MP particles; polymethyl methacrylate (PMMA $\sim 1.18 \text{ g cm}^{-3}$) beads represented 9.3% of the reported APV polymers in that study. The presence of those PMMA MP at the water surface was most probably due to the increased buoyancy conferred by gas bubbles inside the beads (Mani et al., 2015). The nonselective, standardised polymer analysis approach used in the present study enables a more objective assessment of polymer types and proportions, as very small and even barely visible MP particles were included automatically (Primpke et al., 2017b). Due to the fact many studies still rely on bias-afflicted, manual, visual MP selection techniques (Klein et al., 2018; Silva et al., 2018), coupled with the limitation that various research groups use different polymer databases, HQI thresholds and polymer identification algorithms, and resulting clusters (Primpke et al., 2017b), it is possible that widespread APV pollution – potentially emitted from erosion of antifouling paint – is widely overlooked (Mani et al., 2018).

Polymers denser than freshwater ($>1 \text{ g cm}^{-3}$) accounted for $85.1 \pm 17.9\%$ (mean \pm SD) of the numerical proportion of MP per site (Table S3). By contrast, only 5% (Hess et al., 2018) and 8% (Klein et al., 2015) of the MP detected in near-surface compartments of the Rhine were $>1 \text{ g cm}^{-3}$ (Fig. 2). Note that PS was considered denser than freshwater in this study; however, it frequently occurs as low-density buoyant foam in near-surface freshwater compartments

(Moore et al., 2011). The distinct polymer density/river compartment allocation in the Rhine is not entirely corroborated by other studies, e.g., of the Chinese Yangtze (Di and Wang, 2018) and Wen-Rui Tang (Wang et al., 2018) rivers, where polymer particles $>1 \text{ g cm}^{-3}$ accounted for 39% and 41% of MP in the riverbed sediments, respectively. This variation may be the result of different research methodologies and geographies (Hidalgo-Ruz et al., 2012; Silva et al., 2018), but could also suggest specific pollution sources and pathways as each of these rivers endure distinct anthropogenic strains (Dris et al., 2015).

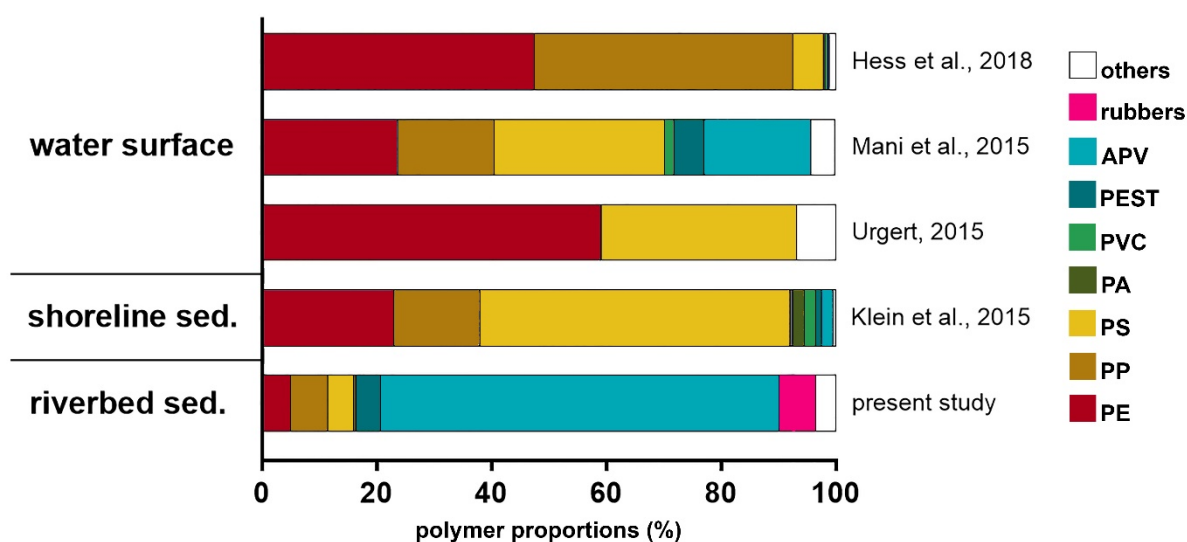


Fig. 2: Mean microplastic polymer cluster proportions reported for three Rhine River compartments in five studies. APV: acrylates/polyurethanes/varnish cluster; PEST: polyester; PVC: polyvinyl chloride; PA: polyamide; PS: polystyrene; PP: polypropylene; PE: polyethylene.

This is the first quantitative evaluation of polymer concentrations down to a particle size of $11 \mu\text{m}$ in benthic riverbed sediments based on a comprehensive sample aliquot analysis. The very low proportion of particles $>500 \mu\text{m}$ positively confirmed as polymers in manual analysis by ATR-FTIR (6.3% *cf.* section 3.2) corroborates the frequently described high bias-affliction of manual MP identification (Ivleva et al., 2017; Lenz et al., 2015; Remy et al., 2015), emphasizing the importance of standardised, bias-mitigating analysis techniques (BASEMAN, 2017; Löder and Gerdts, 2015; Primpke et al., 2017b).

At this point we are able to ascertain that all three hypotheses stated in the introduction can be confirmed: (hA) Benthic Rhine sediments mainly contain small MP of polymers denser than freshwater; (hB) Benthic MP polymer densities contrast near-water surface MP polymers;

(hC) The Rhine River benthic sediments are possibly strongly polluted by antifouling ship paint erosion (*cf.* also section 3.2.).

4.4. Dominance of smallest-size MP in the Rhine riverbed

As plastics fragment into ever-smaller pieces in aquatic media (Lambert and Wagner, 2016), the size frequency distribution of particles is naturally expected to shift and skew toward the smallest detectable size classes (Browne et al., 2011). The MP data from the Rhine riverbed dramatically corroborates this notion, as a mean (\pm SD) of $96.3 \pm 5.7\%$ MP particles per site was $<75 \mu\text{m}$ in diameter (Fig. S10). The striking prevalence of the smallest particle sizes in the Rhine riverbed sediments may be explained by biofouling and the additional grinding up of particles on the riverbed. Biofouling on MP (i) leads to relative increases in the specific density (Besseling et al., 2017), and (ii) at the same time enhances the attachment efficiency of small MP which – coupled with the high abundance of small MP (Browne et al., 2011) – may increase the ability of small MP to form heteroaggregates with natural colloids, and therewith increase the probability of sedimentation (Besseling et al., 2017). In a lotic waterbody, the settling of MP in midstream bed sediments more strongly depends on the particles' sedimentation potential – due to the higher dynamic forces – than in a lentic water body, where all particles, homo- and heteroaggregates $>1 \text{ g cm}^{-3}$ will eventually sink to the ground (Kooi et al., 2018). Once at the riverbed, MP may be continuously ground up into ever finer particles in the moving bedload, which acts as a mill (Frings, 2008). Similarly, ship paint particles are speculated to undergo attrition in dynamic marine sediments (Jones, 2007).

4.5. Sampling method and seasonal influences on sediment MP abundance

The three Rees sites in the centre of the river cross-section, RB2, RD1 and RD2, yielded decreasing MP concentrations with increasing sediment depth: $11.07 \pm 0.6 \times 10^3 \text{ kg}^{-1}$, 7 cm (RB2), $1.79 \pm 0.1 \times 10^3 \text{ kg}^{-1}$, 42 cm (RD1) and $0.89 \pm 0.05 \times 10^3 \text{ kg}^{-1}$, 111 cm, (RD2). Considering that the upper sediment layers usually display the highest levels of MP pollution (Carson et al., 2011; Claessens et al., 2011), the lower mean MP concentrations in the bucket chain dredge samples could be explained by “dilution” of the samples with deeper, less-contaminated sand (Schubert, 2002). As Rhine riverbed sediments are dynamic and subject to regular dredging and deposition of artificial sediments along the shipping routes, the stratification of these sediments does not necessarily represent historical timelines (Frings et al., 2014). Nevertheless, at any point in time, the sediment/water column interface is immediately exposed to water pollution and is therefore the sphere of the latest potential MP retention, possibly explaining the higher MP concentrations in the upper sediment layers.

Significant flushing of MP out of riverbed sediments during high-discharge periods has recently been described (Hurley et al., 2018). At Rees, the bucket chain dredge samples (RD1–2) were collected on February 2, 2016, during river discharge (Q) of $3070 \text{ m}^3 \text{ s}^{-1}$, following a 20-day period of Q dropping to as low as $2020 \text{ m}^3 \text{ s}^{-1}$. The Rees diving bell samples (RB1–3) were taken on March 15, 2016, at $Q = 2670 \text{ m}^3 \text{ s}^{-1}$ following a 40-day period of higher discharges ranging up to $Q = 5350 \text{ m}^3 \text{ s}^{-1}$ (Fig. S11). Despite the period of high discharge between the two sampling dates, the diving bell samples taken on the later date yielded clearly higher MP concentrations, underlining the possible strong effects of the sampling method and potentially the sediment depth and other factors, such as local hydrodynamics (0.89 ± 0.05 and $1.79 \pm 0.1 \times 10^3 \text{ kg}^{-1}$ dredge vs. 3.13 ± 0.44 – $11.07 \pm 0.6 \times 10^3 \text{ kg}^{-1}$ diving bell). However, the relatively low sample size compounds conclusive comparisons at this stage.

4.6. Appraisal of methodology

This is the first study to investigate riverbed MP using automated (FPA) μ FTIR microscopy and image analysis for the 11–500 μm size range (Löder et al., 2015; Primpke et al., 2017b). This method has successfully been demonstrated on samples from wastewater treatment plant in- and effluents (Mintenig et al., 2017; Tagg et al., 2017), as well as Arctic deep sea sediments (Bergmann et al., 2017) and sea ice (Peeken et al., 2018). The greatest advantage of this approach is its exceptional degree of standardisation, which circumvents human bias by (i) avoiding visual pre-selection of potential MP and (ii) automatic comparison of up to 3 million IR spectra against reference libraries (Primpke et al., 2018) in each mapping (Primpke et al., 2017b). On the downside, this method does not accurately reproduce MP particle morphology as (i) only the two-dimensional shape is captured (Primpke et al., 2017b) and (ii) some pixels may be unassigned for identified MP particles as a consequence of weathering (Andrady, 2015) or insufficient removal of biofilms (Lobelle and Cunliffe, 2011), which would alter true particle representation (Primpke et al., 2017b). Like most other MP polymer analysis techniques, FPA μ FTIR-spectroscopy relies on effective sample purification to remove refractory content (Löder and Gerdts, 2015; Tagg et al., 2017). Therefore, heteroaggregation of MP with natural suspended solids – which may possibly yield important indications for MP sedimentation behaviour (Besseling et al., 2017) – cannot be assessed after sample preparation.

MP loss during laboratory processing cannot be ruled out (Löder and Gerdts, 2015). However, we assessed our adapted ZnCl_2 protocol (Imhof et al., 2012) in a pilot spike-recovery test using four particle size classes of PMMA fragments ($\sim 1.18 \text{ g cm}^{-3}$; 62–125 μm ; 125–250 μm ; 250–500 μm and 500–700 μm) in triplicates. Mean recovery rates ranged from 55 to 100%, with the lowest mean retrieval of $55 \pm 8.7\%$ for the smallest size class (Fig. S5). Considering

that $96 \pm 6\%$ of MP particles from the Rhine River sediments were $<75 \mu\text{m}$, the total MP load could be substantially underrepresented. The use of an ultrasonic bath for sample cleansing and separation (Hidalgo-Ruz et al., 2012) may, however, result in the additional fragmentation of MP, and therewith numerical overestimation (Löder and Gerdts, 2015), especially considering likely brittle ship paint fragments.

Acknowledgements

We thank the waterways and shipping administrations (WSA) Duisburg-Rhein and Bingen, Germany for vessel access and technical support. We also thank Nicole Seiler-Kurth, Heidi Schiffer and Hedwig Maria Scharlipp, MGU University of Basel, as well as Vanessa Wirzberger, AWI Helgoland, for laboratory assistance. Special thanks go to Andrea Devlin, chief editor of Science Editing Experts for proof reading and language support. This work was supported by the World Wide Fund for Nature (WWF) Switzerland and the German Federal Ministry of Education and Research (Project BASEMAN - Defining the baselines and standards for microplastics analyses in European waters; BMBF grant 03F0734A). C.L. thanks the Deutsche Bundesstiftung Umwelt (DBU) for financial support.

Author contributions

T.M., P.H., and G.G. designed the study; T.M. performed the field work; T.M. and C.L. processed and prepared the samples for μ FTIR imaging; S.P. conducted the polymer identification and analysis; T.M. and P.H. analysed the data and wrote the manuscript with substantial contributions from and final approval of all authors.

References

- Ali, U., Karim, K.J.B.A., Buang, N.A., 2015. A review of the properties and applications of poly (methyl methacrylate) (PMMA). *Polym. Rev.* 55 (4), 678–705.
doi:10.1080/15583724.2015.1031377.
- Andrady, A.L., 2015. Persistence of plastic litter in the oceans, in: Klages, M., Gutow, L., Bergmann, M. (Eds.), *Marine Anthropogenic Litter*. Springer, pp. 57–72.
- BASEMAN, 2017. Interdisciplinary Research for Good Environmental Status.
<http://www.jpi-oceans.eu/baseman>. Accessed 9 May 2018.
- Bergmann, M., Wirzberger, V., Krumpfen, T., Lorenz, C., Primpke, S., Tekman, M.B., Gerdt, G., 2017. High quantities of microplastic in Arctic deep-sea sediments from the HAUSGARTEN observatory. *Environ. Sci. Technol.* 51 (19), 11000–11010.
doi:10.1021/acs.est.7b03331.
- Besseling, E., Quik, J.T.K., Sun, M., Koelmans, A.A., 2017. Fate of nano- and microplastic in freshwater systems: A modeling study. *Environ. Pollut.* 220 (Pt A), 540–548.
doi:10.1016/j.envpol.2016.10.001.
- Blomqvist, S., 1991. Quantitative sampling of soft-bottom sediments: Problems and solutions. *Mar. Ecol. Prog. Ser.* 72, 295–304. doi:10.3354/meps072295.
- Browne, M.A., Crump, P., Niven, S.J., Teuten, E., Tonkin, A., Galloway, T., Thompson, R., 2011. Accumulation of microplastic on shorelines worldwide: Sources and sinks. *Environ. Sci. Technol.* 45 (21), 9175–9179. doi:10.1021/es201811s.
- Carson, H.S., Colbert, S.L., Kaylor, M.J., McDermid, K.J., 2011. Small plastic debris changes water movement and heat transfer through beach sediments. *Mar. Pollut. Bull.* 62 (8), 1708–1713. doi:10.1016/j.marpolbul.2011.05.032.
- Castañeda, R.A., Avlijas, S., Simard, M.A., Ricciardi, A., Smith, R., 2014. Microplastic pollution in St. Lawrence River sediments. *Can. J. Fish. Aquat. Sci.* 71 (12), 1767–1771.
doi:10.1139/cjfas-2014-0281.
- CCNR, 2018. Information on the waterway Rhine. Central Commission for the Navigation of the Rhine. <https://www.ccr-zkr.org/12030100-en.html>. Accessed 18 December 2018.
- Claessens, M., Meester, S. de, van Landuyt, L., Clerck, K. de, Janssen, C.R., 2011. Occurrence and distribution of microplastics in marine sediments along the Belgian coast. *Mar. Pollut. Bull.* 62 (10), 2199–2204. doi:10.1016/j.marpolbul.2011.06.030.

- Corcoran, P.L., 2015. Benthic plastic debris in marine and fresh water environments. *Environ. Sci. Process. Impact.* 17 (8), 1363–1369. doi:10.1039/c5em00188a.
- Covestro, 2017. Polyurethane Applications.
<https://www.polyurethanes.covestro.com/en/Applications/Overview>. Accessed 28 January 2019.
- Di, M., Wang, J., 2018. Microplastics in surface waters and sediments of the Three Gorges Reservoir, China. *Sci. Tot. Env.* 616-617, 1620–1627.
doi:10.1016/j.scitotenv.2017.10.150.
- Dris, R., Gasperi, J., Tassin, B., 2018. Sources and fate of microplastics in urban areas: A focus on Paris Megacity, in: Wagner, M., Lambert, S., Besseling, E., Biginagwa, F.J. (Eds.), *Freshwater microplastics. Emerging environmental contaminants? The handbook of environmental chemistry. Volume 58.* Springer, pp. 69–83. doi:10.1007/978-3-319-61615-5
- Dris, R., Imhof, H., Sanchez, W., Gasperi, J., Galgani, F., Tassin, B., Laforsch, C., 2015. Beyond the ocean: Contamination of freshwater ecosystems with (micro-)plastic particles. *Environ. Chem.* 12 (5), 539. doi:10.1071/EN14172.
- Duis, K., Coors, A., 2016. Microplastics in the aquatic and terrestrial environment: Sources (with a specific focus on personal care products), fate and effects. *Environ. Sci. Eur.* 28 (2), 1–25. doi:10.1186/s12302-015-0069-y.
- Eerkes-Medrano, D., Thompson, R.C., Aldridge, D.C., 2015. Microplastics in freshwater systems: A review of the emerging threats, identification of knowledge gaps and prioritisation of research needs. *Water res.* 75, 63–82. doi:10.1016/j.watres.2015.02.012.
- Eriksen, M., Lebreton, L.C.M., Carson, H.S., Thiel, M., Moore, C.J., Borerro, J.C., Galgani, F., Ryan, P.G., Reisser, J., 2014. Plastic pollution in the world's oceans: More than 5 trillion plastic pieces weighing over 250,000 tons afloat at sea. *PloS one* 9 (12), e111913. doi:10.1371/journal.pone.0111913.
- Eurostat, 2018. Maritime ports freight and passenger statistics – statistics explained.
https://ec.europa.eu/eurostat/statistics-explained/index.php/Maritime_ports_freight_and_passenger_statistics#Rotterdam.2C_Antwerpen_and_Hamburg_stayed_top_ports. Accessed 29 January 19.
- Farley, K.J., Morel, F.M., 1986. Role of coagulation in the kinetics of sedimentation. *Environ. Sci. Technol.* 20 (2), 187–195. doi:10.1021/es00144a014.

- Fazey, F.M.C., Ryan, P.G., 2016. Biofouling on buoyant marine plastics: An experimental study into the effect of size on surface longevity. *Environ. Pollut.* 210, 354–360. doi:10.1016/j.envpol.2016.01.026.
- Frings, R.M., 2008. Downstream fining in large sand-bed rivers. *Earth-Sci. Rev.* 87 (1-2), 39–60. doi:10.1016/j.earscirev.2007.10.001.
- Frings, R.M., Gehres, N., Promny, M., Middelkoop, H., Schüttrumpf, H., Vollmer, S., 2014. Today's sediment budget of the Rhine River channel, focusing on the Upper Rhine Graben and Rhenish Massif. *Geomorphology* 204, 573–587. doi:10.1016/j.geomorph.2013.08.035.
- GESAMP, 2016. Sources, fate and effects of microplastics in the marine environment: Part two of a global assessment 93. GESAMP, 221 pp. <http://www.gesamp.org/site/assets/files/1275/sources-fate-and-effects-of-microplastics-in-the-marine-environment-part-2-of-a-global-assessment-en.pdf>. Accessed 14 December 2018.
- Hess, M., Diel, P., Mayer, J., Rahm, H., Reifenhäuser, W., Stark, J., Schwaiger, J., 2018. Mikroplastik in Binnengewässern Süd- und Westdeutschlands: Bundesländerübergreifende Untersuchungen in Baden-Württemberg, Bayern, Hessen, Nordrhein-Westfalen und Rheinland-Pfalz, Karlsruhe, Augsburg, Wiesbaden, Recklinghausen, Mainz, 86 pp. https://www.lanuv.nrw.de/fileadmin/lanuvpubl/6_sonderreihen/L%C3%A4nderbericht_Mikroplastik_in_Binnengew%C3%A4ssern.pdf. Accessed 25 May 2018.
- Hidalgo-Ruz, V., Gutow, L., Thompson, R.C., Thiel, M., 2012. Microplastics in the marine environment: A review of the methods used for identification and quantification. *Environ. Sci. Technol.* 46 (6), 3060–3075. doi:10.1021/es2031505.
- Hurley, R., Woodward, J., Rothwell, J.J., 2018. Microplastic contamination of river beds significantly reduced by catchment-wide flooding. *Nat. Geosci.* 11 (4), 251–257. doi:10.1038/s41561-018-0080-1.
- Hurley, R.R., Woodward, J.C., Rothwell, J.J., 2017. Ingestion of microplastics by freshwater tubifex worms. *Environ. Sci. Technol.* 51 (21), 12844–12851. doi:10.1021/acs.est.7b03567.
- ICPR, 2018. The Rhine. International Commission for the Protection of the Rhine. <https://www.iksr.org/en/rhine/>. Accessed 18 December 2018.

- Imhof, H.K., Schmid, J., Niessner, R., Ivleva, N.P., Laforsch, C., 2012. A novel, highly efficient method for the separation and quantification of plastic particles in sediments of aquatic environments. *Limnol. Oceanogr. Meth.* 10 (7), 524–537. doi:10.4319/lom.2012.10.524.
- IT NRW, 2018. Bevölkerung in Nordrhein-Westfalen. Information und Technik Nordrhein-Westfalen. <https://www.it.nrw/bevoelkerung-am-31122017-und-30062018-nach-gemeinden-93051>. Accessed 15 January 2019.
- Ivleva, N.P., Wiesheu, A.C., Niessner, R., 2017. Microplastic in aquatic ecosystems. *Angew. Chem. Int. Edit.* 56 (7), 1720–1739. doi:10.1002/anie.201606957.
- Jambeck, J.R., Geyer, R., Wilcox, C., Siegler, T.R., Perryman, M., Andrady, A., Narayan, R., Law, K.L., 2015. Plastic waste inputs from land into the ocean. *Science* 347 (6223), 768–771. doi:10.1126/science.1260352.
- Ji, Z.-G., 2017. Hydrodynamics and water quality: Modelling rivers, lakes, and estuaries. John Wiley & Sons, Hoboken, NJ.
- Jones, R.J., 2007. Chemical contamination of a coral reef by the grounding of a cruise ship in Bermuda. *Mar. Pollut. Bull.* 54 (7), 905–911. doi:10.1016/j.marpolbul.2007.02.018.
- Jong, M.P.C. de, Battjes, J.A., 2004. Seiche characteristics of Rotterdam Harbour. *Coast. Eng.* 51 (5-6), 373–386. doi:10.1016/j.coastaleng.2004.04.002.
- Karlsson, T.M., Arneborg, L., Broström, G., Almroth, B.C., Gipperth, L., Hassellöv, M., 2018. The unaccountability case of plastic pellet pollution. *Mar. Pollut. Bull.* 129 (1), 52–60. doi:10.1016/j.marpolbul.2018.01.041.
- Klein, S., Dimzon, I.K., Eubeler, J., Knepper, T.P., 2018. Analysis, occurrence, and degradation of microplastics in the aqueous environment, in: Wagner, M., Lambert, S. (Eds.), *Freshwater Microplastics* 58. Springer, pp. 51–67.
- Klein, S., Worch, E., Knepper, T.P., 2015. Occurrence and spatial distribution of microplastics in river shore sediments of the Rhine-Main area in Germany. *Environ. Sci. Technol.* 49 (10), 6070–6076. doi:10.1021/acs.est.5b00492.
- Kooi, M., Besseling, E., Kroeze, C., van Wezel, A.P., Koelmans, A.A., 2018. Modeling the fate and transport of plastic debris in freshwaters: Review and guidance, in: Wagner, M., Lambert, S., Besseling, E., Biginagwa, F.J. (Eds.), *Freshwater microplastics*. Emerging

- environmental contaminants? The handbook of environmental chemistry. Volume 58. Springer, pp. 125–152. doi:10.1007/978-3-319-61615-5
- Kowalski, N., Reichardt, A.M., Waniek, J.J., 2016. Sinking rates of microplastics and potential implications of their alteration by physical, biological, and chemical factors. *Mar. Pollut. Bull.* 109 (1), 310–319. doi:10.1016/j.marpolbul.2016.05.064.
- Lambert, S., Wagner, M., 2016. Formation of microscopic particles during the degradation of different polymers. *Chemosphere* 161, 510–517. doi:10.1016/j.chemosphere.2016.07.042.
- Lebreton, L.C.M., van der Zwet, J., Damsteeg, J.-W., Slat, B., Andrady, A., Reisser, J., 2017. River plastic emissions to the world's oceans. *Nat. Commun.* 8, 15611. doi:10.1038/ncomms15611.
- Lechner, A., Keckeis, H., Lumesberger-Loisl, F., Zens, B., Krusch, R., Tritthart, M., Glas, M., Schludermann, E., 2014. The Danube so colourful: A potpourri of plastic litter outnumbers fish larvae in Europe's second largest river. *Environ. Pollut.* 188, 177–181. doi:10.1016/j.envpol.2014.02.006.
- Lechner, A., Ramler, D., 2015. The discharge of certain amounts of industrial microplastic from a production plant into the River Danube is permitted by the Austrian legislation. *Environ. Pollut.* 200, 159–160. doi:10.1016/j.envpol.2015.02.019.
- Lenz, R., Enders, K., Stedmon, C.A., Mackenzie, D.M.A., Nielsen, T.G., 2015. A critical assessment of visual identification of marine microplastic using Raman spectroscopy for analysis improvement. *Mar. Pollut. Bull.* 100 (1), 82–91. doi:10.1016/j.marpolbul.2015.09.026
- Leslie, H.A., Brandsma, S.H., van Velzen, M.J.M., Vethaak, A.D., 2017. Microplastics en route: Field measurements in the Dutch river delta and Amsterdam canals, wastewater treatment plants, North Sea sediments and biota. *Environ. Int.* 101, 133–142. doi:10.1016/j.envint.2017.01.018.
- Lobelle, D., Cunliffe, M., 2011. Early microbial biofilm formation on marine plastic debris. *Mar. Pollut. Bull.* 62 (1), 197–200. doi:10.1016/j.marpolbul.2010.10.013.
- Löder, M.G.J., Gerdt, G., 2015. Methodology used for the detection and identification of microplastics – A critical appraisal, in: Klages, M., Gutow, L., Bergmann, M. (Eds.), *Marine Anthropogenic Litter*. Springer, pp. 201–227.

- Löder, M.G.J., Kuczera, M., Mintenig, S., Lorenz, C., Gerdt, G., 2015. Focal plane array detector-based micro-Fourier-transform infrared imaging for the analysis of microplastics in environmental samples. *Environ. Chem.* 12 (5), 563. doi:10.1071/EN14205.
- Lorenz, C., Speidel, L., Primpke, S., Gerdt, G., 2017. Using the FlowCam to validate an enzymatic digestion protocol applied to assess the occurrence of microplastics in the southern North Sea, in: Baztan, J., Jorgensen, B., Pahl, S., Thompson, R.C., Vanderlinden, J.-P. (Eds.), *MICRO 2016. Fate and impact of microplastics in marine ecosystems. From the coastline to the open sea.* Elsevier Science, pp. 92–93.
- Mahmood, K., 1987. Reservoir sedimentation: Impact, extent, and mitigation. Technical paper. International Bank for Reconstruction and Development, Washington, DC (USA). <https://www.osti.gov/biblio/5564758>. Accessed 02. March 2020.
- Mani, T., Blarer, P., Storck, F.R., Pittroff, M., Wernicke, T., Burkhardt-Holm, P., 2019. Repeated detection of polystyrene microbeads in the Lower Rhine River. *Environ. Pollut.* 245, 634–641. doi:10.1016/j.envpol.2018.11.036.
- Mani, T., Burkhardt-Holm, P., Segner, H., Zennegg, M., Amaral-Zettler, L., 2018. Microplastics – a potential threat to the remote and pristine ecosystems of the Antarctic seas?, in: *The Expedition PS111 of the Research Vessel POLARSTERN to the southern Weddell Sea in 2018.* Alfred-Wegener-Institut, Helmholtz-Zentrum für Polar- und Meeresforschung. doi:10.2312/BzPM_0718_2018.
- Mani, T., Hauk, A., Walter, U., Burkhardt-Holm, P., 2015. Microplastics profile along the Rhine River. *Sci. Rep.* 5, 17988. doi:10.1038/srep17988.
- Masura, J., Baker, J.E., Foster, G.D., Arthur, C., Herring, C., 2015. Laboratory methods for the analysis of microplastics in the marine environment: recommendations for quantifying synthetic particles in waters and sediments. NOAA technical memorandum NOS-OR&R 48. NOAA, Silver Spring, Maryland, USA. <https://repository.library.noaa.gov/view/noaa/10296#tabs-2>. Accessed 16 August 2018.
- Mellor, B.G., Khanna, A.S. (Eds.), 2006. *Surface coatings for protection against wear.* CRC Press, Cambridge, Eng, 429 pp.
- Mintenig, S.M., Int-Veen, I., Löder, M.G.J., Primpke, S., Gerdt, G., 2017. Identification of microplastic in effluents of waste water treatment plants using focal plane array-based micro-Fourier-transform infrared imaging. *Water res.* 108, 365–372. doi:10.1016/j.watres.2016.11.015.

- Moore, C.J., Lattin, G.L., Zellers, A.F., 2011. Quantity and type of plastic debris flowing from two urban rivers to coastal waters and beaches of Southern California. *RGCI* 11 (1), 65–73. doi:10.5894/rgci194.
- Murphy, F., Ewins, C., Carbonnier, F., Quinn, B., 2016. Wastewater treatment works (wwtw) as a source of microplastics in the aquatic environment. *Environ. Sci. Technol.* 50 (11), 5800–5808. doi:10.1021/acs.est.5b05416.
- Nel, H.A., Dalu, T., Wasserman, R.J., 2018. Sinks and sources: Assessing microplastic abundance in river sediment and deposit feeders in an Austral temperate urban river system. *Sci. Tot. Env.* 612, 950–956. doi:10.1016/j.scitotenv.2017.08.298.
- Ng, A.K.Y., Song, S., 2010. The environmental impacts of pollutants generated by routine shipping operations on ports. *Ocean Coast. Manage.* 53 (5-6), 301–311. doi:10.1016/j.ocecoaman.2010.03.002.
- Nizzetto, L., Bussi, G., Futter, M.N., Butterfield, D., Whitehead, P.G., 2016. A theoretical assessment of microplastic transport in river catchments and their retention by soils and river sediments. *Environ. Sci. Proc. Imp.* 18 (8), 1050–1059. doi:10.1039/c6em00206d.
- Norén, F., 2007. Small plastic particles in coastal Swedish waters. n-research, Lysekil, Sweden. <http://www.n-research.se/pdf/Small%20plastic%20particles%20in%20Swedish%20West%20Coast%20Waters.pdf>. Accessed 23 May 2018.
- NRW Invest, 2016. NI-Standortbroschuere, 28 pp. <https://www.nrwinvest.com/fileadmin/Redaktion/branchen-in-nrw/NI-Standortbroschuere-DE-2016.pdf>. Accessed 13 September 2018.
- Peeken, I., Primpke, S., Beyer, B., Gütermann, J., Katlein, C., Krumpen, T., Bergmann, M., Hehemann, L., Gerdts, G., 2018. Arctic sea ice is an important temporal sink and means of transport for microplastic. *Nat. Commun.* 9 (1), 1505. doi:10.1038/s41467-018-03825-5.
- Penzel, E., Ballard, N., Asua, J.M., 2000. Polyacrylates. *Polymers and Plastics*. Ullmann's Encyclopedia of Industrial Chemistry. Wiley Online Library. doi:10.1002/14356007.a21_157
- Peters, C.A., Bratton, S.P., 2016. Urbanization is a major influence on microplastic ingestion by sunfish in the Brazos River Basin, Central Texas, USA. *Environ. Pollut.* 210, 380–387. doi:10.1016/j.envpol.2016.01.018.

- Primpke, S., Imhof, H., Piehl, S., Lorenz, C., Löder, M., Laforsch, C., Gerdt, G., 2017a. Mikroplastik in der Umwelt. *Chem. Unserer Zeit* 51 (6), 402–412. doi:10.1002/ciuz.201700821.
- Primpke, S., Lorenz, C., Rascher-Friesenhausen, R., Gerdt, G., 2017b. An automated approach for microplastics analysis using focal plane array (FPA) FTIR microscopy and image analysis. *Anal. Methods* 9 (9), 1499–1511. doi:10.1039/C6AY02476A.
- Primpke, S., Wirth, M., Lorenz, C., Gerdt, G., 2018. Reference database design for the automated analysis of microplastic samples based on Fourier transform infrared (FTIR) spectroscopy. *Anal. Bioanal. Chem.* 410 (21), 5131–5141. doi:10.1007/s00216-018-1156-x.
- Pye, K. (Ed.), 1994. *Sediment transport and depositional processes*. Blackwell Scientific Publications, Oxford, 397 pp.
- Quik, J.T.K., Velzeboer, I., Wouterse, M., Koelmans, A.A., van de Meent, D., 2014. Heteroaggregation and sedimentation rates for nanomaterials in natural waters. *Water res.* 48, 269–279. doi:10.1016/j.watres.2013.09.036.
- Remy, F., Collard, F., Gilbert, B., Compère, P., Eppe, G., Lepoint, G., 2015. When microplastic is not plastic: The ingestion of artificial cellulose fibers by macrofauna living in seagrass macrophytodebris. *Environ. Sci. Technol.* 49 (18), 11158–11166.
- Ries, M., 2019. Artificial sediment supply Koblenz. WSA Bingen, personal communication, 12 February 2019.
- Rummel, C.D., Jahnke, A., Gorokhova, E., Kühnel, D., Schmitt-Jansen, M., 2017. Impacts of biofilm formation on the fate and potential effects of microplastic in the aquatic environment. *Environ. Sci. Technol. Lett.* 4 (7), 258–267. doi:10.1021/acs.estlett.7b00164.
- Sanchez, W., Bender, C., Porcher, J.-M., 2014. Wild gudgeons (*Gobio gobio*) from French rivers are contaminated by microplastics: Preliminary study and first evidence. *Environ. Res.* 128, 98–100. doi:10.1016/j.envres.2013.11.004.
- Schmidt, C., Krauth, T., Wagner, S., 2017. Export of plastic debris by rivers into the sea. *Environ. Sci. Technol.* 51 (21), 12246–12253. doi:10.1021/acs.est.7b02368.
- Schubert, J., 2002. Hydraulic aspects of riverbank filtration – field studies. *J. Hydrol.* 266 (3–4), 145–161. doi:10.1016/S0022-1694(02)00159-2.

- Shumchenia, E.J., Guarinello, M.L., King, J.W., 2016. A re-assessment of Narragansett Bay benthic habitat quality between 1988 and 2008. *Estuar. Coast.* 39 (5), 1463–1477. doi:10.1007/s12237-016-0095-z.
- Silva, A.B., Bastos, A.S., Justino, C.I.L., da Costa, J.P., Duarte, A.C., Rocha-Santos, T.A.P., 2018. Microplastics in the environment: Challenges in analytical chemistry – A review. *Anal. Chim. Acta* 1017, 1–19. doi:10.1016/j.aca.2018.02.043.
- Statista, 2018. Amsterdam: total population 2008-2018 | Statistic. <https://www.statista.com/statistics/753235/total-population-of-amsterdam/>. Accessed 29 January 2019.
- Tagg, A.S., Harrison, J.P., Ju-Nam, Y., Sapp, M., Bradley, E.L., Sinclair, C.J., Ojeda, J.J., 2017. Fenton's reagent for the rapid and efficient isolation of microplastics from wastewater. *Chem. Comm.* 53 (2), 372–375. doi:10.1039/c6cc08798a.
- Tittizer, T., Schöll, F., Schleuter, A., 1988. Einsatz von Taucherschacht und Taucherglocke bei benthosbiologischen Untersuchungen. *Deutsche Gewässerkundliche Mitteilungen.* 32 (5/6), 141–144.
- Turner, A., 2010. Marine pollution from antifouling paint particles. *Mar. Pollut. Bull.* 60 (2), 159–171. doi:10.1016/j.marpolbul.2009.12.004.
- Van den Hurk, P., Eertman, R.H.M., Stronkhorst, J., 1997. Toxicity of harbour canal sediments before dredging and after off-shore disposal. *Mar. Pollut. Bull.* 34 (4), 244–249. doi:10.1016/S0025-326X(96)00104-X.
- Van der Wal, M., van der Meulen, M., Tweehuijsen, G., Peterlin, M., Palatinus, A., Viršek, M.K., Coscia, L., Kršan, A., 2015. SFRA0025: Identification and assessment of riverine input of (marine) litter. Final report for the European Commission DG Environment under framework contract No ENV. D, Bristol (Vol. 25). 2/FRA/2012., 208 pp. <http://ec.europa.eu/environment/marine/good-environmental-status/descriptor-10/pdf/iasFinal%20Report.pdf>. Accessed 29 March 2019.
- Van Rijn, L.C., 1984. Sediment transport, part II: Suspended load transport. *J. Hydraul. Eng.* 110 (11), 1613–1641.
- Verlaan, P.A.J., Spanhoff, R., 2000. Massive sedimentation events at the mouth of the Rotterdam waterway. *J. Coastal Res.*, 458–469.

- Wagner, M., Scherer, C., Alvarez-Muñoz, D., Brennholt, N., Bourrain, X., Buchinger, S., Fries, E., Grosbois, C., Klasmeier, J., Marti, T., Rodriguez-Mozaz, S., Urbatzka, R., Vethaak, A.D., Winther-Nielsen, M., Reifferscheid, G., 2014. Microplastics in freshwater ecosystems: What we know and what we need to know. *Environ. Sci. Eur.* 26 (1), 12. doi:10.1186/s12302-014-0012-7.
- Wang, Z., Su, B., Xu, X., Di Di, Huang, H., Mei, K., Dahlgren, R.A., Zhang, M., Shang, X., 2018. Preferential accumulation of small (<300 µm) microplastics in the sediments of a coastal plain river network in eastern China. *Water Res.* 144, 393–401. doi:10.1016/j.watres.2018.07.050.
- Wenzhou Municipal Statistic Bureau, 2011. Wenzhou Population 2010. https://web.archive.org/web/20110927075644/http://www.wenzhou.gov.cn/art/2011/5/10/art_4247_166018.html. Accessed 29 January 2019.
- Wolters, M., 2019. Riverbed dredging at Rees. WSA Duisburg-Rhein, personal communication, 01 February 2019.
- World Shipping Council, 2016. Top 50 World Container Ports. <http://www.worldshipping.org/about-the-industry/global-trade/top-50-world-container-ports>. Accessed 29 January 2019.
- WSV DE, 2016a. Rhine River flow velocity data for Rees (DE) and Andernach (DE) – internal data. Wasserstraßen- und Schifffahrtsverwaltung des Bundes (WSV).
- WSV DE, 2016b. Section profile Rhine Rees – internal document. Wasserstraßen- und Schifffahrtsverwaltung des Bundes (WSV), Aussenbezirk Emmerich.
- WSV DE, 2017. Verkehrsbericht 2017, 115 pp. https://www.gdws.wsv.bund.de/SharedDocs/Downloads/DE/Verkehrsberichte/Verkehrsbericht_2017.pdf?__blob=publicationFile&v=2. Accessed 15 January 2019.
- Xia, F., Qu, L., Wang, T., Luo, L., Chen, H., Dahlgren, R.A., Zhang, M., Mei, K., Huang, H., 2018. Distribution and source analysis of heavy metal pollutants in sediments of a rapid developing urban river system. *Chemosphere* 207, 218–228. doi:10.1016/j.chemosphere.2018.05.090.
- Zheng, J., Yang, D., 2016. Hub-and-spoke network design for container shipping along the Yangtze River. *J. Transp. Geogr.* 55, 51–57. doi:10.1016/j.jtrangeo.2016.07.001.

SI 4: Microplastic pollution in benthic midstream sediments of the Rhine River

SI1 ZnCl₂ density separation and microplastic recovery experiments

As the specifically modified protocol for ZnCl₂ density separation (see section 2.3 of the manuscript) based on (Imhof et al., 2012) used in this study has never been published, a recovery experiment was conducted to assess the efficiency of the protocol. Four size classes of Nile red-dyed, fluorescent polymethyl methacrylate (PMMA, $\rho = 1.18 \text{ g cm}^{-3}$) fragments (62–125 μm , $n = 40$; 125–250 μm , $n = 40$; 250–500 μm , $n = 20$ and 500–1000 μm , $n = 20$) were separately mixed with 60 g of Rhine riverbed sediment (<2 mm). All size class experiments were executed in triplicate. After applying the ZnCl₂ separation protocol according to section 2.3, the supernatant was filtered onto cellulose filter paper (pore size: 3 μm , diameter: 25 mm; Rotilabo-Rundfilter Typ 115A, Carl Roth, Karlsruhe, Germany) and the recovered PMMA particles were visually counted using a fluorescence microscope (Nikon eclipse E 400, Nikon, Tokyo, Japan). Mean microplastic recovery (\pm SD) rates were $100.0 \pm 0.0\%$, $90.0 \pm 5.0\%$, $80.8 \pm 6.3\%$, and $55.0 \pm 8.7\%$ for the 500–1000 μm , 250–500 μm , 125–250 μm , and 62–125 μm size classes, respectively (Fig. S5).

SI2 Blank correction of riverbed sediment microplastic concentrations

Three procedural blanks were run to detect any sample processing-induced microplastics in the samples. The ZnCl₂ density separation (section 2.3 of the manuscript), Fenton's reagent (2.4), focal plane array μFTIR (2.5) and automated analysis of μFTIR data (2.6) were performed without sediment samples. The resulting synthetic polymer abundances (average 97.3 ± 63.7 MP particles per blank) were subsequently subtracted from the microplastic concentrations determined for the Rhine riverbed samples in the respective polymer proportions (Table S1). The microplastic counts for the aliquots of pooled sample analysed ($n = 10$) by micro-Fourier-transform infrared spectroscopy (μFTIR) were blank corrected by subtracting the average blank microplastic count (97.34 , $n = 3$), before extrapolating to the microplastic count for the total volume (100%) of each sediment sample. Microplastic concentrations (MP kg^{-1} sediment) were then calculated based on the dry sediment weight (*cf.* Electronic Supporting Information, ESI).

SI3 Error propagation calculated values derived via FTIR imaging

The following equation was used to calculate the errors for the single samples based on the number of particles (N_p), mass dw (m_s) and the aliquot fractions for the Anodisc-Filtration (f):

$$\Delta N_{DW} = \sqrt{\left(\frac{N_P}{-m_S^2 f} \Delta m_S\right)^2 + \left(\frac{N_P}{m_S - f^2} \Delta f\right)^2 + \left(\frac{1}{m_S f} \Delta N_P\right)^2} \quad (1)$$

The error of the determined value ΔN_{DW} is calculated under the following assumptions: (i) dw sediment Δm_S is weighed at an accuracy of +/- 1 g (section 2.2.); (ii) sub-aliquot volumes for Anodisc-filtration (Δf) was assessed at an accuracy of +/- 1% (2.4.); (iii) FTIR MP particle count accuracy (ΔN_P) is +/- 5% (2.6.).

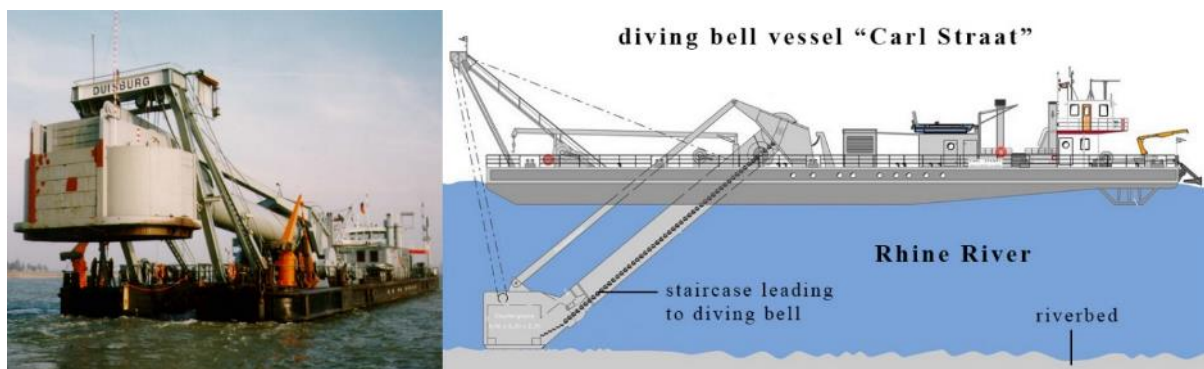


Fig. S1: Diving bell vessel “Carl Straat”. The riverbed can be accessed by foot through a staircase and diving bell that is open on the bottom. Water is kept out using a double door system and artificial adjustment of air pressure in the bell and staircase (0.1 bar per 1.02 m water depth). Images courtesy of the German Waterways and Shipping Administration (WSV), department Duisburg, modified.



Fig. S2: Bucket chain (left arrow, A) vessel with accompanying transport barge (right arrow, A) with the Rhine River visible in the background at Rees, Germany (A). Bucket chain (centre) in action dredging riverbed sediments (direction of hauling: upwards, B). Close-up of sand-gravel riverbed sediment in the dredge bucket (C).

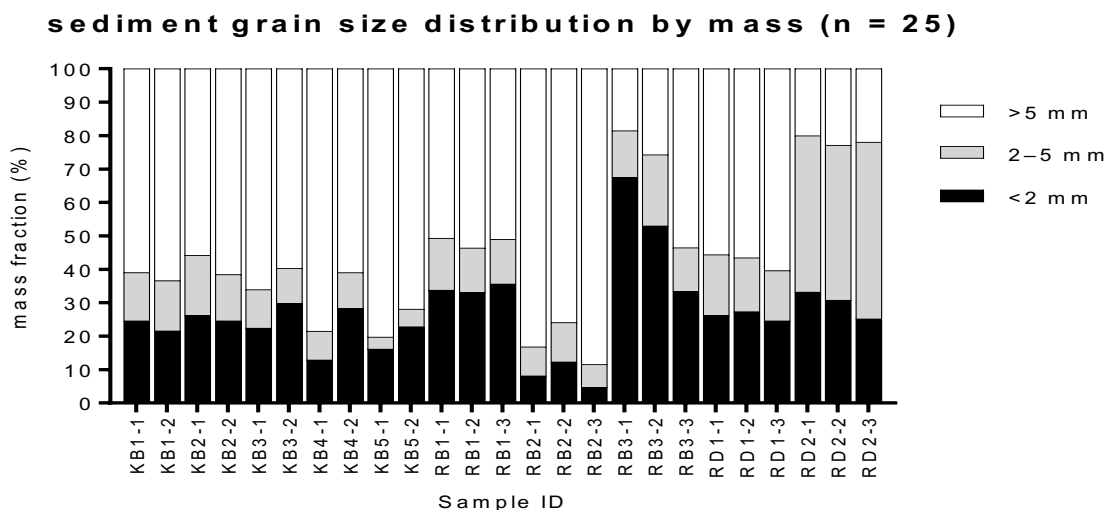


Fig. S3: Percentage mass fractions of grain size classes (>5 mm, 2–5 mm and <2 mm) in the 25 Rhine riverbed sediment samples. K = Koblenz; R = Rees; B = diving bell; D = bucket chain dredger.

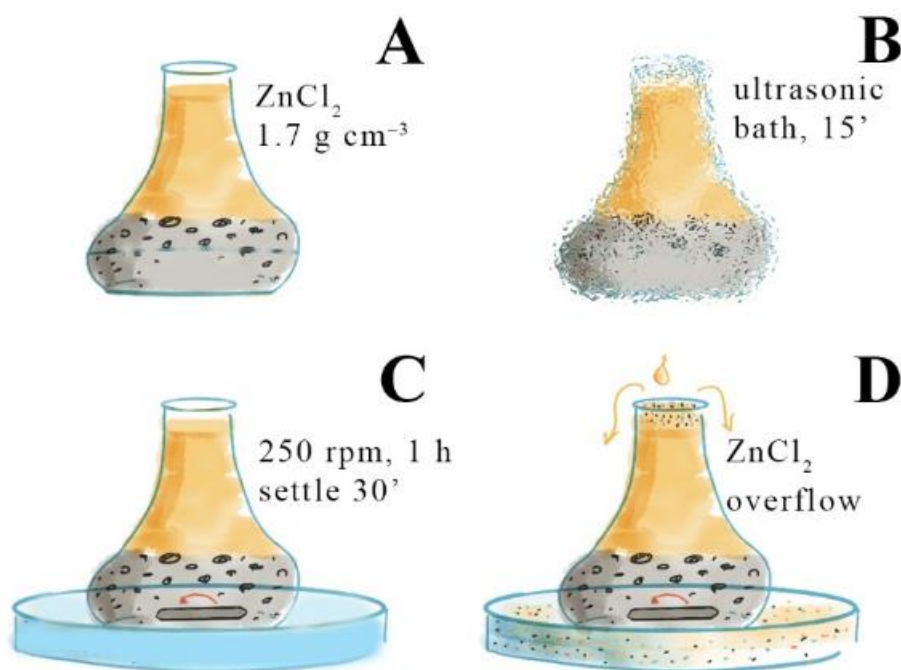


Fig. S4: Schematic depiction of density separation using ZnCl_2 ($\rho \sim 1.7 \text{ g cm}^{-3}$; adapted from Imhof et al., 2012). Dry sample was added to an Erlenmeyer flask (100 mL) and the receptacle was topped up with ZnCl_2 , leaving a 1.5 cm margin below the brim (A). The sealed Erlenmeyer flask was submerged in an ultrasonic bath until the mouth of the flask was 3 cm above the water line and sonicated at 160 W/35 kHz for 15 min (B). Then, the sample was stirred for 1 h at 250 rpm using a PTFE-coated magnetic stirrer bar. The exterior of the flask was cleaned with

distilled water (Aq. dest.), and the flask was placed onto a 14 cm-diameter Petri dish (C). The flask was completely topped up with ZnCl_2 , the contents were allowed to settle for 30 min, then an additional 20 mL of ZnCl_2 was added, inducing overflow of excess liquid and the suspended solids therein into the underlying Petri dish (D).

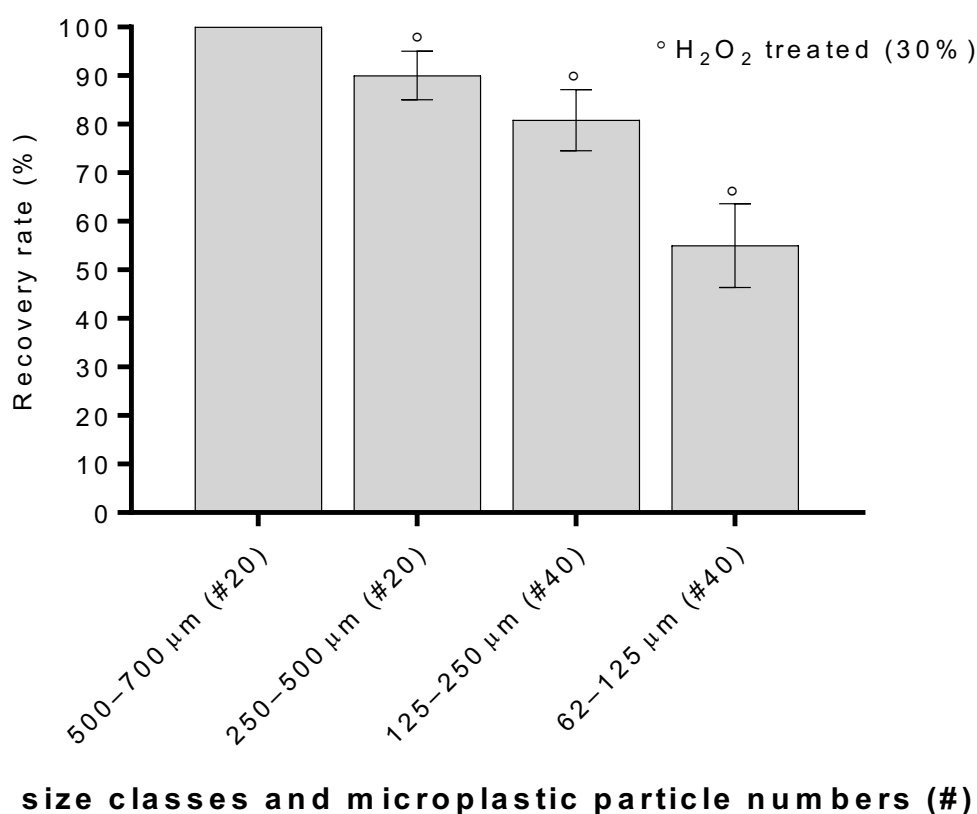


Fig. S5: Density separation spike-recovery experiment ($n = 3$) using ZnCl_2 ($\rho \sim 1.7 \text{ g cm}^{-3}$) and polymethylmethacrylate (PMMA, $\rho 1.18 \text{ g cm}^{-3}$) microplastic particles (62–700 μm). Hashes (#) indicate the number of spiked PMMA particles. All size classes were investigated in triplicate. Error bars indicate standard deviation. Circles above the error bars indicate overnight H_2O_2 treatment (30%).

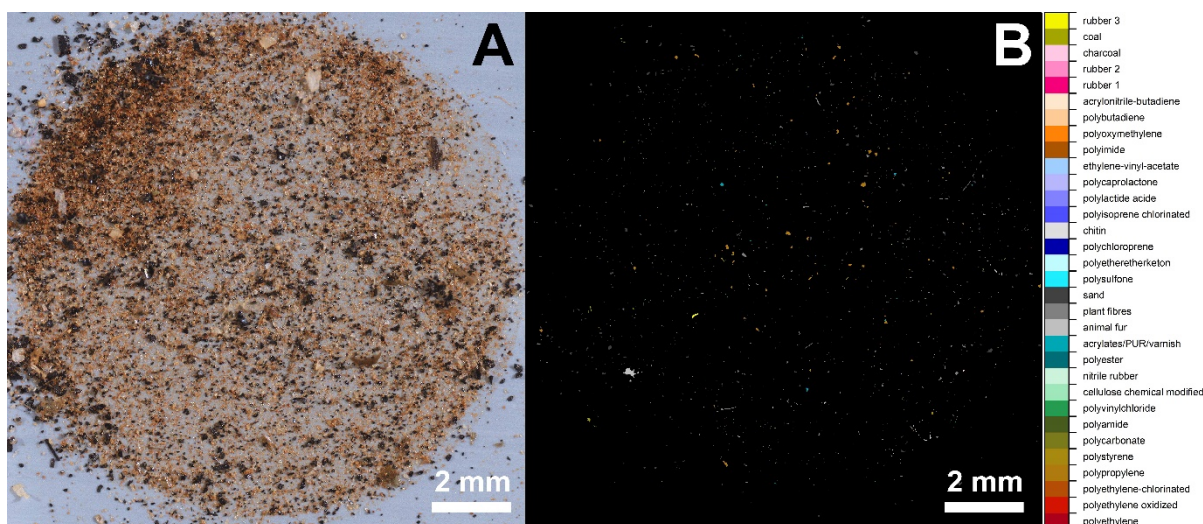


Fig. S6: Visual overview (A) and false colour μ FTIR image (B) of the sample filtrate for site RB3, Rees.

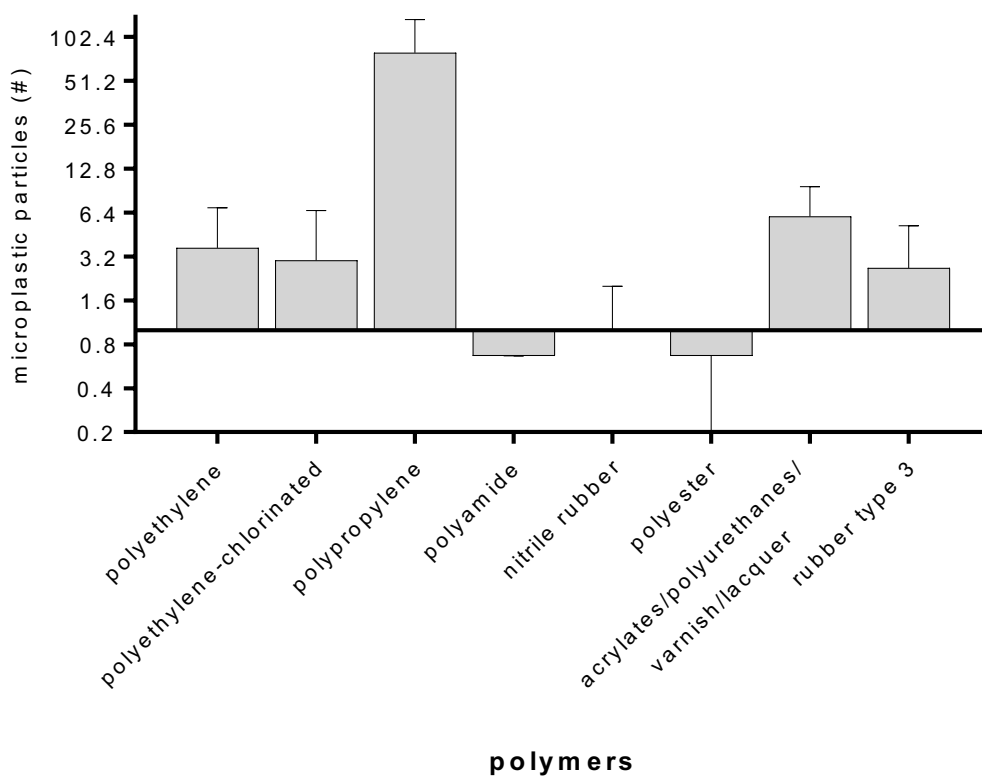


Fig. S7: Mean microplastic particle abundance in the procedural blanks ($n = 3$). Error bars indicate standard deviation. The y-axis is log₂ scaled; 0.67 particles of polyamide and polyester and one nitrile rubber particle were detected.

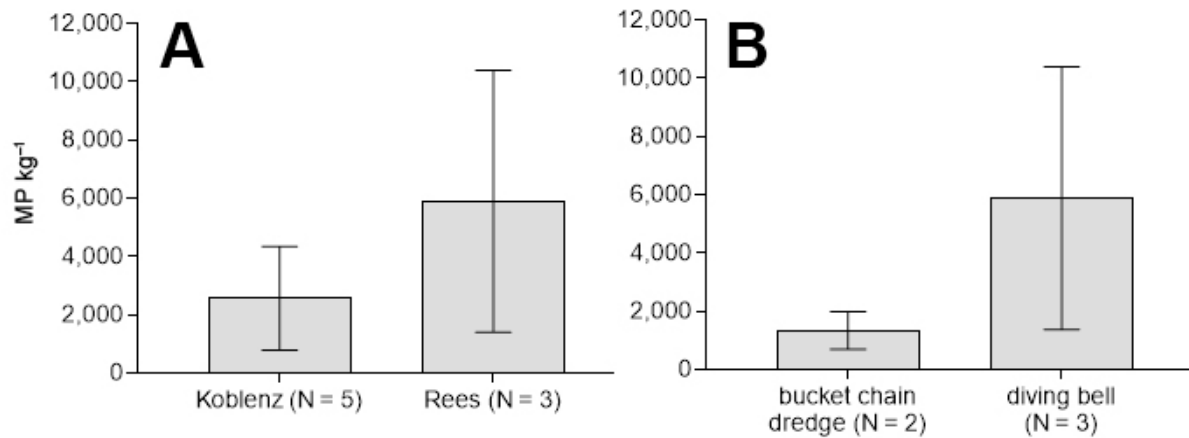


Fig. S8: Mean microplastic concentrations in riverbed sediments (MP kg⁻¹) compared by location, Koblenz vs. Rees (A), and riverbed sampling access mode (B). The access mode was compared at Rees as this was the only location where both were applied (B). Error bars indicate standard deviation. No significant differences were identified (unpaired t-test with Welch's correction, $p > 0.05$).

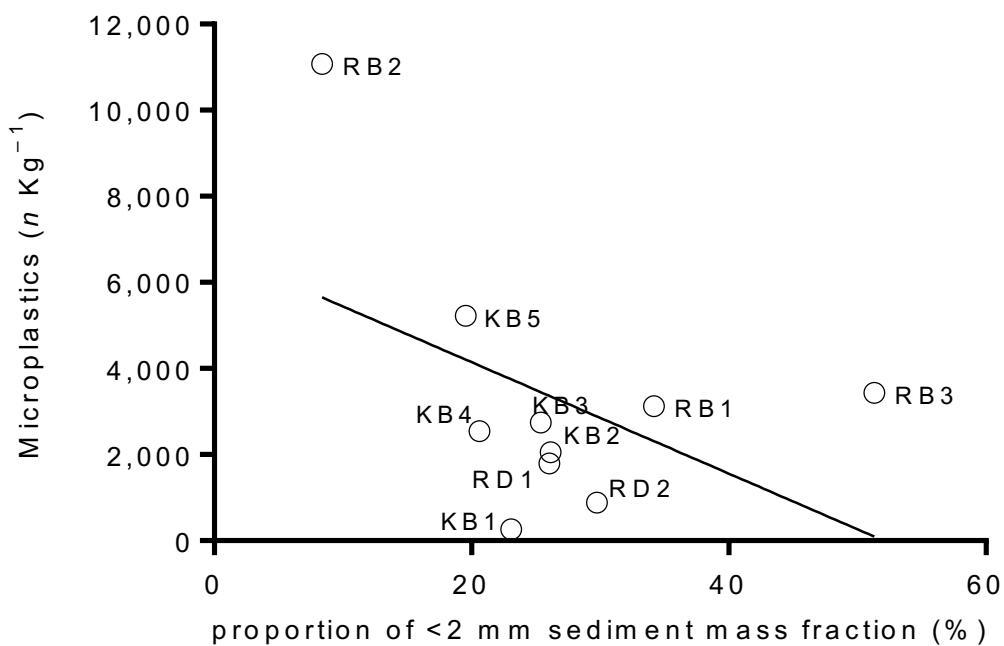


Fig. S9: Linear regression of microplastic concentrations (MP kg⁻¹) and proportion of sand (< 2 mm, %) in the respective sample pool. R square = 0.22; $p = 0.17$. The proportion of sand in the sample was used as a proxy for near-riverbed deposition and flow dynamics.

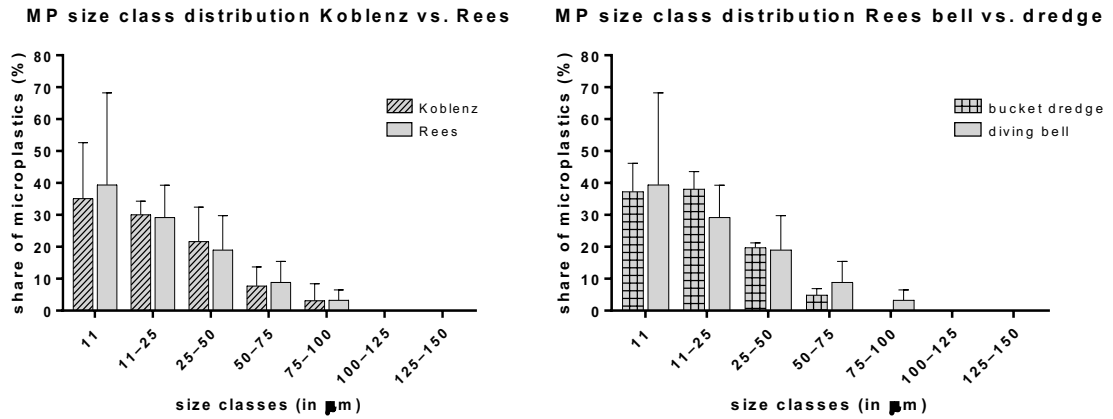


Fig. S10: Size class distribution for the microplastics (<500 µm) identified in all 10 sample pools (n = 25) compared by sampling location (Koblenz vs. Rees, left panel) and by sampling method (bucket chain dredger vs. diving bell, right panel). Size classes <11–150 µm were considered.

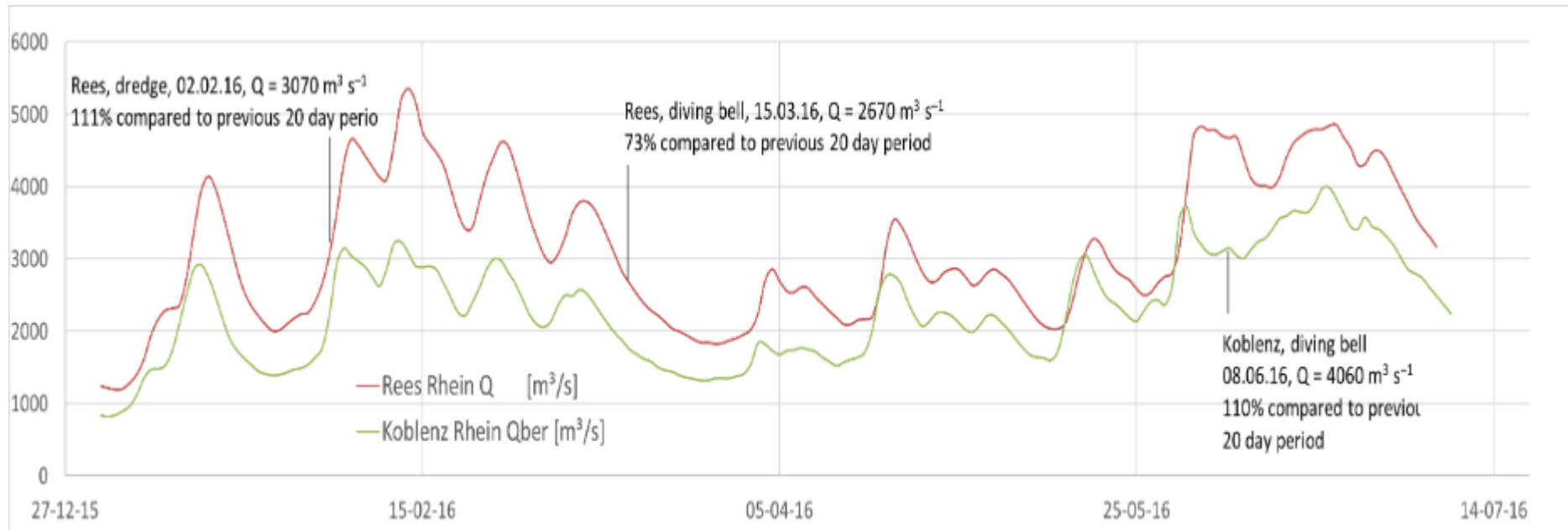


Fig. S11: Rhine River discharge (Q in $\text{m}^3 \text{ s}^{-1}$) at Rees (Rh-km 837.4, red line) and at Bonn (Rh-km 654.8, 56.03 km downstream of the Koblenz sampling sites, blue line) between 01.01.2016 and 08.07.2016. Bucket chain dredge sampling at Rees on 02.02.2016 and diving bell sampling at Rees on 15.03.2016 and Koblenz on 08.06.2016 are indicated (WSV DE, 2016).

Table S1: Sediment sample metadata.

ID ^A	Coordinates	Rhine-kilometre (Rh-km)	Sampling date	Water depth (cm)	Sed. Depth (cm)	Sample ww (g)	Sample dw (g)	Fractions dw (mm, %)			Sample vol. (cm ³) ^B	On Anodic for μ FTIR (%) ^C	MP conc. ($\times 10^3$ MP kg ⁻¹)
								<2	2–5	>5			
KB1-1	N 50°22'47.25	593.95	08.06.2016	700	7	1637	1493	24.6	14.5	61.0	553	100.0	0.26 \pm 0.01
KB1-2	E 7°36'50.74			700	7	1773	1596	21.6	15.0	63.4	591		
KB2-1	N 50°22'46.92	593.95	08.06.2016	650	7	1437	1387	26.2	18.1	55.7	501	58.3	2.74 \pm 0.15
KB2-2	E 7°36'44.71			650	7	1358	1323	24.6	13.9	61.5	471		
KB3-1	N 50°23'10.82	594.8	08.06.2016	650	7	1372	1274	22.4	11.5	66.0	405	26.0	2.05 \pm 0.13
KB3-2	E 7°36'29.68			650	7	1433	1312	29.9	10.4	59.7	452		
KB4-1	N 50°24'0.91	597.05	08.06.2016	650	7	1464	1336	12.9	8.6	78.5	441	91.2	2.54 \pm 0.14
KB4-2	E 7°35'8.19			650	7	1625	1404	28.3	10.7	61.0	513		
KB5-1	N 50°24'42.43	598.77	08.06.2016	650	7	1617	1481	16.2	3.6	80.2	546	7.5	5.22 \pm 0.75
KB5-2	E 7°34'10.37			650	7	1749	1556	22.9	5.2	71.9	589		
RB1-1	N 51°45'23.47	837.41	15.03.2016	750	7	950	878	33.7	15.6	50.7	325	7.6	3.13 \pm 0.44
RB1-2	E 6°23'42.27			750	7	1145	1080	33.1	13.2	53.6	396		
RB1-3				750	7	1461	1162	35.6	13.3	51.0	437		
RB2-1	N 51°45'20.11	837.41	15.03.2016	750	7	851	812	8.1	8.7	83.1	304	67.9	11.07 \pm 0.6
RB2-2	E 6°23'42.28			750	7	894	845	12.3	11.8	75.9	410		
RB2-3				750	7	1097	1058	4.7	6.8	88.5	385		
RB3-1	N 51°45'14.64	837.41	15.03.2016	500	7	952	817	67.6	14.0	18.5	330	77.9	3.43 \pm 0.19
RB3-2	E 6°23'40.40			500	7	970	859	53.0	21.3	25.7	426		
RB3-3				500	7	1205	1140	33.4	13.1	53.5	446		
RD1-1	N 51°45'18.68	837.52	02.02.2016	577	42	1368	1297	26.2	18.2	55.6	497	42.1	1.79 \pm 0.1
RD1-2	E 6°23'35.60			577	42	1424	1408	27.3	16.1	56.5	532		
RD1-3				577	42	1366	1326	24.6	15.1	60.3	522		
RD2-1	N 51°45'17.87	837.52	02.02.2016	508	111	1291	1226	33.3	46.7	20.0	450	53.2	0.89 \pm 0.05
RD2-2	E 6°23'35.59			508	111	1245	1195	30.8	46.4	22.8	450		
RD2-3				508	111	1279	1238	25.2	52.9	21.9	511		

^A K = Koblenz; R = Rees; B = diving bell; D = bucket chain dredger.

^B Net sample volume determined by porosity assessment, described in section 2.2 of the main article.

^C Percentage of ZnCl₂ density separation supernatant filtered onto the Anodisc (0.22 μ m) and analysed by FPA μ FTIR.

Table S2: Literature overview of microplastics in benthic and littoral sediments of lotic waterbodies.

Lotic waterbody	Compartment	MP conc. ($\times 10^3$ MP kg ⁻¹)	MP size (μ m)	Sampling method	MP identification	Reference
St. Lawrence River, including lakes (Canada, CA)	Benthos	0–1.5	400–2160	Petite Ponar Grab; Peterson Grab; 10 sites	Visual selection, diff. scanning calorimetry ($n = \text{n.a.}$)	(Castañeda et al., 2014)
Wen-Rui Tang River estuary (China, CN)	Benthos	18.69–74.8	20–5000	Peterson grab; 12 sites	Visual selection, μ FTIR ($n = 595$)	(Wang et al., 2018)
Yangtze River (CN)	Benthos	0.03–0.3	48–5000	Van Veen Grab; 29 sites	Visual selection, μ Raman ($n = 174$)	(Di and Wang, 2018)
Amsterdam canals (Netherlands, NL)	Benthos	0.07–10.5	10–5000	Van Veen Grab; 6 sites	Visual selection, μ FTIR (subsample 6%)	(Leslie et al., 2017)
Rhine estuary, Port of Rotterdam (NL)	Benthos	3.01–3.6	10–5000	Van Veen Grab; 2 sites	Visual selection, μ FTIR (subsample 6%)	(Leslie et al., 2017)
18 rivers or channels in Irwell and Upper Mersey catchments (UK)	Benthos	0.3–4.8	79–4779	Cylinder resuspension technique; 40 sites	Visual selection, FTIR ($n = 100$)	(Hurley et al., 2018)
Leach, Lambourn and Cut rivers (UK)	Benthos	0.19 ± 0.04 – 0.66 ± 0.08	1000–4000	Stainless steel spoon; 4 sites	Raman ($n = 336$)	(Horton et al., 2017)
Bloukrans River System (South Africa, ZA)	Benthos	0.006 ± 0.004 – 0.16 ± 0.14	63–5000	Quadrat and hand device; 30 sites	Comprehensive visual selection and identification	(Nel et al., 2018)
Rhine (DE)	Benthos	0.26 ± 0.01 – 11.07 ± 0.6	11–5033	Quadrat and steel hand spade; 10 sites	FPA μ FTIR; visual selection ATR-FTIR ($> 500 \mu\text{m}$)	Present study
L. Ontario trib., Don, Humber, Etobicoke, Red Hill (CA)	Littoral	0.04–27.83	63–2000	Petite Ponar Grab; 7 sites	Raman ($n = 90$)	(Ballent et al., 2016)
Ottawa River (CA)	Littoral	0.11–0.45	>100	Ekman bottom grab sampler; 10 sites	Comprehensive visual selection and identification	(Vermaire et al., 2017)
Beijiang River (CN)	Littoral	0.18 ± 0.07 – 0.54 ± 0.11	1–5000	Quadrat and stainless steel shovel; 8 sites	Comprehensive visual selection and μ FTIR	(Wang et al., 2017)
Seven rivers or channels in the Shanghai urban area (CN)	Littoral	0.05 ± 0.01 – 1.6 ± 0.19	>1	quadrat and shovel; 7 sites	μ FTIR ($n = \text{n.a.}$)	(Peng et al., 2018)
Rhine, Main (DE)	Littoral	0.23–3.76	63–5000	Stainless steel spoon	ATR-FTIR ($n = \text{n.a.}$)	(Klein et al., 2015)
Elbe, Mosel, Neckar, Rhine (DE)	n.a.	0.03–0.06	n.a.	n.a.	n.a.	(Wagner et al., 2014)

Table S3: Numerical proportions of polymer types by total MP concentrations (MP kg⁻¹), ordered by number of sites of occurrence from left to right.

Site	Total (× 10 ³ MP kg ⁻¹)	(%)																	
		APV*	CPE	EPDM*	PEST*	PE	PS*	PA*	NR	EVA	Rubber	PP	CMC*	OPE	PC*	PVC*	PCP	PLA*	ACNB*
KB1	0.26 ± 0.01	77.07	0.00	0.00	0.00	16.66	0.00	0.00	0.00	0.00	6.26	0.00	0.00	0.00	0.00	0.00	0.00	0.00	
KB2	2.74 ± 0.15	75.70	1.07	5.87	5.84	2.14	0.00	0.64	0.00	0.00	0.00	4.57	1.04	0.00	0.00	0.00	0.00	3.12	
KB3	2.05 ± 0.13	64.31	2.05	0.00	24.52	0.00	0.00	0.00	2.86	0.00	6.26	0.00	0.00	0.00	0.00	0.00	0.00	0.00	
KB4	2.54 ± 0.14	85.18	2.50	3.50	2.66	0.85	0.00	0.72	0.28	2.87	0.72	0.00	0.00	0.00	0.00	0.72	0.00	0.00	
KB5	5.22 ± 0.75	83.12	0.00	0.00	4.14	0.00	12.74	0.00	0.00	0.00	0.00	0.00	0.00	0.00	0.00	0.00	0.00	0.00	
RB1	3.13 ± 0.44	38.90	0.00	13.26	0.00	12.91	27.95	0.00	0.00	6.99	0.00	0.00	0.00	0.00	0.00	0.00	0.00	0.00	
RB2	11.07 ± 0.6	81.77	0.66	0.98	0.00	0.00	0.00	1.01	0.96	1.11	0.00	0.00	12.19	0.44	0.66	0.00	0.22	0.00	
RB3	3.43 ± 0.19	33.40	0.60	1.22	0.62	0.60	1.25	1.55	0.46	1.87	1.25	57.18	0.00	0.00	0.00	0.00	0.00	0.00	
RD1	1.79 ± 0.1	78.47	6.03	8.85	4.10	0.35	2.20	0.00	0.00	0.00	0.00	0.00	0.00	0.00	0.00	0.00	0.00	0.00	
RD2	0.89 ± 0.05	78.29	3.93	9.74	0.00	0.00	0.00	0.00	0.00	0.00	0.00	4.50	0.00	0.00	0.00	0.00	0.00	3.53	

APV: acrylates/polyurethanes/varnish cluster; CPE: chlorinated polyethylene; EPDM: ethylene-propylene-diene rubber; PEST: polyester; PE: polyethylene; PS: polystyrene; PA: polyamide; NR: nitrile rubber; EVA: ethylene-vinyl-acetate; PP: polypropylene; CMC: chemically modified cellulose; OPE: oxidised polyethylene; PC: polycarbonate; PVC: polyvinylchloride; PCP: polychloroprene; PLA: polylactide acide; ACNB: acrylonitrile-butadiene.

* specific density >1 g cm⁻¹

References

- Ballent, A., Corcoran, P.L., Madden, O., Helm, P.A., Longstaffe, F.J., 2016. Sources and sinks of microplastics in Canadian Lake Ontario nearshore, tributary and beach sediments. *Mar. Poll. Bull.* 110 (1), 383–395. doi:10.1016/j.marpolbul.2016.06.037.
- Castañeda, R.A., Avlijas, S., Simard, M.A., Ricciardi, A., Smith, R., 2014. Microplastic pollution in St. Lawrence River sediments. *Can. J. Fish. Aquat. Sci.* 71 (12), 1767–1771. doi:10.1139/cjfas-2014-0281.
- Di, M., Wang, J., 2018. Microplastics in surface waters and sediments of the Three Gorges Reservoir, China. *Sci. Tot. Env.* 616-617, 1620–1627. doi:10.1016/j.scitotenv.2017.10.150.
- Horton, A.A., Svendsen, C., Williams, R.J., Spurgeon, D.J., Lahive, E., 2017. Large microplastic particles in sediments of tributaries of the River Thames, UK – Abundance, sources and methods for effective quantification. *Mar. Poll. Bull.* 114 (1), 218–226. doi:10.1016/j.marpolbul.2016.09.004.
- Hurley, R., Woodward, J., Rothwell, J.J., 2018. Microplastic contamination of river beds significantly reduced by catchment-wide flooding. *Nat. Geosci.* 11 (4), 251–257. doi:10.1038/s41561-018-0080-1.
- Imhof, H.K., Schmid, J., Niessner, R., Ivleva, N.P., Laforsch, C., 2012. A novel, highly efficient method for the separation and quantification of plastic particles in sediments of aquatic environments. *Limnol. Oceanogr. Meth.* 10 (7), 524–537. doi:10.4319/lom.2012.10.524.
- Klein, S., Worch, E., Knepper, T.P., 2015. Occurrence and spatial distribution of microplastics in river shore sediments of the Rhine-Main area in Germany. *Environ. Sci. Technol.* 49 (10), 6070–6076. doi:10.1021/acs.est.5b00492.
- Leslie, H.A., Brandsma, S.H., van Velzen, M.J.M., Vethaak, A.D., 2017. Microplastics en route: Field measurements in the Dutch river delta and Amsterdam canals, wastewater treatment plants, North Sea sediments and biota. *Environ. Int.* 101, 133–142. doi:10.1016/j.envint.2017.01.018.
- Nel, H.A., Dalu, T., Wasserman, R.J., 2018. Sinks and sources: Assessing microplastic abundance in river sediment and deposit feeders in an Austral temperate urban river system. *Sci. Tot. Env.* 612, 950–956. doi:10.1016/j.scitotenv.2017.08.298.

- Peng, G., Xu, P., Zhu, B., Bai, M., Li, D., 2018. Microplastics in freshwater river sediments in Shanghai, China: A case study of risk assessment in mega-cities. *Environ. Pollut.* 234, 448–456. doi:10.1016/j.envpol.2017.11.034.
- Vermaire, J.C., Pomeroy, C., Herczegh, S.M., Haggart, O., Murphy, M., Schindler, D.E., 2017. Microplastic abundance and distribution in the open water and sediment of the Ottawa River, Canada, and its tributaries. *FACETS* 2 (1), 301–314. doi:10.1139/facets-2016-0070.
- Wagner, M., Scherer, C., Alvarez-Muñoz, D., Brennholt, N., Bourrain, X., Buchinger, S., Fries, E., Grosbois, C., Klasmeier, J., Marti, T., Rodriguez-Mozaz, S., Urbatzka, R., Vethaak, A.D., Winther-Nielsen, M., Reifferscheid, G., 2014. Microplastics in freshwater ecosystems: What we know and what we need to know. *Environ. Sci. Eur.* 26 (1), 12. doi:10.1186/s12302-014-0012-7.
- Wang, J., Peng, J., Tan, Z., Gao, Y., Zhan, Z., Chen, Q., Cai, L., 2017. Microplastics in the surface sediments from the Beijiang River littoral zone: Composition, abundance, surface textures and interaction with heavy metals. *Chemosphere* 171, 248–258. doi:10.1016/j.chemosphere.2016.12.074.
- Wang, Z., Su, B., Xu, X., Di Di, Huang, H., Mei, K., Dahlgren, R.A., Zhang, M., Shang, X., 2018. Preferential accumulation of small (<300 µm) microplastics in the sediments of a coastal plain river network in eastern China. *Water Res.* 144, 393–401. doi:10.1016/j.watres.2018.07.050.
- WSV DE, 2016. Abflussdaten Tagesmittel Rees und Bonn – internal data received. <http://undine.bafg.de>.

Final Discussion Dissertation

The research papers presented in this dissertation thesis were primarily designed and elaborated to enhance the knowledge on the degree and quality of microplastics (MP) pollution in the Rhine River – one of Europe’s main streams and one of the World’s most busy inland waterways. It had become evident from earlier studies (Klein et al., 2015; Mani et al., 2015; Van der Wal et al., 2015) that the Rhine River is not spared from plastic pollution, which might not come as a surprise, considering the vast population, industry, shipping and leisure pressure (ICPR, 2018). On its 1,230 km route from the Swiss Alps through France, Germany and the Netherlands to the North Sea, the Rhine River is a pivotal symbol of identity for many regions. The catchment is home to ~50 million humans and ~20 millions of them receive their daily drinking water from the Rhine, this being one major, but by far not the only reason to protect this precious resource from pollution. The Rhine River has a long history of human settlements reaching from far before the Romans until today. This large biosphere is still preferentially inhabited by grand numbers of people, birds, fish, insects and other animals. Over the past two centuries the course of the River has been repeatedly straightened to facilitate its economical exploitation and gain land, creating new opportunities but also threats, such as higher flooding risk and severe riverbed scouring (Uekoetter, 2018). Evermore corrective engineering measures are required to keep these dynamics at bay. Also, pollution to the Rhine River has a long and tragic history, from being a public sewer collector for centuries up to the devastating chemical catastrophe of Schweizerhalle near Basel in 1986 (Giger, 2009) and the nowadays increasing levels of micro pollutants and more recently, evidently, MP (Forter, 2000). Other anthropogenic footprints are e.g. displayed by the upstream invasion of non-native invasive species (Hirsch et al., 2016; Kalchhauser et al., 2013). And although, blessedly, the general ecological status of the Rhine habitat has improved over the past decades, even allowing for the Atlantic Salmon to reach Basel again (Mertens, 2011), these modern micro, nano and molecular threats pose new endangerments which call for urgent prevention and remediation measures. The basis for promising and efficient action against MP pollution is solid evidence on sources, concentrations, quantities, and dynamics, which this dissertation aspired to contribute to.

Searching for MP sources on a way towards better accountability

In Paper 1 (“Repeated detection of polystyrene microbeads in the Lower Rhine River”) the critical topic of traceability of MP waste in aquatic environments was addressed. As even large plastic waste items in the environment, such as bags, fishing lines and uncountable further examples are extremely difficult to trace to their origins, the challenge is mightily magnified

with decreasing particle size. To foster accountability for environmental plastic pollution it is crucial to detect substantial sources and fluxes in order to attribute them to their emitters. It had been reported that the Rhine River carries considerable amounts of primary MP beads in its surface waters (Mani et al., 2015; Urgert, 2015; Van der Wal et al., 2015). In a sustained forensic effort, the likely source area of this characteristic, solid PS microbead type, repeatedly occurring in the Lower Rhine River, was narrowed down. Through a longitudinal spot sampling investigation it became apparent that their concentrations strikingly and repeatedly increased from 0.05 to 9.2 MP m⁻³ along a stretch of 20 km. Rigorous chemical and optical analysis (infrared and Raman spectroscopy as well as scanning electron microscopy) unveiled polystyrene-divinylbenzene (PS-DVB) ion-exchange resin beads which highly likely originated from industrial effluents after water purification. Such beads have occurred in all of our sampling campaigns on ten different days between 2014 and 2017 downstream of Leverkusen (DE), substantiating their continuous emissions. The high likeliness of industrial point source emissions was discussed in person with the head of environmental politics at one of the riparian, possibly relevant, large industry parks. It was conveyed to us that this topic will be taken up on the internal agenda and rectification measures to potential spill will be addressed. Secondary MP generally vastly dominate the proportion of environmental MP, they are, however, practically impossible to link to their origins, due to a lack of distinct characteristics on comparison to e.g. the investigated microbeads in Paper 1 (Fahrenfeld et al., 2019). Nevertheless, one next important step must be to tackle the enormous challenge of also tracing such types. Possibly a way forward is to distinctly chemically fingerprint all produced polymers (Cartier et al., 2018).

Gearing up for the next challenges – method development for MP research

The study presented in Paper 1 focused on a very specific and visually securely recognisable type of spherical MP. Therefore, the initial processing of samples to access the particles in question was comparatively straight forward requiring NaCl–density separation and careful visual sorting under a stereomicroscope. When, however, the target MP is not defined and a comprehensive analysis of environmental MP of all polymers, sizes, types, shapes and colours is intended, reliable detection of MP requires efficient and reliable purification and/or separation of MP from their surrounding environmental matrix. Many traditional separation and purification techniques involve expensive and hazardous chemicals and are time-costly and prone to sample contamination and sample loss (Imhof et al., 2012; Ivleva et al., 2017; Löder et al., 2017). So to get ready for the high-sample-number seasonal MP emission dynamics investigation presented in Paper 3 (“Seasonal microplastics variation in nival and pluvial

stretches of the Rhine River – From the Swiss catchment towards the North Sea”) we set out to refine an oil-based separation technique originally proposed by Crichton et al. (2017) the result of which is presented in Paper 2 (“Using castor oil to separate microplastics from four different environmental matrices”). In this process, the challenges of high time cost, financial costs, environmental and health hazard as well as sample contamination potential were targeted. Furthermore, the technique was tested on four different environmental matrices, successfully demonstrating the harmonisation potential of such all-rounder techniques to foster comparability of methods for investigations of different environmental compartments (BASEMAN, 2017). It was demonstrated in our spike-recovery experiment that using the high molecular weight castor oil to separate four different polymer type MP from four different environmental matrices is a promising way to proceed as we were able to reliably recover $99 \pm 4\%$ of spiked MP.

Taking into account seasonal changes in MP concentrations and fluxes

One great challenge when studying environmental phenomena is to identify its spatial and temporal representativeness. In snapshot data an erratic event may fundamentally influence the detected pattern, potentially completely skewing and biasing the consequential evaluation and the work’s scientific and societal reception. It was a general ambition of this dissertation to follow up on leads set out by early Rhine River research to gain better insight into their validity (Klein et al., 2015; Mani et al., 2015; Urgert, 2015; Van der Wal et al., 2015). While Paper 1 is a geographical follow-up on the striking occurrence of microbeads encountered in a July 2014 longitudinal sampling campaign (Mani et al., 2015), Paper 3 aimed to gain insight on temporal variation of MP concentrations and total MP freights by at the same time this study expanded the previously set scope in the upstream direction to three important Swiss Rhine River tributaries. As a result of this study, there was no clearly visible relation between the discharge levels and MP concentrations which implies that regime dominated seasonal discharge patterns most certainly mainly govern the amount of MP moved towards the North Sea. Hence, according to the downstream prevailing pluvial discharge regime, November–May and specifically February are the most likely main contributing time periods for MP input towards the estuary and North Sea region. Going along the same argumentation, however, for there to be comparable MP concentrations in the river between all investigated times of year, as was the case in the presented Paper 3, elevated MP immissions levels are required to maintain the similar MP concentrations. It is assumed that the higher discharge rates, simultaneously rising the water level and often being the result of previous rainfall events, thus washing waste into the stream from the shoreline and from runoff, could explain this compensating quasi-

equilibrium dynamic. The main polymers PE, PP, PS represent the world's and Europe's main plastic demand and are also the most commonly found polymers in worldwide environmental MP studies. Their buoyancy in freshwater make them prominent components in water surface investigations and it is a different question what is to be found beneath the water surface and potentially on the riverbed itself. Exploring new ground in the Rhine River, Paper 4 ("Microplastic pollution in benthic midstream sediments of the Rhine River") presented our investigation on the Rhine floor.

Getting to the bottom of things – investigating MP on the Rhine riverbed

As rivers are often regarded as loyal conveyor belts, transporting their pollution downstream, there is rising evidence that MP may be retained (Hurley et al., 2018; Klein et al., 2015). When rivers act as MP sinks their ecosystem will accumulate pollution by preventing it to move downstream towards the sea. It had been shown that dammed and slack river water as well as shorelines retain MP but the question remained what happens in the midstream sediments of a large, dynamic river in undammed stretches (Castañeda et al., 2014; Klein et al., 2015; Zhang et al., 2015). In an attempt to find out if plastics settle and remain in the bed sediments of the Rhine River we took a diving bell and a dredging vessel to access the bottom (Paper 4). Using state-of-the-art analysis techniques in collaboration with Alfred Wegener Institute Helgoland, we identified concentrations of $0.26\text{--}11.01 \times 10^3 \text{ MP kg}^{-1}$. These MP concentrations in the Rhine River at Rh-km 837 were comparable to those reported from the Rhine estuary (Leslie et al., 2017), evoking further questions about accumulation and distribution patterns. As the vast majority of particles were of larger density than freshwater ($85 \pm 18\%$) a high proportion of suspected ship paint particles (acrylates/polyurethanes/varnish) was detected ($70 \pm 19\%$). This was a novel finding for the Rhine ecosystem and calls for further research with respect to mechanical and physical degradation of ship hull coatings and potential consequential accumulation or downstream transport of the resulting emission. With this study, a further important piece of the puzzle was provided for understanding the distribution and allocation of MP in the different compartments of the Rhine and of rivers in general. Still missing today is a comprehensive investigation of mid-water column MP to finally provide all constituents for reliable MP flux modelling in the Rhine. This would certainly be a highly interesting endeavour and something I might consider for future research.

Outlook and conclusion

As Plastic production, consumption and waste is still on the rise today (Ellen Mc Arthur Foundation, 2016) it becomes obvious that pollution needs to be tackled swiftly, comprehensively and effectively. The vast amounts of plastic waste are reflective of a linear economy where aggressive production and consumption is incentivised and negative externalities are paid by the state and the general public (Kramm et al., 2018; Wagner et al., 2018). Primary MP emission reduction initiatives such as “beat the microbead” (Plastic Soup Foundation, 2019), “zero pellet loss” or “operation clean sweep” (PlasticsEurope, 2017), numerous national bans on microbeads in cosmetics e.g. in the US, the UK, Taiwan and India (Plastic Soup Foundation, 2019), single use plastic bans, among other places in Europe, Morocco, Rwanda and China (The Guardian, 2017) and further measures are on the rise. Nevertheless, legal national and international preventative action against plastic pollution of the environment is disproportionately low, surprisingly so also in high developed countries of Western Europe (European Union, 2018). Considering that 40% of plastics are produced for packaging it is no wonder that the daily European plastic waste amounts to approximately 75,000 tons (PlasticsEurope, 2017). Other major usage is in longer life applications such as construction (20%), automotive (10%) and electronics (6%, PlasticsEurope, 2017). Many European states with high standard waste systems still export considerable amounts of plastic garbage to regions where landfilling is modus operandi (Bing et al., 2015). China, which had imported a cumulative 45% of global exported plastic waste since 1992, now refuses to accept the foreign waste, thus opening a next Pandora’s box for the future global waste pathways (Brooks et al., 2018). Despite the existence of the Basel Convention which ought to govern the export of hazardous and other waste, plastics is not regulated thereunder (Brooks et al., 2018; Voinov Kohler, 2017). Neither is plastic and MP waste considered under the Rotterdam Convention for hazardous chemicals and pesticides in international trade (Rotterdam Convention, 1998), despite their proven toxic potential (Gallo et al., 2018; Lohmann, 2017).

In favour of accountability and tracing of plastic waste, the following lines shall give insight into further research and policy steps I would pursue for the future:

- a) Closing the knowledge gap in the water column. As vast data of so many river compartments is steadily compiling, there remains still a soaring question about quantities and quality of plastic and MP moving downstream the Rhine below the surface but above the ground. In a phone call from a fisherman of the Lower Rhine I learned that his submerged nets tend to dramatically fill with sanitary and household

waste – especially during and after high discharge events. I have been an astounded witness to vast MP waste at the shores of Basel, but during all of my sampling experience I have not spotted the macroplastic waste according to the anecdotal report of the fisherman, as the items may be submerged beneath the water surface. So to provide this pivotal puzzle piece, it would be a tempting mission to specifically address the mid-water-column.

- b) Further, more knowledge is needed regarding specific and detailed cause and effects of plastic and MP in the Rhine as well as in other rivers. Despite the enormous challenge such investigations would pose, I believe that now moving towards the point sources and also diffuse sources needs to be completed.
- c) The reason for the still shy but steady boom in global reduction measures against single use plastic waste is the item's lack of value in the first place. After large Swiss supermarkets put a minute fee of 0.05 CHF on single use plastic bags, up to then freely received on the counter, demand for these lightweight receptacles immediately plummeted by 80% (Tagesanzeiger, 2018). Obviously, they weren't even worth 0.05 Swiss francs to the consumers (Dikgang et al., 2012). This example strongly indicates that there is a vast plastic consumption reduction potential in a myriad of other products not necessarily always needed, especially packaging. Starting from the items least valuable to society, I am in favour to set ambitious reduction targets in order to then rigorously follow up on cutting away at the unnecessary polymer products on the market which are most prone to pollute.
- d) Apart from that, I strongly support a “de-hysterisation” of the environmental plastic debate. Many reports are riding on a hype in demonising plastics without sufficient reflection on its enormous societal value when managed appropriately (BBC, 2018). There is not much dispute about the devastating extents ugly and dense plastic waste can have, and there is no two ways about where we shall move as mankind, but ongoing hysteria and alarmism – when not justified – leads to inflation of impulsive claims (Backhaus and Wagner, 2018). False reports and medial attention seeking lead to a concerning and counterproductive devalorisation of the cause. To keep sharp analysis and crisp recommendations for remediation up our sleeves, the really bad news must be distinguishable from the everyday “bad news” for media selling purposes. I will always aspire to contribute factually, objective and sober to the utterly important discussion about the future of – and inevitably – with plastics.

After plastics made their glorious run through society – and are expected to continue to do so – the downsides of such immensely durable material has become evident. Finally, I am reminded of Johann Wolfgang von Goethes “Zauberlehrling” whose broom, which initially proves a superb assistant, suddenly catastrophically turns against him. In Goethe’s poem the master turns up in the end to quickly resolve the disaster. For the plastic disaster, unfortunately, there is no grown master in sight yet. May the extended knowledge – gradually, steadily and hopefully soon – will lead to tangible solutions towards an environment free of plastic waste.

References

- Backhaus, T., Wagner, M., 2018. Microplastics in the environment: Much ado about nothing? A debate, 26 pp. *Global Challenges*. doi:10.1002/gch2.201900022
- BASEMAN, 2017. Interdisciplinary Research for Good Environmental Status. <http://www.jpi-oceans.eu/baseman>. Accessed 9 May 2018.
- BBC, 2018. Drowning in plastic. <https://www.bbc.co.uk/programmes/b0bmbn47>. Accessed 01 April 2018.
- Bing, X., Bloemhof-Ruwaard, J., Chaabane, A., van der Vorst, J., 2015. Global reverse supply chain redesign for household plastic waste under the emission trading scheme. *J. Clean. Prod.* 103, 28–39. doi:10.1016/j.jclepro.2015.02.019.
- Brooks, A.L., Wang, S., Jambeck, J.R., 2018. The Chinese import ban and its impact on global plastic waste trade. *Science advances* 4 (6), eaat0131. doi:10.1126/sciadv.aat0131.
- Cartier, L.E., Krzemnicki, M.S., Lendvay, B., Meyer, J.B., 2018. DNA fingerprinting of pearls, corals and ivory: A brief review of applications in gemmology. *Journ. of Gemm.* 36 (2), 152–160. doi:10.15506/JoG.2018.36.2.152.
- Castañeda, R.A., Avlijas, S., Simard, M.A., Ricciardi, A., Smith, R., 2014. Microplastic pollution in St. Lawrence River sediments. *Can. J. Fish. Aquat. Sci.* 71 (12), 1767–1771. doi:10.1139/cjfas-2014-0281.
- Crichton, E.M., Noël, M., Gies, E.A., Ross, P.S., 2017. A novel, density-independent and FTIR-compatible approach for the rapid extraction of microplastics from aquatic sediments. *Anal. Methods* 9 (9), 1419–1428. doi:10.1039/C6AY02733D.
- Dikgang, J., Leiman, A., Visser, M., 2012. Elasticity of demand, price and time: Lessons from South Africa's plastic-bag levy. *Appl. Econ.* 44 (26), 3339–3342. doi:10.1080/00036846.2011.572859.
- Ellen Mc Arthur Foundation, 2016. The new plastics economy: Rethinking the future of plastics & catalysing action, 68 pp. https://www.ellenmacarthurfoundation.org/assets/downloads/publications/NPEC-Hybrid_English_22-11-17_Digital.pdf. Accessed 01 April 2019.
- European Union, 2018. Directive of the European parliament and of the council on the reduction of the impact of certain plastic products on the environment, 33 pp. <https://eur->

lex.europa.eu/legal-content/en/ALL/?uri=CELEX%3A52018PC0340 Accessed on 09 March 2020.

- Fahrenfeld, N.L., Arbuckle-Keil, G., Naderi Beni, N., Bartelt-Hunt, S.L., 2019. Source tracking microplastics in the freshwater environment. *TrAC Trend. Anal. Chem.* 112, 248–254. doi:10.1016/j.trac.2018.11.030.
- Forster, M., 2000. *Farbenspiel: Ein Jahrhundert Umweltnutzung durch die Basler chemische Industrie*. Zugl.: Basel, Univ., Diss, 1998. Chronos, Zürich, 543 pp.
- Gallo, F., Fossi, C., Weber, R., Santillo, D., Sousa, J., Ingram, I., Nadal, A., Romano, D., 2018. Marine litter plastics and microplastics and their toxic chemicals components: The need for urgent preventive measures. *Environ. Sci. Eur.* 30 (1), 13. doi:10.1186/s12302-018-0139-z.
- Giger, W., 2009. The Rhine red, the fish dead – The 1986 Schweizerhalle disaster, a retrospect and long-term impact assessment. *Environ. Sci. Pollut. Res. Int.* 16 Suppl. 1, S98–111. doi:10.1007/s11356-009-0156-y.
- Hirsch, P.E., N’Guyen, A., Adrian-Kalchhauser, I., Burkhardt-Holm, P., 2016. What do we really know about the impacts of one of the 100 worst invaders in Europe? A reality check. *Ambio* 45 (3), 267–279. doi:10.1007/s13280-015-0718-9.
- Hurley, R., Woodward, J., Rothwell, J.J., 2018. Microplastic contamination of river beds significantly reduced by catchment-wide flooding. *Nat. Geosci.* 11 (4), 251–257. doi:10.1038/s41561-018-0080-1.
- ICPR, 2018. *The Rhine. International Commission for the Protection of the Rhine.* <https://www.iksr.org/en/rhine/>. Accessed 18 December 2018.
- Imhof, H.K., Schmid, J., Niessner, R., Ivleva, N.P., Laforsch, C., 2012. A novel, highly efficient method for the separation and quantification of plastic particles in sediments of aquatic environments. *Limnol. Oceanogr. Methods* 10 (7), 524–537. doi:10.4319/lom.2012.10.524.
- Ivleva, N.P., Wiesheu, A.C., Niessner, R., 2017. Microplastic in aquatic ecosystems. *Angew. Chem. Int. Edit.* 56 (7), 1720–1739. doi:10.1002/anie.201606957.
- Kalchhauser, I., Mutzner, P., Hirsch, P., Burkhardt-Holm, P., 2013. Arrival of round goby *Neogobius melanostomus* (Pallas, 1814) and bighead goby *Ponticola kessleri* (Günther, 1861) in the High Rhine (Switzerland). *BIR* 2 (1), 79–83. doi:10.3391/bir.2013.2.1.14.

- Klein, S., Worch, E., Knepper, T.P., 2015. Occurrence and spatial distribution of microplastics in river shore sediments of the Rhine-Main area in Germany. *Environ. Sci. Technol.* 49 (10), 6070–6076. doi:10.1021/acs.est.5b00492.
- Kramm, J., Völker, C., Wagner, M., 2018. Superficial or substantial: Why care about microplastics in the anthropocene? *Environ. Sci. Technol.* 52 (6), 3336–3337. doi:10.1021/acs.est.8b00790.
- Leslie, H.A., Brandsma, S.H., van Velzen, M.J.M., Vethaak, A.D., 2017. Microplastics en route: Field measurements in the Dutch river delta and Amsterdam canals, wastewater treatment plants, North Sea sediments and biota. *Environ. Int.* 101, 133–142. doi:10.1016/j.envint.2017.01.018.
- Löder, M.G.J., Imhof, H.K., Ladehoff, M., Löschel, L.A., Lorenz, C., Mintenig, S., Piehl, S., Primpke, S., Schrank, I., Laforsch, C., Gerdt, G., 2017. Enzymatic purification of microplastics in environmental samples. *Environ. Sci. Technol.* 51 (24), 14283–14292. doi:10.1021/acs.est.7b03055.
- Lohmann, R., 2017. Microplastics are not important for the cycling and bioaccumulation of organic pollutants in the oceans – But should microplastics be considered POPs themselves? *Integr. Environ. Assess.* 13 (3), 460–465. doi:10.1002/ieam.1914.
- Mani, T., Hauk, A., Walter, U., Burkhardt-Holm, P., 2015. Microplastics profile along the Rhine River. *Sci. Rep.* 5, 17988. doi:10.1038/srep17988.
- Mertens, M., 2011. *Der Lachs: Ein Fisch kehrt zurück*. Haupt, Bern.
- Plastic Soup Foundation, 2019. Beat the Microbead. <https://www.beatthemicrobead.org>. Accessed 01 April 2019.
- PlasticsEurope, 2017. Operation Clean Sweep, 28 pp. <https://www.plasticseurope.org/en/resources/publications/367-plasticseurope-operation-clean-sweep-report-2017>. Accessed 01 April 2019.
- Tagesanzeiger, 2018. Die 5-Rappen-Gebühr zeigt Wirkung – und wie. <https://www.tagesanzeiger.ch/wirtschaft/standardverbrauch-von-raschelsaekli-ging-um-84-prozent-zurueck/story/16111216>. Accessed 01 April 2019.
- The Guardian, 2017. Kenya brings in world’s toughest plastic bag ban: Four years jail or \$40,000 fine. <https://www.theguardian.com/environment/2017/aug/28/kenya-brings-in-worlds-toughest-plastic-bag-ban-four-years-jail-or-40000-fine>. Accessed 01 April 2019.

- Uekoetter, F., 2018. In the reflection of water. A transnational environmental history of the Upper Rhine (1800-2000). Franz Steiner Verlag, Germany.
- Urgert, W., 2015. Microplastics in the rivers Meuse and Rhine: Developing guidance for a possible future monitoring program. Masterthesis, Heerlen, The Netherlands, 106 pp. <https://www.riwa-rijn.org/wp-content/uploads/2015/11/master-thesis-NW-Wilco-Urgert-838144036-DEFINITIEF-16-10-2015.pdf> Accessed 09 March 2020.
- Van der Wal, M., Van der Meulen, M., Tweehuijsen, G., Peterlin, M., Palatinus, A., Virsek, M.K., Coscia, L., Krsan, A., 2015. SFRA0025: Identification and assessment of riverine input of (marine) litter.: Final report for the European Commission DG Environment under framework contract No ENV. D, Bristol (Vol. 25). 2/FRA/2012., 208 pp. <http://ec.europa.eu/environment/marine/good-environmental-status/descriptor-10/pdf/iasFinal%20Report.pdf>. Accessed 29 March 2019.
- Voinov Kohler, J., 2017. The Basel Convention on the Control of Transboundary Movements of Hazardous Wastes and their Disposal 1989, in: Elgar encyclopedia of environmental law. Edward Elgar Publishing, Cheltenham, UK, pp. 331–342.
- Wagner, M., Lambert, S., Besseling, E., Biginagwa, F.J. (Eds.), 2018. Freshwater microplastics: Emerging environmental contaminants? The handbook of environmental chemistry. Volume 58. Springer, 303 pp. doi:10.1007/978-3-319-61615-5
- Zhang, K., Gong, W., Lv, J., Xiong, X., Wu, C., 2015. Accumulation of floating microplastics behind the Three Gorges Dam. Environ. Pollut. 204, 117–123. doi:10.1016/j.envpol.2015.04.023.

Final Acknowledgements Dissertation

I would like to extend my warmest gratitude towards these kind people for supporting me:

Patricia Holm, Gunnar Gerdts, Ruedi Bösiger, Nicole Seiler-Kurth, Heidi Schiffer, Claudia Lorenz, Sebastian Primpke, Helmut Segner and Jürg Utzinger

Irene Adrian-Kalchhauser, Dieter Biemann, Pascal Blarer, Sascha Borer, Sophie Bosshart, Karen Bussmann, Renato Goldschmidt, Philipp Hirsch, Christian Hossli, Clara Leistenschneider, Bridget, Ueli, Hannah, Sarah and Christoph Mani, Rolf Nagelschmidt, Anouk N’Guyen, Hedwig Scharlipp, Mike Schröder, Denise Staubli, Sandrine Straub, Kai Trurnit, Joschka Wiegler and Martin Wolters

Final References Dissertation

- AFT Fluorotec, 2016. The properties and advantages of PTFE.
<https://www.fluorotec.com/news/blog/the-properties-and-advantages-of-polytetrafluoroethylene-ptfe/>. Accessed 21 February 2019.
- Ali, U., Karim, K.J.B.A., Buang, N.A., 2015. A review of the properties and applications of poly (methyl methacrylate) (PMMA). *Polym. Rev.* 55 (4), 678–705.
doi:10.1080/15583724.2015.1031377.
- Andrady, A.L., 2011. Microplastics in the marine environment. *Mar. Pollut. Bull.* 62 (8), 1596–1605. doi:10.1016/j.marpolbul.2011.05.030.
- Andrady, A.L., 2015. Persistence of plastic litter in the oceans, in: Klages, M., Gutow, L., Bergmann, M. (Eds.), *Marine Anthropogenic Litter*. Springer, pp. 57–72.
- Andrady, A.L., 2017. The plastic in microplastics: A review. *Mar. Pollut. Bull.* 119 (1), 12–22. doi:10.1016/j.marpolbul.2017.01.082.
- Andrady, A.L., Pegram, J.E., Tropsha, Y., 1993. Changes in carbonyl index and average molecular weight on embrittlement of enhanced-photodegradable polyethylenes. *J. Environ. Polym. Degr.* 1 (3), 171–179. doi:10.1007/BF01458025.
- Araujo, C.F., Nolasco, M.M., Ribeiro, A.M.P., Ribeiro-Claro, P.J.A., 2018. Identification of microplastics using Raman spectroscopy: Latest developments and future prospects. *Water Res.* 142, 426–440. doi:10.1016/j.watres.2018.05.060.
- Arshady, R., 1992. Suspension, emulsion, and dispersion polymerization: A methodological survey. *Colloid Polym. Sci.* 270 (8), 717–732. doi:10.1007/BF00776142.
- Backhaus, T., Wagner, M., 2018. Microplastics in the environment: Much ado about nothing? A debate, 26 pp. *Global Challenges*. doi:10.1002/gch2.201900022
- Ballent, A., Corcoran, P.L., Madden, O., Helm, P.A., Longstaffe, F.J., 2016. Sources and sinks of microplastics in Canadian Lake Ontario nearshore, tributary and beach sediments. *Mar. Poll. Bull.* 110 (1), 383–395. doi:10.1016/j.marpolbul.2016.06.037.
- Barcelo, D., Rocha-Santos, T.A.P., Duarte, A.C. (Eds.), 2017. Characterization of microplastics by Raman spectroscopy. *Comprehensive Analytical Chemistry* 75, 33 pp.
- Barnes, D.K.A., Galgani, F., Thompson, R.C., Barlaz, M., 2009. Accumulation and fragmentation of plastic debris in global environments. *Philosophical transactions of the*

- Royal Society of London. Series B, Biological sciences 364 (1526), 1985–1998.
doi:10.1098/rstb.2008.0205.
- BASEMAN, 2017. Interdisciplinary Research for Good Environmental Status.
<http://www.jpi-oceans.eu/baseman>. Accessed 9 May 2018.
- BBC, 2018. Drowning in plastic. <https://www.bbc.co.uk/programmes/b0bmbn47>. Accessed 01 April 2018.
- Bergmann, M., Lutz, B., Tekman, M.B., Gutow, L., 2017. Citizen scientists reveal: Marine litter pollutes Arctic beaches and affects wild life. *Mar. Pollut. Bull.* 125 (1-2), 535–540.
doi:10.1016/j.marpolbul.2017.09.055.
- Bergmann, M., Wirzberger, V., Krumpfen, T., Lorenz, C., Primpke, S., Tekman, M.B., Gerdts, G., 2017. High quantities of microplastic in Arctic deep-sea sediments from the HAUSGARTEN observatory. *Environ. Sci. Technol.* 51 (19), 11000–11010.
doi:10.1021/acs.est.7b03331.
- Besseling, E., Foekema, E.M., van Franeker, J.A., Leopold, M.F., Kühn, S., Bravo Rebolledo, E.L., Heße, E., Mielke, L., IJzer, J., Kamminga, P., Koelmans, A.A., 2015. Microplastic in a macro filter feeder: Humpback whale *Megaptera novaeangliae*. *Mar. Pollut. Bull.* 95 (1), 248–252. doi:10.1016/j.marpolbul.2015.04.007.
- Besseling, E., Quik, J.T.K., Sun, M., Koelmans, A.A., 2017. Fate of nano- and microplastic in freshwater systems: A modeling study. *Environ. Pollut.* 220 (Pt A), 540–548.
doi:10.1016/j.envpol.2016.10.001.
- BfG, 2017. Pegel Rhein Bonn. http://undine.bafg.de/rhein/pegel/rhein_pegel_bonn.html.
Accessed 10 January 2018.
- BfG, 2017. Pegel Rhein Rees. http://undine.bafg.de/rhein/pegel/rhein_pegel_rees.html.
Accessed 10 January 2018.
- BfG, 2017. Pegel Rhein Ruhr Hattingen.
http://undine.bafg.de/rhein/pegel/rhein_pegel_hattingen.html. Accessed 5 January 2018.
- BfG, 2017. Pegel Rhein Ruhrort Duisburg.
http://undine.bafg.de/rhein/pegel/rhein_pegel_ruhrort.html. Accessed 5 January 2018.
- Bing, X., Bloemhof-Ruwaard, J., Chaabane, A., van der Vorst, J., 2015. Global reverse supply chain redesign for household plastic waste under the emission trading scheme. *J. Clean. Prod.* 103, 28–39. doi:10.1016/j.jclepro.2015.02.019.

- Birley, A.W., 2012 // 1991. Plastic materials: properties and applications. Springer, 1205 pp.
- Biron, M. (Ed.), 2004. Thermosets and Composites. Elsevier Science, Oxford.
- Blarer, P., Burkhardt-Holm, P., 2016. Microplastics affect assimilation efficiency in the freshwater amphipod *Gammarus fossarum*. *Environ. Sci. Pollut. R. Int.* 23 (23), 23522–23532. doi:10.1007/s11356-016-7584-2.
- Blarer, P., Kull, G., 2018. Swiss Litter Report, Zurich, 65 pp.
https://storage.googleapis.com/wzukusers/user-15533811/documents/5b867b8f51528JrYbIoW/Swiss%20Litter%20Report_final_180710.pdf. Accessed 30 March 2019.
- Blettler, M.C.M., Abrial, E., Khan, F.R., Sivri, N., Espinola, L.A., 2018. Freshwater plastic pollution: Recognizing research biases and identifying knowledge gaps. *Water Res.* 143, 416–424. doi:10.1016/j.watres.2018.06.015.
- Blomqvist, S., 1991. Quantitative sampling of soft-bottom sediments: Problems and solutions. *Mar. Ecol. Prog. Ser.* 72, 295–304. doi:10.3354/meps072295.
- BMJV, 2016. Deutsches Bundesministerium für Justiz und Verbraucherschutz. Verordnung über die Anforderungen an das Einleiten von Abwasser in Gewässer, Annex 29: Eisen- und Stahlerzeugung. BMJV. http://www.gesetze-im-internet.de/abwv/anhang_29.html. Accessed 15 January 2018.
- Bosker, T., Behrens, P., Vijver, M.G., 2017. Determining global distribution of microplastics by combining citizen science and in-depth case studies. *Integr. Environ. Assess. Manag.* 13 (3), 536–541. doi:10.1002/ieam.1908.
- Boucher, J., Faure, F., Pompini, O., Plummer, Z., Wieser, O., Felipe de Alencastro, L., 2019. (Micro) plastic fluxes and stocks in Lake Geneva basin. *TrAC Trends in Analytical Chemistry* 112, 66–74. doi:10.1016/j.trac.2018.11.037.
- Brooks, A.L., Wang, S., Jambeck, J.R., 2018. The Chinese import ban and its impact on global plastic waste trade. *Science advances* 4 (6), eaat0131. doi:10.1126/sciadv.aat0131.
- Browne, M.A., Crump, P., Niven, S.J., Teuten, E., Tonkin, A., Galloway, T., Thompson, R., 2011. Accumulation of microplastic on shorelines worldwide: Sources and sinks. *Environ. Sci. Technol.* 45 (21), 9175–9179. doi:10.1021/es201811s.
- Brydson, J.A., 1999. *Plastics Materials*. Elsevier Science, Oxford, United Kingdom.

- Bundesamt für Umwelt BAFU, 2018. Hydrologisches Jahrbuch der Schweiz 2017. 44 pp.
https://naturwissenschaften.ch/uuid/61b20431-cbe0-5f94-8511-c50e3c95b90b?r=20190807115818_1565140005_88713df7-d203-5932-ae9a-0b9e3ecb3adf. Accessed 31 March 2020.
- Bundesamt für Umwelt BAFU, 2019. Hydrologische Daten und Vorhersagen.
https://www.hydrodaten.admin.ch/de/messstationen_zustand.html. Accessed 14 April 2019.
- Carpenter, E.J., Anderson, S.J., Harvey, G.R., Miklas, H.P., Peck, B.B., 1972. Polystyrene spherules in coastal waters. *Science* 178 (4062), 749–750.
doi:10.1126/science.178.4062.749.
- Carpenter, E.J., Smith, K.L., 1972. Plastics on the Sargasso sea surface. *Science* 175 (4027), 1240–1241.
- Carson, H.S., Colbert, S.L., Kaylor, M.J., McDermid, K.J., 2011. Small plastic debris changes water movement and heat transfer through beach sediments. *Mar. Pollut. Bull.* 62 (8), 1708–1713. doi:10.1016/j.marpolbul.2011.05.032.
- Cartier, L.E., Ali, S.H., Krzemnicki, M.S., 2018. Blockchain, chain of custody and trace elements: An overview of tracking and traceability opportunities in the gem Industry. *Journ. of Gemm.* 36 (3), 212–227. doi:10.15506/JoG.2018.36.3.212.
- Cartier, L.E., Krzemnicki, M.S., Lendvay, B., Meyer, J.B., 2018. DNA fingerprinting of pearls, corals and ivory: A brief review of applications in gemmology. *Journ. of Gemm.* 36 (2), 152–160. doi:10.15506/JoG.2018.36.2.152.
- Castañeda, R.A., Avlijas, S., Simard, M.A., Ricciardi, A., Smith, R., 2014. Microplastic pollution in St. Lawrence River sediments. *Can. J. Fish. Aquat. Sci.* 71 (12), 1767–1771. doi:10.1139/cjfas-2014-0281.
- CCNR, 2018. Information on the waterway Rhine. Central Commission for the Navigation of the Rhine. <https://www.ccr-zkr.org/12030100-en.html>. Accessed 18 December 2018.
- Choi, S.-S., Kim, Y.-K., 2012. Analysis of residual monomers in poly(acrylonitrile-co-butadiene-co-styrene). *Macromol. Res.* 20 (6), 585–589. doi:10.1007/s13233-012-0080-8.
- Claessens, M., Meester, S. de, van Landuyt, L., Clerck, K. de, Janssen, C.R., 2011. Occurrence and distribution of microplastics in marine sediments along the Belgian coast. *Mar. Pollut. Bull.* 62 (10), 2199–2204. doi:10.1016/j.marpolbul.2011.06.030.

- Claessens, M., van Cauwenberghe, L., Vandegehuchte, M.B., Janssen, C.R., 2013. New techniques for the detection of microplastics in sediments and field collected organisms. *Mar. Pollut. Bull.* 70 (1-2), 227–233. doi:10.1016/j.marpolbul.2013.03.009.
- Cole, G., Sherrington, C., 2016. Study to quantify pellet emission in the UK - Report to Fidra. Eunomia. <https://www.eunomia.co.uk/reports-tools/study-to-quantify-pellet-emissions-in-the-uk/>. Accessed 09 June 2018.
- Cole, M., Lindeque, P., Halsband, C., Galloway, T.S., 2011. Microplastics as contaminants in the marine environment: A review. *Mar. Pollut. Bull.* 62 (12), 2588–2597. doi:10.1016/j.marpolbul.2011.09.025.
- Cole, M., Webb, H., Lindeque, P.K., Fileman, E.S., Halsband, C., Galloway, T.S., 2014. Isolation of microplastics in biota-rich seawater samples and marine organisms. *Sci. Rep.* 4, 4528. doi:10.1038/srep04528.
- Corcoran, P.L., 2015. Benthic plastic debris in marine and fresh water environments. *Environ. Sci. Process. Impact.* 17 (8), 1363–1369. doi:10.1039/c5em00188a.
- Covestro, 2017. Polyurethane Applications. <https://www.polyurethanes.covestro.com/en/Applications/Overview>. Accessed 28 January 2019.
- Cózar, A., Echevarría, F., González-Gordillo, J.I., Irigoien, X., Ubeda, B., Hernández-León, S., Palma, A.T., Navarro, S., García-de-Lomas, J., Ruiz, A., Fernández-de-Puelles, M.L., Duarte, C.M., 2014. Plastic debris in the open ocean. *P. Natl. Acad. Sci. USA* 111 (28), 10239–10244. doi:10.1073/pnas.1314705111.
- Crichton, E.M., Noël, M., Gies, E.A., Ross, P.S., 2017. A novel, density-independent and FTIR-compatible approach for the rapid extraction of microplastics from aquatic sediments. *Anal. Methods* 9 (9), 1419–1428. doi:10.1039/C6AY02733D.
- Currie, R.I., Foxton, P., 1957. A new quantitative plankton net. *J. Mar. Biol. Ass.* 36 (01), 17. doi:10.1017/S0025315400017033.
- De Dardel, F., 2015. Ion exchange resin structure. http://dardel.info/IX/resin_structure.html#gel_macro. Accessed 3 October 2018.
- Dekiff, J.H., Remy, D., Klasmeier, J., Fries, E., 2014. Occurrence and spatial distribution of microplastics in sediments from Norderney. *Environ. Pollut.* 186, 248–256. doi:10.1016/j.envpol.2013.11.019.

- Derraik, J.G.B., 2002. The pollution of the marine environment by plastic debris: A review. *Mar. Pollut. Bull.* 44 (9), 842–852. doi:10.1016/S0025-326X(02)00220-5.
- Di, M., Wang, J., 2018. Microplastics in surface waters and sediments of the Three Gorges Reservoir, China. *Sci. Tot. Env.* 616-617, 1620–1627. doi:10.1016/j.scitotenv.2017.10.150.
- Dikgang, J., Leiman, A., Visser, M., 2012. Elasticity of demand, price and time: Lessons from South Africa’s plastic-bag levy. *Appl. Econ.* 44 (26), 3339–3342. doi:10.1080/00036846.2011.572859.
- Dris, R., Gasperi, J., Rocher, V., Saad, M., Renault, N., Tassin, B., 2015. Microplastic contamination in an urban area: A case study in Greater Paris. *Environ. Chem.* 12 (5), 592. doi:10.1071/EN14167.
- Dris, R., Gasperi, J., Saad, M., Mirande, C., Tassin, B., 2016. Synthetic fibers in atmospheric fallout: A source of microplastics in the environment? *Mar. Pollut. Bull.* 104 (1-2), 290–293. doi:10.1016/j.marpolbul.2016.01.006.
- Dris, R., Gasperi, J., Tassin, B., 2018. Sources and fate of microplastics in urban areas: A focus on Paris Megacity, in: Wagner, M., Lambert, S., Besseling, E., Biginagwa, F.J. (Eds.), *Freshwater microplastics. Emerging environmental contaminants? The handbook of environmental chemistry. Volume 58.* Springer, pp. 69–83. doi:10.1007/978-3-319-61615-5
- Dris, R., Imhof, H., Sanchez, W., Gasperi, J., Galgani, F., Tassin, B., Laforsch, C., 2015. Beyond the ocean: Contamination of freshwater ecosystems with (micro-)plastic particles. *Environ. Chem.* 12 (5), 539. doi:10.1071/EN14172.
- Duis, K., Coors, A., 2016. Microplastics in the aquatic and terrestrial environment: Sources (with a specific focus on personal care products), fate and effects. *Environ. Sci. Eur.* 28 (1), 2. doi:10.1186/s12302-015-0069-y.
- Eerkes-Medrano, D., Thompson, R.C., Aldridge, D.C., 2015. Microplastics in freshwater systems: A review of the emerging threats, identification of knowledge gaps and prioritisation of research needs. *Water Res.* 75, 63–82. doi:10.1016/j.watres.2015.02.012.
- Ellen Mc Arthur Foundation, 2016. *The new plastics economy: Rethinking the future of plastics & catalysing action*, 68 pp. https://www.ellenmacarthurfoundation.org/assets/downloads/publications/NPEC-Hybrid_English_22-11-17_Digital.pdf. Accessed 01 April 2019.

- Elwas, 2018. ELWAS KARTE NRW. <http://www.elwasweb.nrw.de/elwas-web/index.jsf#>. Accessed 10 January 2018.
- Eriksen, M., Lebreton, L.C.M., Carson, H.S., Thiel, M., Moore, C.J., Borerro, J.C., Galgani, F., Ryan, P.G., Reisser, J., 2014. Plastic pollution in the world's oceans: More than 5 trillion plastic pieces weighing over 250,000 tons afloat at sea. *PloS one* 9 (12), e111913. doi:10.1371/journal.pone.0111913.
- Eriksen, M., Mason, S., Wilson, S., Box, C., Zellers, A., Edwards, W., Farley, H., Amato, S., 2013. Microplastic pollution in the surface waters of the Laurentian Great Lakes. *Mar. Pollut. Bull.* 77 (1-2), 177–182. doi:10.1016/j.marpolbul.2013.10.007.
- European Union, 2018. Directive of the European parliament and of the council on the reduction of the impact of certain plastic products on the environment, 33 pp. <https://eur-lex.europa.eu/legal-content/en/ALL/?uri=CELEX%3A52018PC0340> Accessed on 09 March 2020.
- European Union, 2018. Strategy for plastics in a circular economy. https://ec.europa.eu/commission/publications/documents-strategy-plastics-circular-economy_en. Accessed 10 October 2018.
- Eurostat, 2018. Maritime ports freight and passenger statistics – statistics explained. https://ec.europa.eu/eurostat/statistics-explained/index.php/Maritime_ports_freight_and_passenger_statistics#Rotterdam.2C_Antwerpen_and_Hamburg_stayed_top_ports. Accessed 29 January 19.
- Fahrenfeld, N.L., Arbuckle-Keil, G., Naderi Beni, N., Bartelt-Hunt, S.L., 2019. Source tracking microplastics in the freshwater environment. *TrAC Trend. Anal. Chem.* 112, 248–254. doi:10.1016/j.trac.2018.11.030.
- Farley, K.J., Morel, F.M., 1986. Role of coagulation in the kinetics of sedimentation. *Environ. Sci. Technol.* 20 (2), 187–195. doi:10.1021/es00144a014.
- Faure, F., Corbaz, M., Baecher, H., Alencastro, L.F. de, 2012. Pollution due to plastics and microplastics in Lake Geneva and in the Mediterranean Sea. *Arch. Sci.* 65 (157–164). https://www.unige.ch/sphn/Publications/ArchivesSciences/AdS%202004-2015/AdS%202012%20Vol%2065%20Fasc%201/157-164_16_Faure_65.pdf Accessed on 09 March 2020.

- Faure, F., Demars, C., Wieser, O., Kunz, M., Alencastro, L.F. de, 2015. Plastic pollution in Swiss surface waters: Nature and concentrations, interaction with pollutants. *Environ. Chem.* 12 (5), 582. doi:10.1071/EN14218.
- Fazey, F.M.C., Ryan, P.G., 2016. Biofouling on buoyant marine plastics: An experimental study into the effect of size on surface longevity. *Environ. Pollut.* 210, 354–360. doi:10.1016/j.envpol.2016.01.026.
- Feldman, D., 2002. Polymer weathering: Photo-oxidation. *J. Polym. Environ.* 10 (4), 163–173. doi:10.1023/A:1021148205366.
- Felsing, S., Kochleus, C., Buchinger, S., Brennholt, N., Stock, F., Reifferscheid, G., 2018. A new approach in separating microplastics from environmental samples based on their electrostatic behavior. *Environ. Pollut.* 234, 20–28. doi:10.1016/j.envpol.2017.11.013.
- Fendall, L.S., Sewell, M.A., 2009. Contributing to marine pollution by washing your face: Microplastics in facial cleansers. *Mar. Pollut. Bull.* 58 (8), 1225–1228. doi:10.1016/j.marpolbul.2009.04.025.
- Ferreira, P., Fonte, E., Soares, M.E., Carvalho, F., Guilhermino, L., 2016. Effects of multi-stressors on juveniles of the marine fish *Pomatoschistus microps*: Gold nanoparticles, microplastics and temperature. *Aquat. Toxicol.* 170, 89–103. doi:10.1016/j.aquatox.2015.11.011.
- Finkelstein, N.H., 2008. *Plastics*. Marshall Cavendish Benchmark.
- Foley, C.J., Feiner, Z.S., Malinich, T.D., Höök, T.O., 2018. A meta-analysis of the effects of exposure to microplastics on fish and aquatic invertebrates. *Sci. Total Environ.* 631–632, 550–559. doi:10.1016/j.scitotenv.2018.03.046.
- Forster, M., 2000. *Farbenspiel: Ein Jahrhundert Umweltnutzung durch die Basler chemische Industrie*. Zugl.: Basel, Univ., Diss, 1998. Chronos, Zürich, 543 pp.
- Fossi, M.C., Bainsi, M., Panti, C., Galli, M., Jiménez, B., Muñoz-Arnanz, J., Marsili, L., Finoia, M.G., Ramírez-Macías, D., 2017. Are whale sharks exposed to persistent organic pollutants and plastic pollution in the Gulf of California (Mexico)? First ecotoxicological investigation using skin biopsies. *Comparative biochemistry and physiology. Toxicol. Pharm.: CBP* 199, 48–58. doi:10.1016/j.cbpc.2017.03.002.
- Frings, R.M., 2008. Downstream fining in large sand-bed rivers. *Earth-Sci. Rev.* 87 (1-2), 39–60. doi:10.1016/j.earscirev.2007.10.001.

- Frings, R.M., Gehres, N., Promny, M., Middelkoop, H., Schüttrumpf, H., Vollmer, S., 2014. Today's sediment budget of the Rhine River channel, focusing on the Upper Rhine Graben and Rhenish Massif. *Geomorphology* 204, 573–587. doi:10.1016/j.geomorph.2013.08.035.
- Fujita, I., Muste, M., Kruger, A., 1998. Large-scale particle image velocimetry for flow analysis in hydraulic engineering applications. *J. Hydraul. Res.* 36 (3), 397–414. doi:10.1080/00221689809498626.
- Gallo, F., Fossi, C., Weber, R., Santillo, D., Sousa, J., Ingram, I., Nadal, A., Romano, D., 2018. Marine litter plastics and microplastics and their toxic chemicals components: The need for urgent preventive measures. *Environ. Sci. Eur.* 30 (1), 13. doi:10.1186/s12302-018-0139-z.
- GESAMP, 2016. Sources, fate and effects of microplastics in the marine environment: Part two of a global assessment 93. GESAMP, 221 pp. <http://www.gesamp.org/site/assets/files/1275/sources-fate-and-effects-of-microplastics-in-the-marine-environment-part-2-of-a-global-assessment-en.pdf>. Accessed 14 December 2018.
- Gewert, B., Ogonowski, M., Barth, A., MacLeod, M., 2017. Abundance and composition of near surface microplastics and plastic debris in the Stockholm Archipelago, Baltic Sea. *Mar. Pollut. Bull.* 120 (1-2), 292–302. doi:10.1016/j.marpolbul.2017.04.062.
- Geyer, R., Jambeck, J.R., Law, K.L., 2017a. Production, use, and fate of all plastics ever made. *Sci. Adv.* 3 (7), e1700782. doi:10.1126/sciadv.1700782.
- Geyer, R., Jambeck, J.R., Law, K.L., 2017b. Supplementary Material, Production, use, and fate of all plastics ever made. *Sci. Adv.* 3 (7), e1700782. doi:10.1126/sciadv.1700782.
- Giger, W., 2009. The Rhine red, the fish dead – The 1986 Schweizerhalle disaster, a retrospect and long-term impact assessment. *Environ. Sci. Pollut. Res. Int.* 16 Suppl. 1, S98–111. doi:10.1007/s11356-009-0156-y.
- Gregory, M.R., 2009. Environmental implications of plastic debris in marine settings – entanglement, ingestion, smothering, hangers-on, hitch-hiking and alien invasions. *Philosophical transactions of the Royal Society of London. Series B, Biological sciences* 364 (1526), 2013–2025. doi:10.1098/rstb.2008.0265.
- Hartmann, N.B., Hüffer, T., Thompson, R.C., Hassellöv, M., Verschoor, A., Daugaard, A.E., Rist, S., Karlsson, T., Brennholt, N., Cole, M., Herrling, M.P., Hess, M.C., Ivleva, N.P.,

- Lusher, A.L., Wagner, M., 2019. Are we speaking the same language? Recommendations for a definition and categorization framework for plastic debris. *Environ. Sci. Technol.* 53 (3), 1039–1047. doi:10.1021/acs.est.8b05297.
- Hernandez, E., Nowack, B., Mitrano, D.M., 2017. Polyester textiles as a source of microplastics from households: A mechanistic study to understand microfiber release during washing. *Environ. Sci. Technol.* 51 (12), 7036–7046. doi:10.1021/acs.est.7b01750.
- Hess, M., Diel, P., Mayer, J., Rahm, H., Reifenhäuser, W., Stark, J., Schwaiger, J., 2018. Mikroplastik in Binnengewässern Süd- und Westdeutschlands: Bundesländerübergreifende Untersuchungen in Baden-Württemberg, Bayern, Hessen, Nordrhein-Westfalen und Rheinland-Pfalz, Karlsruhe, Augsburg, Wiesbaden, Recklinghausen, Mainz, 86 pp.
https://www.lanuv.nrw.de/fileadmin/lanuvpubl/6_sonderreihen/L%C3%A4nderbericht_Mikroplastik_in_Binnengew%C3%A4ssern.pdf. Accessed 25 May 2018.
- Hidalgo-Ruz, V., Gutow, L., Thompson, R.C., Thiel, M., 2012. Microplastics in the marine environment: A review of the methods used for identification and quantification. *Environ. Sci. Technol.* 46 (6), 3060–3075. doi:10.1021/es2031505.
- Hirsch, P.E., N’Guyen, A., Adrian-Kalchhauser, I., Burkhardt-Holm, P., 2016. What do we really know about the impacts of one of the 100 worst invaders in Europe? A reality check. *Ambio* 45 (3), 267–279. doi:10.1007/s13280-015-0718-9.
- Holm, P., Schulz, G., Athanasopulu, K., 2013. Mikroplastik - ein unsichtbarer Störenfried. *Biologie in unserer Zeit* 43 (1), 27–33. doi:10.1002/biuz.201310497.
- Hong, S.H., Shim, W.J., Hong, L., 2017. Methods of analysing chemicals associated with microplastics: A review. *Anal. Methods* 9 (9), 1361–1368. doi:10.1039/C6AY02971J.
- Horton, A.A., Svendsen, C., Williams, R.J., Spurgeon, D.J., Lahive, E., 2017. Large microplastic particles in sediments of tributaries of the River Thames, UK – Abundance, sources and methods for effective quantification. *Mar. Poll. Bull.* 114 (1), 218–226. doi:10.1016/j.marpolbul.2016.09.004.
- Huck, C.W., Bonn, G.K., 2005. Poly(styrene-divinylbenzene) based media for liquid chromatography. *Chem. Eng. Technol.* 28 (12), 1457–1472. doi:10.1002/ceat.200500265.
- Huerta Lwanga, E., Gertsen, H., Gooren, H., Peters, P., Salánki, T., van der Ploeg, M., Besseling, E., Koelmans, A.A., Geissen, V., 2016. Microplastics in the terrestrial

- ecosystem: Implications for *Lumbricus terrestris* (Oligochaeta, Lumbricidae). *Environ. Sci. Technol.* 50 (5), 2685–2691. doi:10.1021/acs.est.5b05478.
- Hurley, R., Woodward, J., Rothwell, J.J., 2018. Microplastic contamination of river beds significantly reduced by catchment-wide flooding. *Nat. Geosci.* 11 (4), 251–257. doi:10.1038/s41561-018-0080-1.
- Hurley, R.R., Woodward, J.C., Rothwell, J.J., 2017. Ingestion of microplastics by freshwater tubifex worms. *Environ. Sci. Technol.* 51 (21), 12844–12851. doi:10.1021/acs.est.7b03567.
- ICPR, 2018. The Rhine. International Commission for the Protection of the Rhine. <https://www.iksr.org/en/rhine/>. Accessed 18 December 2018.
- Imhof, H.K., Schmid, J., Niessner, R., Ivleva, N.P., Laforsch, C., 2012. A novel, highly efficient method for the separation and quantification of plastic particles in sediments of aquatic environments. *Limnol. Oceanogr. Methods* 10 (7), 524–537. doi:10.4319/lom.2012.10.524.
- Inamuddin, D., Luqman, M. (Eds.), 2012. *Ion Exchange Technology II: Applications*. Springer. 434 pp.
- IT NRW, 2018. Bevölkerung in Nordrhein-Westfalen. Information und Technik Nordrhein-Westfalen. <https://www.it.nrw/bevoelkerung-am-31122017-und-30062018-nach-gemeinden-93051>. Accessed 15 January 2019.
- Ivleva, N.P., Wiesheu, A.C., Niessner, R., 2017. Microplastic in aquatic ecosystems. *Angew. Chem. Int. Edit.* 56 (7), 1720–1739. doi:10.1002/anie.201606957.
- Jahnke, A., Arp, H.P.H., Escher, B.I., Gewert, B., Gorokhova, E., Kühnel, D., Ogonowski, M., Potthoff, A., Rummel, C., Schmitt-Jansen, M., Toorman, E., MacLeod, M., 2017. Reducing uncertainty and confronting ignorance about the possible impacts of weathering plastic in the marine environment. *Environ. Sci. Technol. Lett.* 4 (3), 85–90. doi:10.1021/acs.estlett.7b00008.
- Jambeck, J.R., Geyer, R., Wilcox, C., Siegler, T.R., Perryman, M., Andrady, A., Narayan, R., Law, K.L., 2015. Plastic waste inputs from land into the ocean. *Science* 347 (6223), 768–771. doi:10.1126/science.1260352.

- Jemec, A., Horvat, P., Kunej, U., Bele, M., Kržan, A., 2016. Uptake and effects of microplastic textile fibers on freshwater crustacean *Daphnia magna*. *Environ. Pollut.* 219, 201–209. doi:10.1016/j.envpol.2016.10.037.
- Ji, Z.-G., 2017. Hydrodynamics and water quality: Modelling rivers, lakes, and estuaries. John Wiley & Sons, Hoboken, NJ.
- Jones, R.J., 2007. Chemical contamination of a coral reef by the grounding of a cruise ship in Bermuda. *Mar. Pollut. Bull.* 54 (7), 905–911. doi:10.1016/j.marpolbul.2007.02.018.
- Jong, M.P.C. de, Battjes, J.A., 2004. Seiche characteristics of Rotterdam Harbour. *Coast. Eng.* 51 (5-6), 373–386. doi:10.1016/j.coastaleng.2004.04.002.
- Kalchhauser, I., Mutzner, P., Hirsch, P., Burkhardt-Holm, P., 2013. Arrival of round goby *Neogobius melanostomus* (Pallas, 1814) and bighead goby *Ponticola kessleri* (Günther, 1861) in the High Rhine (Switzerland). *BIR* 2 (1), 79–83. doi:10.3391/bir.2013.2.1.14.
- Käppler, A., Fischer, D., Oberbeckmann, S., Schernewski, G., Labrenz, M., Eichhorn, K.-J., Voit, B., 2016. Analysis of environmental microplastics by vibrational microspectroscopy: FTIR, Raman or both? *Anal. Bioanal. Chem.* 408 (29), 8377–8391. doi:10.1007/s00216-016-9956-3.
- Karlsson, T.M., Arneborg, L., Broström, G., Almroth, B.C., Gipperth, L., Hassellöv, M., 2018. The unaccountability case of plastic pellet pollution. *Mar. Pollut. Bull.* 129 (1), 52–60. doi:10.1016/j.marpolbul.2018.01.041.
- Kawecki, D., Scheeder, P.R.W., Nowack, B., 2018. Probabilistic material flow analysis of seven commodity plastics in Europe. *Environ. Sci. Technol.* 52 (17), 9874–9888. doi:10.1021/acs.est.8b01513.
- Kettler, R., 2001. Statistique des déchets 2000, Avec données 2001 sur la planification des UIOM.: Doc. Environ. 95. Off. fédéral l'environnement.
<https://www.admin.ch/gov/fr/accueil/documentation/communiques.msg-id-8421.html>.
Accessed 02 March 2020.
- Kirstein, I.V., Kirmizi, S., Wichels, A., Garin-Fernandez, A., Erler, R., Löder, M., Gerdts, G., 2016. Dangerous hitchhikers? Evidence for potentially pathogenic *Vibrio* spp. on microplastic particles. *Mar. Environ. Res.* 120, 1–8. doi:10.1016/j.marenvres.2016.07.004.
- Klages, M., Gutow, L., Bergmann, M. (Eds.), 2015. Marine Anthropogenic Litter. Springer, 447 pp.

- Klein, S., Dimzon, I.K., Eubeler, J., Knepper, T.P., 2018. Analysis, occurrence, and degradation of microplastics in the aqueous environment, in: Wagner, M., Lambert, S. (Eds.), *Freshwater Microplastics* 58. Springer, pp. 51–67.
- Klein, S., Worch, E., Knepper, T.P., 2015. Occurrence and spatial distribution of microplastics in river shore sediments of the Rhine-Main area in Germany. *Environ. Sci. Technol.* 49 (10), 6070–6076. doi:10.1021/acs.est.5b00492.
- Kleinn, J., Frei, C., Gurtz, J., Lüthi, D., Vidale, P.L., Schär, C., 2005. Hydrologic simulations in the Rhine basin driven by a regional climate model. *J. Geophys. Res.* 110 (D4), 224. doi:10.1029/2004JD005143.
- Koelmans, A.A., Besseling, E., Foekema, E.M., 2014. Leaching of plastic additives to marine organisms. *Environ. Pollut.* 187, 49–54. doi:10.1016/j.envpol.2013.12.013.
- Kooi, M., Besseling, E., Kroeze, C., van Wezel, A.P., Koelmans, A.A., 2018. Modeling the fate and transport of plastic debris in freshwaters: Review and guidance, in: Wagner, M., Lambert, S., Besseling, E., Biginagwa, F.J. (Eds.), *Freshwater microplastics. Emerging environmental contaminants? The handbook of environmental chemistry. Volume 58.* Springer, pp. 125–152. doi:10.1007/978-3-319-61615-5
- Kowalski, N., Reichardt, A.M., Waniek, J.J., 2016. Sinking rates of microplastics and potential implications of their alteration by physical, biological, and chemical factors. *Mar. Pollut. Bull.* 109 (1), 310–319. doi:10.1016/j.marpolbul.2016.05.064.
- Kramm, J., Völker, C., Wagner, M., 2018. Superficial or substantial: Why care about microplastics in the anthropocene? *Environ. Sci. Technol.* 52 (6), 3336–3337. doi:10.1021/acs.est.8b00790.
- Lambert, S., Wagner, M., 2016. Formation of microscopic particles during the degradation of different polymers. *Chemosphere* 161, 510–517. doi:10.1016/j.chemosphere.2016.07.042.
- Lebreton, L.C.M., van der Zwet, J., Damsteeg, J.-W., Slat, B., Andrady, A., Reisser, J., 2017. River plastic emissions to the world's oceans. *Nat. Commun.* 8, 15611. doi:10.1038/ncomms15611.
- Lechner, A., Keckeis, H., Lumesberger-Loisl, F., Zens, B., Krusch, R., Tritthart, M., Glas, M., Schludermann, E., 2014. The Danube so colourful: A potpourri of plastic litter outnumbered fish larvae in Europe's second largest river. *Environ. Pollut.* 188, 177–181. doi:10.1016/j.envpol.2014.02.006.

- Lechner, A., Ramler, D., 2015. The discharge of certain amounts of industrial microplastic from a production plant into the River Danube is permitted by the Austrian legislation. *Environ. Pollut.* 200, 159–160. doi:10.1016/j.envpol.2015.02.019.
- Lenntech, 2018. Ion exchange resins. <https://www.lenntech.com/products/resins/ixresins.htm>. Accessed 02. March 2020.
- Lenz, R., Enders, K., Stedmon, C.A., Mackenzie, D.M.A., Nielsen, T.G., 2015. A critical assessment of visual identification of marine microplastic using Raman spectroscopy for analysis improvement. *Mar. Pollut. Bull.* 100 (1), 82–91. doi:10.1016/j.marpolbul.2015.09.026
- Leslie, H.A., Brandsma, S.H., van Velzen, M.J.M., Vethaak, A.D., 2017. Microplastics en route: Field measurements in the Dutch river delta and Amsterdam canals, wastewater treatment plants, North Sea sediments and biota. *Environ. Int.* 101, 133–142. doi:10.1016/j.envint.2017.01.018.
- Liebezeit, G., Dubaish, F., 2012. Microplastics in beaches of the East Frisian islands Spiekeroog and Kachelotplate. *Bull. Environ. Contam. Toxicol.* 89 (1), 213–217. doi:10.1007/s00128-012-0642-7.
- Liedermann, M., Gmeiner, P., Pessenlehner, S., Haimann, M., Hohenblum, P., Habersack, H., 2018. A methodology for measuring microplastic transport in large or medium rivers. *Water* 10 (4), 414. doi:10.3390/w10040414.
- Lin-Vien, D. (Ed.), 2006. *The Handbook of infrared and raman characteristic frequencies of organic molecules*, [Repr.] ed. Academic Press, San Diego, 503 pp.
- Lin, Z.H., Guan, C.J., Feng, X.L., Zhao, C.X., 2006. Synthesis of macroreticular p-(ω -sulfonic-perfluoroalkylated) polystyrene ion-exchange resin and its application as solid acid catalyst. *J. Mol. Catal A-Chem.* 247 (1-2), 19–26. doi:10.1016/j.molcata.2005.11.008.
- Lobelle, D., Cunliffe, M., 2011. Early microbial biofilm formation on marine plastic debris. *Mar. Pollut. Bull.* 62 (1), 197–200. doi:10.1016/j.marpolbul.2010.10.013.
- Löder, M.G.J., Gerdt, G., 2015. Methodology used for the detection and identification of microplastics – A critical appraisal, in: Klages, M., Gutow, L., Bergmann, M. (Eds.), *Marine Anthropogenic Litter*. Springer, pp. 201–227.
- Löder, M.G.J., Imhof, H.K., Ladehoff, M., Löschel, L.A., Lorenz, C., Mintenig, S., Piehl, S., Primpke, S., Schrank, I., Laforsch, C., Gerdt, G., 2017. Enzymatic purification of

- microplastics in environmental samples. *Environ. Sci. Technol.* 51 (24), 14283–14292. doi:10.1021/acs.est.7b03055.
- Löder, M.G.J., Kuczera, M., Mintenig, S., Lorenz, C., Gerdt, G., 2015. Focal plane array detector-based micro-Fourier-transform infrared imaging for the analysis of microplastics in environmental samples. *Environ. Chem.* 12 (5), 563. doi:10.1071/EN14205.
- Lohmann, R., 2017. Microplastics are not important for the cycling and bioaccumulation of organic pollutants in the oceans – But should microplastics be considered POPs themselves? *Integr. Environ. Assess.* 13 (3), 460–465. doi:10.1002/ieam.1914.
- Lorenz, C., Speidel, L., Primpke, S., Gerdt, G., 2017. Using the FlowCam to validate an enzymatic digestion protocol applied to assess the occurrence of microplastics in the southern North Sea, in: Baztan, J., Jorgensen, B., Pahl, S., Thompson, R.C., Vanderlinden, J.-P. (Eds.), MICRO 2016. Fate and impact of microplastics in marine ecosystems. From the coastline to the open sea. Elsevier Science, Amsterdam, Boston, Heidelberg, London, New York, Oxford, Paris, San Diego, San Francisco, Singapore, Sydney, Tokyo, pp. 92–93.
- Lots, F.A.E., Behrens, P., Vijver, M.G., Horton, A.A., Bosker, T., 2017. A large-scale investigation of microplastic contamination: Abundance and characteristics of microplastics in European beach sediment. *Mar. Pollut. Bull.* 123 (1-2), 219–226. doi:10.1016/j.marpolbul.2017.08.057.
- Mahmood, K., 1987. Reservoir sedimentation: Impact, extent, and mitigation. Technical paper. International Bank for Reconstruction and Development, Washington, DC (USA). <https://www.osti.gov/biblio/5564758>. Accessed 02. March 2020.
- Mani, T., Blarer, P., Storck, F.R., Pittroff, M., Wernicke, T., Burkhardt-Holm, P., 2019. Repeated detection of polystyrene microbeads in the Lower Rhine River. *Environ. Pollut.* 245, 634–641. doi:10.1016/j.envpol.2018.11.036.
- Mani, T.; Burkhardt-Holm, P., 2020. Seasonal microplastics variation in nival and pluvial stretches of the Rhine River – From the Swiss catchment towards the North Sea. *Sci. Total Environ.* 707, 135579. doi:10.1016/j.scitotenv.2019.135579.
- Mani, T., Burkhardt-Holm, P., Segner, H., Zennegg, M., Amaral-Zettler, L., 2018. Microplastics – a potential threat to the remote and pristine ecosystems of the Antarctic seas?, in: The Expedition PS111 of the Research Vessel POLARSTERN to the southern

- Weddell Sea in 2018. Alfred-Wegener-Institut, Helmholtz-Zentrum für Polar- und Meeresforschung. doi:10.2312/BzPM_0718_2018.
- Mani, T., Frehland, S., Kalberer, A., Burkhardt-Holm, P., 2019. Using castor oil to separate microplastics from four different environmental matrices. *Anal. Methods* 11 (13), 1788–1794. doi:10.1039/C8AY02559B.
- Mani, T., Hauk, A., Walter, U., Burkhardt-Holm, P., 2015. Microplastics profile along the Rhine River. *Sci. Rep.* 5, 17988. doi:10.1038/srep17988.
- Mani, T., Primpke, S., Lorenz, C., Gerdt, G., Burkhardt-Holm, P., 2019. Microplastic pollution in benthic midstream sediments of the Rhine River. *Environ. Sci. Technol.* 53 (10), 6053–6062. doi:10.1021/acs.est.9b01363.
- Masura, J., Baker, J.E., Foster, G.D., Arthur, C., Herring, C., 2015. Laboratory methods for the analysis of microplastics in the marine environment: recommendations for quantifying synthetic particles in waters and sediments. NOAA technical memorandum NOS-OR&R 48. NOAA, Silver Spring, Maryland, USA.
<https://repository.library.noaa.gov/view/noaa/10296#tabs-2>. Accessed 16 August 2018.
- Mato, Y., Isobe, T., Takada, H., Kanehiro, H., Ohtake, C., Kaminuma, T., 2001. Plastic resin pellets as a transport medium for toxic chemicals in the marine environment. *Environ. Sci. Technol.* 35 (2), 318–324. doi:10.1021/es0010498.
- McCormick, A., Hoellein, T.J., Mason, S.A., Schlupe, J., Kelly, J.J., 2014. Microplastic is an abundant and distinct microbial habitat in an urban river. *Environ. Sci. Technol.* 48 (20), 11863–11871. doi:10.1021/es503610r.
- Mellor, B.G., Khanna, A.S. (Eds.), 2006. *Surface coatings for protection against wear*. CRC Press, Cambridge, Eng, 429 pp.
- Mertens, M., 2011. *Der Lachs: Ein Fisch kehrt zurück*. Haupt, Bern.
- Miller, W.S., Castagna, C.J., Pieper, A.W., 2009. Understanding ion-exchange resins for water treatment systems. *Water Technologies & Solutions*, 13 pp.
<https://www.nguyenthanhmy.com/courses/Ion-Exchange-Polymers-01.pdf>. Accessed 02. March 2020.
- Mintenig, S.M., Int-Veen, I., Löder, M.G.J., Primpke, S., Gerdt, G., 2017. Identification of microplastic in effluents of waste water treatment plants using focal plane array-based

- micro-Fourier-transform infrared imaging. *Water Res.* 108, 365–372.
doi:10.1016/j.watres.2016.11.015.
- Moore, C.J., Lattin, G.L., Zellers, A.F., 2011. Quantity and type of plastic debris flowing from two urban rivers to coastal waters and beaches of Southern California. *RGCI* 11 (1), 65–73. doi:10.5894/rgci194.
- Murphy, F., Ewins, C., Carbonnier, F., Quinn, B., 2016. Wastewater treatment works (wwtw) as a source of microplastics in the aquatic environment. *Environ. Sci. Technol.* 50 (11), 5800–5808. doi:10.1021/acs.est.5b05416.
- Napper, I.E., Thompson, R.C., 2016. Release of synthetic microplastic plastic fibres from domestic washing machines: Effects of fabric type and washing conditions. *Mar. Pollut. Bull.* 112 (1-2), 39–45. doi:10.1016/j.marpolbul.2016.09.025.
- Nel, H.A., Dalu, T., Wasserman, R.J., 2018. Sinks and sources: Assessing microplastic abundance in river sediment and deposit feeders in an Austral temperate urban river system. *Sci. Tot. Env.* 612, 950–956. doi:10.1016/j.scitotenv.2017.08.298.
- Ng, A.K.Y., Song, S., 2010. The environmental impacts of pollutants generated by routine shipping operations on ports. *Ocean Coast. Manage.* 53 (5-6), 301–311.
doi:10.1016/j.ocecoaman.2010.03.002.
- Nizzetto, L., Bussi, G., Futter, M.N., Butterfield, D., Whitehead, P.G., 2016. A theoretical assessment of microplastic transport in river catchments and their retention by soils and river sediments. *Environ. Sci. Proc. Imp.* 18 (8), 1050–1059. doi:10.1039/c6em00206d.
- Norén, F., 2007. Small plastic particles in coastal Swedish waters. n-research, Lysekil, Sweden.
https://www.researchgate.net/profile/Fredrik_Noren/publication/284312290_Small_plastic_particles_in_Coastal_Swedish_waters/links/571203c608ae4ef74525ec38/Small-plastic-particles-in-Coastal-Swedish-waters.pdf?origin=publication_detail. Accessed 23 May 2018.
- NRW Invest, 2016. NI-Standortbroschuere, 28 pp.
<https://www.nrwinvest.com/fileadmin/Redaktion/branchen-in-nrw/NI-Standortbroschuere-DE-2016.pdf>. Accessed 13 September 2018.
- Nuelle, M.-T., Dekiff, J.H., Remy, D., Fries, E., 2014. A new analytical approach for monitoring microplastics in marine sediments. *Environ. Pollut.* 184, 161–169.
doi:10.1016/j.envpol.2013.07.027.

- O’Brine, T., Thompson, R.C., 2010. Degradation of plastic carrier bags in the marine environment. *Mar. Poll. Bull.* 60 (12), 2279–2283. doi:10.1016/j.marpolbul.2010.08.005.
- Oehlmann, J., Schulte-Oehlmann, U., Kloas, W., Jagnytsch, O., Lutz, I., Kusk, K.O., Wollenberger, L., Santos, E.M., Paull, G.C., van Look, K.J.W., Tyler, C.R., 2009. A critical analysis of the biological impacts of plasticizers on wildlife. *Philosophical transactions of the Royal Society of London. Series B, Biological sciences* 364 (1526), 2047–2062. doi:10.1098/rstb.2008.0242.
- Ohtake, Y., Kobayashi, T., Asabe, H., Murakami, N., 1998. Studies on biodegradation of LDPE – observation of LDPE films scattered in agricultural fields or in garden soil. *Polym. Degrad. Stabil.* 60 (1), 79–84. doi:10.1016/S0141-3910(97)00032-3.
- Park, I., Seo, I.W., Kim, Y.D., Han, E.J., 2017. Turbulent mixing of floating pollutants at the surface of the river. *J. Hydraul. Eng.* 143 (8), 4017019. doi:10.1061/(ASCE)HY.1943-7900.0001319.
- Peeken, I., Primpke, S., Beyer, B., Gütermann, J., Katlein, C., Krumpfen, T., Bergmann, M., Hehemann, L., Gerdts, G., 2018. Arctic sea ice is an important temporal sink and means of transport for microplastic. *Nat. Commun.* 9 (1), 1505. doi:10.1038/s41467-018-03825-5.
- Peng, G., Xu, P., Zhu, B., Bai, M., Li, D., 2018. Microplastics in freshwater river sediments in Shanghai, China: A case study of risk assessment in mega-cities. *Environ. Pollut.* 234, 448–456. doi:10.1016/j.envpol.2017.11.034.
- Penzel, E., Ballard, N., Asua, J.M., 2000. Polyacrylates. *Polymers and Plastics. Ullmann's Encyclopedia of Industrial Chemistry.* Wiley Online Library. doi:10.1002/14356007.a21_157
- Peters, C.A., Bratton, S.P., 2016. Urbanization is a major influence on microplastic ingestion by sunfish in the Brazos River Basin, Central Texas, USA. *Environ. Pollut.* 210, 380–387. doi:10.1016/j.envpol.2016.01.018.
- Plastic Soup Foundation, 2019. Beat the Microbead. <https://www.beatthemicrobead.org>. Accessed 01 April 2019.
- PlasticsEurope, 2017. Operation Clean Sweep, 28 pp. <https://www.plasticseurope.org/en/resources/publications/367-plasticseurope-operation-clean-sweep-report-2017>. Accessed 01 April 2019.

- PlasticsEurope, 2017. Plastic – the Facts 2017, 44 pp.
https://www.plasticseurope.org/application/files/5715/1717/4180/Plastics_the_facts_2017_FINAL_for_website_one_page.pdf. Accessed 23 August 2018.
- Primpke, S., Imhof, H., Piehl, S., Lorenz, C., Löder, M., Laforsch, C., Gerdt, G., 2017. Mikroplastik in der Umwelt. *Chem. Unserer Zeit* 51 (6), 402–412.
doi:10.1002/ciuz.201700821.
- Primpke, S., Lorenz, C., Rascher-Friesenhausen, R., Gerdt, G., 2017. An automated approach for microplastics analysis using focal plane array (FPA) FTIR microscopy and image analysis. *Anal. Methods* 9 (9), 1499–1511. doi:10.1039/C6AY02476A.
- Primpke, S., Wirth, M., Lorenz, C., Gerdt, G., 2018. Reference database design for the automated analysis of microplastic samples based on Fourier transform infrared (FTIR) spectroscopy. *Anal. Bioanal. Chem.* 410 (21), 5131–5141. doi:10.1007/s00216-018-1156-x.
- Pye, K. (Ed.), 1994. Sediment transport and depositional processes. Blackwell Scientific Publications, Oxford, 397 pp.
- Quik, J.T.K., Velzeboer, I., Wouterse, M., Koelmans, A.A., van de Meent, D., 2014. Heteroaggregation and sedimentation rates for nanomaterials in natural waters. *Water Res.* 48, 269–279. doi:10.1016/j.watres.2013.09.036.
- Remy, F., Collard, F., Gilbert, B., Compère, P., Eppe, G., Lepoint, G., 2015. When microplastic is not plastic: The ingestion of artificial cellulose fibers by macrofauna living in seagrass macrophytodetritus. *Environ. Sci. Technol.* 49 (18), 11158–11166.
- Rice, M.R., Gold, H.S., 1984. Polypropylene as an adsorbent for trace organics in water. *Anal. Chem.* 56 (8), 1436–1440. doi:10.1021/ac00272a052.
- Rillig, M.C., 2012. Microplastic in terrestrial ecosystems and the soil? *Environ. Sci. Technol.* 46 (12), 6453–6454. doi:10.1021/es302011r.
- Rochman, C.M., Browne, M.A., Halpern, B.S., Hentschel, B.T., Hoh, E., Karapanagioti, H.K., Rios-Mendoza, L.M., Takada, H., Teh, S., Thompson, R.C., 2013. Policy: Classify plastic waste as hazardous. *Nature* 494 (7436), 169–171. doi:10.1038/494169a.
- Rodrigues, M.O., Abrantes, N., Gonçalves, F.J.M., Nogueira, H., Marques, J.C., Gonçalves, A.M.M., 2018. Spatial and temporal distribution of microplastics in water and sediments

- of a freshwater system (Antuã River, Portugal). *Sci. Total Environ.* 633, 1549–1559. doi:10.1016/j.scitotenv.2018.03.233.
- Rohde, W., Wloka, V., 2011. Ion exchanger moulded body and method for producing same PCT/EP09/64350. 2009. USA, 9 pp. <https://patents.google.com/patent/EP2352635A2/en>. Accessed 09 March 2020.
- Rummel, C.D., Jahnke, A., Gorokhova, E., Kühnel, D., Schmitt-Jansen, M., 2017. Impacts of biofilm formation on the fate and potential effects of microplastic in the aquatic environment. *Environ. Sci. Technol. Lett.* 4 (7), 258–267. doi:10.1021/acs.estlett.7b00164.
- Salimon, J., Noor, D.A.M., Nazrizawati, A.T., Firdaus, M.Y.M., Noraishah, A., 2010. Fatty acid composition and physicochemical properties of Malaysian castor bean *Ricinus communis* L. seed oil. *Sains Malays.* 39 (5), 761–764.
- Sanchez, W., Bender, C., Porcher, J.-M., 2014. Wild gudgeons (*Gobio gobio*) from French rivers are contaminated by microplastics: Preliminary study and first evidence. *Environ. Res.* 128, 98–100. doi:10.1016/j.envres.2013.11.004.
- Scheurer, M., Bigalke, M., 2018. Microplastics in Swiss floodplain soils. *Environ. Sci. Technol.* 52 (6), 3591–3598. doi:10.1021/acs.est.7b06003.
- Schmidt, C., Krauth, T., Wagner, S., 2017. Export of plastic debris by rivers into the sea. *Environ. Sci. Technol.* 51 (21), 12246–12253. doi:10.1021/acs.est.7b02368.
- Schubert, J., 2002. Hydraulic aspects of riverbank filtration – field studies. *J. Hydrol.* 266 (3–4), 145–161. doi:10.1016/S0022-1694(02)00159-2.
- Secchi, E.R., Zarzur, S., 1999. Plastic debris ingested by a Blainville's beaked whale, *Mesoplodon densirostris*, washed ashore in Brazil. *Aquat. Mamm.* 25 (1), 21–24.
- Sedlak, D., 2017. Three lessons for the microplastics voyage. *Environ. Sci. Technol.* 51 (14), 7747–7748. doi:10.1021/acs.est.7b03340.
- Shim, S.E., Yang, S., Choi, H.H., Choe, S., 2004. Fully crosslinked poly(styrene-co-divinylbenzene) microspheres by precipitation polymerization and their superior thermal properties. *J. Polym. Sci. A Polym. Chem.* 42 (4), 835–845. doi:10.1002/pola.11028.
- Shumchenia, E.J., Guarinello, M.L., King, J.W., 2016. A re-assessment of Narragansett Bay benthic habitat quality between 1988 and 2008. *Estuar. Coast.* 39 (5), 1463–1477. doi:10.1007/s12237-016-0095-z.

- Siegfried, M., Koelmans, A.A., Besseling, E., Kroeze, C., 2017. Export of microplastics from land to sea. A modelling approach. *Water Res.* 127, 249–257. doi:10.1016/j.watres.2017.10.011.
- Silva-Cavalcanti, J.S., Silva, J.D.B., França, E.J.d., Araújo, M.C.B.d., Gusmão, F., 2017. Microplastics ingestion by a common tropical freshwater fishing resource. *Environ. Pollut.* 221, 218–226. doi:10.1016/j.envpol.2016.11.068.
- Silva, A.B., Bastos, A.S., Justino, C.I.L., da Costa, J.P., Duarte, A.C., Rocha-Santos, T.A.P., 2018. Microplastics in the environment: Challenges in analytical chemistry – A review. *Anal. Chim. Acta.* 1017, 1–19. doi:10.1016/j.aca.2018.02.043.
- Song, Y.K., Hong, S.H., Jang, M., Han, G.M., Jung, S.W., Shim, W.J., 2017. Combined effects of uv exposure duration and mechanical abrasion on microplastic fragmentation by polymer type. *Environ. Sci. Technol.* 51 (8), 4368–4376. doi:10.1021/acs.est.6b06155.
- Spreafico, M., Weingartner, R., Leibundgut, C. (Eds.), 1992. *Hydrological atlas of Switzerland*. EDMZ, Bern, 11 pp.
- Statista, 2018. Amsterdam: total population 2008-2018 | Statistic. <https://www.statista.com/statistics/753235/total-population-of-amsterdam/>. Accessed 29 January 2019.
- Steer, M., Cole, M., Thompson, R.C., Lindeque, P.K., 2017. Microplastic ingestion in fish larvae in the western English Channel. *Environ. Pollut.* 226, 250–259. doi:10.1016/j.envpol.2017.03.062.
- Stolte, A., Forster, S., Gerdtts, G., Schubert, H., 2015. Microplastic concentrations in beach sediments along the German Baltic coast. *Mar. Pollut. Bull.* 99 (1-2), 216–229. doi:10.1016/j.marpolbul.2015.07.022.
- Tagesanzeiger, 2018. Die 5-Rappen-Gebühr zeigt Wirkung – und wie. <https://www.tagesanzeiger.ch/wirtschaft/standardverbrauch-von-raschelsaeckli-ging-um-84-prozent-zurueck/story/16111216>. Accessed 01 April 2019.
- Tagg, A.S., Harrison, J.P., Ju-Nam, Y., Sapp, M., Bradley, E.L., Sinclair, C.J., Ojeda, J.J., 2017. Fenton’s reagent for the rapid and efficient isolation of microplastics from wastewater. *Chem. Comm.* 53 (2), 372–375. doi:10.1039/c6cc08798a.
- Ter Halle, A., Ladirat, L., Gendre, X., Goudouneche, D., Pusineri, C., Routaboul, C., Tenailleau, C., Duployer, B., Perez, E., 2016. Understanding the fragmentation pattern of

marine plastic debris. *Environ. Sci. Technol.* 50 (11), 5668–5675.

doi:10.1021/acs.est.6b00594.

Terepocki, A.K., Brush, A.T., Kleine, L.U., Shugart, G.W., Hodum, P., 2017. Size and dynamics of microplastic in gastrointestinal tracts of Northern Fulmars (*Fulmarus glacialis*) and Sooty Shearwaters (*Ardenna grisea*). *Mar. Pollut. Bull.* 116 (1-2), 143–150. doi:10.1016/j.marpolbul.2016.12.064.

The Guardian, 2017. Kenya brings in world's toughest plastic bag ban: Four years jail or \$40,000 fine. <https://www.theguardian.com/environment/2017/aug/28/kenya-brings-in-worlds-toughest-plastic-bag-ban-four-years-jail-or-40000-fine>. Accessed 01 April 2019.

Thompson, R.C., Olsen, Y., Mitchell, R.P., Davis, A., Rowland, S.J., John, A.W.G., McGonigle, D., Russell, A.E., 2004. Lost at sea: Where is all the plastic? *Science*. 304 (5672), 838. doi:10.1126/science.1094559.

Tittizer, T., Schöll, F., Schleuter, A., 1988. Einsatz von Taucherschacht und Taucherglocke bei benthosbiologischen Untersuchungen. *Deutsche Gewässerkundliche Mitteilungen*. 32 (5/6), 141–144.

Triebskorn, R., Braunbeck, T., Grummt, T., Hanslik, L., Huppertsberg, S., Jekel, M., Knepper, T.P., Kraus, S., Müller, Y.K., Pittroff, M., Ruhl, A.S., Schmiege, H., Schür, C., Strobel, C., Wagner, M., Zumbülte, N., Köhler, H.-R., 2019. Relevance of nano- and microplastics for freshwater ecosystems: A critical review. *TrAC Trend. Anal. Chem.* 110, 375–392. doi:10.1016/j.trac.2018.11.023.

Tsyurupa, M.P., Davankov, V.A., 2006. Porous structure of hypercrosslinked polystyrene: State-of-the-art mini-review. *React. Funct. Polym.* 66 (7), 768–779. doi:10.1016/j.reactfunctpolym.2005.11.004.

Turner, A., 2010. Marine pollution from antifouling paint particles. *Mar. Pollut. Bull.* 60 (2), 159–171. doi:10.1016/j.marpolbul.2009.12.004.

Uekoetter, F., 2018. In the reflection of water. A transnational environmental history of the Upper Rhine (1800-2000). Franz Steiner Verlag, Germany.

Urgert, W., 2015. Microplastics in the rivers Meuse and Rhine: Developing guidance for a possible future monitoring program. Masterthesis, Heerlen, The Netherlands, 106 pp. <https://www.riwa-rijn.org/wp-content/uploads/2015/11/master-thesis-NW-Wilco-Urgert-838144036-DEFINITIEF-16-10-2015.pdf> Accessed 09 March 2020.

- Van Cauwenberghe, L., Vanreusel, A., Mees, J., Janssen, C.R., 2013. Microplastic pollution in deep-sea sediments. *Environ. Pollut.* 182, 495–499. doi:10.1016/j.envpol.2013.08.013.
- Van den Hurk, P., Eertman, R.H.M., Stronkhorst, J., 1997. Toxicity of harbour canal sediments before dredging and after off-shore disposal. *Mar. Pollut. Bull.* 34 (4), 244–249. doi:10.1016/S0025-326X(96)00104-X.
- Van der Wal, M., van der Meulen, M., Tweehuijzen, G., Peterlin, M., Palatinus, A., Viršek, M.K., Coscia, L., Kršan, A., 2015. SFRA0025: Identification and assesment of riverine input of (marine) litter. Final report for the European Commission DG Environment under framework contact No ENV. D, Bristol (Vol. 25). 2/FRA/2012., 208 pp. <http://ec.europa.eu/environment/marine/good-environmental-status/descriptor-10/pdf/iasFinal%20Report.pdf>. Accessed 29 March 2019.
- Van Rijn, L.C., 1984. Sediment transport, part II: Suspended load transport. *J. Hydraul. Eng.* 110 (11), 1613–1641.
- Verbunt, M., Zappa, M., Gurtz, J., Kaufmann, P., 2006. Verification of a coupled hydrometeorological modelling approach for alpine tributaries in the Rhine basin. *Journal of Hydrology* 324 (1-4), 224–238. doi:10.1016/j.jhydrol.2005.09.036.
- Verlaan, P.A.J., Spanhoff, R., 2000. Massive sedimentation events at the mouth of the Rotterdam waterway. *J. Coastal Res.*, 458–469.
- Vermaire, J.C., Pomeroy, C., Herczegh, S.M., Haggart, O., Murphy, M., Schindler, D.E., 2017. Microplastic abundance and distribution in the open water and sediment of the Ottawa River, Canada, and its tributaries. *FACETS* 2 (1), 301–314. doi:10.1139/facets-2016-0070.
- Voinov Kohler, J., 2017. The Basel Convention on the Control of Transboundary Movements of Hazardous Wastes and their Disposal 1989, in: *Elgar encyclopedia of environmental law*. Edward Elgar Publishing, Cheltenham, UK, pp. 331–342.
- Von Moos, N., Burkhardt-Holm, P., Köhler, A., 2012. Uptake and effects of microplastics on cells and tissue of the blue mussel *Mytilus edulis* L. after an experimental exposure. *Environ. Sci. Technol.* 46 (20), 11327–11335. doi:10.1021/es302332w.
- Wagner, M., Lambert, S., Besseling, E., Biginagwa, F.J. (Eds.), 2018. Freshwater microplastics: Emerging environmental contaminants? *The handbook of environmental chemistry*. Volume 58. Springer, 303 pp. doi:10.1007/978-3-319-61615-5

- Wagner, M., Scherer, C., Alvarez-Muñoz, D., Brennholt, N., Bourrain, X., Buchinger, S., Fries, E., Grosbois, C., Klasmeier, J., Marti, T., Rodriguez-Mozaz, S., Urbatzka, R., Vethaak, A.D., Winther-Nielsen, M., Reifferscheid, G., 2014. Microplastics in freshwater ecosystems: What we know and what we need to know. *Environ. Sci. Eur.* 26 (1), 12. doi:10.1186/s12302-014-0012-7.
- Wang, J., Peng, J., Tan, Z., Gao, Y., Zhan, Z., Chen, Q., Cai, L., 2017. Microplastics in the surface sediments from the Beijiang River littoral zone: Composition, abundance, surface textures and interaction with heavy metals. *Chemosphere* 171, 248–258. doi:10.1016/j.chemosphere.2016.12.074.
- Wang, W., Ndungu, A.W., Li, Z., Wang, J., 2017. Microplastics pollution in inland freshwaters of China: A case study in urban surface waters of Wuhan, China. *Sci.Total Environ.* 575, 1369–1374. doi:10.1016/j.scitotenv.2016.09.213.
- Wang, Z., Su, B., Xu, X., Di Di, Huang, H., Mei, K., Dahlgren, R.A., Zhang, M., Shang, X., 2018. Preferential accumulation of small (<300 µm) microplastics in the sediments of a coastal plain river network in eastern China. *Water Res.* 144, 393–401. doi:10.1016/j.watres.2018.07.050.
- Weaton & Lefevre, 2000. Ion-Exchange resins. http://msdssearch.dow.com/PublishedLiteratureDOWCOM/dh_0032/0901b803800326ca.pdf. Accessed 15 January 2018.
- Wenzhou Municipal Statistic Bureau, 2011. Wenzhou Population 2010. https://web.archive.org/web/20110927075644/http://www.wenzhou.gov.cn/art/2011/5/10/art_4247_166018.html. Accessed 29 January 2019.
- Winterling, H., Sonntag, N., 2011. Rigid Polystyrene Foam (EPS, XPS). *Kunststoffe international* 10, 18–22.
- World Shipping Council, 2016. Top 50 World Container Ports. <http://www.worldshipping.org/about-the-industry/global-trade/top-50-world-container-ports>. Accessed 29 January 2019.
- Wright, S.L., Kelly, F.J., 2017. Plastic and human health: A micro issue? *Environ. Sci. Technol.* 51 (12), 6634–6647. doi:10.1021/acs.est.7b00423.
- WSV DE, 2017. Verkehrsbericht 2017, 115 pp. https://www.gdws.wsv.bund.de/SharedDocs/Downloads/DE/Verkehrsberichte/Verkehrsbericht_2017.pdf?__blob=publicationFile&v=2. Accessed 15 January 2019.

- Xia, F., Qu, L., Wang, T., Luo, L., Chen, H., Dahlgren, R.A., Zhang, M., Mei, K., Huang, H., 2018. Distribution and source analysis of heavy metal pollutants in sediments of a rapid developing urban river system. *Chemosphere* 207, 218–228. doi:10.1016/j.chemosphere.2018.05.090.
- Xiong, X., Wu, C., Elser, J.J., Mei, Z., Hao, Y., 2019. Occurrence and fate of microplastic debris in middle and lower reaches of the Yangtze River – From inland to the sea. *Sci. Total Environ.* 659, 66–73. doi:10.1016/j.scitotenv.2018.12.313.
- Yonkos, L.T., Friedel, E.A., Perez-Reyes, A.C., Ghosal, S., Arthur, C.D., 2014. Microplastics in four estuarine rivers in the Chesapeake Bay, U.S.A. *Environ. Sci. Technol.* 48 (24), 14195–14202. doi:10.1021/es5036317.
- Zeng, E.Y., 2018. microplastic contamination in aquatic environments: An emerging matter of environmental urgency. Elsevier Science. doi:10.1016/C2016-0-04784-8
- Zettler, E.R., Mincer, T.J., Amaral-Zettler, L.A., 2013. Life in the “plastisphere”: Microbial communities on plastic marine debris. *Environ. Sci. Technol.* 47 (13), 7137–7146. doi:10.1021/es401288x.
- Zhang, G.S., Liu, Y.F., 2018. The distribution of microplastics in soil aggregate fractions in southwestern China. *Sci. Total Environ.* 642, 12–20. doi:10.1016/j.scitotenv.2018.06.004.
- Zhang, K., Gong, W., Lv, J., Xiong, X., Wu, C., 2015. Accumulation of floating microplastics behind the Three Gorges Dam. *Environ. Pollut.* 204, 117–123. doi:10.1016/j.envpol.2015.04.023.
- Zheng, J., Yang, D., 2016. Hub-and-spoke network design for container shipping along the Yangtze River. *J. Transp. Geogr.* 55, 51–57. doi:10.1016/j.jtrangeo.2016.07.001.

Curriculum Vitae

Name:

Thomas Alexander Mani (from Diemtigen, BE, Switzerland)

Place and date of birth:

Salisbury (UK), 22. February 1987

Address:

Zollstrasse 16, 8005 Zürich, Switzerland

Tel.:

+41 (0)79 617 11 96

E-Mail:

t.mani@gmx.ch

Nationalities:

Swiss and British

Education:

2015–2019: PhD in Environmental Sciences, University of Basel, Switzerland

2012–2015: M. Sc. in Sustainable Development, University of Basel, Switzerland

2008–2012: B. A. in Geography and English, University of Basel, Switzerland

Publications

Journal papers

- Mani, Thomas; Burkhardt-Holm, Patricia (2020): **Seasonal microplastics variation in nival and pluvial stretches of the Rhine River – From the Swiss catchment towards the North Sea.** In *Science of the Total Environment* 707, 135579
DOI: 10.1016/j.scitotenv.2019.135579.
- Holm, Patricia; Mani, Thomas; Kalberer, Andreas (2019): **Mikroplastik – Zivilisationsmüll in und um den Rhein herum.** In *Regio Basiliensis* 60 (2), pp. 121–129.
- Mani, Thomas; Primpke, Sebastian; Lorenz, Claudia; Gerdts, Gunnar; Burkhardt-Holm, Patricia (2019): **Microplastic pollution in benthic midstream sediments of the Rhine River.** In *Environmental Science & Technology* 53, pp. 6053–6062.
DOI: 10.1021/acs.est.9b01363
- Mani, Thomas; Frehland, Stefan; Kalberer, Andreas; Burkhardt-Holm, Patricia (2019): **Using castor oil to separate microplastics from four different environmental matrices.** In *Analytical Methods* 11 (13), pp. 1788–1794. DOI: 10.1039/C8AY02559B.
- Mani, Thomas; Blarer, Pascal; Storck, Florian R.; Pittroff, Marco; Wernicke, Theo; Burkhardt-Holm, Patricia (2019): **Repeated detection of polystyrene microbeads in the Lower Rhine River.** In *Environmental Pollution* 245, pp. 634–641.
DOI: 10.1016/j.envpol.2018.11.036.
- Mani, Thomas; Hauk, A.; Walter, U.; Burkhardt-Holm, P. (2015): **Microplastics profile along the Rhine River.** In *Scientific Reports* 5, 17988 (2015). DOI: 10.1038/srep17988

Chapters in edited works

- Mani, Thomas; Burkhardt-Holm, Patricia; Segner, Helmut; Zenneg, Markus; Amaral-Zettler, Linda: **Microplastics - a potential threat to the remote and pristine ecosystems of the Antarctic seas?** In Schröder, Michael, Ed.: *The Expedition PS111 of the Research Vessel Polarstern to the southern Weddell Sea in 2018* (2018). DOI:10.2312/BzPM_0718_2018.
- Mani, Thomas; Hauk, Armin; Walter, Ulrich; Burkhardt-Holm, Patricia: **Mikroplastik im Rhein zwischen Basel und Rotterdam.** In Holger Schüttrumpf, Ed.: *47. IWASA Internationales Wasserbau-Symposium Aachen 2017 – Living Rivers – Neues aus Praxis und Forschung!* (Shaker Verlag, Düren, Germany, 2017).